

**Physiological and Molecular Investigations of Manganese Transforming Bacteria**

**Author**

Wright, Mitchell Henry

**Published**

2014

**Thesis Type**

Thesis (PhD Doctorate)

**School**

School of Biomolecular and Physical Sciences

**DOI**

[10.25904/1912/3277](https://doi.org/10.25904/1912/3277)

**Downloaded from**

<http://hdl.handle.net/10072/368137>

**Griffith Research Online**

<https://research-repository.griffith.edu.au>

# **Physiological and Molecular Investigations of Manganese Transforming Bacteria**

**Mitchell Henry Wright**

B. Biotech (Hons 1.a)



School of Natural Sciences

Griffith Science

Griffith University

Submitted in fulfilment of the requirements

of the degree of Doctor of Philosophy

**July 2014**



**Dedicated to my Grandma, Catherine Wright**

30/01/1918 - 24/07/2013

**Rest in Peace**

## Statement of Originality

This work, entitled **Physiological and Molecular Investigations of Manganese Transforming Bacteria**, has not previously been submitted for a degree or diploma in any university. To the best of my knowledge and belief, the thesis contains no material previously published or written by another person except where due reference is made in the thesis itself.

**Mitchell Henry Wright**

October 23<sup>rd</sup>, 2014

## Acknowledgements

I would like to express my gratitude to my supervisors Dr. Anthony Greene and Prof. Bharat Patel for their guidance and encouragement through my PhD. They were paramount in helping me complete my dissertation, and I will be forever grateful for their help.

I would like to thank my fellow PhD student and good friend Saad Farooqui for helping me through the tough times in the lab. Your friendship helped me step back when things weren't working and I'll cherish the times spent discussing and analysing results together. I would like to thank Adam Mazins, Alan White, James Cameron, Chang Siang Sheng Randall, Wong Wai Mun Mitchell, Joseph Adelskov, Subash Baral, Josh Ong Yong Ming and Lim Yi Jie for their assistance in the lab.

In addition I would like to thank Angela Dickson for her vast knowledge of the ins and outs of Griffith University and for assisting me no matter how obscure the request. Your support and friendship made my time at Griffith University a pleasure. My proof-reader and editor, Charlotte Bouchereau; I have no idea how you understood the jargon that is my writing, but your assistance in comprehending and deciphering my work is a sheer feat and is greatly appreciated. For his diagram editing, I would like to thank Daryle Santos – his knowledge of image editing software assisted in this thesis preparation.

Finally I would like to thank those closest to me on a personal level. Alexandra McMEnamin, thanks for being my best friend and roommate and listening to me ramble on about scientific terminology even though you had no idea what I was talking about. To my father, Ian Wright, you have always been there supporting me, no matter what. For helping me become the person I am today, I am eternally thankful. For any friends, family and faculty not mentioned who have helped me through; I thank you all.

## Publications Arising From This Thesis

### Journal articles:

**Wright, M.H., Farooqui, S.M. & Greene, A.C.** (2014). Manganese Oxidising Characteristics of *Shewanella* Strains. *Geochimica et Cosmochimica Acta*. (Submitted)

**Farooqui, S.M., Wright, M.H. & Greene, A.C.** (2014). *Idiomarina minutum* sp. nov., a haloalkaliphilic bacterium capable of forming ultra-small cells under non-optimal conditions. *Antonie van Leeuwenhoek*. (Submitted)

**Wright, M.H., Greene, A.C. & Patel, B.K.C.** (2014). Metagenomic 16S rRNA analyses of Paralana Hot Springs in the Northern Flinders Ranges of South Australia. *Appl. Environ. Microbiol.* (In preparation).

**Wright, M.H., Greene, A.C. & Patel, B.K.C.** (2014). Draft genome sequence of *Bacillus* sp. strain PMO, a manganese transforming bacterium. *Journal of Bacteriology*. (In preparation).

### Conference proceedings:

**Wright, M.H., Patel, B.K.C. & Greene, A.C.** (2012). Thermophilic bacteria from Paralana Hot Springs in the Northern Flinders Ranges of South Australia. *The Australian Society for Microbiology*. Brisbane, Australia. **July 1<sup>st</sup> – 4<sup>th</sup>, 2012.**

## Abstract

Bacteria plays a critical role in the geochemical cycling of manganese in aquatic environments. They are readily able to transform manganese through oxidative and reductive processes. In natural environments, it is well known that some bacteria are able to oxidise Mn(II) to Mn(IV) under aerobic conditions, while others reduce Mn(IV) to Mn(II) under anaerobic conditions. In the current project, manganese transforming bacteria were investigated on both a physiological and molecular basis to further understand bacterial transformation.

Paralana hot springs (PHS), an aqueous environment rich in heavy metals, was used as a model environment in the study. The diversity of microorganisms in PHS was initially investigated using both culture dependent and independent techniques. Metagenomic 16S rRNA screening revealed bacteria belonging to 24 different phyla, 11 of which have been previously determined to contain manganese oxidisers. Mesophilic and thermophilic bacteria were detected and isolated, with many able to oxidise and/or reduce manganese as well as other metals (including iron, arsenic, cobalt, manganese, molybdenum, selenium, uranium and vanadium). Subsequent 16S rRNA analysis of obtained isolates revealed a number of novel bacteria, including the manganese transforming bacteria; *Bacillus* sp. DLH-1207, *Bacillus* sp. PMO and *Paenibacillus* sp. AEM-1106.

The manganese transforming isolates from PHS were investigated further in comparison with several known manganese reducing *Shewanella* species. Characterisation studies revealed that all isolates were nutritionally diverse mesophiles, with optimal growth exhibited at near-neutral/neutral pH and in the presence of 1-2.5% NaCl. All were capable of manganese oxidation under aerobic conditions and were also able to reduce under anaerobic conditions. This was the first time any *Shewanella* species were shown to oxidise manganese. In fact, it has rarely been observed that the same organism is capable of both manganese oxidation and reduction. In addition to oxygen and manganese, respiration was observed using iron, vanadium, uranium, cobalt and nitrate as electron acceptors. Products of manganese oxidation by the bacteria were confirmed as manganese dioxide by FTIR-spectroscopy and had an average oxidation state of 1.93, actually indicating  $MnO_{1.93}$ .

The immobilisation potential of biogenic  $MnO_2$  was assessed against various heavy metals present in industrial contamination. Single metal immobilisation studies determined that biogenic  $MnO_2$  was effective in the removal of copper, chromium, lithium, lead, cobalt, arsenic and nickel when both the  $MnO_2$  was formed prior to the addition of metal and co-precipitated in the presence of metals. In all the dilutions tested (undiluted, 1:10 and 1:100 dilutions), zinc, copper, nickel, cadmium and chromium were removed from simulated waste waters. When multiple metals were added to cultures, there was a higher level of zinc and copper immobilisation, but lower levels with nickel cadmium and chromium immobilisation. The immobilisation potential of biogenic oxides against simulated waste waters from an industrial waste system has not been previously described.

Finally, the genomic and metabolic profile of *Bacillus* sp. PMO was probed for genes associated with metal transformation and metabolism. Subsystem analysis by RAST revealed numerous metabolic subsystems, including those involved in the metabolism of carbohydrates, iron, manganese, sulphate, nitrate and fermentation. It showed that transport and metal uptake occurs through both cytochrome transport systems and siderophores. Manganese oxidation studies detected a multicopper oxidase responsible for Mn(II) oxidation. BLAST analysis of this protein revealed high levels of homology across several other organisms, which indicates that manganese oxidation in *Firmicutes* may occur in a much larger range of organisms than first anticipated.

The current work extends our knowledge of the diversity of microorganisms in a radioactive hot spring, and in particular manganese transforming bacteria. It provides important information regarding the ability of bacteria to oxidise and reduce manganese and the properties of oxides produced. These type of bacteria are likely to have a major role ecologically, and may be useful industrial applications including the potential for bioremediation of toxic metals. Genome studies of *Bacillus* sp. PMO provides a framework for future molecular and physiological studies of this strain.

## Table of Contents

<b>Statement of Originality</b>	<b>iii</b>
<b>Acknowledgements</b>	<b>iv</b>
<b>Publications Arising From This Thesis</b>	<b>v</b>
<b>Abstract</b>	<b>vi</b>
<b>Table of Contents</b>	<b>ix</b>
<b>List of Figures</b>	<b>xvii</b>
<b>List of Tables</b>	<b>xxvii</b>
<b>List of Abbreviations</b>	<b>xxxii</b>

## Chapter 1: Introduction

<b>1.1 General Introduction</b>	<b>2</b>
<b>1.2 Geomicrobiology</b>	<b>4</b>
1.2.1 Aerobic processes	4
1.2.2 Anaerobic processes	6
1.2.3 Extremophiles	9
1.2.4 Metal tolerant bacteria	12
<b>1.3 Microbial Reduction</b>	<b>13</b>
1.3.1 Dissimilatory metal reducing bacteria	13
1.3.2 Mechanisms of microbial reduction	13
1.3.3 Manganese(IV) reduction	17
1.3.4 Microbial reduction of other metals	18
1.3.4.1 <i>Iron(III) reduction</i>	18
1.3.4.2 <i>Vanadium(V) reduction</i>	18
1.3.4.3 <i>Uranium(VI) reduction</i>	19

<b>1.4 Manganese Oxidation</b>	<b>20</b>
1.4.1 Manganese oxidisers	20
1.4.2 Mechanisms of manganese oxidation	21
1.4.2.1 Direct oxidation	22
1.4.2.2 Indirect oxidation	23
1.4.3 Manganese oxidising bacteria	23
1.4.4 Iron oxidising bacteria	25
<b>1.5 Manganese</b>	<b>27</b>
1.5.1 The element	27
1.5.2 Manganese minerals in nature	27
1.5.3 Manganese cycling in nature	29
1.5.4 Industrial significance	30
<b>1.6 Project Aims and Overview</b>	<b>31</b>

## **Chapter 2: Materials and Methods**

<b>2.1 Research Plan</b>	<b>34</b>
<b>2.2 Chemicals, Buffers and Media</b>	<b>36</b>
2.2.1 Chemicals and reagents	36
2.2.2 Buffers	36
2.2.3 Media	36
2.2.3.1 Preparation and anaerobic techniques	36
2.2.3.2 Great Artesian Basin (GAB) medium	37
2.2.3.3 Peptone Yeast Extract (PYE) medium	38
2.2.3.4 Patel Lab (PL) media	39
2.2.3.5 Vitamins and trace elements	40
2.2.3.6 Preparation of stock solutions	41

<b>2.3 Sample Collection and Source of Cultures</b>	<b>42</b>
2.3.1 Paralana hot springs	42
2.3.2 Water content and pH of samples	45
2.3.3 <i>Shewanella</i> species	45
<b>2.4 Enrichment and Isolation</b>	<b>46</b>
2.4.1 Aerobic enrichments	46
2.4.2 Anaerobic enrichments	46
2.4.3 Purification of aerobes	46
2.4.4 Purification of anaerobes	46
2.4.5 Culture purity and storage	46
<b>2.5 Growth Characteristics</b>	<b>47</b>
2.5.1 Temperature optimisation	47
2.5.2 pH optimisation	47
2.5.3 Salinity tolerance	47
2.5.4 Microscopy and gram staining	48
2.5.5 Antibiotic sensitivity	48
2.5.6 Chlorophyll detection	48
2.5.7 Determination of cell density by turbidity	49
2.5.8 Determination of cell numbers by Most Probable Number (MPN) technique	49
<b>2.6 Growth Characteristics</b>	<b>50</b>
2.6.1 Time course of manganese transformations	50
2.6.2 Effect of Mn(II) concentration on oxidation	51
2.6.3 Effect of Mn(IV) concentration on reduction	51

<b>2.7 Immobilisation of Metals by Biogenic Oxides</b>	<b>52</b>
2.7.1 Individual metals	52
2.7.2 Simulated waste waters	53
<b>2.8 Metal Determination</b>	<b>54</b>
2.8.1 Manganese assay	54
2.8.2 Iron assay	54
2.8.3 Cobalt assay	54
2.8.4 Vanadium assay	54
2.8.5 Uranium assay	55
2.8.6 Atomic absorption spectroscopy (AAS)	55
2.8.7 Inductively coupled plasma optical emission spectroscopy (ICP-OES)	55
<b>2.9 Metal Determination</b>	<b>56</b>
2.9.1 Sample preparation	56
2.9.2 Chemical synthesis of amorphous MnO <sub>2</sub>	56
2.9.3 Average oxidation states	56
2.9.4 Fourier transform infra-red spectroscopy (FTIR-Spec)	57
2.9.5 Scanning electron microscopy (SEM)	57
<b>2.10 Molecular Techniques</b>	<b>58</b>
2.10.1 Bacterial DNA extraction and purification	58
2.10.2 Agarose gel electrophoresis	59
2.10.3 PCR amplification of 16S rRNA genes	59
2.10.4 Oligonucleotides used in PCR and sequencing	60
2.10.5 Purification of PCR products	61
2.10.6 Automated dye terminator cycle sequencing	61
2.10.7 Community DNA extraction and purification	62

<b>2.11 Molecular Analysis</b>	<b>63</b>
2.11.1 Bacterial DNA extraction and purification	63
2.11.2 Metagenomic analysis	63
2.11.3 Ion Torrent PGM whole genome sequencing	64
2.11.4 Whole genome sequence assembly and alignment	64

### **Chapter 3: Culture Dependent and Independent Analysis of Paralana Hot Springs**

<b>3.1 Introduction</b>	<b>67</b>
3.1.1 Paralana hot springs (PHS)	67
3.1.2 Great Artesian Basin (GAB)	69
3.1.3 Microbial detection	71
<b>3.2 Chemical Analysis of PHS Waters</b>	<b>72</b>
<b>3.3 Aerobic Screening</b>	<b>73</b>
3.3.1 Thermophilic aerobic enrichments	73
3.3.2 Aerobic cell content in PHS sediments	74
3.3.3 16S rRNA sequencing and phylogenetic analysis of aerobes	74
<b>3.4 Anaerobic Screening</b>	<b>77</b>
3.4.1 Thermophilic anaerobic enrichments	77
3.4.2 Anaerobic cell content in Paralana spring sediments	78
3.4.3 16S rRNA sequencing and phylogenetic analysis of anaerobes	79
<b>3.5 Manganese Oxidising Bacteria</b>	<b>81</b>
3.5.1 Thermophilic anaerobic enrichments	81
3.5.2 16S rRNA sequencing and phylogenetic analysis of manganese oxidisers	81

<b>3.6 Culture Independent Diversity Profile</b>	<b>85</b>
3.6.1 16S rRNA gene amplicon analysis	85
3.6.2 Phylum Distribution	86
3.6.3 Detection of chlorophylls and bacteriochlorophylls	89
<b>3.7 Discussion</b>	<b>92</b>

## Chapter 4: Manganese Transformation Characteristics of Paralana Isolates and *Shewanella* species

<b>4.1 Introduction</b>	<b>101</b>
<b>4.2 Visual Inference of Bacterial MnO<sub>2</sub> Production</b>	<b>102</b>
<b>4.3 Optimisation Studies</b>	<b>103</b>
4.3.1 Temperature optimum	103
4.3.2 pH optimum	103
4.3.3 Salinity optimum	103
4.3.4 Antibiotic susceptibility	107
4.3.5 Electron donor utilisation	108
4.3.6 Electron acceptor utilisation	109
<b>4.4 Manganese Transformation Characteristics</b>	<b>110</b>
4.4.1 Manganese reduction	110
4.4.2 Manganese oxidation	113
<b>4.5 Manganese Oxide Characterisation</b>	<b>119</b>
4.5.1 Average oxidation states of oxides	119
4.5.2 Scanning electron microscopy (SEM) of oxides	120
4.5.3 FTIR analysis of oxides	120
<b>4.6 Discussion</b>	<b>129</b>

## Chapter 5: Immobilisation of Toxic Metals by Biogenic MnO<sub>2</sub>

<b>5.1 Introduction</b>	<b>137</b>
5.1.1 Metal immobilization by biogenic MnO <sub>2</sub>	137
5.1.2 Bioremediation	139
<b>5.2 Single Metal Immobilisation by Manganese Oxides</b>	<b>140</b>
<b>5.3 Bioremediation of Waste Waters by Biogenic Oxides</b>	<b>145</b>
<b>5.4 Discussion</b>	<b>150</b>

## Chapter 6: Genomic Analysis of *Bacillus* sp. PMO

<b>6.1 Introduction</b>	<b>153</b>
6.1.1 Whole genome sequencing	154
6.1.2 Genes associated with manganese oxide reduction	155
6.1.3 Genes associated with manganese oxidation	157
<b>6.2 Genomic Analysis of <i>Bacillus</i> sp. PMO</b>	<b>159</b>
<b>6.3 Genes Associated with Carbohydrate Metabolism</b>	<b>161</b>
6.3.1 Overview	161
<b>6.4 Genes Associated with Iron Acquisition and Electron Transfer</b>	<b>162</b>
6.4.1 Overview	162
6.4.2 Siderophore genes	164
<b>6.5 Genes Associated with the Transport of Manganese</b>	<b>165</b>
6.5.1 Overview	165
6.5.2 Siderophore genes	165

<b>6.6 Genes Associated With Manganese Oxidation</b>	<b>166</b>
6.6.1 Identification of associated manganese oxidation genes	166
6.6.2 Multicopper oxidase gene analysis	166
6.6.3 Predicted role of MCO in Mn(II) oxidation	168
6.6.4 Significance of the MCO enzyme	168
<b>6.7 Discussion</b>	<b>169</b>

## **Chapter 7: Thesis Summary and Future Direction**

<b>7.1 Thesis Summary</b>	<b>172</b>
<b>7.2 Genomic Analysis of <i>Bacillus</i> sp. PMO</b>	<b>176</b>

## **References**

<b>8.1 Reference List</b>	<b>180</b>
---------------------------	------------

## **Appendices**

<b>Appendix 1 – Most Probable Number (MPN) Table</b>	<b>207</b>
<b>Appendix 2 – Calculation of Average Oxidation States (O/Mn ratio)</b>	<b>208</b>

## List of Figures

### Chapter 1: Introduction

- Figure 1.1:** Phylogenetic tree of life based on genetic variability between organisms **2**  
belonging to the domains Bacteria, Archaea and Eukaryota. The root connecting all  
branches shows the earliest common ancestor and is theorised to have occurred  
approximately 3.6 billion years ago (Orchid Bioinformatics, 2013).
- Figure 1.2:** Chemical equation of glucose in cellular respiration. The breakdown of **5**  
glucose in the presence of oxygen, ADP and free phosphate ions results in the  
generation of carbon dioxide, water and 38 molecules of ATP (Berg *et al.*, 2002).
- Figure 1.3:** Oxidation of glyceraldehyde-3-phosphate to 1,3 bisphosphoglycerate. **7**  
Electrons are removed from the carbon (red) and used in the reduction of  $\text{NAD}^+$ . An  
inorganic phosphate replaces the removed carbon (Paustian, 2000).
- Figure 1.4:** Reduction of acetaldehyde to ethanol through the oxidation of NADH **7**  
back to  $\text{NAD}^+$  (Paustian, 2000).
- Figure 1.5:** Oxidation-reduction potentials for various acceptors used in bacterial **9**  
respiration at pH 7 and 25°C (Modified from Weidemeier *et al.*, 1999).
- Figure 1.6:** Different mechanisms used by bacteria in metal reduction. **14**
- Figure 1.7:** Representative neighbour joining, unrooted phylogram of Mn(II) **24**  
oxidising bacteria (Tebo *et al.*, 2005).

**Figure 1.8:** Maximum-likelihood 16S rRNA dendrogram of known iron oxidising Proteobacteria. Acidophilic (red), nitrate-dependent (black), phototrophic (blue) and neutrophilic aerobic (green) iron oxidisers are shown. GenBank accession numbers are given in the parenthesis. Scale bar indicates 5 nucleotide changes per 100 nucleotides. Taken from Hedrich *et al.*, 2011. **26**

**Figure 1.9:** The major features of manganese oxidation in nature. Adapted from Nealson, 2006. **29**

**Figure 1.10:** Manganese cycling in terrestrial and marine environmental systems. Oxidation and reduction is largely driven by microbial transformation but the process is also dependent on surrounding environmental conditions. Adapted from Marshall *et al.*, 1979. **30**

## Chapter 2: Materials and Methods

**Figure 2.1:** Outline of research plan used to address aims to better understand the mechanisms and environments of manganese transforming. **35**

**Figure 2.2:** The geographical location of Paralana hot springs (30°17'49"S, 139°44'15"E) within Australia (Google Maps, 2013). **42**

**Figure 2.3:** Images of Paralana hot springs. **43**

**Figure 2.4:** Overhead representative map of PHS with significant geographical features. **44**

**Chapter 3: Culture Dependent and Independent Analysis of Paralana Hot Springs**

<b>Figure 3.1:</b> Evidence of microbial mats at Paralana hot springs.	<b>68</b>
<b>Figure 3.2:</b> The Great Artesian Basin of Eastern and Southern Australia and its subsurface geographical features (Bekesi <i>et al.</i> , 2013).	<b>70</b>
<b>Figure 3.3:</b> Cross-section of GAB showing various attributes of the basin (Bekesi <i>et al.</i> , 2013).	<b>70</b>
<b>Figure 3.4:</b> A dendrogram depicting the phylogenetic position of <i>Bacillus</i> sp. PMO and its closest relatives. GenBank accession numbers are given in the parenthesis. Scale bar indicates 2 nucleotide changes per 100 nucleotides.	<b>82</b>
<b>Figure 3.5:</b> A dendrogram depicting the phylogenetic position of <i>Bacillus</i> sp. DLH-1207 and its closest relatives. GenBank accession numbers are given in the parenthesis. Scale bar indicates 3 nucleotide changes per 100 nucleotides.	<b>83</b>
<b>Figure 3.6:</b> A dendrogram depicting the phylogenetic position of <i>Paenibacillus</i> sp. AEM-1106 and its closest relatives. GenBank accession numbers are given in the parenthesis. Scale bar indicates 2 nucleotide changes per 100 nucleotides.	<b>84</b>
<b>Figure 3.7:</b> FastQC quality score distribution across PHS diversity profile sequence data.	<b>85</b>
<b>Figure 3.8:</b> FastQC quality score of individual position reads of PHS diversity profile sequence data.	<b>86</b>
<b>Figure 3.9:</b> KRONA diagram depicting relative distributions (phylum) following 454 sequencing of PHS diversity profile sequence data.	<b>88</b>

**Figure 3.10:** Chlorophyll detection by scanning UV-Vis spectroscopy (350nm-700nm). Primary absorbance peaks are presented. **90**

**Figure 3.11:** Bacteriochlorophyll detection by scanning UV-Vis spectroscopy (700nm-1050nm). Primary absorbance peaks are presented. **90**

**Figure 3.12:** Cross-section of Paralana hot springs and its surrounding aquifers. The close proximity of the GAB and the springs suggests that the basin may have attributed to the waters of PHS. (Brugger *et al.*, 2005) **97**

#### **Chapter 4: Manganese Transformation Characteristics of Paralana Isolates and *Shewanella* species**

**Figure 4.1:** Bacterial manganese oxidation [A], growth without oxidation [B] and the control [C]. **102**

**Figure 4.2:** Growth curves of *Shewanella* sp. and Paralana isolates. Grown aerobically on PYE media, 0.2% yeast extract, pH 7. **104**

**Figure 4.3:** pH curves of *Shewanella* sp. and Paralana isolates. Grown aerobically on PYE media, 0.2% yeast extract, under optimal temperature. **105**

**Figure 4.4:** Salinity curves of *Shewanella* sp. and Paralana isolates. Grown aerobically on PYE media, 0.2% yeast extract, under optimal temperature and pH. **106**

**Figure 4.5:** Manganese reduction curves of *Shewanella* sp. and PHS isolates. Grown aerobically on PYE media, 0.2% yeast extract, under optimal temperature and pH. **111**

**Figure 4.6:** Manganese reduction time curves of *Shewanella* sp. and PHS isolates. **112**

Grown aerobically on PYE media, 0.2% yeast extract, 3mM manganese dioxide under optimal temperature and pH.

**Figure 4.7:** Manganese oxidation curves of *Shewanella* sp. and PHS isolates. Grown **114**

aerobically on PYE media, 0.2% yeast extract, under optimal temperature and pH.

**Figure 4.8a:** Manganese transformation and relative cellular growth of *Shewanella* **115**

*denitrificans* OS517. Grown aerobically on PYE media, 0.02% yeast extract, 3mM Mn(IV), under optimal temperature and pH. \*Isolates were deoxygenated with N<sub>2</sub> gas and re-enriched with 0.2% yeast extract.

**Figure 4.8b:** Manganese transformation and relative cellular growth of *Shewanella* **115**

*oneidensis* MR-1. Grown aerobically on PYE media, 0.02% yeast extract, 3mM Mn(IV), under optimal temperature and pH. \*Isolates were deoxygenated with N<sub>2</sub> gas and re-enriched with 0.2% yeast extract.

**Figure 4.8c:** Manganese transformation and relative cellular growth of *Shewanella* **116**

*putrefaciens* CN-32. Grown aerobically on PYE media, 0.02% yeast extract, 3mM Mn(IV), under optimal temperature and pH. \*Isolates were deoxygenated with N<sub>2</sub> gas and re-enriched with 0.2% yeast extract.

**Figure 4.8d:** Manganese transformation and relative cellular growth of *Shewanella* **116**

*loihica* PV4. Grown aerobically on PYE media, 0.02% yeast extract, 3mM Mn(IV), under optimal temperature and pH. \*Isolates were deoxygenated with N<sub>2</sub> gas and re-enriched with 0.2% yeast extract.

- Figure 4.8e:** Manganese transformation and relative cellular growth of *Shewanella putrefaciens* 200. Grown aerobically on PYE media, 0.02% yeast extract, 3mM Mn(IV), under optimal temperature and pH. \**Isolates were deoxygenated with N<sub>2</sub> gas and re-enriched with 0.2% yeast extract.* 117
- Figure 4.8f:** Manganese transformation and relative cellular growth of *Bacillus sp.* PMO. Grown aerobically on PYE media, 0.02% yeast extract, 3mM Mn(IV), under optimal temperature and pH. \**Isolates were deoxygenated with N<sub>2</sub> gas and re-enriched with 0.2% yeast extract.* 117
- Figure 4.8g:** Manganese transformation and relative cellular growth of *Bacillus sp.* DLH-1207. Grown aerobically on PYE media, 0.02% yeast extract, 3mM Mn(IV), under optimal temperature and pH.. \**Isolates were deoxygenated with N<sub>2</sub> gas and re-enriched with 0.2% yeast extract.* 118
- Figure 4.8h:** Manganese transformation and relative cellular growth of *Paenibacillus sp.* AEM-1106. Grown aerobically on PYE media, 0.02% yeast extract, 3mM Mn(IV), under optimal temperature and pH. \**Isolates were deoxygenated with N<sub>2</sub> gas and re-enriched with 0.2% yeast extract.* 118
- Figure 4.9a:** Scanning electron microscopy of analytical grade manganese dioxide. *Bar = 10 $\mu$ m (1,000x magnification).* 121
- Figure 4.9b:** Scanning electron microscopy of analytical grade manganese dioxide. *Bar = 5 $\mu$ m (5,000x magnification).* 121
- Figure 4.10a:** Scanning electron microscopy of chemically synthesised manganese dioxide. *Bar = 10 $\mu$ m (1,000x magnification).* 122

- Figure 4.10b:** Scanning electron microscopy of chemically synthesised manganese dioxide. *Bar = 5 $\mu$ m (5,000x magnification).* **122**
- Figure 4.11a:** Scanning electron microscopy of manganese dioxide transformed by *Shewanella putrefaciens* CN-32. *Bar = 10 $\mu$ m (1,000x magnification).* **123**
- Figure 4.11b:** Scanning electron microscopy of *Shewanella putrefaciens* CN-32 and the produced manganese dioxide. *Bar = 5 $\mu$ m (5,000x magnification).* **123**
- Figure 4.12a:** Scanning electron microscopy of manganese dioxide transformed by *Shewanella loihica* PV-4. *Bar = 10 $\mu$ m (1,000x magnification).* **124**
- Figure 4.12b:** Scanning electron microscopy of *Shewanella loihica* PV-4 and the produced manganese dioxide. *Bar = 5 $\mu$ m (5,000x magnification).* **124**
- Figure 4.13a:** Scanning electron microscopy of manganese dioxide transformed by *Bacillus* sp. PMO. *Bar = 10 $\mu$ m (1,000x magnification).* **125**
- Figure 4.13b:** Scanning electron microscopy of *Bacillus* sp. PMO and the produced manganese dioxide. *Bar = 5 $\mu$ m (5,000x magnification).* **125**
- Figure 4.14:** FTIR-Spectroscopy of organically produced manganese samples of analytical grade and chemically produced MnO<sub>2</sub>. Major absorbance peaks are displayed. **126**
- Figure 4.15:** FTIR-Spectroscopy of organically produced manganese samples of *Shewanella putrefaciens* CN-32, *Shewanella loihica* PV-4 and *Bacillus* sp. PMO. Major absorbance peaks of *Bacillus* sp. PMO are displayed. **127**

**Figure 4.16:** FTIR-Spectroscopy overlay of the bacterially produced, analytical grade and chemically produced manganese samples. **128**

## Chapter 5: Immobilisation of Toxic Metals by Biogenic MnO<sub>2</sub>

**Figure 5.1:** Structural model of biogenic manganese oxides and subsequent adsorption of metals (as ions) on hexagonal birnessite. Mn(IV) vacancies are compensated by charge-balancing cations (excluded from diagram). Adapted from Miyata *et al.*, 2007. **138**

**Figure 5.2:** Adsorbed Pb(II) on hexagonal birnessite, depicting [A] double edged sharing and [B] triple corner sharing to lead. Adapted from Spiro *et al.*, 2010. **138**

**Figure 5.3:** Adsorption of various metals by biogenic manganese oxides (oxidised by *Shewanella putrefaciens* CN-32) in conjunction with bacterial growth and after growth/oxidation. **142**

**Figure 5.4:** Adsorption of various metals by biogenic manganese oxides (oxidised by *Shewanella loihica* PV-4) in conjunction with bacterial growth and after growth/oxidation. **143**

**Figure 5.5:** Adsorption of various metals by biogenic manganese oxides (oxidised by *Bacillus* sp. PMO) in conjunction with bacterial growth and after growth/oxidation. **144**

**Figure 5.6:** Metal immobilisation of simulated waste waters by manganese oxides produced by *Shewanella putrefaciens* CN-32. **147**

**Figure 5.7:** Metal immobilisation of simulated waste waters by manganese oxides produced by *Shewanella loihica* PV-4. **148**

**Figure 5.8:** Metal immobilisation of simulated waste waters by manganese oxides produced by *Bacillus* sp. PMO. **149**

## Chapter 6: Genomic Analysis of *Bacillus* sp. PMO

**Figure 6.1:** Electron transfer pathways for *Shewanella* spp. [A] and *Geobacter* spp. [B] during reduction of solid metal oxides. In system [A], proteins form complexes with the metal oxide and subsequent reduction transpires, while in system [B] electron transfer is conferred through type IV pili. Important proteins are visualised (red) and their encoding genes are detailed in Table 6.1. Figure adapted from Shi *et al.*, 2007. **155**

**Figure 6.2:** Genes associated with subsystems and their distributions in different subsystems as identified by RAST. Subsystems in bold are discussed in more detail in this chapter. **160**

**Figure 6.3:** Genes associated with carbohydrate metabolism, further classified into subcategories. **161**

**Figure 6.4:** Genes associated with iron acquisition and metabolism, further classified into subcategories; iron acquisition in *Streptococcus* (13 genes; 42%), heme, hemin uptake and utilization systems in Gram Positives (4 genes; 13%), ABC transporter [iron.B12.siderophore.hemin] (8 genes; 26%), hemin transport system (4 genes; 13%) and iron siderophore sensor and receptor system (2 genes; 6%). **162**

**Figure 6.5:** *HasA* hemophore binding to extracellular iron. The hemophore delivers the bound iron to the *HasR* receptor and transported into the cell by the *TonB* system. Diagram adapted from Wandersman and Stojiljkovic, 2000. **164**

**Figure 6.6:** Multiple alignment of *MCO* amino acid sequence (*Bacillus* sp. PMO) against other *MCO* proteins of significant similarity by use of CLUSTAL. Shaded amino acids represent identical residues between all *MCO* proteins. GenBank accession numbers: *Bacillus anthracis* CDC 684 (**WP\_009880000.1**), *Bacillus cereus* (**WP\_002052239.1**), *Bacillus thuringiensis* (**WP\_000833194.1**), *Staphylococcus cohnii* (**WP\_025687215.1**), *Bacillus weihenstephanensis* (**WP\_012260745.1**), *Bacillus mycoides* (**WP\_003188542.1**). **167**

**Figure 6.7:** The predicted role of *MCO* in the two-step oxidation of Mn(II) to Mn(IV). **168**

**Figure 6.8:** Multiple alignment of *MCO* amino acid sequence (*Bacillus* sp. PMO) against the *MCO* enzyme of *Bacillus* sp. SG-1 (**WP\_006837219.1**) by use of CLUSTAL. Sequence alignment revealed similarity at four sites on the *Bacillus* sp. SG-1 *MCO* protein; positions **51-94** (14/44 matches, 32% similarity), **253-316** (21/73 matches, 29% similarity), **690-724** (15/35 matches, 43% similarity) and **1093-1139** (19/48 matches; 40% similarity). **170**

## List of Tables

### Chapter 1: Introduction

**Table 1.1:** Various sub-classes of extremophiles. The term extremophile, while often applying to prokaryotic organisms, can be extended to eukaryotes in select examples. **11**

Table adapted from Rothschild and Mancinelli, 2001.

**Table 1.2:** The appearance, crystalline structure and chemical formulae of common manganese minerals **26**

### Chapter 2: Materials and Methods

**Table 2.1:** List of buffers used in various experimentation. All buffers were prepared under sterile conditions and buffers containing sensitive compounds stored at -20°C until used. **36**

**Table 2.2:** Chemical composition of GAB media (per litre of distilled H<sub>2</sub>O). Following preparation the media was pH adjusted to required level and heat sterilised. **37**

**Table 2.3:** Chemical composition of PYE media (per litre of distilled H<sub>2</sub>O). Following preparation the media was pH adjusted to required level and heat sterilised. **38**

**Table 2.4:** Chemical composition of PL media (per litre of distilled H<sub>2</sub>O). Following preparation the media was pH adjusted to required level and heat sterilised. **39**

**Table 2.5:** Chemical composition of Zeikus trace element solution (per litre of distilled H<sub>2</sub>O). Following preparation media was heat sterilised and stored at 4°C for future use. **40**

**Table 2.6:** Chemical composition of Wolin's solution (per litre of distilled H<sub>2</sub>O). Following preparation the solution was filter sterilised into a 15mL falcon tube and stored at 4°C for future use. **41**

**Table 2.7:** Yearly average level of heavy metal pollutants in the Tajola Industrial Estate, Mumbai, India in 2000 (Lokhande *et al.*, 2011). Metals used to synthesise wastewaters were as followed: chromium chloride; cadmium chloride; nickel chloride; zinc chloride and copper chloride. **53**

**Table 2.8:** Chemical composition of each PCR reaction (for a total of 49µL). Preparation of master mix was performed under sterile conditions. **59**

**Table 2.9:** Cycling criteria for amplification of 16S rRNA of bacterial samples. **60**

**Table 2.10:** Comprehensive list of primers used for PCR amplification and sequencing as well as the sequences and location on the *E. coli* 16S rRNA gene (Brosius *et al.*, 1981; Frank *et al.*, 2008). **60**

**Table 2.11:** List of reagents and quantities used for big-dye sequencing. Quantity of sample used varied depending on DNA concentration of purified PCR product. Unless specified otherwise, primers used for sequencing were Fd1 and Rd1 (3.2µM). **61**

**Chapter 3: Culture Dependent and Independent Analysis of Paralana Hot Springs**

<b>Table 3.1:</b> Trace element concentrations of macronutrients and heavy metals in pool samples P1W, P1S, P2W and P2S.	<b>72</b>
<b>Table 3.2:</b> Water pH of pool samples P1W, P1S, P2W and P2S	<b>72</b>
<b>Table 3.3:</b> Aerobic enrichments of PHS environmental samples. Grown on various electron donors in conjunction with PL media (60°C, pH 7.5).	<b>73</b>
<b>Table 3.4:</b> Most probable numbers of aerobes present within each pool sample. Grown on PL medium (60°C, pH 7.5, 0.2% yeast extract).	<b>74</b>
<b>Table 3.5:</b> Aerobic PHS isolates. Grown on various electron donors, temperatures and pH in conjunction with PL media.	<b>75</b>
<b>Table 3.6:</b> Presence of growth/reduction in conjunction with various electron acceptors. Grown anaerobically on PL medium (60°C, pH 7.5, 0.2% yeast extract).	<b>77</b>
<b>Table 3.7:</b> Most probable numbers of anaerobes present within each pool sample. Grown anaerobically on PL medium with various electron acceptors (60°C, pH 7.5, 0.2% yeast extract).	<b>78</b>
<b>Table 3.8:</b> Anaerobes present in Paralana pool samples. Samples grown anaerobically with PL medium (60°C, pH 7.5, 0.2% yeast extract).	<b>80</b>
<b>Table 3.9:</b> Presence of manganese oxidation in conjunction with various electron donors. Grown on PL medium (37°C, pH 7.5, with 2mM Mn <sup>2+</sup> ).	<b>81</b>

**Table 3.10:** PHS diversity profile sequence distribution organized by phylum. **87**  
 Erroneous sequences removed and relative percentages adjusted.

**Table 3.11:** Detected sequences within the phylum Firmicutes. **89**

**Table 3.12:** Major chlorophylls and bacteriochlorophylls and their occurrences in **91**  
 PHS waters.

### Chapter 4: Manganese Transformation Characteristics of Paralana Isolates and *Shewanella* species

**Table 4.1:** Antibiotic susceptibility across the *Shewanella* spp. (CN-32, PV-4, 200, **107**  
 OS517 and MR-1) and PHS isolates (PMO, DLH-1207 and AEM-1106). Samples  
 were tested on PYE media agar plates and grown under optimal conditions. +  
*indicates the isolate was resistant against a tested antibiotic.*

**Table 4.2:** Electron donor utilisation across the *Shewanella* spp. (CN-32, PV-4, 200, **108**  
 OS517 and MR-1) and PHS isolates (PMO, DLH-1207 and AEM-1106). Samples  
 were tested aerobically on PYE media and grown under optimal conditions.

**Table 4.3:** Electron acceptor utilisation across the *Shewanella* spp. (CN-32, PV-4, **109**  
 200, OS517 and MR-1) and PHS isolates (PMO, DLH-1207 and AEM-1106).  
 Samples were tested on PYE media and grown under optimal conditions, 0.2% yeast  
 extract.

**Table 4.4:** Relative oxidation states and manganese oxide content of chemically **119**  
 synthesised, analytical grade MnO<sub>2</sub> and the produced oxides by *Shewanella*  
*putrefaciens* CN-32, *Shewanella loihica* PV-4 and *Bacillus* sp. PMO

## Chapter 5: Immobilisation of Toxic Metals by Biogenic MnO<sub>2</sub>

**Table 5.1:** Metal immobilisation of individual metals by bacterially produced manganese oxides. Immobilisations at percentages  $\geq 90\%$  are highlighted in bold. **141**

**Table 5.2:** Metal immobilisation of simulated waste waters by bacterially produced manganese oxides. Immobilisations at percentages  $\geq 90\%$  are highlighted in bold. **146**

## Chapter 6: Genomic Analysis of *Bacillus* sp. PMO

**Table 6.1:** Representative genes associated with Mn(IV) oxide reduction. **156**

**Table 6.2:** Representative genes associated with Mn(II) oxidation. **158**

**Table 6.3:** Genes, roles and features associated with iron acquisition and metabolism. **163**

## List of Abbreviations

<b>A</b>	Adenine
<b>AAS</b>	Atomic absorption spectroscopy
<b>ADP</b>	Adenosine diphosphate
<b>AGRF</b>	Australian Genome Research Facility
<b>ATP</b>	Adenosine triphosphate
<b>C</b>	Cytosine
<b>Contig</b>	Contiguous sequence
<b>DES</b>	Double edge sharing
<b>DMRB</b>	Dissimilatory metal reducing bacteria
<b>FTIR</b>	Fourier transform infrared spectroscopy
<b>G</b>	Guanine
<b>GAB</b>	Great Artesian Basin
<b>ICP-OES</b>	Inductively coupled plasma atomic emission spectroscopy
<b>KEGG</b>	Kyoto Encyclopaedia of Genes and Genomes
<b>LCV</b>	Leukocrystal violet
<b>MCO</b>	Multi copper oxidase
<b>MIRA</b>	Mimicking Intelligent Read Assembly
<b>MPN</b>	Most probable number
<b>NADH</b>	Nicotinamide adenine dinucleotide
<b>PCR</b>	Polymerase chain reaction
<b>PHS</b>	Paralana hot springs
<b>PL</b>	Patel lab
<b>PYE</b>	Peptone yeast extract
<b>QIIME</b>	Quantitative Insights Into Microbial Ecology

<b>RAST</b>	Rapid Annotations using Subsystem Technology
<b>RDP</b>	Ribosomal Database Project
<b>roH<sub>2</sub>O</b>	Reverse osmosis water
<b>sdH<sub>2</sub>O</b>	Sterilised water
<b>TCS</b>	Triple corner sharing
<b>T</b>	Thymine
<b>U</b>	Uracil
<b>WGS</b>	Whole genome sequencing

# Chapter 1

Introduction

## 1.1 General Introduction

The evolution of carbon-based life on planet Earth saw the divergence of anaerobic, single-celled prokaryotes into the three domains of life; Bacteria, Archaea and Eukaryota (Figure 1.1). The specifics surrounding the geological evolution of Earth are greatly debated within the scientific community; however it is widely accepted that the earth formed approximately 4.54 billion years ago and began as an anoxic ball of magma, whose mass was derived from meteorite strikes over hundreds of millions of years. This, in addition to the radioactive decay of various unstable elements created the Earth's molten crust and provided the base of what would become modern Earth (Valley, 2005). Eventually, the earth cooled and during these times simple organic molecules formed that were essential to the generation of life. The beginning of life can be traced back to approximately 3.6 billion years ago when the first prokaryotic organisms are theorised to have appeared. These organisms were hyperthermophilic anaerobes that utilised iron and other metals in respiration and hence are the earliest known evolutionary ancestor shared among all forms of life today (Romano & Conway, 1996).

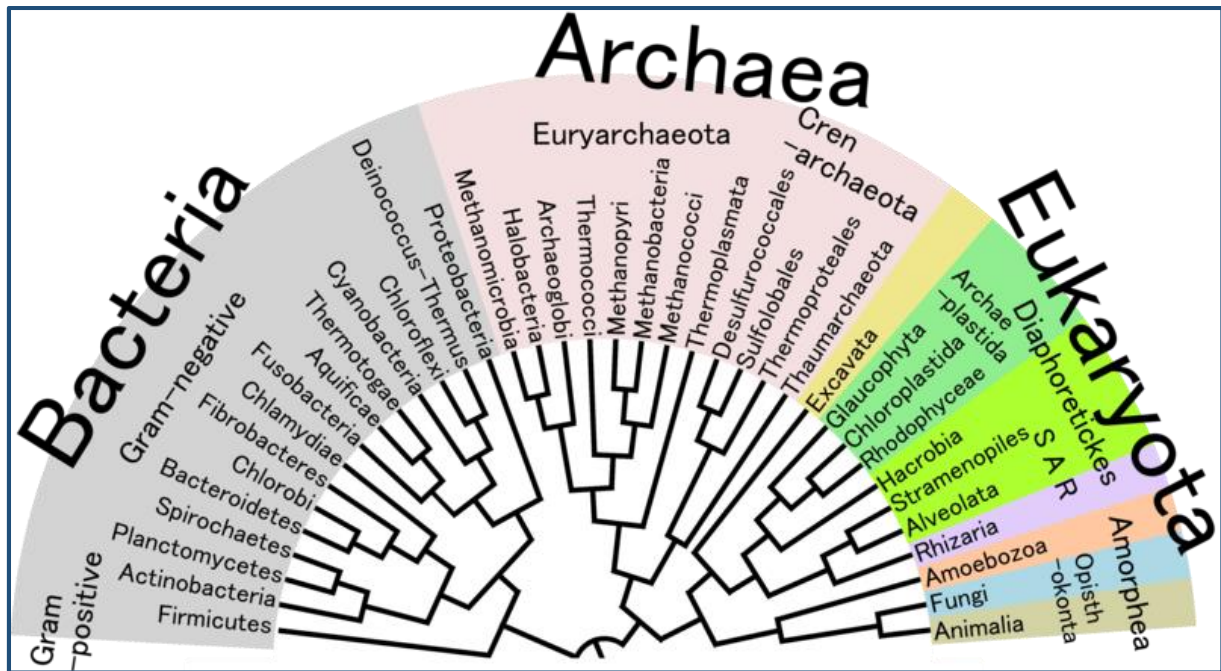


**Figure 1.1:** Phylogenetic tree of life based on genetic variability between organisms belonging to the domains Bacteria, Archaea and Eukaryota. The root connecting all branches shows the earliest common ancestor and is theorised to have occurred approximately 3.6 billion years ago (Orchid Bioinformatics, 2013).

Bacteria and Archaea are unicellular, prokaryotes that are able to exist in a range of environments unsuitable for eukaryotic growth. These organisms have evolved to tolerate and even thrive under a range of extreme temperatures, pH ranges, pressure and salinity, as they possess unique environmental and chemical resistances. However, aside from genetic differences, Bacteria and Archaea have several distinct traits. Archaea are similar in size and shape to bacteria, however can use different carbon sources and have unique metabolic pathways (Deppenmeier *et al.*, 1996). Prokaryotes carry out important processes in the environment such as cycling of carbon, metals and other elements, deposition and solubilisation of mineral structures and the detoxification of environmental contaminants. The interaction between microbes and the geochemistry of the surrounding environment is studied in geomicrobiology. It dictates to a large extent how and what microbes are able to survive in particular environments (such as waters and sediments).

## 1.2 Geomicrobiology

### 1.2.1 Aerobic processes

Aerobic bacteria (aerobes) are organisms that utilise oxygen for cellular respiration. Aerobes are present almost everywhere that oxygen is accessible; existing in waters, soils and many other environments, including human hosts. Typically a few microns in length, aerobes are found in a variety of shapes and often have flagella that assist in cellular movement. Through evolutionary adaptations, aerobes have been found in habitats with extreme pH or temperature, having developed complex adaptation mechanisms suitable for their surroundings. Aerobes generate energy through oxidative phosphorylation; a process where oxygen is coupled with an organic nutrient source to produce adenosine triphosphate (ATP), the main source of energy for cells (Higgins *et al.*, 1986). Aerobes are highly nutritionally diverse and use a multitude of electron donors, including sugars, amino acids, aromatics, hydrocarbons and degraded organic materials. Additionally, some aerobes are also chemolithotrophs; able to use inorganics (such as CO<sub>2</sub>) in energy synthesis. Finally, aerobes play a crucial role in the cycling of various compounds in aquatic environments, with oxidation of inorganics (such as manganese, iron, sulphur and ammonia) occurring largely as a result of microbial activity.

Aerobes, like eukaryotic organisms, utilise oxygen as a terminal electron acceptor. However, due to the absence of mitochondria this process occurs within the cytoplasmic membrane via ATPases. ATPases are membrane-bound ion channels that assist in the production of ATP through the coupling of ion movement with conversion of ATP to ADP, thus producing an energy favourable reaction (Kemp *et al.*, 2001). Generation of ATP in cellular respiration requires a nutrient source in addition to oxygen. This nutrient source is generally in the form of a simple sugar (glucose), however bacteria are able to use various nutrient sources from organic extracts to single amino acids, as well as inorganics (in the case of autotrophic bacteria) (Jurtshuk Jr., 1996). In terms of glucose, breakdown in the presence of oxygen and free phosphate ions produces carbon dioxide, water and ATP. The chemical equation of this process is:



**Figure 1.2:** Chemical equation of glucose in cellular respiration. The breakdown of glucose in the presence of oxygen, ADP and free phosphate ions results in the generation of carbon dioxide, water and 38 molecules of ATP (Berg *et al.*, 2002).

### 1.2.2 Anaerobic processes

Anaerobic bacteria (anaerobes) are organisms that use alternative electron acceptors or fermentation for cellular respiration, as oxygen often is toxic. In addition to aerobic bacteria, several sub-classes of anaerobic bacteria are found in nature. These are categorised as followed: obligate anaerobes (die in the presence of oxygen); facultative anaerobes (can grow with or without oxygen); and aerotolerant anaerobes (do not use oxygen for metabolism but can grow in the presence of oxygen). Depending on the genetic makeup of the organism, these bacteria either produce energy through fermentation or cellular respiration (with the exception of aerotolerant bacteria which are strictly fermentative). Obligate anaerobes are capable of fermentation and cellular respiration depending on nutrient availability. Facultative anaerobes are capable of using oxygen as well as other acceptors. Although, oxygen generates more ATP than anaerobic respiration or fermentation and therefore is preferred by bacteria over the less favourable alternatives. Anaerobes also play a role in the environmental cycling of various inorganics through microbial reduction; with some facultative anaerobes able to both reduce selected compounds (under anoxic conditions) and then re-oxidise that same compound (under oxic conditions). This is most widely researched topic in iron and manganese cycling, however this process is not limited to just these metals.

Fermentation is an energy producing process where organic molecules are used as both electron donors and electron acceptors. Fermentation occurs when oxygen (or other suitable electron acceptors) are absent and is used to generate energy when the electron transport chain is unusable for metabolism (Thauer *et al.*, 1977). In glucose fermentation, the energy produced from the breakdown of glucose to pyruvate allows for phosphorylation of ADP and the subsequent reduction of nicotinamide adenine dinucleotide ( $\text{NAD}^+$ ; Figure 1.3). Pyruvate is then further broken down into acetaldehyde, and  $\text{CO}_2$  is produced as a by-product. Finally, the two produced acetaldehydes are converted to ethanol with  $\text{NADH}$  converted back to  $\text{NAD}^+$  (Figure 1.4; Paustian, 2000).

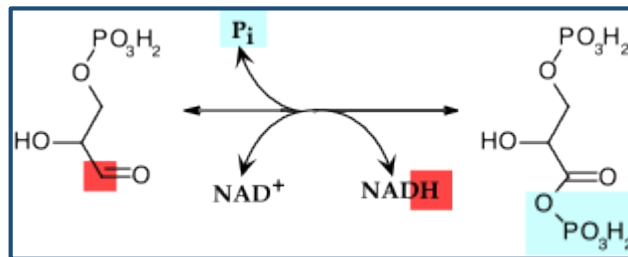


**Figure 1.3:** Oxidation of glyceraldehyde-3-phosphate to 1,3 bisphosphoglycerate. Electrons are removed from the carbon (red) and used in the reduction of  $\text{NAD}^+$ . An inorganic phosphate replaces the removed carbon (Paustian, 2000).

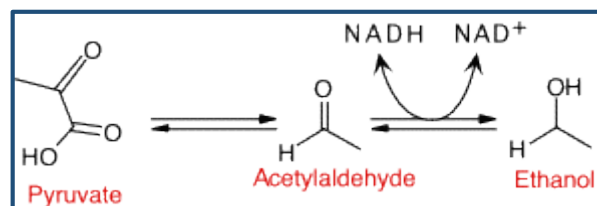


**Figure 1.4:** Reduction of acetaldehyde to ethanol through the oxidation of  $\text{NADH}$  back to  $\text{NAD}^+$  (Paustian, 2000).

While the energy produced is inferior compared to anaerobic respiration (net gain of 2ATP), bacteria have numerous fermentative pathways they can utilise to generate energy in conditions that lack appropriate electron acceptors. Glucose as a source is just one example of microbial fermentation and the pathways and products produced vary depending on the organic utilised. Another example of microbial fermentation is the conversion of lactate to lactic acid, which uses the Embden-Meyerhoff-Parnas (EMP) pathway (Paustian, 2000).

Anaerobes can use alternative electron acceptors (not oxygen) to produce energy via oxidative phosphorylation. Oxygen as the terminal electron acceptor in respiration is favoured over alternatives as it releases more energy during electron transfer (also known as reduction potential). Obligate anaerobes are unable to use oxygen and instead require different acceptors. These are primarily ionic compounds (nitrates, sulphates, etc.) or metal complexes (ferric iron, manganese oxide, etc.) present within an anoxic environment. Many bacteria are capable of reducing multiple compounds and preference for reduction is determined by which is more thermodynamically favourable (Weidemeier *et al.*, 1999). Figure 1.5 highlights typical electron acceptors and the respective redox potentials (millivolts) of each.

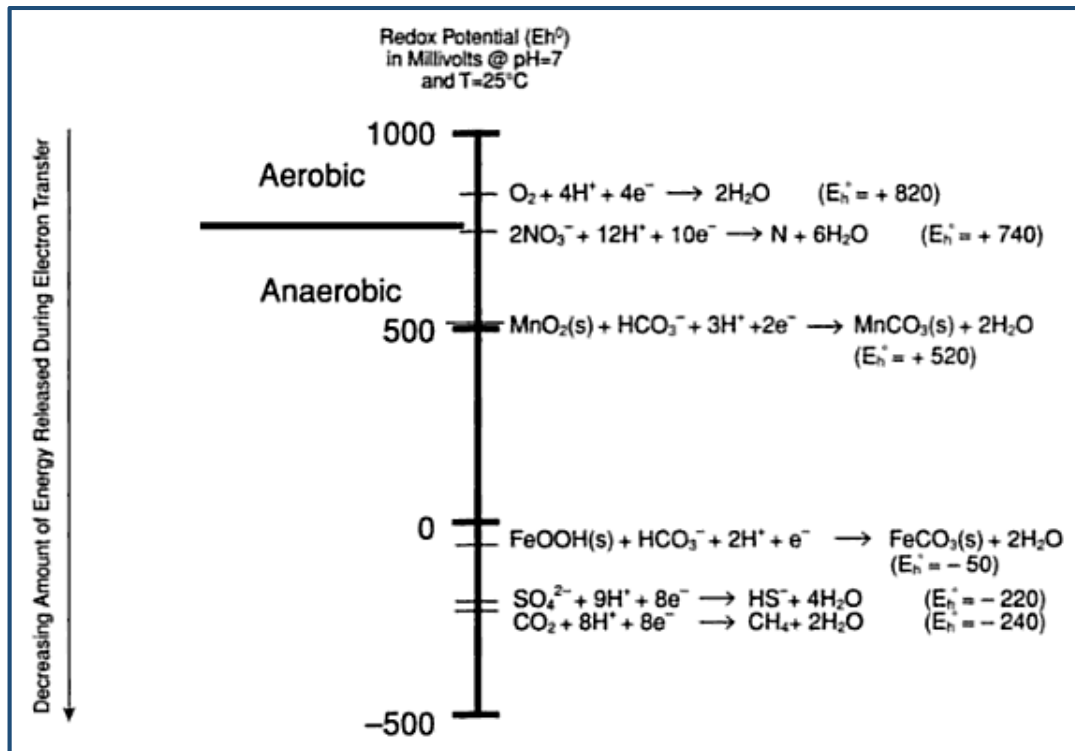


**Figure 1.5:** Oxidation-reduction potentials for various acceptors used in bacterial respiration at pH 7 and 25°C (Modified from Weidemeier *et al.*, 1999).

### 1.2.3 Extremophiles

Extremophiles are bacteria that proliferate under extreme conditions. Extremophiles are found in environments of extreme temperature, pH, salinity and in the presence of inorganics that would inhibit the growth of normal organisms. Through evolutionary adaptations extremophiles developed defence mechanisms to combat the lethal effects of the surrounding environment. Environmental extremes can affect the transportation of nutrients, enzyme activity, translation and cell division, membrane integrity, protein denaturation and folding, etc. but extremophiles have developed means of counteracting this damage (D'Amico *et al.*, 2006). It is important to note however that the term extremophile is not limited to bacteria but can refer to organisms from the domains Bacteria, Archaea and Eukaryota (Stetter, 1999).

Extremophiles fall under several sub-categories classified through the supposed environmental extreme/s they live in. Organisms that grow under extreme temperatures are termed thermophiles (optimal growth at  $\geq 60^{\circ}\text{C}$ ) and psychrophiles (optimal growth at  $\leq 15^{\circ}\text{C}$ ; Li and Lu, 2005). Organisms that grow under extreme acidic or alkaline environments are termed acidophiles (optimal growth at  $\text{pH} \leq 3$ ) and alkaliphiles (optimal growth at  $\text{pH} \geq 9$ ). Halophiles are organisms that can tolerate extreme levels of salt and are often unable to survive in its absence (Burg, 2003). Metalotolerant organisms are those that can not only tolerate, but are still able to thrive in the presence of high concentrations of heavy-metals (Avoscan et al., 2007). Environments that host extremophiles can have uniform conditions (saline lakes, acidic waters) while others can be variable (hot springs with a heat gradient away from a heat source). These along with several other sub-classes are described in Table 1.1.

**Table 1.1:** Various sub-classes of extremophiles. The term extremophile, while often applying to prokaryotic organisms, can be extended to eukaryotes in select examples. Table adapted from Rothschild and Mancinelli, 2001.

Environmental Parameter	Type	Definition	Examples
Temperature	Hyperthermophile	Growth >80°C	<i>Pyrolobus fumarii</i>
	Thermophile	Growth 60-80°C	<i>Synechococcus lividis</i>
	Mesophile	Growth 15-60°C	<i>Homo sapiens</i>
	Psychrophile	Growth <15°C	<i>Psychrobacter</i> spp.
Radiation			<i>Deinococcus radiodurans</i>
Pressure	Barophile	Weight-loving	<i>Shewanella benthica</i>
	Piezophile	Pressure-loving	
Gravity	Hypergravity	>1g	None known
	Hypogravity	<1g	None known
Vacuum		Tolerates space devoid of matter	Tardigrades
Desiccation	Xerophiles	Anhydrobiotic	<i>Artemia salina</i>
Salinity	Halophiles	Salt-loving (≥2M NaCl)	<i>Dunaliella salina</i>
pH	Alkaliphile	pH >9	<i>Natronbacterium</i> spp.
	Acidophile	Low pH-loving	<i>Cyanidium caldarium</i>
Oxygen Tension	Anaerobe	Cannot tolerate O <sub>2</sub>	<i>Methanococcus jannaschii</i>
	Microaerophile	Tolerates some O <sub>2</sub>	<i>Clostridium</i> spp.
	Aerobe	Requires O <sub>2</sub>	<i>Homo sapiens</i>
Chemical Extremes	Gases	Can tolerate/reduce high concentrations of metals	<i>Ferroplasma acidarmanus</i>
	Metals		<i>Ralstonia</i> spp.

#### 1.2.4 Metal tolerant bacteria

Metal resistant bacteria (or metalotolerant bacteria) are specialised bacteria that are capable of both survival and growth in the presence of otherwise toxic concentrations of heavy metals. Bacteria have been discovered in numerous environments containing heavy metals, surviving where other organisms would die through specialised evolutionary adaptations (Duxbury & Bicknell, 1983). These bacteria have developed unique detoxifying mechanisms designed to impede the hazardous effects caused by heavy metal toxication. Metal tolerance has been found as a result of two unique systems; through inhibition by bacterially produced proteins (to form a protein-metal complex) or through the complete blockage of uptake via altered membrane transportation pathways (Hassen *et al.*, 1998). In many instances, bacteria resistant to a specific metal are often also able to use the metal in energy generation. Protein and genomic analysis on metalotolerant bacteria has resulted in the discovery of a variety of metal tolerance mechanisms. Proteins that confer metal resistance are not always metal specific and are often capable of providing resistance against multiple metals with similar characteristics. Genes encoding for metal resistance are typically activated in one of two ways; either by passive expression of the protein or through activation of gene transcription by the toxic metal itself (Bontidean *et al.*, 2000).

## 1.3 Microbial Reduction

### 1.3.1 Dissimilatory metal reducing bacteria

Dissimilatory metal reducing bacteria (DMRB) couple organic electron donors with heavy metals for energy production in cellular respiration. Metal reducers have been discovered capable of oxidising a wide variety of organic acids, alcohols and organics in conjunction with numerous metals. In addition to energy requirements, metal reduction has been linked as a detoxification mechanism to prevent growth inhibition (Lovley, 1991). Metals used by DMRB include: iron(III); vanadium(V); chromium(VI); molybdenum(VI); cobalt(III); manganese(IV); selenium(VI); arsenic(V); technetium(VII); plutonium(IV); uranium(VI); palladium(II); gold(III); silver(I); and mercury(II) (Lovley, 1991; Lovley, 2001; Carpentier *et al.*, 2003). Metal-reducing characteristics in microorganisms have been evident for decades and were first proven with iron and manganese reducing bacteria (Lovley and Phillips, 1986).

### 1.3.2 Mechanisms of microbial reduction

DMRB employ a range of different techniques when coupling metals with cellular respiration. Soluble metals are easily accessed by bacteria and often involve a simple electron exchange; however, solid metals are often more difficult for reducers to utilise in anaerobic respiration. DMRB are able to reduce metals in a variety of ways, including: direct cell contact; secretion of a Chelator; utilisation of an electron shuffle system; and nanowire electron transportation. Descriptions of these mechanisms are seen in Figure 1.6.

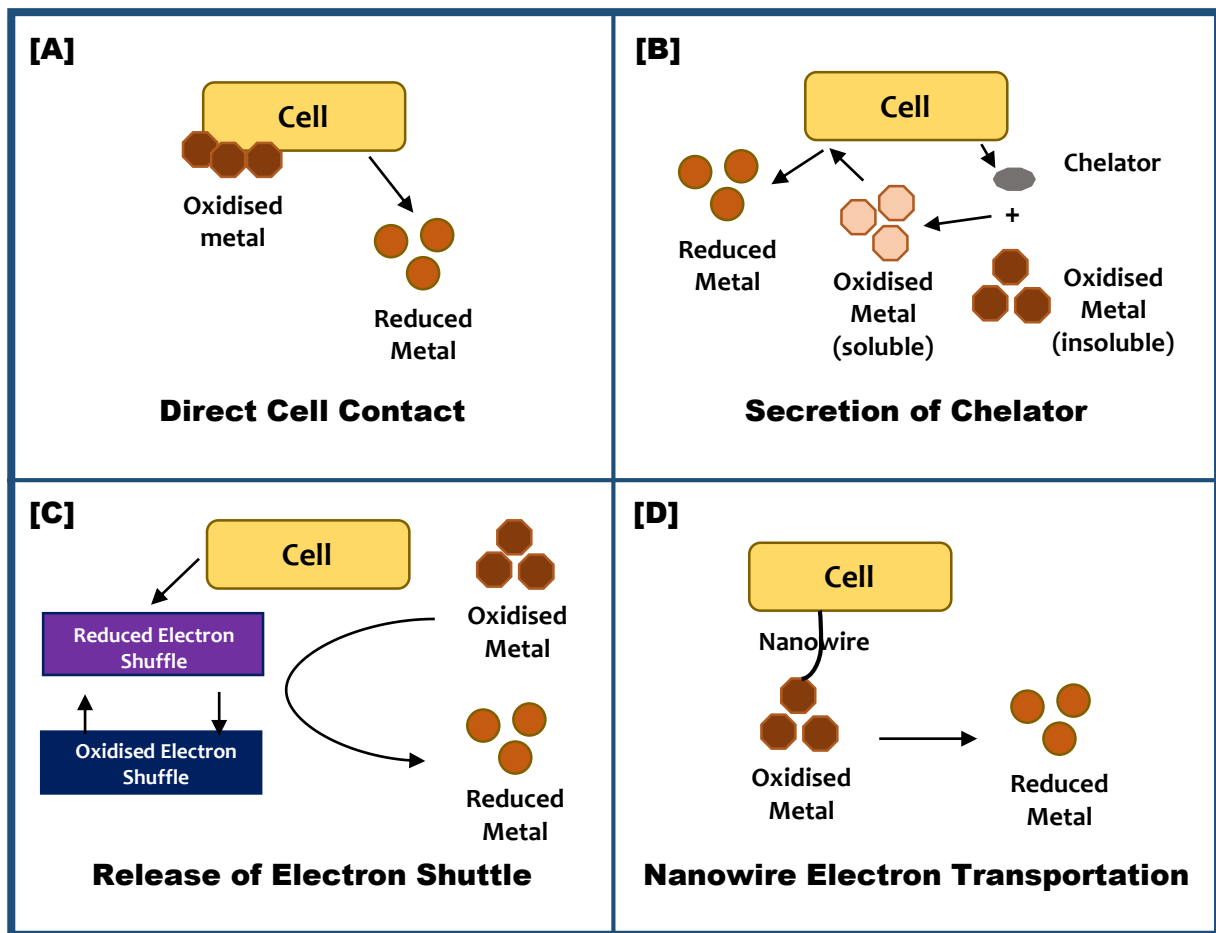


**Figure 1.6:** Different mechanisms used by bacteria in metal reduction.

Bacterial metal reduction through direct cell contact (Figure 1.6A) is achieved through electron transfer between cells and extracellular metal oxides. Electron transfer in this way begins with outer membrane proteins (c-type cytochromes) binding to the metal. Specialised enzymes (reductases) then mediate electron transfer in conjunction with an appropriate electron donor. This is well documented in *Shewanella putrefaciens* MR-1, a known metal reducer. In the case of iron, outer membrane proteins bind oxidised iron which allows the terminal Fe(III) reductase to reduce iron in anaerobic respiration (Belialev *et al.*, 2001). Note that this is one example of one metal reducing system and that bacteria have different systems and also various metals have specific systems for reduction.

Some deep-water bacteria are able to secrete chelating agents that bind to metals, increasing their solubility for microbial reduction (Figure 1.6B). Environmental metal under anoxic conditions is typically scarce and often unsuitable for use in anaerobic respiration. Bacteria (as well as some microalgae) have developed chelating agents they secrete into the environment that bind to these metals; increasing their solubility for cellular utilisation. Little is known about the chelating agents produced by bacteria, however a bacterially secreted iron chelator has been described by the Barbeau group. Iron reducers can produce siderophores, which are the strongest known binding agents of iron. Once bound, the Fe(III)-siderophore complex leads to the formation of lower-affinity Fe(III) ligands and the subsequent reduction of Fe(III) in anaerobic respiration (Barbeau *et al.*, 2001).

When bacteria are unable to reduce metals directly, metal reduction can be achieved through an electron shuttle (Figure 1.7C). In this process, bacteria indirectly transfer electrons to third party substances (organic matter, etc.) which then in turn reduce metal oxides in the environment. The shuttle is then re-oxidised and the process is repeated to reduce the remaining metal oxides (Lovely and Harris, 1999).

Nanowire electron transfer (Figure 1.6D) is the use of bacterial pili to reduce metals for use in anaerobic respiration. Bacteria that lack outer membrane c-type cytochromes are unable to directly reduce metals, so they must rely on other mechanisms to produce energy. Recent research into bacteria lacking these c-type cytochromes resulted in the discovery of organisms capable of nanowire electron transfer. In this process, electrons are transferred through highly conductive pili on the outer cell surfaces to the surface of the metal. Pili as a transport system between cell-cell and cell-environment have been extensively studied, however, the use of nanowire electron transfer for anaerobic respiration is a relatively recent discovery and the extent and range of metals to which these organisms can reduce is not conclusive. It is theorised that the pili are attached to cytochromes that make them electrically conductive (Reguera *et al.*, 2005).

### 1.3.3 Manganese(IV) reduction

Bacteria are able to utilise Mn(IV) as a terminal electron acceptor in cellular respiration. Naturally occurring Mn(IV) exists predominantly as nodule deposits of MnO<sub>2</sub>, formed through both geochemical and microbial generation. Under anoxic conditions deprived of oxygen, some bacteria have developed evolutionary mechanisms that allow them to use Mn(IV) as an alternative to oxygen; reducing the insoluble Mn(IV) to the soluble Mn(II) (Lovley, 1991). Solubilized manganese plays a crucial role in oceanic microorganism communities which are important in several biological processes (Bhattacharyya-Pakrasi *et al.*, 2002). These include nutritional purposes as a trace element and as a water oxidiser during photosynthesis (Spratt Jr *et al.*, 1994).

The reduction of manganese in nature occurs not only as a result of specific chemical interactions but also arises through biological conversion by a range of bacteria and fungi. (Tebo *et al.*, 2004). The organic conversion of Mn(III,IV) to Mn(II) is evident in both bacteria and fungi originating from diverse environments. Such environments include mine drainage systems, soils, rock surfaces and various water systems abundant in Mn(IV) (Santelli *et al.*, 2010; Thompson *et al.*, 2005). Manganese reducers significantly alter the biogeochemistry of an environment rich in manganese. Additionally, the presence of manganese within a system has been found to affect various biological processes of these organisms including carbon fixation and photosynthesis (Tebo *et al.*, 2004).

### 1.3.4 Microbial reduction of other metals

#### 1.3.4.1 Iron(III) reduction

Bacterial reduction of iron is observed in nature and as well as in microbial cultures. Depending on the environmental conditions, iron in nature exists in both the divalent and trivalent state (the redox changes between Fe(III) and Fe(II) play vital roles in subsequent anoxic redox processes that is greatly influenced by bacterial transformation). Research into iron reducing bacteria has highlighted the importance of these bacteria in the environmental cycling of iron (Lovley, 1993). To date, numerous ferric iron-reducing bacteria have been isolated from a diverse range of anoxic environments including soils, deep terrestrial subsurfaces, hot springs and sludge sediments (Straub *et al.*, 2001).

#### 1.3.4.2 Vanadium(V) reduction

Although present in trace concentrations, vanadium is another transition metal present in nature. Under neutral pH and anaerobic conditions, vanadium is environmentally present as vanadium(IV) and vanadium(V). Vanadium(IV) is present as vanadyl ions that are insoluble in solution and vanadium(V) as vanadate ions that are soluble in water (Rehder, 1991; Rehder 1992). Several bacteria have been identified capable of vanadium reduction, including *Pseudomonas* sp. and *Shewanella oneidensis*. These organisms, in addition to other metals, are able to reduced V(V) to V(IV) coupled with an electron donor for use in anaerobic respiration. Organisms capable of vanadium reduction have great potential in the bioremediation of vanadium-contaminated sites; with the biological conversion into an insoluble metal offering a means of physically removing wastes from the environment.

#### 1.3.4.3 Uranium(VI) reduction

Uranium as U(VI) is a toxic, water soluble metallic element that is highly radioactive and detrimental to human health (Lovley *et al.*, 1991). Tight government regulations limit everyday exposure, however extraction of uranium at mining sites often results in environmental contamination that is difficult to remove. Reduction of U(VI) to U(IV) *in situ* is a desired outcome during industrial process as U(IV) is much less toxic and forms a precipitate in water (Schiebe *et al.*, 2009). Reduction through anaerobic respiration with U(VI) as the terminal electron acceptor on environmental contamination offers an effective means of removing unwanted waste products.

Organisms belonging to several genera have been discovered capable of reducing U(VI) and include some species of *Geobacter*, *Anaeromyxobacter*, *Desulfosporosinus*, *Desulfovibrio* and *Acidovorax* sp. (Cardenas *et al.*, 2008). Additionally, several species from *Clostridium* sp. have been discovered capable of reducing uranium as uranyl –acetate, -citrate and –nitrate (Gao & Francis., 2008; Wright, 2010). These works demonstrate that the *Clostridium* sp. are often dominant bacteria found in sediment contaminated with uranium and play a major role in natural reduction of uranium in sediments and uranium mines (Gao & Francis., 2008; Nevin, *et al.*, 2003; Wright, 2010). While bacteria have been found across numerous genera, very few organisms able to reduce uranium have been isolated and assessed.

## 1.4 Manganese Oxidation

### 1.4.1 Manganese oxidisers

Manganese oxidising microorganisms are organisms that are able to oxidise Mn(II) to Mn(IV). Manganese oxidation by microorganisms is ubiquitous in nature; with microorganisms capable of oxide production present in lakes, marine basins, sediments, fresh and salt water systems, and groundwater systems high in organic matter (Villalobos *et al.*, 2003). Bacteria and fungi belonging to multiple genera have been found to be capable of this process and compared to natural manganese oxidation, oxidation proceeds at several orders of magnitude faster than without a biological catalyst (Miyata *et al.*, 2007). Manganese oxidation does not assist microorganisms metabolically and is independent of cellular growth. In addition to live cells, bacterial oxidation has been observed in metabolically inactive spores of a variety of *Bacillus* sp. (Francis and Tebo, 2002).

The mechanisms of microbial manganese oxidation have been widely researched, however it is not clear why microorganisms have evolved to be capable of biological oxidation. As microbial oxidation offers no direct metabolic advantage to microorganisms, several theories exist that may account for this evolutionary trait. Firstly, it is hypothesised that oxidation may be an energy storage mechanism, providing an electron acceptor for facultative organisms in environments that alternate between oxic and anoxic conditions. Additionally, the genes responsible for oxidation may be an evolutionary redundancy that may have had a more significant use but now has no direct benefit to the organisms (Tebo *et al.*, 1997). MnO<sub>2</sub> is readily able to adsorb toxic metals and it has been theorised that manganese oxidation may be a defence mechanism against metal toxicity. Studies have shown that *Leptothrix discophora* SS-1 (a known oxidiser) exhibited increased oxidation rates when exposed to non-toxic levels of copper, however the group responsible determined this was not a result of metal toxicity (Gheriany *et al.*, 2011). Finally, oxidation may have been an evolutionary coincidence; a

mutation of an already existing reductases or metabolic cofactors (Tebo *et al.*, 2005). Whatever the reason, microbial manganese oxidation plays a vital role in environmental manganese cycling.

#### **1.4.2 Mechanisms of manganese oxidation**

The mechanisms of manganese oxidation by microorganisms can be divided into two sub-groups: direct oxidation; and indirect oxidation. Direct oxidation (Section 1.5.2.1) is oxidation that occurs as a direct result of microbial enzymatic conversion. Electron transfer is induced by enzyme-metal interactions and is directly influence by the presence of Mn(II) oxidisers. Indirect oxidation (Section 1.5.2.2) is the conversion of Mn(II) through environmental changes brought on by incidental cellular processes. The change of environmental conditions results in the lowering of  $E_h$  of oxidation and the microorganism acts as an indirect catalyst of Mn(II) conversion without directly being involved with the reaction itself (Nealson *et al.*, 1988).

#### 1.4.2.1 Direct oxidation

Three major Mn(II) oxidising models have been determined through analysis of distinct bacteria: *Leptothrix discophora* SS-1, *Pseudomonas putida* MnB1 / GB-1 and *Bacillus sp.* SG-1 (Brouwers *et al.*, 2000; Caspi *et al.*, 1998; van Waasbergen *et al.*, 1996). All three organisms all share the ability to oxidise Mn(II) on an exopolymer matrix surrounding the cell. However each have secondary oxidation characteristics unique to each organism. *L. discophora* oxidises enzymatically on an extracellular sheath, although strain SS-1 is a mutant that releases the oxidation factor into the supernatant (Brouwers *et al.*, 2000; Tebo *et al.*, 2004). The manganese oxidation activity of *Bacillus sp.* SG-1 is localised on the outermost layer of the spores (exosporium) and the oxidation activity of *P. putida* MnB1 / GB-1 occurs on the membrane glycocalyx (Caspi *et al.*, 1998; Tebo *et al.*, 2004; van Waasbergen *et al.*, 1996). Not all manganese oxidation mechanisms convert Mn(II) in the same way. In fact there are several different chemical pathways associated with enzyme mediated manganese oxidation in microorganisms. The following are some of the well-known reactions linked to microbial Mn(II) oxidation (Nealson, 2006).



These reactions can occur as a biotic or abiotic reaction in the environment. It is important to note that for this reaction to occur that environmental conditions must heavily favour oxide formation or be rich in microorganisms capable of catalysing these reactions.

#### 1.4.2.2 Indirect oxidation

Indirect oxidation occurs when Mn(II) conversion is achieved through incidental cellular processes (acting as a catalyst). Indirect oxidation can occur in several ways and is present in both bacteria and fungi. Firstly, organisms that alter the surrounding pH and/or redox conditions of their surrounding environment can result in catalysis of Mn(II) oxidation. In phytoplankton communities, it was observed that the surrounding water was ~pH10 and supersaturated with oxygen as a result of cellular metabolism. These conditions favoured Mn(II) oxidation, which occurred at a very fast rate without the aid of a direct biological catalyst (Richardson *et al.*, 1988). Secondly, metabolic end products resulting from cellular activity have been found to have the ability to chemically oxidize Mn(II) (Hullo *et al.*, 2001). Recent studies by Learman *et al.* (2011) found oxidation of Mn(II) by *Roseobacter* sp. AzwK-3b to occur through the biological production of a redox reactant superoxide. This then readily oxidises Mn(II) through electron transfer, without the direct inclusion of biological conversion.

#### 1.4.3 Manganese oxidising bacteria

Numerous bacteria have been identified as manganese oxidisers; isolated from various environments and exhibiting high levels of phylogenetically diversity between isolates. In addition to oxidation by fungi, extensive research has been performed on the mechanisms and the variety of manganese oxidisers. Investigations of these organisms has resulted in oxidising isolates across a broad range of phyla, with bacteria belonging to Firmicutes, Actinobacteria and Proteobacteria capable of enzymatic oxidation (Tebo *et al.*, 2005).

Perhaps the most extensively researched of all Mn(II) oxidisers, *Bacillus* sp. SG-1 has helped gain much insight into the mechanisms and understandings of manganese oxidation. *Bacillus* sp. SG-1 has been found to enzymatically achieve microbial oxidation of manganese under a large range of temperatures (3°C – 70°C), Mn(II) concentrations (nano- to millimolar) and relative ionic strength (fresh and saltwater) (Francis and Tebo, 2002). In addition to *Bacillus* sp. SG-1, there are over 30 strains across multiple genera that have been discovered. Figure 1.7 demonstrates a representative phylogram of known Mn(II) oxidising bacteria.

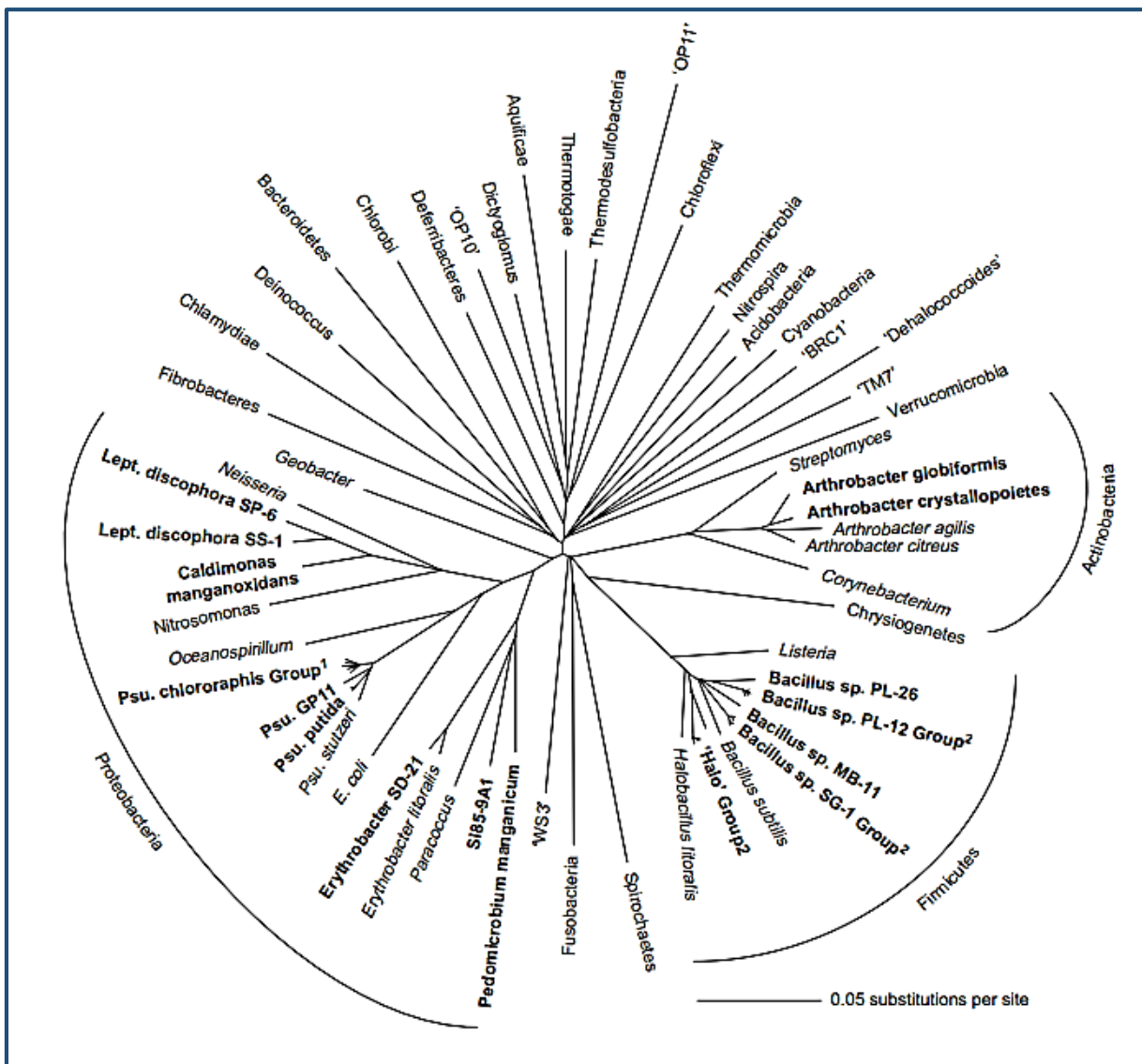


**Figure 1.7:** Representative neighbour joining, unrooted phylogram of Mn(II) oxidising bacteria

(Tebo *et al.*, 2005).

#### 1.4.4 Iron oxidising bacteria

Bacteria that oxidise iron are the most widely researched group of metal transformers and are greatly responsible for iron cycling in nature. Similar to Mn(II) oxidation, the conversion of ferrous iron (Fe(II)) to ferric iron (Fe(III)) occurs in marine/ocean environments and results in the production of an insoluble, orange/dark brown metal compound. When the pH of an environment is  $\geq 4$ , Fe(II) exists as an insoluble compound, compared to pH  $\leq 4$  at which point Fe(II) is present as an aqueous species. Bacteria responsible for the production of ferrous iron are often able to use this in anaerobic respiration, coupling it with an appropriate electron donor and reproducing ferric iron (Lovley, 1991; Straub *et al.*, 2001; Emerson & Floyd., 2005; Weber *et al.*, 2006).

Iron oxidising bacteria are not limited to obligate aerobes; facultative anaerobes and strict anaerobes have also been discovered that are capable of ferrous iron production. Additionally, both mesophilic and acidophilic bacteria are responsible for iron transformation each with their own oxidation subsystems. One of the most studied Fe(II) oxidisers is *Acidithiobacillus ferrooxidans*, an acidophile that has a major role in bioleaching (Valdés *et al.*, 2008). The majority of iron oxidising bacteria are Proteobacteria, though the phyla Firmicutes and Nitrospirae also contain bacteria capable of iron oxidation (Hedrich *et al.*, 2011). Figure 1.8 provides a representative dendrogram of *Acidithiobacillus ferrooxidans* and other known iron oxidising Proteobacteria; contrasting mesophiles, nitrate-dependent, neutrophilic and acidophilic oxidisers.

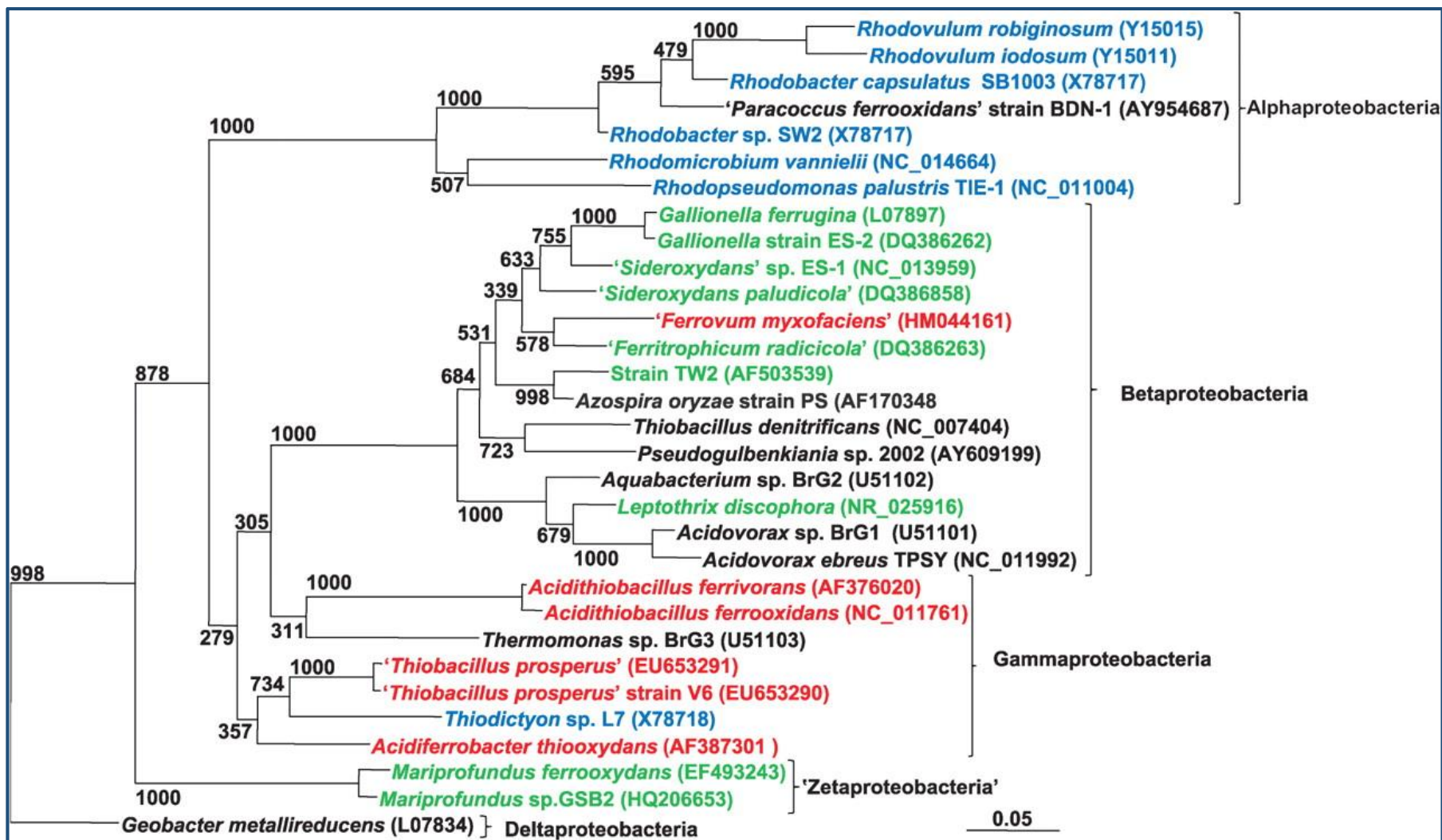


**Figure 1.8:** Maximum-likelihood 16S rRNA dendrogram of known iron oxidising Proteobacteria. Acidophilic (red), nitrate-dependent (black), phototrophic (blue) and neutrophilic aerobic (green) iron oxidisers are shown. GenBank accession numbers are given in the parenthesis. Scale bar indicates 5 nucleotide changes per 100 nucleotides. Taken from Hedrich *et al.*, 2011.

## 1.5 Manganese

### 1.5.1 The element

Manganese is the 25<sup>th</sup> chemical element on the periodic table and is designated by the symbol Mn. It is the twelfth most abundant element found in the earth's crust, however exists almost entirely in mineral form or as an alloy. Manganese is also present in oceanic waters both solubilized and as nodules on the oceans floor (an estimated 500 billion nodules existing in nature; Wang *et al.*, 2009). It is non-magnetic and is found in nature both as a free element and as part of many minerals. Manganese has valency states of -3 to +7, with the +2, +3 and +4 form most common in the environment. Manganese can be soluble (Mn(II)) or insoluble (Mn(IV)) and predominately exists as a brownish-blackish oxide (Nealson, 1983).

### 1.5.2 Manganese minerals in nature

Manganese can form a wide variety of minerals, including borates, carbonates, oxides, phosphates, silicates, sulphates, borosilicates, arsenates, sulphosalts and sulphates and exists in over 100 forms naturally. Manganese oxides are the most common form of manganese, playing a significant role in the environment, affecting both groundwater and bulk soil compositions (Post, 1999). The formation of manganese oxides and other compounds are determined by a combination of bioavailability of constituents and surrounding environmental conditions. In fact, many of these compounds have industrial significance and are mined from natural deposits for commercial trade due to their diverse range of uses. Table 1.2 depicts common manganese compounds, highlighting both the chemical and physical diversities between manganese minerals.

**Table 1.2:** The appearance, crystalline structure and chemical formulae of common manganese minerals

Mineral	Formulae	Molecular weight	Appearance	References
<b>Alabandite</b>	MnS	87.00 g/mol	Black / Lead grey / Brownish grey	McCummon, 1991
<b>Birnessite</b>	$(\text{Na}_{0.3}\text{Ca}_{0.1}\text{K}_{0.1})(\text{Mn}^{4+}, \text{Mn}^{3+})_{2.4} \cdot 1.5 \text{H}_2\text{O}$	215.71 g/mol	Dark brown / Black	Post & Veblen, 1990
<b>Cryptomelane</b>	$\text{K}(\text{Mn}^{4+}, \text{Mn}^{2+})_8\text{O}_{16}$	734.59 g/mol	Black / Gray / Blue grey	Post <i>et al.</i> , 1982
<b>Groutite</b>	$\alpha\text{-MnOOH}$	87.94 g/mol	Blue black	Wyckoff, 1963
<b>Hausmannite</b>	$\text{Mn}^{2+}\text{Mn}^{3+}_2\text{O}_4$	228.81 g/mol	Brownish black, Greyish	Baron <i>et al.</i> , 1998
<b>Jacobsite</b>	$(\text{Mn}^{2+}, \text{Fe}^{2+}, \text{Mg})(\text{Fe}^{3+}, \text{Mn}^{3+})_2\text{O}_4$	227.38 g/mol	Iron black / Black	Lucchesi <i>et al.</i> , 1997
<b>Manganite</b>	$\gamma\text{-MnOOH}$	87.94 g/mol	Black / Grey / Greyish black	Kohler <i>et al.</i> , 1997
<b>Manganosite</b>	MnO	70.94 g/mol	Green / Greenish black	Pacalo and Graham, 1991
<b>Pyrolusite</b>	$\beta\text{-MnO}_2$	86.94 g/mol	Steel grey / Iron grey	Wyckoff, 1963
<b>Ramsdellite</b>	$\text{MnO}_2$	86.94 g/mol	Iron black / Black / Steel grey	Post & Heaney, 2004
<b>Rhodochrosite</b>	$\text{MnCO}_3$	114.95 g/mol	Pinkish red / Red / Rose red	Graf, 1961
<b>Romanèchite</b>	$((\text{Ba}, \text{H}_2\text{O})_2(\text{Mn}^{+4}, \text{Mn}^{+3})_5\text{O}_{10})$	544.25 g/mol	Greyish black / Black / Steel grey	Turner & Post, 1988

### 1.5.3 Manganese cycling in nature

Manganese cycling in nature is the natural redox of  $\text{Mn(IV)} \rightleftharpoons \text{Mn(II)}$  and is largely dependent on the physical, chemical and environmental factors. The preferred oxidation states of manganese are dependent on the environments pH and oxygen availability. Under anoxic conditions and at lower pH, Mn(II) is thermodynamically favoured whereas Mn(III,IV) are the favoured forms at higher pH levels and in the presence of oxygen (Figure 1.9). The high activation energy required for manganese oxidation means that a catalyst is often required; typically through microbial conversion by bacteria or fungi (Tebo *et al.*, 2004). In marine environments, maximum oxidation was found to occur just above the oxic / anoxic region; that is the region where saturation oxygen dissipates and anaerobic conditions prevail (Nealson *et al.*, 1988). Mn(II) produced in this way is subsequently used as an alternative electron acceptor in anaerobic respiration, where it is reduced back to Mn(IV). Figure 1.10 shows common features of manganese oxidation in nature.

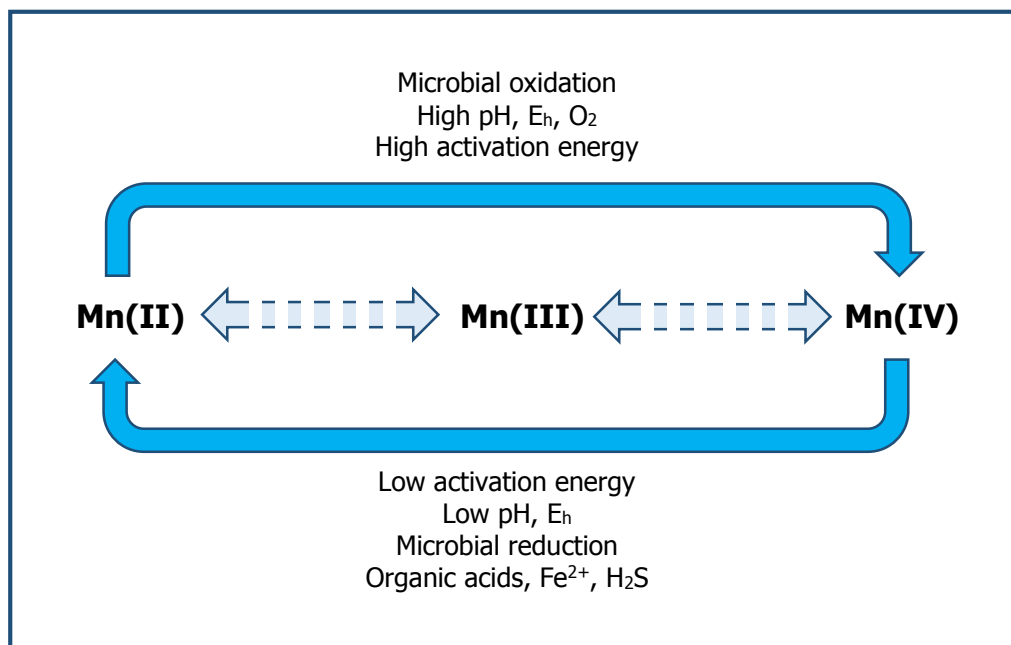


**Figure 1.9:** The major features of manganese oxidation in nature. Adapted from Nealson, 2006.

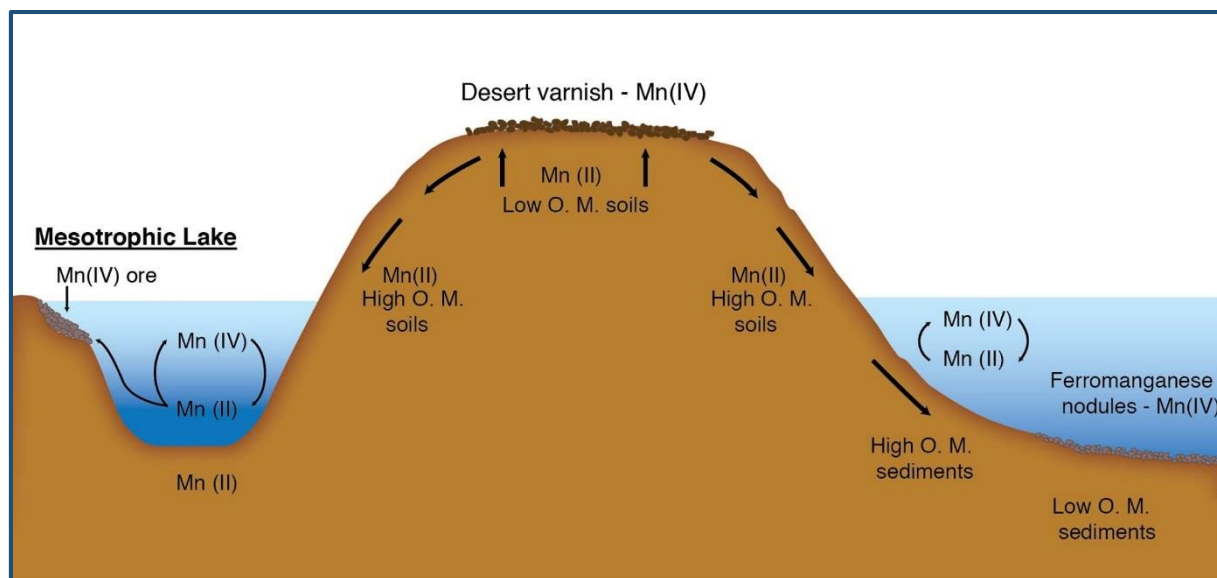


**Figure 1.10:** Manganese cycling in terrestrial and marine environmental systems. Oxidation and reduction is largely driven by microbial transformation but the process is also dependent on surrounding environmental conditions. Adapted from Marshall *et al.*, 1979.

#### 1.5.4 Industrial significance

Manganese nodules are mined and exported for use as a cofactor in a range of industrial products. Manganese is used in the manufacturing of many products, however is primarily used as a cofactor in stainless steel manufacturing (accounting for 85% - 90% of total demand) (Zhang & Cheng, 2007). The addition of manganese to stainless steel is essential for its sulphur-fixing properties; forming a high melting sulphide which prevents the formation of iron sulphides. Stainless steel produced with manganese is known as Hadfield Steel and compared to other steel alloys is generally tougher, harder and has better workability at high temperatures (Dastur and Leslie, 1981). Manganese dioxide is the major component of dry-cell batteries due to its high depolarizing activity. Activity is directly related to the structure of the oxide, with the more disordered and non-crystalline resulting in a higher activity (Greene & Madgwick, 1991).

## 1.6 Project Aims and Overview

This thesis examines several aspects of manganese transforming bacteria. It explores a radioactively heated environment known for its high levels of trace metals, the manganese transforming characteristics of bacteria, several previously unreported manganese oxidisers, the bioremediation potential of the produced oxides, and a genomic analysis of one of these transformers. More specifically, this thesis intends to investigate and address the following aims:

- (1) Investigate a unique environment rich in trace metals likely to contain manganese transforming bacteria.**

PHS was selected as an ideal location for investigation as its relative isolation from civilisation and its extreme environmental conditions (temperature, radioactivity, metal concentration) resulting in an uncontaminated water source which could potentially reveal novel organisms. Chapter 3 investigates the springs in-depth, characterising the environment from both a geochemical and microbiological approach. In addition to isolation of selected bacteria, a culture independent study was performed to detect the presence of manganese transformers that may be present in the spring. Isolates capable of manganese oxidation and reduction were stored and used in subsequent investigation.

**(2) Kinetic studies and characterisation of manganese oxidising bacteria and investigations of produced oxides.**

Early studies on manganese transformers focused solely on either manganese reduction or oxidation, with very little work done on both. *Shewanella* sp. represent the widest researched metal reducers, and the transformation characteristics of these bacteria were tested alongside the PHS isolates. This thesis is the first published work that characterises and identifies *Shewanella* sp. as manganese oxidisers and additionally also discusses three newly discovered Firmicutes. The redox characteristics of these organisms were investigated and biogenic MnO<sub>2</sub> analysed.

**(3) Assess the bioremediation potential of biogenic manganese oxide in the removal of toxic metals from wastewaters.**

The ability for manganese oxides to immobilize soluble toxic metals offers potential in the bioremediation of contaminated waste sites. Chapter 5 investigates the bioremediation potential biogenic MnO<sub>2</sub> of select isolates which was tested against individual metals as well as under simulated waste water conditions. The metal tolerances of these isolates were also investigated to determine suitability for *in situ* bioremediation of toxic water.

**(4) Analyse the genes responsible for manganese oxidation by *Bacillus* sp. PMO**

The PHS isolate, *Bacillus* sp. PMO, was selected for genomic analysis to determine the gene(s) responsible for manganese oxidation. Chapter 6 investigates this bacterium, which was selected due to its close phylogenetic proximity to the most widely researched Mn(II) oxidiser, *Bacillus* sp. SG-1.

**Finally, conclusions and recommendations for future work are summarised and presented in Chapter 7.**

# Chapter 2

Materials and Methods

## 2.1 Research Plan

The central theme behind the research plan was to thoroughly investigate the bacterial flora present within Paralana hot springs and subsequently focus on those organisms capable of manganese transformation. Water and sedimentary samples were collected and the bacterial diversity contained therein was determined by culture dependent and independent techniques. In addition, chemical analysis was performed on the samples to determine trace metal composition (Chapter 3). Manganese transforming bacteria obtained through isolations were investigated further in composite with several *Shewanella* sp. in addition to the chemical composition and attributes of the transformed manganese (Chapter 4). The bioremediation potential of these organisms was assessed using manganese dioxide as a metal immobilisation agent for removing various heavy metals (Chapter 5). Finally, a manganese transforming bacteria was selected and whole genome sequence performed to compare the manganese transforming genes with those present in other bacteria (Chapter 6). A comprehensive research plan is outlined in Figure 2.1.

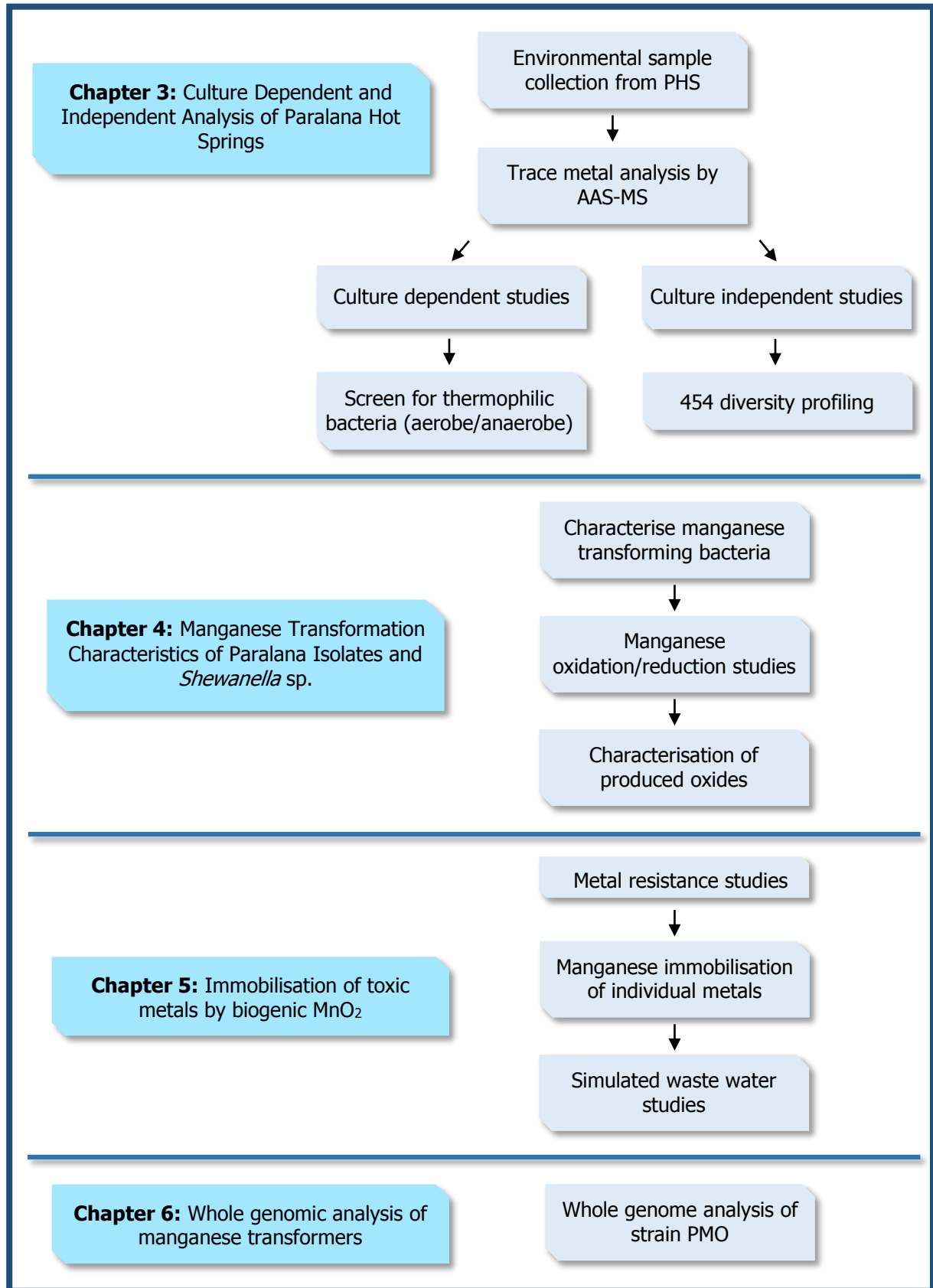


**Figure 2.1:** Outline of research plan used to address aims to better understand the mechanisms and environments of manganese transforming.

## 2.2 Chemicals, Buffers and Media

### 2.2.1 Chemicals and reagents

All chemicals and reagents used are analytical grade and molecular biology grade unless otherwise specified.

### 2.2.2 Buffers

**Table 2.1:** List of buffers used in various experimentation. All buffers were prepared under sterile conditions and buffers containing sensitive compounds stored at -20°C until used.

Buffer	Composition
<b>6x loading buffer</b>	0.25% bromophenol blue, 40% sucrose
<b>TAE buffer</b>	40mM Tris-acetate, 2mM EDTA
<b>TE buffer</b>	10mM Tris-Cl (pH 7.4), 1mM EDTA (pH 8.0)
<b>QG buffer</b>	5.5M guanidine thiocyanate, 20mM Tris-HCl (pH 6.6)
<b>PE buffer</b>	10mM Tris-Cl (pH 7.5), 80% ethanol
<b>EB buffer</b>	10mM Tris-Cl (pH 8.5)
<b>P1 buffer</b>	50mM Tris-Cl (pH 8.0), 10mM EDTA, 100µg/mL RNaseA

### 2.2.3 Media

#### 2.2.3.1 Preparation and anaerobic techniques

All media were prepared by dissolving each individual constituent in deionised water, with additional metals added when required. The solutions pH was adjusted to as required using 0.5M HCl / NaOH then reconfirmed after sterilisation. Aerobic medium was dispensed in 9mL aliquots into test tubes which were then sterilised for 15 minutes at 121°C and 1.05kg.cm<sup>-2</sup> pressure. When solid aerobic media was required for colony isolation, an additional 16g/l bacteriological agar was added to the media and was sterilised. The media was then poured into Gamma sterilised plates under aseptic conditions inside a lamina-flow hood.

Anaerobic medium was prepared using the anaerobic technique described by Hungate (1950). The medium was prepared firstly by boiling it for 15 minutes to remove dissolved oxygen within the solution. The medium was subsequently cooled with a stream of N<sub>2</sub> gas to approximately 60°C and 9mL aliquots dispensed into Hungate while being deoxygenated with N<sub>2</sub> gas. Hungate tubes containing medium were then autoclaved for 15 minutes at 121°C and 1.05kg.cm<sup>-2</sup> pressure.

#### 2.2.3.2 Great Artesian Basin (GAB) medium

GAB medium was utilised to support the growth of microbes from Paralana hot springs. The media was used for aerobic enrichments, and contained the following constituents (Table 2.2):

**Table 2.2:** Chemical composition of GAB media (per litre of distilled H<sub>2</sub>O). Following preparation the media was pH adjusted to the required level and heat sterilised.

<b>Chemical</b>	<b>Concentration (g/L)</b>
<b>NH<sub>4</sub>Cl</b>	1.00
<b>KH<sub>2</sub>PO<sub>4</sub></b>	0.30
<b>K<sub>2</sub>HPO<sub>4</sub></b>	0.60
<b>MgCl<sub>2</sub>.6H<sub>2</sub>O</b>	0.50
<b>CaCl<sub>2</sub>.H<sub>2</sub>O</b>	0.10
<b>NaHCO<sub>3</sub></b>	3.20
<b>NaCl</b>	2.00

### 2.2.3.3 Peptone Yeast Extract (PYE) medium

PYE media was used to support the bacterial oxidation of manganese in aerobic samples. In addition, the media was also used for anaerobic reduction of manganese by manganese transforming bacteria and contained the following constituents (Table 2.3):

**Table 2.3:** Chemical composition of PYE media (per litre of distilled H<sub>2</sub>O). Following preparation the media was pH adjusted to the required level and heat sterilised.

Chemical	Concentration (g/L)
Yeast extract	1.00
Peptone	1.50
NaCl	7.50
(NH <sub>4</sub> ) <sub>2</sub> SO <sub>4</sub>	1.00
HEPEs	2.40

PYE media was utilised for growth and manganese transformation in *Shewanella* sp. as well as PHS bacterium isolated using GAB medium. In addition to the constituents comprising PYE media, an addition of 1-9mM MnCl<sub>2</sub>.6H<sub>2</sub>O (manganese oxidation) or 1-14mM MnO<sub>2</sub> (manganese reduction) was added for manganese transformation studies.

## 2.2.3.4 Patel Lab (PL) media

Patel lab media was utilised for the enrichment and isolation of anaerobic organisms and contained the following constituents (Table 2.4):

**Table 2.4:** Chemical composition of PL media (per litre of distilled H<sub>2</sub>O). Following preparation the media was pH adjusted to the required level and heat sterilised.

Chemical	Concentration (g/L)
NH <sub>4</sub> Cl	1.00
KH <sub>2</sub> PO <sub>4</sub>	0.30
K <sub>2</sub> HPO <sub>4</sub>	0.60
MgCl <sub>2</sub> .6H <sub>2</sub> O	0.10
NaCl	1.00
HEPEs	12.00
CaCl <sub>2</sub> .2H <sub>2</sub> O	0.10
Yeast extract	0.20
Wolin's vitamin solution	1mL
Zeikus' trace element solution	1mL

In addition to selected electron donors, a stock solution of either sodium nitrate, sodium sulphate, sodium sulphite, sodium arsenate, potassium dichromate, cobalt EDTA, ferric ammonium citrate, manganese oxide, sodium molybdenate, sodium selenate, uranyl acetate and sodium orthovanadate were added (in varying concentrations depending on the compound) to tubes containing PL media for use as a terminal electron acceptor.

## 2.2.3.5 Vitamins and trace elements

Zeikus' trace element solution (Zeikus *et al.*, 1979) was prepared for use in PL media to provide microorganisms with trace elements, promoting growth and contained the following constituents (Table 2.5):

**Table 2.5:** Chemical composition of Zeikus trace element solution (per litre of distilled H<sub>2</sub>O).

Following preparation media was heat sterilised and stored at 4°C for future use.

Vitamin	Concentration (g/L)
<b>FeCl<sub>3</sub>.4H<sub>2</sub>O</b>	0.20
<b>MnCl<sub>2</sub>.4H<sub>2</sub>O</b>	0.10
<b>CoCl<sub>2</sub>.6H<sub>2</sub>O</b>	0.017
<b>CaCl<sub>2</sub>.2H<sub>2</sub>O</b>	0.10
<b>ZnCl<sub>2</sub></b>	0.10
<b>CuCl<sub>2</sub></b>	0.02
<b>H<sub>3</sub>BO<sub>3</sub></b>	0.01
<b>NaMoO<sub>4</sub>.2H<sub>2</sub>O</b>	0.01
<b>NaCl</b>	1.00
<b>Na<sub>2</sub>SeO<sub>3</sub></b>	0.02
<b>Nitilotriacetic acid</b>	12.00

The pH of the solution was adjusted to pH 6.5 and was sterilised for 15 minutes at 121°C and 1.05kg.cm<sup>-2</sup> pressure. The solution was stored at 4°C.

Wolin's vitamin solution (Wolin *et al.*, 1963) was prepared for use in PL media as an added nutrient source. The solution was filter-sterilised using a Millex GS 0.22 $\mu$ m Filter, stored at 4°C and contained the following constituents (Table 2.6):

**Table 2.6:** Chemical composition of Wolin's solution (per litre of distilled H<sub>2</sub>O). Following preparation the solution was filter sterilised into a 15mL falcon tube and stored at 4°C for future use.

Vitamin	Concentration (mg/L)
<b>Biotin</b>	2.00
<b>Folic acid</b>	2.00
<b>Pyridoxine-HCl</b>	10.00
<b>Riboflavin</b>	5.00
<b>Thiamine</b>	5.00
<b>Nicotinic acid</b>	5.00
<b>Pantothenic acid</b>	5.00
<b>Vitamin B12</b>	0.10
<b>Para-amino benzoic acid</b>	5.00
<b>Thiotic acid</b>	5.00

#### 2.2.3.6 Preparation of stock solutions

Stock solutions of utilisable electron donors and electron acceptors were prepared anaerobically in Schott bottles. The substrates were dissolved in distilled H<sub>2</sub>O to the required concentration and the pH was neutralised using 0.5M HCl / NaOH (if required). The solutions were then transferred to 100mL serum bottles and slowly boiled. The serum bottles were then cooled with a stream of N<sub>2</sub> gas for approximately 5 minutes to ensure the uptake of N<sub>2</sub> gas into the solution. Stock solutions were either autoclaved for 40 minutes at 121°C and 1-1.5kg.cm<sup>-2</sup> pressure, or if heat sterilisation would affect the compounds integrity, filter sterilisation was achieved using a Millex GS 0.22 $\mu$ m micro filter.

## 2.3 Sample Collection and Source of Cultures

### 2.3.1 Paralana hot springs

Paralana hot springs was selected as the site for sample collection due to its relative isolation from other water sources as well as the high concentrations of heavy metals in the neighbouring environments. Located in outback South Australia ( $30^{\circ}17'S$ ,  $139^{\circ}44'E$ ; Figure 2.4), it is a naturally occurring hot spring with the unique trait that it is partially heated by radioactive decay in addition to a magmatic heat source (discussed in greater detail in Section 3.1.1). The springs consist of a primary large pool connected to a smaller pool (via a small stream). The cooler areas of the spring play host to a variety of aquatic organisms and evidence of microbial mats are present (Figure 2.3).



**Figure 2.2:** The geographical location of Paralana hot springs ( $30^{\circ}17'49''S$ ,  $139^{\circ}44'15''E$ ) within Australia (Google Maps, 2013).



Figure 2.3: Images of Paralana hot springs.

Surface water samples (0-1M) were collected from the springs using sterile 2L plastic storage containers. Soil samples (0-30cm deep) were collected using 500mL plastic sterile storage containers. Samples were stored at 4°C until used for enrichments/other analysis. The term ‘Primary Pool’ refers to the pool containing the heat source with the ‘Secondary Pool’ connected by a small stream. Samples used for analysis were termed: **P1W** (Primary pool water sample), **P1S** (Primary pool sediment sample), **P2W** (Secondary pool water sample) and **P2S** (Secondary pool sediment sample) (Figure 2.4).

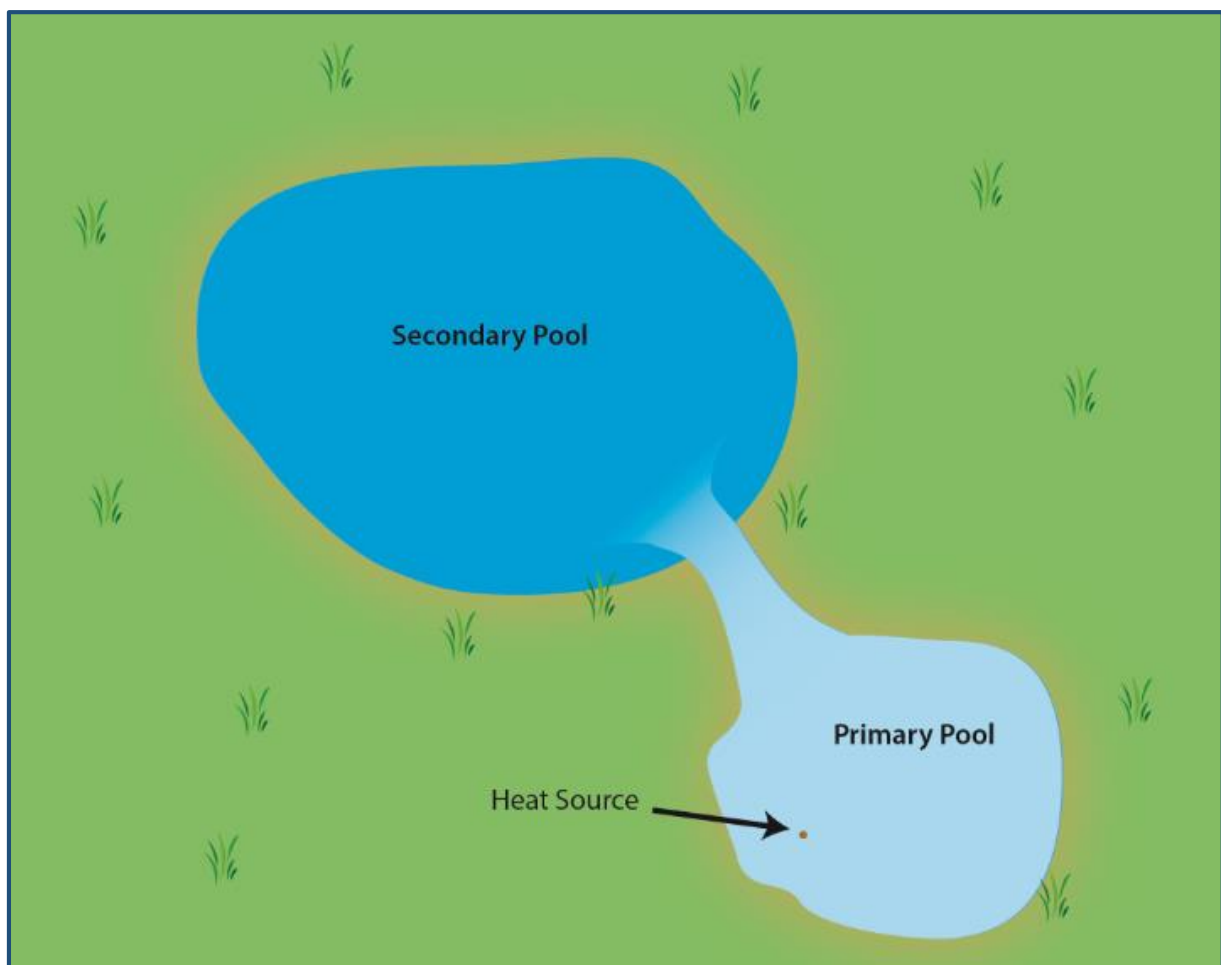


**Figure 2.4:** Overhead illustrative map of PHS with significant geographical features.

### 2.3.2 Water content and pH of samples

An adapted method for calculating percentage water content was used to determine the quantity of water in PHS sediment samples (Gardner & Klute, 1986). 100g soil samples were weighed out on a sterile Petrie dish within 48 hours of original collection (termed “wet weight”). Samples were spread out to maximise surface area and left uncovered for 96 hours in 75°C incubator. The samples were then weighed again (termed “dry weight”). Water content in each sample were determined using the following mathematic formulae.

$$\left( \frac{\text{Dry weight}}{\text{Wet weight}} \right) \times 100 = \text{Percent dry weight (PDW)}$$

$$100 - \text{PDW} = \text{Percentage water content}$$

Soil pH was determined using a method by the Shivaji group (2011). Approx. 50g of soil samples were ground down into fine particles using a sterilised mortar and pestle and passed through a 2mm sieve. 10g of each sample were mixed with 50mL of RO H<sub>2</sub>O containing 0.1% CaCl<sub>2</sub> (performed in triplicate) and allowed to settle for 10 minutes. The pH was measured and the mean pH was calculated across samples.

### 2.3.3 *Shewanella* species

*Shewanella oneidensis* MR-1, *Shewanella putrefaciens* 200, *Shewanella putrefaciens* CN-32, *Shewanella loihica* PV-4 and *Shewanella denitrificans* OS217 were kindly donated by Professor Kenneth Nealson of the University of Southern California, U.S.A.

## **2.4 Enrichment and Isolation**

### **2.4.1 Aerobic enrichments**

Aerobic enrichments were performed by adding 1mL of PHS waters to 9mL of medium and were amended with an appropriate electron donor. Enrichments were left to incubate for 72 hours and those positive for growth were used for aerobic isolations (Section 2.4.3).

### **2.4.2 Anaerobic enrichments**

Anaerobic enrichments were performed by adding 1mL of PHS waters to 9mL of deoxygenated medium and were amended with an appropriate electron donor and acceptor. Enrichments were left to incubate for 72 hours and those positive for growth were used for anaerobic isolations (Section 2.4.4).

### **2.4.3 Purification of aerobes**

Isolate purifications of aerobes in liquid media were achieved through streaking of environmental samples onto agar plates. Following positive growth, individual colonies were selected based on size and morphology and subcultured for downstream experimentation.

### **2.4.4 Purification of anaerobes**

Isolate purifications of anaerobes in liquid media were achieved through the dilution to extinction method, with 1:10 serial dilutions into Hungate tubes containing the same constituents as the original enrichment culture. The lowest serial dilution that showed positive growth was selected and the dilution process was repeated in triplicate.

### **2.4.5 Culture purity and storage**

Culture purity was determined by the visualisation of cells with light microscopy and 16S rRNA gene sequencing performed confirmed culture purity. Pure isolates were stored at -80°C in a 1:1 glycerol-growth medium. Cultures stored were in log phase when frozen.

## **2.5 Growth Characteristics**

### **2.5.1 Temperature optimisation**

Temperature optimisation was determined by inoculating 1mL of fresh culture into 9mL of respective enrichment medium. Electron donors and pH levels known to support growth were used for temperature optimisation, with increments of 5°C from 10°C to 60°C (for aerobic isolates) and 40°C to 70°C (for anaerobic isolates) tested. Growth was assessed after 48 hours by measuring the relative cell densities under each condition. All temperature optimisation studies were performed in triplicate unless otherwise stated.

### **2.5.2 pH optimisation**

pH optimisation was determined by inoculating 1mL of fresh culture into 9mL of respective enrichment medium across a range of different pH levels (pH 5 – 9; increments of 0.5). Electron donors known to support growth and optimal temperature were used for pH optimisation and growth was assessed after 48 hours by measuring the relative cell densities under each condition. All pH optimisation studies were performed in triplicate unless otherwise stated.

### **2.5.3 Salinity tolerance**

The effects of salinity on growth were analysed by inoculating 1mL of fresh culture into 9mL of respective enrichment medium across a range of salt concentrations (0% - 20%; varying increments). Electron donors known to support growth and optimal temperature/pH were used for salinity tolerance and growth was assessed after 48 hours by measuring the relative cell densities under each condition. All salinity tolerance studies were performed in triplicate unless otherwise stated.

#### **2.5.4 Microscopy and gram staining**

The cell wall compositions of isolates were determined using Hucker's gram staining method (Hucker and Conn, 1923). 5 droplets of each sample were heat fixed to sterilised glass microscope slides. Samples were then flooded with Hucker's Crystal Violet Solution for 1 minute, and then briefly rinsed with sdH<sub>2</sub>O. An iodine solution was then applied to the smear for a further minute and then briefly rinsed with sdH<sub>2</sub>O. The samples were then rinsed with 95% ethanol until decolouration of the slide had occurred and then counterstained with safranin for 20-60 seconds. After a final rinse using sdH<sub>2</sub>O, the slides were blot dried and examined at 100x magnification using a BX-40 light microscope (Olympus Optical Co. Ltd). Bacterium that stained purple were deemed gram-positive and those stained pink were deemed gram-negative.

#### **2.5.5 Antibiotic sensitivity**

Resistance to various antibiotics was tested using solid agar plates of growth medium and Mast Diagnostic antibiotic disks. 1cm antibiotic disks containing 3µg tetracycline, 10µg gentamycin, 30µg cephalosporin, 5µg ciprofloxacin, 10µg ampicillin and 10µg chloramphenicol were placed on agar plates coated with liquid cultures. Plates were inoculated at optimal conditions and antibiotic sensitivity was determined by inhibition (or lack) of growth surrounding the antibiotic disks.

#### **2.5.6 Chlorophyll detection**

Environmental water was spun down from the primary PHS sample (50mL aliquots for a combined total of 300mL) and washed in a potassium phosphate buffer (100 mM KCl, 3mM KH<sub>2</sub>PO<sub>4</sub>, pH 7) in triplicate (Hanada *et al.*, 2002). Cells were subsequently disrupted by vortexing (using a Hwashin 250VM Vortex) in a 2:1 chloroform/methanol extract. Cells were spun down (using a Nüve NF-200 centrifuge) at 2,822 rcf for 5 minutes and the lower phase

taken. Absorption peaks were observed and recorded using a Agilent 8453 UV-Vis spectrometer using the original 2:1 chloroform/methanol extract as a standard.

### **2.5.7 Determination of cell density by turbidity**

Growth of organisms which utilise oxygen as an electron acceptor were determined by measuring the turbidity of the liquid cultures. Turbidity was measured by transferring 1mL of culture to a plastic cuvette and measured at 600nm using a Shimadzu UV-2550 UV spectrometer. The spectrometer was calibrated using respective, sterilised medium to zero the spectrometer. All growth studies were performed in triplicate and a mean was calculated.

### **2.5.8 Determination of cell numbers by Most Probable Number (MPN) technique**

Estimates of cellular growth in cultures containing interfering compounds were determined using the most probable numbers (MPN) technique (Halvorsen and Ziegler, 1933). Pure isolate-containing cultures were serially diluted (1:10)  $10^{-9}$  dilutions into tubes containing 9mL of respective medium. All transfers were performed using sterilised syringes and performed in triplicate as per the MPN procedure. Tubes were vortexed to avoid cell clumping, they included the appropriate electron donor/acceptor and they were grown under optimal conditions. Estimates of cellular growth were derived using the MPN index, which is based on the pattern of the triplicate enrichments truncating at the dilution containing at least one culture with positive growth. Cultures were deemed a positive enrichment if turbidity was observed. The MPN of each sample were determined using the MPN formula devised by Greenberg *et al.* (1992). Comprehensive values comprising the MPN table can be found in Appendix 1.

## 2.6 Oxidation-reduction studies

### 2.6.1 Time course of manganese transformations

The reducing/oxidising capabilities of transforming bacteria were determined by assessing the relative conversion of manganese. For transformation at varying concentrations, bacteria were cultured in appropriate media with increasing concentrations of manganese (chemically produced manganese oxide for reduction;  $\text{MnCl}_2 \cdot 6\text{H}_2\text{O}$  for oxidation) and grown under optimal conditions. After maximum growth/transformation was observed, final concentrations were detected using the Leuco crystal violet (LCV) assay (Section 2.8.1). For growth/transformation over time, bacteria were culture in an appropriate media in conjunction with a fixed manganese concentration (chemically produced  $\text{MnO}_2$  for reduction;  $\text{MnCl}_2 \cdot 6\text{H}_2\text{O}$  for oxidation) and grown under optimal conditions on an orbital shaker (120 rpm) under optimal conditions. Samples were taken at predetermined time intervals and final concentrations of manganese were detected using the LCV assay. In manganese reduction studies, growth was determined by quantifying cell turbidity (Section 2.5.5). In manganese oxidation studies where the insoluble oxide influenced turbidity, the MPN technique was used (Section 2.5.6). Growth was tested as a function of time by measuring the relative growth level of enrichment cultures at regular intervals. In aerobic cultures and anaerobic cultures containing soluble electron acceptors, growth was assessed using the cell density method (Section 2.5.5). Growth in where there were solid precipitates was determined using the MPN method (Section 2.5.6).

### **2.6.2 Effect of Mn(II) concentration on oxidation**

Manganese oxidising strains were grown to mid-log phase and 1mL of each culture was inoculated into 100 mL volumes of PYE medium supplemented with increasing concentrations of  $\text{MnCl}_2 \cdot 6\text{H}_2\text{O}$  (1mM – 9mM; 1mM increments). Enrichments were incubated on an orbital shaker (120 rpm) under optimal conditions, and after 20 days manganese oxide concentration was measured.

### **2.6.3 Effect of Mn(IV) concentration on reduction**

Manganese reducing strains were grown to mid-log phase and 1mL of each culture was inoculated into 100 mL volumes of PYE medium supplemented with increasing concentrations of chemically produced  $\text{MnO}_2$  (1mM – 14mM; 1mM increments). Enrichments were incubated under optimal conditions and after 5 days manganese oxide concentration was measured.

## 2.7 Immobilisation of Metals by Biogenic Oxides

### 2.7.1 Individual metals

The immobilisation potential of biologically produced manganese oxides were tested in conjunction with several heavy metals. Manganese transformers were grown under optimal conditions and immobilisation potential was tested against two criteria; addition of metals to enrichment cultures following growth and growth in conjunction with individual metals. Stock solutions of copper chloride (20mM), potassium chromate (10mM), lithium chloride (10mM), lead chloride (10mM), cobalt chloride (10mM), sodium arsenate (10mM) and nickel chloride (10mM) were made with roH<sub>2</sub>O and stored until use. For cultures grown in conjunction with various heavy metals, a 1:1 ratio of each metal to roH<sub>2</sub>O was added when preparing enrichment media. For cultures grown independently of heavy metals, a 1:1 ratio of stock metal solution was added to the enrichment after complete transformation had occurred. The samples were then spun down and supernatant carefully decanted before being analysed via AAS (Section 2.8.6). Cultures devoid of additional heavy metals and stock roH<sub>2</sub>O were tested as controls to avoid fallacious results.

### 2.7.2 Simulated waste waters

In addition to singular heavy metals, manganese transforming bacteria were exposed to simulated waste waters to analyse concurrent immobilisation of several heavy metals. Simulated waters taken from Tajola Industrial Estate (as effluent) were synthesised and tested for potential bioremediation treatment (Lokhande *et al.*, 2011; Table 2.7). Manganese transformers were grown under optimal conditions and immobilisation potential tested with addition of enrichment to simulated wastewaters (Neat, 1:10 and 1:100 dilutions). Samples were analysed using ICP-OES (Section 2.8.7) to determine overall immobilisation potential. Cultures devoid of additional heavy metals and stock  $\text{roH}_2\text{O}$  were tested as controls to avoid fallacious results.

**Table 2.7:** Yearly average level of heavy metal pollutants in the Tajola Industrial Estate, Mumbai, India in 2000 (Lokhande *et al.*, 2011). Metals used to synthesise wastewaters were as followed: chromium chloride; cadmium chloride; nickel chloride; zinc chloride and copper chloride.

Heavy metal	Average concentration (ppm)
Chromium	30.40
Cadmium	24.40
Nickel	21.50
Zinc	26.70
Copper	21.50

## 2.8 Metal Determination

### 2.8.1 Manganese assay

Manganese transformation was detected by the LCV assay (Spratt Jr. *et al.*, 1994). 0.05g of LCV was added to 1mL glacial acetic acid and made up to 100mL with sdH<sub>2</sub>O. Following this, 0.1mL enrichment sample was added to 3mL LCV solution and left to sit for 10 minutes. Samples were visualised at 592nm with a Shimadzu UV-2550 UV spectrometer. Absorbance was plotted against a standard curve of known concentrations of Mn(II)/Mn(IV).

### 2.8.2 Iron assay

The reduction of Fe(III) (as ferric ammonium citrate) was inferred by a visual colour change from a reddish-brown colour to a black insoluble Fe(II) oxide that precipitated at the bottom of the culture medium. Reduction was confirmed using the ferrozine assay (Sorensen, 1982). 3mL of ferrozine reagent (1g/L in 50mM HEPEs buffer) was mixed with 0.1mL of enrichment sample and visualised at 562nm with a Shimadzu UV-2550 UV spectrometer.

### 2.8.3 Cobalt assay

Positive growth of microorganisms were detected in anaerobic tubes containing cobalt(III) (as cobalt-EDTA). The reduction of cobalt(III) to cobalt(II) was inferred by a visual colour change from a violet colour to a colourless solution. In enrichments where low levels of reduction were present the sample was visualised at 592nm with a Shimadzu UV-2550 UV spectrometer.

### 2.8.4 Vanadium assay

The reduction of V(V) (as sodium orthovanadate) to V(IV) was inferred by a visual colour change from colourless to aqua (either soluble or as a precipitate). Enrichments where low levels of reduction was present a diphenylcarbazide (DPC) assay was utilised to confirm results (Carpentier *et al.*, 2003). 250µL of 1% (wt/vol) DPC in acetone was added to 250µL of 2M

H<sub>2</sub>SO<sub>4</sub> and was combined with 500µL of diluted enrichment sample. After sitting for 10 minutes, samples were visualised at 320nm with a Shimadzu UV-2550 UV spectrometer.

### **2.8.5 Uranium assay**

The reduction of U(VI) (as uranyl acetate) to U(IV) was inferred by evidence of growth in tubes containing uranyl acetate under anaerobic conditions. To confirm reduction, an adapted 2-(5-bromo-2-pyridylazo)-5-diethylaminophenol (bromo-PADAP) method was used (Lyle & Tamizi, 1978). 0.1mL of enrichment sample was added to a solution containing 0.5mL bromo-PADAP solution (0.02% bromo-PADAP in 100% ethanol), 0.8mL 100% ethanol and 3.6mL sdH<sub>2</sub>O and left to sit for 15 minutes. The sample was visualised at 578nm with a Shimadzu UV-2550 UV spectrometer.

### **2.8.6 Atomic absorption spectroscopy (AAS)**

Atomic absorption spectroscopy was used to determine the concentration of various individual metals after immobilisation by biogenic manganese oxides (Section 2.7.1) and in bioremediation assessment of simulated waste waters (Section 2.7.2). Samples were processed with the facilities and assistance from Mr Scott Byrnes of the school of Environmental Sciences, Griffith University Nathan campus, and samples were analysed using an Avanta Sigma AAS (GBS).

### **2.8.7 Inductively coupled plasma optical emission spectroscopy (ICP-OES)**

ICP-OES was used to detect trace levels of manganese following titration analysis. Samples were processed with the facilities and assistance from Mr Alan White of the School of Chemistry, Griffith University Nathan campus and analysed using an Optima 8300 ICP-OES (Perkin Elmer).

## 2.9 Manganese oxide characterisation

### 2.9.1 Sample preparation

The biogenically synthesised manganese oxides were centrifuged 25,155 rcf for 10 minutes using an Allegra 25R™ centrifuge (Beckman Coulter) and supernatant carefully removed. The residual solids were resuspended with 467µL of P1 buffer (containing 100µg/mL RnaseA) and transferred into a sterile 1.5mL Eppendorf tube. 8µL of lysozyme (60mg/mL) and 16µL of achromopeptidase (10mg/mL) was added, gently mixed and incubated at 37°C for 2 hours to remove adsorbed Mn(II) ions. Following this, an acid wash (dilute sulphuric acid; 0.03M, pH 1.5) was used in triplicate to remove soluble components and organic materials. Finally, diH<sub>2</sub>O washes were performed until the pH was neutralised.

### 2.9.2 Chemical synthesis of amorphous MnO<sub>2</sub>

Synthesis of amorphous manganese dioxide was achieved using an adapted KmnO<sub>4</sub> / MnCl<sub>2</sub> precipitation technique (Lovley & Phillips, 1986). A 200mL MnCl<sub>2</sub> solution (6g/L) was slowly added to a 200mL KmnO<sub>4</sub> solution (3.2g/L, pH 8.5) and stirred using a magnetic stirrer for 30 minutes. Amorphous MnO<sub>2</sub> was produced (black precipitate) and was centrifuged and washed with distilled water 6 times to remove unwanted salts. The powder was air-dried at 50°C for 24 hours.

### 2.9.3 Average oxidation states

The average oxidation state analysis was used to measure the average valence state of the manganese in a sample. It is important to note that this is an average measure as it does not distinguish between different valence states if more than one exists in a sample. For manganese oxide, the average oxidation state (x) is presented as MnO<sub>x</sub> where x is the aggregate average across all oxide states. The method used for determining this average oxidation state is adapted from an iodometric method by Murray et al. (1984; Appendix 2).

Approximately 10mg of each pre-prepared sample were weighed out into a 50ml beaker. A composite mixture of 10mL roH<sub>2</sub>O, 1mL 20% v/v H<sub>2</sub>SO<sub>4</sub> and 1mL alkaline NaI solution (comprising 32g NaOH and 60g NaI in 100mL roH<sub>2</sub>O) was added to the sample and left to sit for 18 hours. Following this, the sample was filtered into a 100ml beaker using a Millex GS 0.45µm micro filter. 1mL of 1% (w/v) starch solution was added to the filtrate. To determine the total oxidising equivalents, the liberated I<sub>2</sub> from each sample was titrated with 5mM sodium thiosulphate using a 50mL burette. The titration was deemed complete when the blue colour dissipated. The solution was brought up to 100mL in a volumetric flask with roH<sub>2</sub>O and the manganese concentration was determined by ICP-OES (Section 2.8.7).

#### **2.9.4 Fourier transform infra-red spectroscopy (FTIR)**

FTIR was used to compare the purity and relative spectras of chemical grade, analytical grade, chemically produced (Section 2.9.2) and biologically produced manganese oxides. Solid samples (powder) were processed with the facilities and assistance from Mr Alan White of the School of Chemistry, Griffith University Nathan campus and analysed using a Spectrum 2 System FTIR spectrometer (Perkin Elmer).

#### **2.9.5 Scanning electron microscopy (SEM)**

SEM was used to visualise the differences in chemical grade, analytical grade, chemically produced (Section 2.9.2) and biologically produced manganese oxides as well as determine the structural characteristics of manganese transforming bacteria. Samples were crushed with a sterilised pestle and mortar and loaded onto a carbon tape before being visualised at 1,000x, 3,000x and 5000x magnification. Samples were processed with the facilities and assistance from Mr Glenn Walker of the Australian National Fabrication Facility, Brisbane Australia and analysed using a JSM-6510LV Scanning Electron Microscope (Jeol USA).

## 2.10 Molecular Techniques

### 2.10.1 Bacterial DNA extraction and purification

DNA extraction of bacterial samples was achieved using a modified method of Marmur (1961). Enrichments were transferred to 50mL falcon tubes and spun at 25,155 rcf for 10 minutes using an Allegra 25R™ centrifuge (Beckman Coulter). The subsequent supernatant was drained, the pellet resuspended with 467µL of P1 buffer (containing 100µg/mL RnaseA) and transferred into a sterile 1.5mL Eppendorf tube. 8µL of lysozyme (60mg/mL) and 16µL of achromopeptidase (10mg/mL) was added, gently mixed and incubated at 37°C for 1 hour. Post incubation 30µL of 10% SDS and 3µL of proteinase K (20mg/mL) was added, gently inverted and incubated at 50°C for an additional hour. The DNA was then purified from the suspension by extracting it with 525µL of a 25:24:1 mixture of phenol: chloroform: isoamylalcohol and inverted gently for 10 minutes. The suspension was centrifuged at 17,970 rcf for 15 minutes and then the upper phase was transferred to a sterile 1.5mL Eppendorf tube. An equal volume of -20°C 100% ethanol was added to precipitate out the DNA. The solution was then centrifuged at 17,970 rcf for 15 minutes, the ethanol was removed and the DNA pellet thoroughly dried in a 50°C incubator. The DNA pellet was then resuspended by adding 40µL TE buffer and the DNA quality assessed by agarose gel electrophoresis (Section 2.10.2).

### 2.10.2 Agarose gel electrophoresis

Agarose gel electrophoresis was utilised to analyse the concentration and purity of extracted DNA and PCR products. Agarose gels were prepared by weighing out 0.75g agarose and adding it to 50mL 1x TAE buffer for a final gel concentration of 1.5%. Agarose was dissolved by boiling and allowing it to cool to 55°C. 0.1µg/mL ethidium bromide was added and thoroughly swirled through before the solution was transferred to a horizontal electrophoresis apparatus and allowed to set. The gel was then submerged with 1x TAE buffer and 200ng of λHindIII ladder standard for assistance in determining DNA fragment size. 5µL of each DNA sample was mixed with 2µL of 6x loading buffer and loaded into the electrophoresis apparatus. Electrophoresis occurred for 40 minutes at 120V, 80mA and gels were then visualised under UV light for further analysis.

### 2.10.3 PCR amplification of 16S rRNA genes

The Polymerase Chain Reaction (PCR) method was used to amplify 16S rRNA genes from extracted bacterial DNA. PCR was achieved through the use of *MangoTaq* polymerase system and reactions prepared in 49µL aliquots of reagents containing:

**Table 2.8:** Chemical composition of each PCR reaction (for a total of 49µL). Preparation of master mix was performed under sterile conditions.

Reagent	Volume per reaction (µL)
5x MangoTaq reaction buffer	10.00
MgCl <sub>2</sub> (50mM)	2.00
iTaq-dNTP's (100mM)	1.00
MangoTaq DNA polymerase	0.50
Forward Primer *	1.00
Reverse Primer *	1.00
sdH <sub>2</sub> O	33.50

\* A comprehensive list of primers used is found in Section 2.10.4

1  $\mu$ L of each bacterial DNA sample was added to each reaction and a negative control containing sdH<sub>2</sub>O was incorporated to ensure the accuracy of results. Samples were overlaid with 50  $\mu$ L sterilised mineral oil and cycling achieved using a Corbett Research Palm Cycler CP-002. In total PCR was achieved in 32 cycles of the following times/temperatures:

**Table 2.9:** Cycling criteria for amplification of 16S rRNA of bacterial samples.

Temperature	Time	Number of cycles
94°C	2 minutes	1
94°C	1 minute	30
50°C	1 minute	
72°C	1.5 minutes	
72°C	10 minutes	1
25°C	-	-

#### 2.10.4 Oligonucleotides used in PCR and sequencing

Universal oligonucleotides used for PCR amplification and sequencing of DNA samples are described in Table 2.10. Primer stocks were diluted to a concentration of 50  $\mu$ M in Tris-HCl (pH 8) and this concentration of primer was used for PCR. For sequencing, primers were diluted to a concentration of 3.2  $\mu$ M in sdH<sub>2</sub>O.

**Table 2.10:** Comprehensive list of primers used for PCR amplification and sequencing as well as the sequences and location on the *E. coli* 16S rRNA gene (Brosius *et al.*, 1981; Frank *et al.*, 2008).

Primer	<i>E. coli</i> position	Primer Sequence 5' -> 3'
<b>Fd1</b>	8 – 27	AGA GTT TGA TCC TGG CTC AG
<b>Rd1</b>	1542 – 1526	AAG GAG GTG ATC CAG CC
<b>F1</b>	339 – 357	CTC CTA CGG GAG GCA GCA G
<b>R6</b>	1513 – 1494	TAC GGT TAC CTT GTT ACG AC
<b>27F</b>	27 – 43	AGA GTT TGA TCM TGG CTC AG
<b>1492R</b>	1492 – 1477	TAC CTT GTT ACG ACT T

### 2.10.5 Purification of PCR products

Successful PCR amplicons were run on a 1.5% agarose gel and products were visualised over a UV-transilluminator and excised with a sterilised scalpel. PCR products were then removed from the gel and purified using QIAquick PCR purification spin columns in conjunction with the recommended protocol by the manufacturer (QIAGEN Pty Ltd, Australia). Alternatively, PCR products in solution were purified using SureClean+ (Bioline) as per the manufacturer's protocol.

### 2.10.6 Automated dye terminator cycle sequencing

Sanger sequencing was used to determine the 16S rRNA sequences of the isolates. Sequencing reactions were prepared in 0.2mL sterile centrifuge tubes and contained a collective 20µL of master mix (Table 2.11) and purified PCR product as per the manufacturers instruction (Applied Biosystems, Australia). The volume of PCR product required was determined by agarose gel electrophoresis (requiring ~200ng sample) and all reactions included a negative control of sdH<sub>2</sub>O.

**Table 2.11:** List of reagents and quantities used for big-dye sequencing. Quantity of sample used varied depending on DNA concentration of purified PCR product. Unless specified otherwise, primers used for sequencing were Fd1 and Rd1 (3.2µM).

Reagent	Volume per reaction (µL)
Purified PCR product	1.00 – 4.00
ABI BigDye™ v3.1	4.0
10x Taq buffer	2.0
Forward / Reverse Primer	1.0
sdH <sub>2</sub> O*	9.00 – 13.00

### **2.10.7 Community DNA extraction and purification**

Community DNA extraction of PHS water samples was achieved by spinning down a large quantity of water to obtain a pellet for downstream processing. 1L of PHS water obtained from directly above the heat source (20 x 50ml falcon tubes) was spun down at 25,155 rcf for 10 minutes using an Allegra 25R™ centrifuge (Beckman Coulter). Supernatant was discarded and pellets were collected and combined into a 15ml falcon tube, before a final spin at 17,970 rcf for 15 minutes. The aggregate sample was sent to the Australian Genome Research Facility (Adelaide).

## 2.11 Molecular Analysis

### 2.11.1 Bacterial DNA extraction and purification

Sequence data was imported into the sequence alignment editor (BioEdit v.7.0.9.0) and the individual chromatograms examined and any data generated in error were fixed when applicable. Also, contiguous sequences were formed through Bioedit (Hall, 1999) and analysed using blastn from GenBank (Altschul *et al.*, 2001). Individual sequences were inputted into the Ribosomal Database Project (RDP) to determine relative taxonomy and the sequence data of the 20 closest relatives exported (Cole *et al.*, 2014). Nearest evolutionary neighbours and isolate sequences were imported alongside into PhylogenyFR and unrooted dendrograms were constructed based on this information (Dereeper *et al.*, 2008).

### 2.11.2 Metagenomic analysis

Total community DNA for Metagenomic analysis was extracted and purified using the community DNA extraction method (Section 2.10.7). Samples were sequenced by AGRF using a Roche 454 GS-FLX system (Hoffmann-La Roche, Switzerland) targeting the 27F – 519R region of the 16S rRNA bacterial gene. Sequencing base quality and read data were assessed using the FastQC software prior to quantitative analysis (Babraham Bioinformatics). Quality control and annotation of 16S rRNA amplicons sequences was achieved by AGRF to determine the relative phyla distributions and organisms present within the water sample. Amplicons that were of insufficient size, quality or did not return a result were categorized under ‘Other’. Community data was visualised using a KRONA distribution diagram (Ondov *et al.*, 2011).

### **2.11.3 Ion Torrent PGM whole genome sequencing**

High molecular weight DNA for whole genome sequencing was prepared using the DNA extraction method (Section 2.10.1). Samples were run on agarose gel electrophoresis (Section 2.10.2) to determine concentration (>200ng purified DNA was required) and downstream sequencing utilised to confirm DNA purity. Finally, the DNA concentration of the sample was verified using agarose gel electrophoresis using 200ng of  $\lambda$ HindIII ladder as a standard. DNA samples were subsequently submitted to the Australian Genome Research Facility (AGRF) and processed using an Ion Torrent PGM Sequencer (Life Technologies) using a 318chip, 200bp reads.

### **2.11.4 Whole genome sequence assembly and alignment**

Whole genome sequences obtained through Ion Torrent Sequencing were aligned and assembled through the assembly programs Mimicking Intelligent Read Assembly (MIRA) and Newbler. Sequence assembly through MIRA is based on an overlap-layout-consensus approach where sequences of low quality are removed by the MIRA protocol before sequence alignment occurs. The alignments produced are then checked for errors using the Waterman alignment algorithm (Smith & Waterman, 1981) and following contigs produced. Newbler is a Linux based platform used to identify overlap reads and constructs contigs based on these reads. The software is then used to collaborate generated contigs based on quality (quantified as a quality score). Contigs can then be organised into scaffolds using pair end information (Trivedi *et al.*, 2014). The assembled sequences are finally analysed and genetic and metabolic profiles of the organism were generated.

Genomic annotations for *Bacillus* sp. PMO were performed using the Rapid Annotation using Subsystem Technology (RAST). Assembled and aligned sequences (MIRA and Newbler) were submitted to the RAST server and subsystems in the genomes and metabolic profiles of the strains were obtained. Sequences were annotated through the RAST server to the genomic programs FIGfams, GLIMMER2, KEGG and SEED which assigned gene functions and identified protein encoding rRNA and tRNA genes (Aziz *et al.*, 2008). This process also predicts the subsystems that are represented in the genome and reconstructs a metabolic profile of the organism (KEGG) and the annotated genome can be compared with other genomes (SEED) (Overbeek *et al.*, 2005).

# Chapter 3

Culture Dependent and  
Independent Analysis of  
Paralana Hot Springs

## 3.1 Introduction

### 3.1.1 Paralana hot springs

Situated in South Australia, Paralana hot springs (PHS) is a hydrothermal geographic phenomenon as it heated by radioactive decay in addition to the archetypal, geothermal heat source. The surrounding Mt Painter and Mt Gee regions are rich in mineral deposits, especially uranium at Olympic Dam and Beverly where the world's largest deposits are situated. With radon and uranium present, astonishingly, evidence of bacterial communities and biofilms are palpable at this previously thought-to-be uninhabitable environment. Moreover, the presence of epithermal Cu-Fe and Fe-U mineral deposits is indicative that metal-reducing bacteria encompass the necessary energy requirements to survive (Brugger *et al.*, 2005).

Very few investigations have looked at the microbial ecology of environments analogous to PHS. The geographical characteristics of Paralana position it to be an ideal milieu for thermotolerant and thermophilic bacterial growth, with many of these capable of metal reduction. The deposits in surrounding areas are commercially mined for export to foreign countries and are also a source of heat for the spring. Evidence of biofilms in the form of microbial mats (Figure 3.1) suggests that bacterial organisms are capable of surviving, even in the presence of radioactive elements. These microbial mats grow in temperature gradients as the water flows away from the source of heat; seeping water connecting with rock fractures at the bottom of the pool. Generally, analogous studies of heated environments have involved artesian and volcanically heated water systems; with very few studies having focused on radioactively heated pools.



**Figure 3.1:** Evidence of microbial mats at Paralana hot springs.

The temperature of the waters of PHS is (on average) 57°C with a neutral pH (7-8). With declining temperature gradients away from the springs heat source, the waters contain numerous heavy metals in trace levels, however there are relatively high concentrations of Uranium (up to 600 ppb) and Radon (concentrations of ~10,900 Bq/m<sup>3</sup>) (Brugger *et al.*, 2005). It is predicted that through evolutionary mechanisms, thermotolerant/thermophilic organisms have become capable of utilising various metals as an electron acceptors and donors, and many have potential to convert these into non-toxic variants. This environment is therefore an important aim of research due to its potential in bioremediation through the presence of metal transforming bacteria.

### 3.1.2 Great Artesian Basin (GAB)

The Great Artesian Basin (GAB) is an aquifer that underlies ~20% of the Australian continent. The GAB is a thermally heated, oxic/anoxic subsurface environment with temperatures ranging from 30°C to 100°C (depending on depth) and shares several geographical conditions to PHS. The GAB is important the livelihood of rural Australian communities, providing fresh water to them through various bores (Kanso et al., 2002). Additionally, the GAB is of great significance from a microbiological stand point as it has remained relatively isolated since its formation over 100 million years ago (Wright, 2010). Figure 3.2 and Figure 3.3 depicts the GAB and the significant attributes of this environment.

The GAB is of specific interest as a comparator to PHS as it is probable to be a significant source of the hot springs' water, possibly from a direct subsurface link to the GAB. Additionally, sections of the GAB also have elevated metal concentrations, similar to PHS (Brugger *et al.*, 2005). It is therefore assumed that the microbial ecology of the two locations share a degree of similarity. However, the presence of radioactivity incorporated into PHS from the surrounding environment will likely influence the type of microbes present.

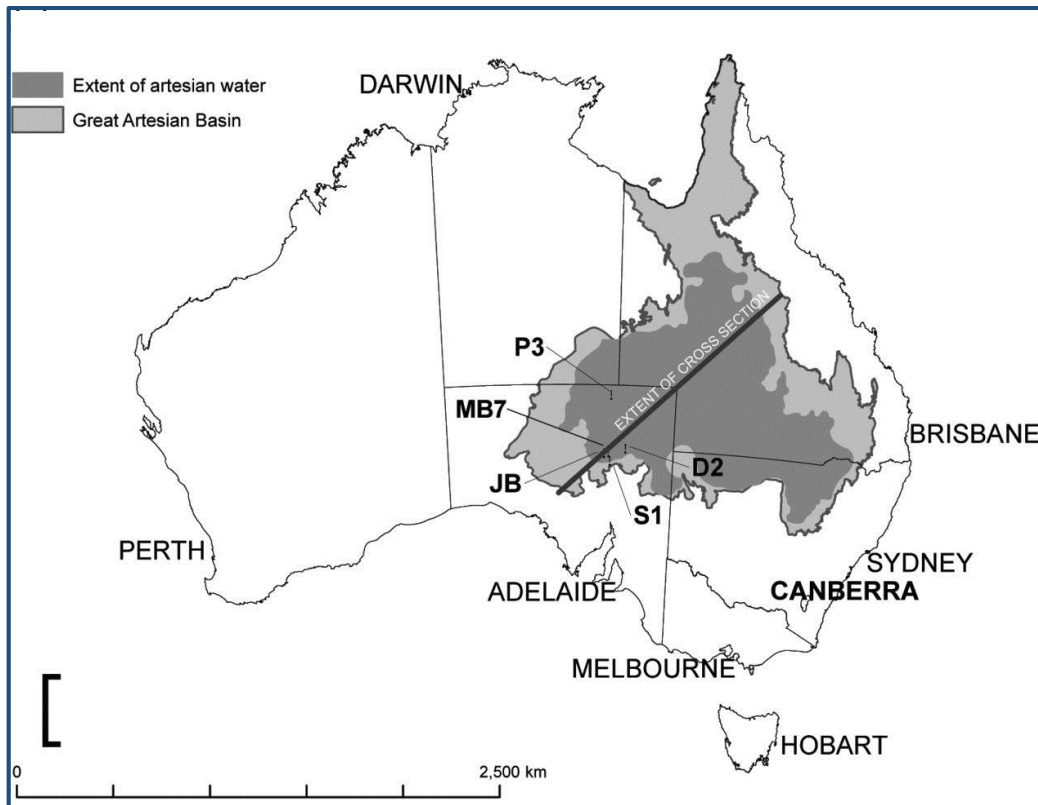


**Figure 3.2:** The Great Artesian Basin of Eastern and Southern Australia and its subsurface geographical features (Bekesi *et al.*, 2013).

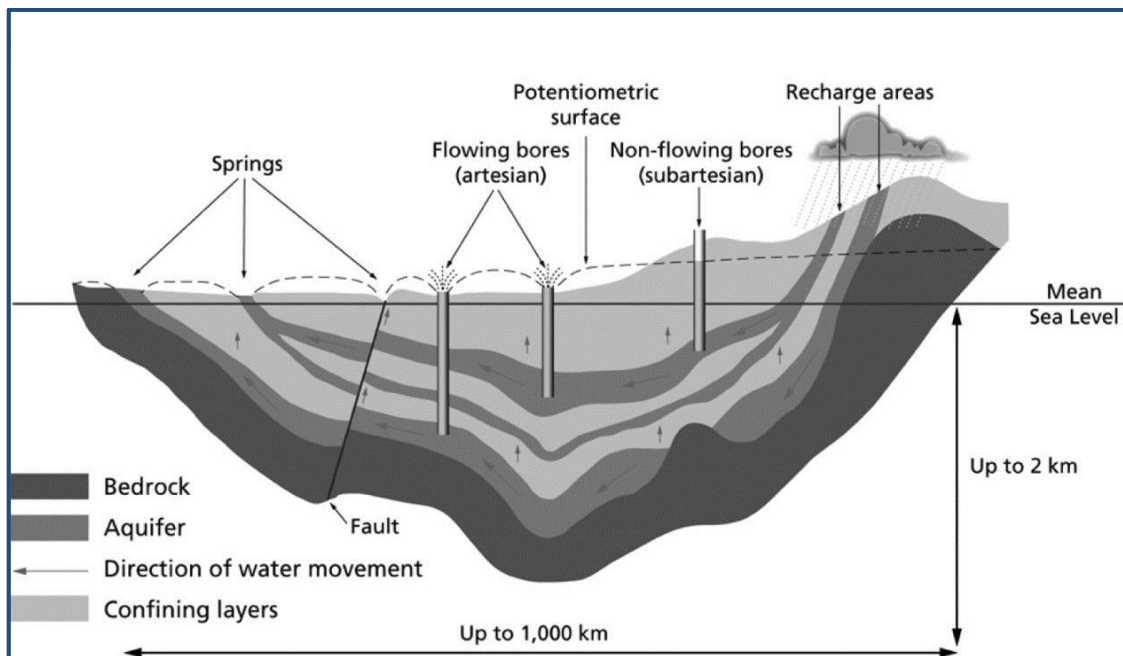


**Figure 3.3:** Cross-section of GAB showing various attributes of the basin (Bekesi *et al.*, 2013).

### 3.1.3 Microbial detection

Detection of microbes in an environmental sample provides an insight of the types of organisms present and the mechanisms that they possess. From an environmental standpoint, the identification of microorganisms helps understand the ecological influence these organisms may have in the cycling of various compounds, breakdown/production of metabolites, etc. Microbial identification is achieved through two different methods; culture dependent and culture independent analysis.

Culture dependent studies involve obtaining pure isolates through enrichments of sample sediments/waters and identification through 16S rRNA sequencing. Culture medium designed to mimic the environment of interest is combined with sample waters/sediment incubated under conditions similar to the original environment. Through this, pure cultures are obtained through one of several microbiological techniques (agar streaking, dilutions to extinction, agar shakes) and the isolate is regrown for further analysis. The isolate is then subject to genetic screening (typically 16S rRNA sequencing for bacteria) and characterisation studies performed. Culture dependent analysis of an environment offers a great deal of information on some organisms, but precludes those organisms not targeted by enrichments and is by no means a representative study.

Culture independent studies involve metagenomic analysis of samples to obtain representative data of organisms present within a location. Total DNA is extracted from an environmental sample and is then also subject to genetic screening (typically 16S rRNA sequencing for bacteria). Sequences are then processed and are the subject of bioinformatics; offering phyla distribution, organisms present (both cultured and uncultured). Studies of this nature provide a significant amount of information about the microbial community within an environment but offer very little information about the functions and characteristics of these organisms.

### 3.2 Chemical Analysis of PHS Waters

Trace element concentrations of primary pool samples P1W, P1S, P2W and P2S were assessed to detect metals present for microbial reduction. In addition to macronutrients (calcium, magnesium, potassium and sodium) concentrations of arsenic, chromium, cobalt, iron, manganese, molybdenum, selenium, uranium and vanadium were determined (Table 3.1). To assist in growth optimisation, pH was also established for each pool sample (Table 3.2).

**Table 3.1:** Trace element concentrations of macronutrients and heavy metals in pool samples P1W, P1S, P2W and P2S.

Elements by ICP-OES		Concentrations in Each Pool Sample			
Element	Units	P1W	P1S	P2W	P2S
Arsenic	ppb	44	28	18	20
Calcium	ppm	44	42	22	130
Chromium	ppb	0.9	0.5	0.2	1.7
Cobalt	ppb	0.1	0.1	< 0.1	1.1
Iron	ppb	37	240	< 5	2200
Magnesium	ppm	16	16	17	34
Manganese	ppb	0.3	1.9	< 0.1	140
Molybdenum	ppb	79	50	3.4	49
Potassium	ppm	25	25	28	35
Selenium	ppb	< 1	< 1	< 1	< 1
Sodium	ppm	300	290	320	310
Uranium	ppb	93	15	4.2	19
Vanadium	ppb	6.9	3.5	0.3	5.2

**Table 3.2:** Water pH of pool samples P1W, P1S, P2W and P2S

	P1W	P1S	P2W	P2S
pH	7.08	7.19	8.22	7.58

### 3.3 Aerobic Screening

#### 3.3.1 Thermophilic aerobic enrichments

The utilisation of various electron donors by bacteria was assessed between PHS pool samples. Growth in all pools was exhibited in conjunction with yeast extract, lactate and L-Asparagine whereas L-Glucose (isomer of D-Glucose) exhibited no growth. Bacteria present in pools P1W and P1S contained bacteria capable of utilising the largest variety of electron donors (growth in 9 out of 10 tested), with P2S presenting growth in 8 out of 10 tested. Sample P2W showed the lowest range of varied growth, occurring only on yeast extract, lactate and L-Asparagine (Table 3.3). Yeast extract was determined to yield the highest levels of growth and was chosen as the primary donor for future screening studies.

**Table 3.3:** Aerobic enrichments of PHS environmental samples. Grown on various electron donors in conjunction with PL media (60°C, pH 7.5).

Electron Donors		Growth			
Donor	Conc.	P1W	P1S	P2W	P2S
L-Asparagine	10mM	+	+	+	+
Casamino acids	0.1%	+	+	-	-
Fructose	10mM	+	+	-	+
Galactose	10mM	+	+	-	+
D-Glucose	10mM	+	+	-	+
L-Glucose	10mM	-	-	-	-
Lactate	5mM	+	+	+	+
Maltose	10mM	+	+	-	+
Succinate	10mM	+	+	-	+
Yeast extract	0.2%	+	+	+	+

### 3.3.2 Aerobic cell content in PHS sediments

The numbers of aerobes present within each pool were determined using the MPN studies. Growth was tested at 60°C, pH 7.5 and with 0.2% yeast extract. Pool P2S was deemed to possess the highest cell count of  $2.0 \times 10^5$  bacteria per 100ml under these conditions, with P2W exhibiting the lowest numbers with only  $2.5 \times 10^4$  bacteria per 100ml (Table 3.4).

**Table 3.4:** Most probable numbers of aerobes present within each pool sample. Grown on PL medium (60°C, pH 7.5, 0.2% yeast extract).

Condition Tested	Bacterial Count / 100mL			
	P1W	P1S	P2W	P2S
Aerobic	$7.5 \times 10^4$ cells/100 ml	$1.1 \times 10^5$ cells/100 ml	$2.5 \times 10^4$ cells/100 ml	$2.0 \times 10^5$ cells/100 ml

### 3.3.3 16S rRNA sequencing and phylogenetic analysis of aerobes

From the enrichments studies (Table 3.3), 34 strains were obtained through colony isolation. These isolates were sequenced to determine if novel thermophiles were present in the pool samples (Table 3.5).

**Table 3.5:** Aerobic PHS isolates. Grown on various electron donors, temperatures and pH in conjunction with PL media.

Isolate	e <sup>-</sup> Donor	pH	Temperature	Closest Neighbour (%)
MAE-001	D-Glucose	7.5	60°C	<i>Anoxybacillus gonensis</i> (94%)
MAE-011	Maltose	7.5	60°C	<i>Anoxybacillus thermarum</i> (95%)
MAE-015	Lactate	7.5	60°C	<i>Anoxybacillus kamchatkensis</i> (95%)
MAE-002	D-Glucose	7.5	60°C	<i>Anoxybacillus kamchatkensis</i> (98%)
MAE-004	Yeast extract	7.5	60°C	<i>Anoxybacillus kualawohkensis</i> (99%)
MAE-008	Casamino acid	7.5	60°C	<i>Anoxybacillus flavithermus</i> (94%)
MAE-009	Fructose	7.5	60°C	<i>Anoxybacillus kamchatkensis</i> (98%)
MAE-014	Galactose	7.5	60°C	<i>Anoxybacillus gonensis</i> (98%)
MAE-020	L-Asparagine	7.5	60°C	<i>Anoxybacillus thermarum</i> (95%)
MAE-017	Lactate	7.5	60°C	<i>Anoxybacillus gonensis</i> (93%)
MAE-021	L-Asparagine	7.5	60°C	<i>Anoxybacillus kamchatkensis</i> (97%)
MAE-003	D-Glucose	7.5	60°C	<i>Anoxybacillus gonensis</i> (96%)
MAE-006	Yeast extract	7.5	60°C	<i>Anoxybacillus kamchatkensis</i> (97%)
MAE-010	Fructose	7.5	60°C	<i>Anoxybacillus flavithermus</i> (97%)
MAE-012	Maltose	7.5	60°C	<i>Geobacillus caldoproteolyticus</i> (94%)
PXF-009	Lactate	7.5	50°C	<i>Anoxybacillus kamchatkensis</i> (97%)
PXF-010	Arabinose	7.5	50°C	<i>Anoxybacillus amylolyticus</i> (99%)
PXF-011	Yeast extract	7.5	50°C	<i>Anoxybacillus contaminans</i> (95%)
PXF-012	L-Glucose	7.5	50°C	<i>Anoxybacillus contaminans</i> (98%)
PXF-013	Maltose	7.5	50°C	<i>Anoxybacillus voinovskiensis</i> (99%)
PXF-014	Peptone	7.5	50°C	<i>Anoxybacillus amylolyticus</i> (98%)
PXF-015	Mannitol	7.5	50°C	<i>Anoxybacillus amylolyticus</i> (99%)

<b>PXF-016</b>	Raffinose	7.5	50°C	<i>Anoxybacillus contaminans</i> (95%)
<b>PXF-018</b>	Uracil	7.5	50°C	<i>Anoxybacillus contaminans</i> (99%)
<b>PXF-019</b>	Valine	7.5	50°C	<i>Anoxybacillus kamchatkensis</i> (99%)
<b>PXF-020</b>	Xylose	7.5	50°C	<i>Anoxybacillus kamchatkensis</i> (99%)
<b>PXF-021</b>	Yeast extract	7.5	50°C	<i>Anoxybacillus kamchatkensis</i> (99%)
<b>PXH-001</b>	2,5-dihydroxybenzoate	7.5	60°C	<i>Anoxybacillus kamchatkensis</i> (99%)
<b>SFD-004</b>	Fructose	7.2	65°C	<i>Anoxybacillus amylolyticus</i> (98%)
<b>SFD-007</b>	Glucose	7.2	65°C	<i>Geobacillus thermoglucosidasius</i> (97%)
<b>SFD-009</b>	Lactate	7.2	65°C	<i>Anoxybacillus amylolyticus</i> (99%)
<b>SFD-010</b>	Arabinose	7.2	65°C	<i>Geobacillus stearothermophilus</i> (99%)
<b>SFD-011</b>	L-Asparagine	7.2	65°C	<i>Geobacillus stearothermophilus</i> (99%)
<b>SFD-012</b>	L-Glucose	7.2	65°C	<i>Anoxybacillus amylolyticus</i> (98%)

### 3.4 Anaerobic Screening

#### 3.4.1 Thermophilic anaerobic enrichments

Growth in conjunction with various electron acceptors was assessed between PHS pool samples. Growth in all samples was exhibited in tubes containing selenium and vanadium and high levels of growth observed in tubes containing iron (as ferric citrate) in pools P1W, P1S and P2S. No growth was evident with chromium. Pool P1S was found to contain bacteria capable of growth under most conditions (9 out of 13 tested) with the lowest variety of growth in sample P2W (growth in 2 out of 13 tested). Visual reduction was observed in tubes containing iron, cobalt and vanadium. For nitrate, sulphate, sulphite, molybdenum, arsenic and selenium it is deduced these substrates were utilised in bacterial metabolism as no growth was observed in tubes without a terminal electron acceptor (Table 3.6).

**Table 3.6:** Presence of growth/reduction in conjunction with various electron acceptors. Grown anaerobically on PL medium (60°C, pH 7.5, 0.2% yeast extract).

Electron Acceptors		Reduction			
Acceptor	Conc.	P1W	P1S	P2W	P2S
No acceptor	N/A	-	-	-	-
Nitrate	10mM	+	+	-	-
Sulphate	10mM	+	+	-	-
Sulphite	2.5mM	-	+	-	-
Arsenic	1mM	+	+	-	-
Chromium	1.25mM	-	-	-	-
Cobalt	1mM	-	-	-	+
Iron	2mM	+	+	-	+
Manganese	4mM	+	+	-	-
Molybdenum	1mM	-	+	-	+
Selenium	1mM	+	+	+	+
Uranium	2.5mM	-	+	-	-
Vanadium	5mM	+	+	+	+

### 3.4.2 Anaerobic cell content in Paralana spring sediments

The numbers of anaerobes present within each pool were determined using the MPN technique. In addition to sulphate, iron, uranium and vanadium were tested to determine numbers of bacteria capable of reducing these metals. Bacterial growth coupled with sulphate was determined to be the most commonly used donor, yielding  $8.0 \times 10^5$  cells/100 ml (P1W) and  $2.5 \times 10^6$  cells/100 ml (P1S). In terms of bacterial reduction, pool P2S was found to be the most active (in terms of cellular growth across tested metals) with  $4.5 \times 10^5$  cells/100 ml (iron) and  $1.5 \times 10^5$  cells/100 ml (vanadium). Respectively, cellular growth was lowest in pool P2W with anaerobic respiration evident only in vanadium, with  $2.5 \times 10^3$  cells/100 ml (Table 3.7). In fact, vanadium was the only electron acceptor to show growth in all four samples.

**Table 3.7:** Most probable numbers of anaerobes present within each pool sample. Grown anaerobically on PL medium with various electron acceptors (60°C, pH 7.5, 0.2% yeast extract).

Condition Tested	Bacterial Count / 100mL			
	P1W	P1S	P2W	P2S
<b>Sulphate</b>	$8.0 \times 10^5$ cells/100 ml	$2.5 \times 10^6$ cells/100 ml	-	-
<b>Manganese</b>	$2.0 \times 10^4$ cells/100 ml	$4.0 \times 10^4$ cells/100 ml	-	-
<b>Iron</b>	$8.0 \times 10^3$ cells/100 ml	$9.5 \times 10^4$ cells/100 ml	-	$4.5 \times 10^5$ cells/100 ml
<b>Uranium</b>	-	$6.0 \times 10^5$ cells/100 ml	-	-
<b>Vanadium</b>	$2.0 \times 10^5$ cells/100 ml	$9.0 \times 10^3$ cells/100 ml	$2.5 \times 10^3$ cells/100 ml	$1.5 \times 10^5$ cells/100 ml

### **3.4.3 16S rRNA sequencing and phylogenetic analysis of anaerobes**

Since a variety of electron acceptors were used by PHS organisms, various donors in addition to yeast extract were used alongside these in the isolation of metal reducers. This resulted in 9 isolates and obtained through dilution to extinction series. These isolates were sequenced to determine the presence of the most abundant thermophilic anaerobic metal reducers within the pool samples (Table 3.8).

**Table 3.8:** Anaerobes present in Paralana pool samples. Samples grown anaerobically with PL medium (60°C, pH 7.5, 0.2% yeast extract).

Isolate	e <sup>-</sup> Acceptor	e <sup>-</sup> Donor	pH	Temperature	Closest Neighbour (%)
MNA-002	Vanadium	Maltose	7.5	60°C	<i>Thermobrachium celere</i> (91%)
MNA-003	Cobalt	Yeast extract	7.5	60°C	<i>Thermobrachium celere</i> (90%)
MNA-004	Cobalt	Glucose	7.5	60°C	<i>Thermobrachium celere</i> (91%)
MNA-006	Iron	Yeast extract	7.5	60°C	<i>Caloramator australicus</i> (96%)
MNA-008	Selenium	Yeast extract	7.5	60°C	<i>Anoxybacillus pushchinoensis</i> (98%)
MNA-009	Iron	Fructose	7.5	60°C	<i>Caloramator australicus</i> (95%)
MNA-010	Nitrate	Glucose	7.5	60°C	<i>Anoxybacillus kamchatkensis</i> (99%)
UAY-001	Uranium	Yeast extract	7.2	60°C	<i>Clostridium thermosuccinogenes</i> (98%)
IHW-1405	Iron	Yeast extract	7.5	60°C	<i>Thermobrachium celere</i> (91%)

### 3.5 Manganese Oxidising Bacteria

#### 3.5.1 Manganese oxidising bacterial enrichments

Following on from the initial analysis of aerobes, PHS pool samples were screened for presence of both thermophilic and mesophilic aerobes capable of oxidising metals, specifically manganese. No thermophilic manganese oxidising bacteria were detected however were detected at 37°C. Manganese oxidation activity was exhibited in samples P1W (with yeast extract and glucose) and P2S (with yeast extract) and occurred 5-7 days after initial growth had been observed in enrichment tubes. Aerobic growth was evident in samples P1S and P2W; however no subsequent oxidation was observed (Table 3.9).

**Table 3.9:** Presence of manganese oxidation in conjunction with various electron donors. Grown on PL medium (37°C, pH 7.5, with 2mM Mn<sup>2+</sup>).

Electron Donors		Oxidation			
Donor	Conc.	P1W	P1S	P2W	P2S
Casamino acids	0.1%	-	-	-	-
D-Glucose	10mM	+	-	-	-
Fructose	10mM	-	-	-	-
Galactose	10mM	-	-	-	-
Yeast extract	0.2%	+	-	-	+

#### 3.5.2 16S rRNA sequencing and phylogenetic analysis of manganese oxidisers

From the aerobic enrichments, 3 strains were obtained through colony isolation (*Bacillus* sp. PMO, *Bacillus* sp. DLH-1207 and *Bacillus* sp. AEM-1106). 16S rRNA sequencing revealed that strain PMO was 99% similar to *Bacillus anthracis*, strain DLH-1207 was 97% similar to *Bacillus megatarium* and strain AEM-1106 was 98% similar to *Paenibacillus alvei*. From these results, phylogenetic trees were established to visually represent manganese oxidising populations present within each pool sample (Figure 3.4; Figure 3.5; Figure 3.6).

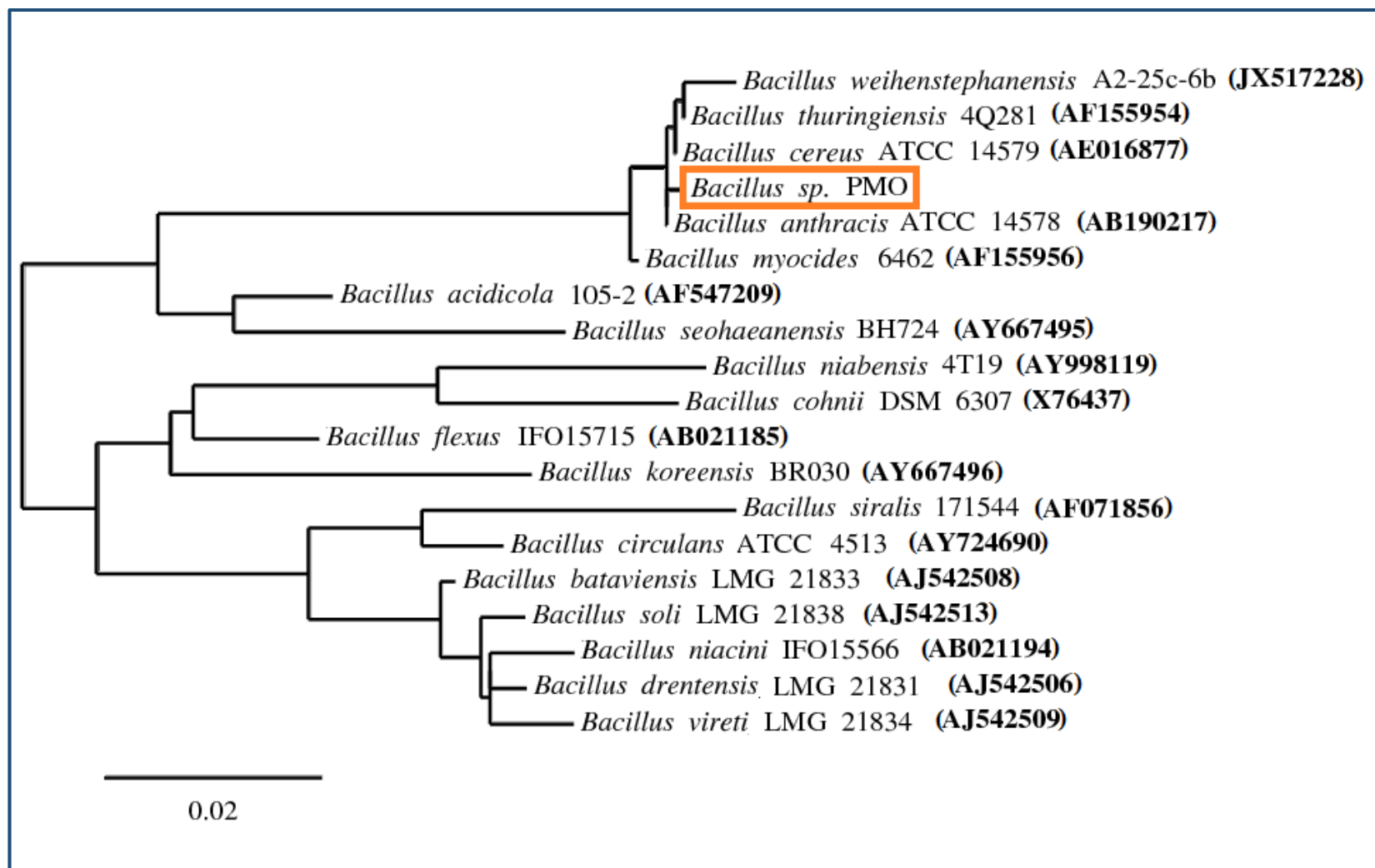


**Figure 3.4:** A dendrogram depicting the phylogenetic position of *Bacillus* sp. PMO and its closest relatives. GenBank accession numbers are given in the parenthesis. Scale bar indicates 2 nucleotide changes per 100 nucleotides.

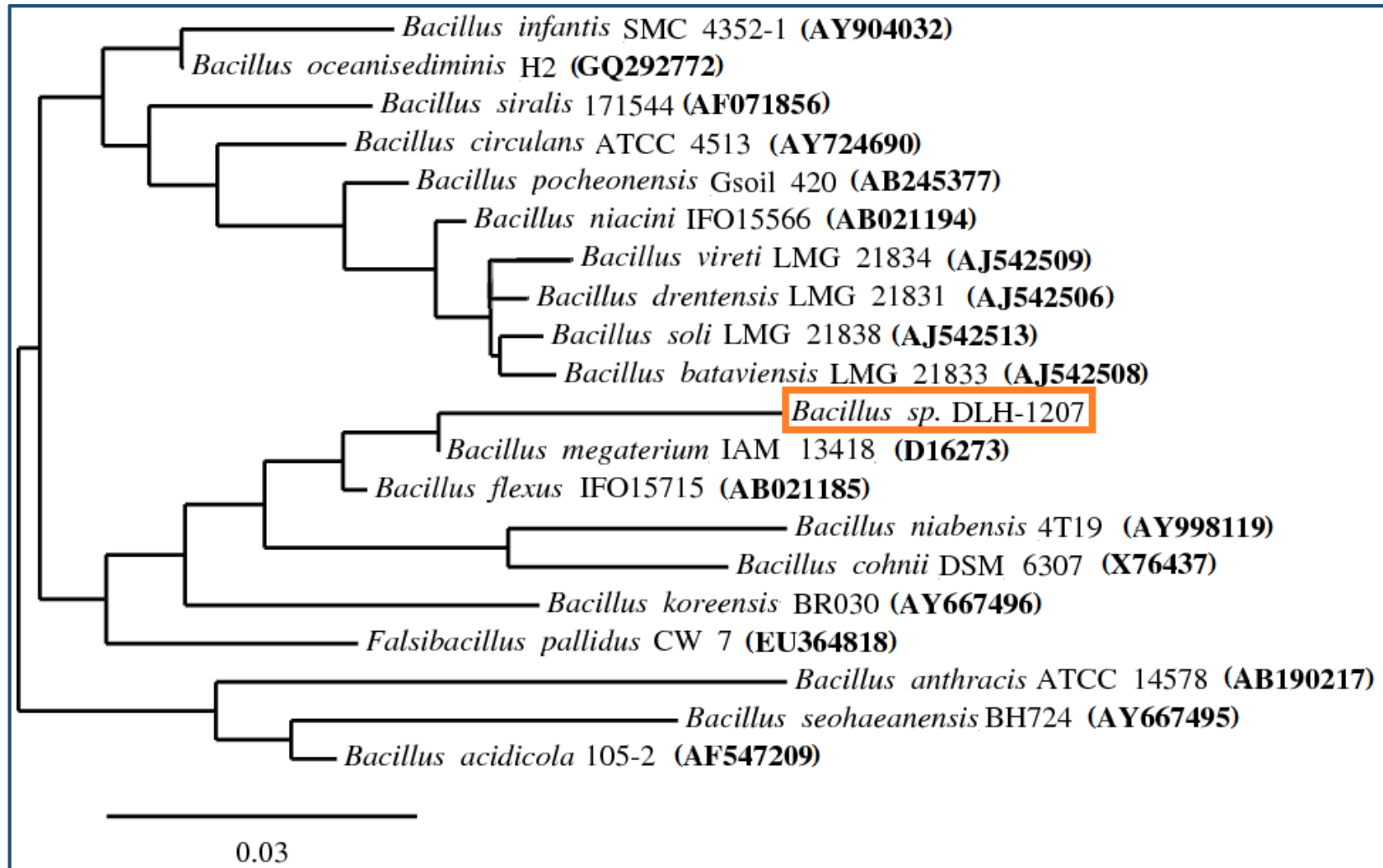


**Figure 3.5:** A dendrogram depicting the phylogenetic position of *Bacillus sp. DLH-1207* and its closest relatives. GenBank accession numbers are given in the parenthesis. Scale bar indicates 3 nucleotide changes per 100 nucleotides.

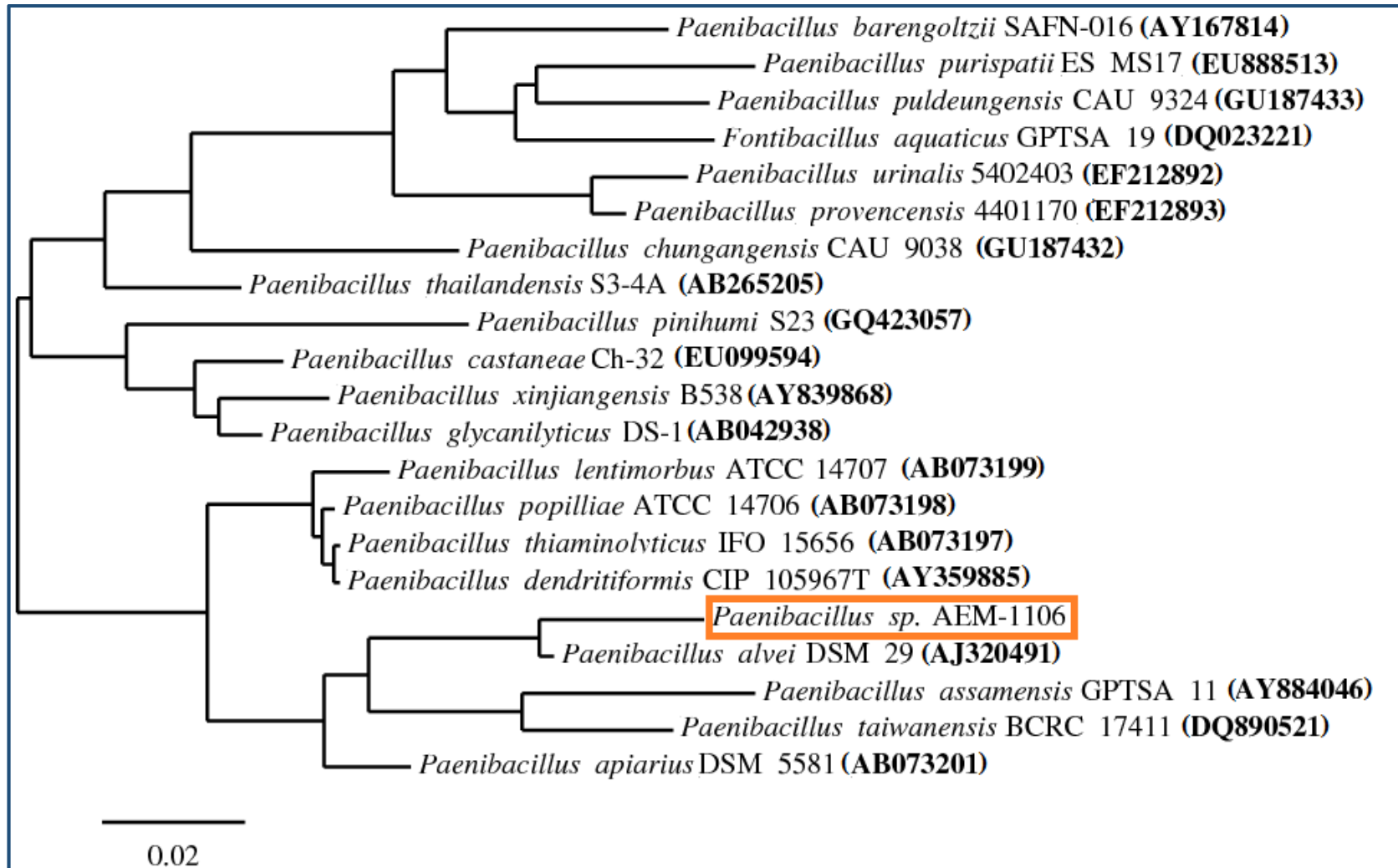


**Figure 3.6:** A dendrogram depicting the phylogenetic position of *Paenibacillus sp. AEM-1106* and its closest relatives. GenBank accession numbers are given in the parenthesis. Scale bar indicates 2 nucleotide changes per 100 nucleotides.

## 3.6 Culture Independent Diversity Profile

### 3.6.1 16S rRNA gene amplicon analysis

A data set of 13,949 sequences was produced from an aqueous PHS water sample cloned on the 16S rRNA gene at bases 27 – 519. Sequence analysis revealed bacteria across 21 phyla (14 cultivated, 6 uncultivated and 1 unclassified) with Cyanobacteria most prevalent within the data set (36.69%). Analysis of sequence data returned a GC-content of 56%. Quality analysis of sequence data gave a mode phred score of 37 (Figure 3.7). Individual per base sequence quality across all bases is seen in Figure 3.8. 18.18% of sequences were not appropriately grouped or used within the diversity profile and were termed ‘other’. These are predominately a result of chimera formation, non-16S rRNA binding or fragments of insufficient size/quality.

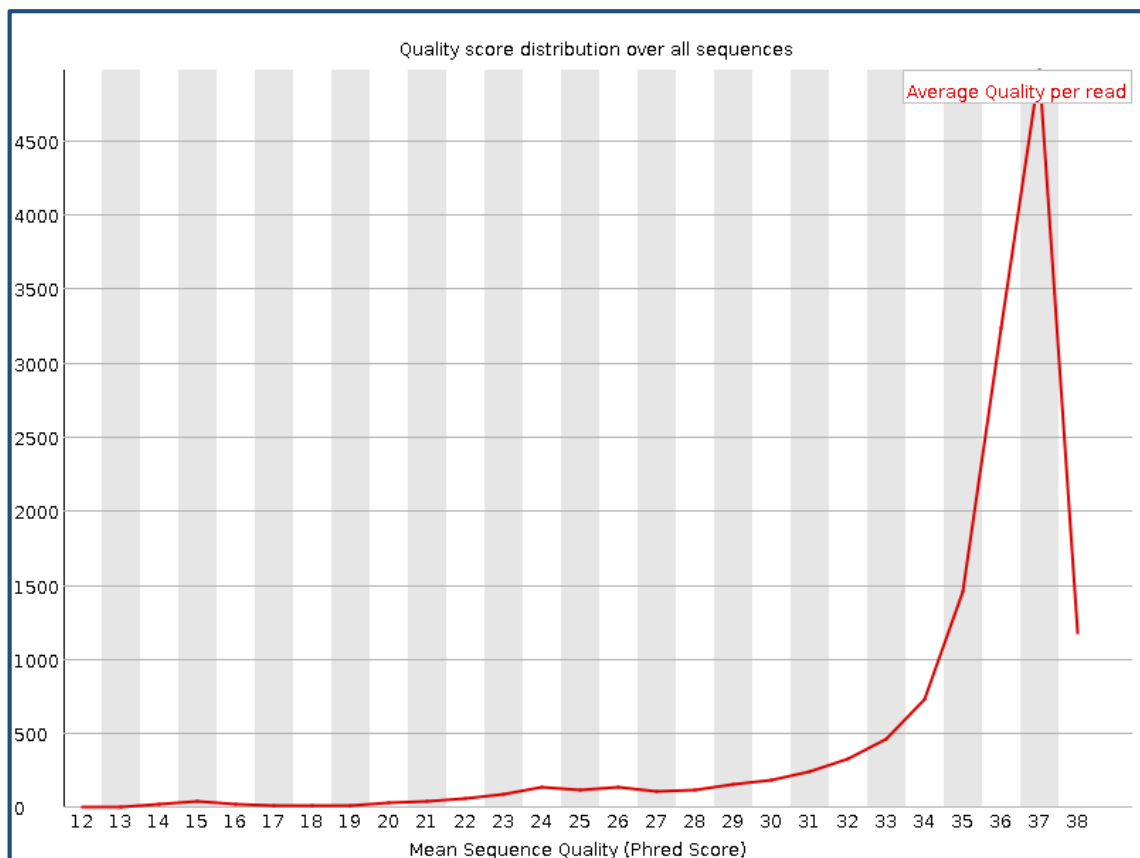


**Figure 3.7:** FastQC quality score distribution across PHS diversity profile sequence data.

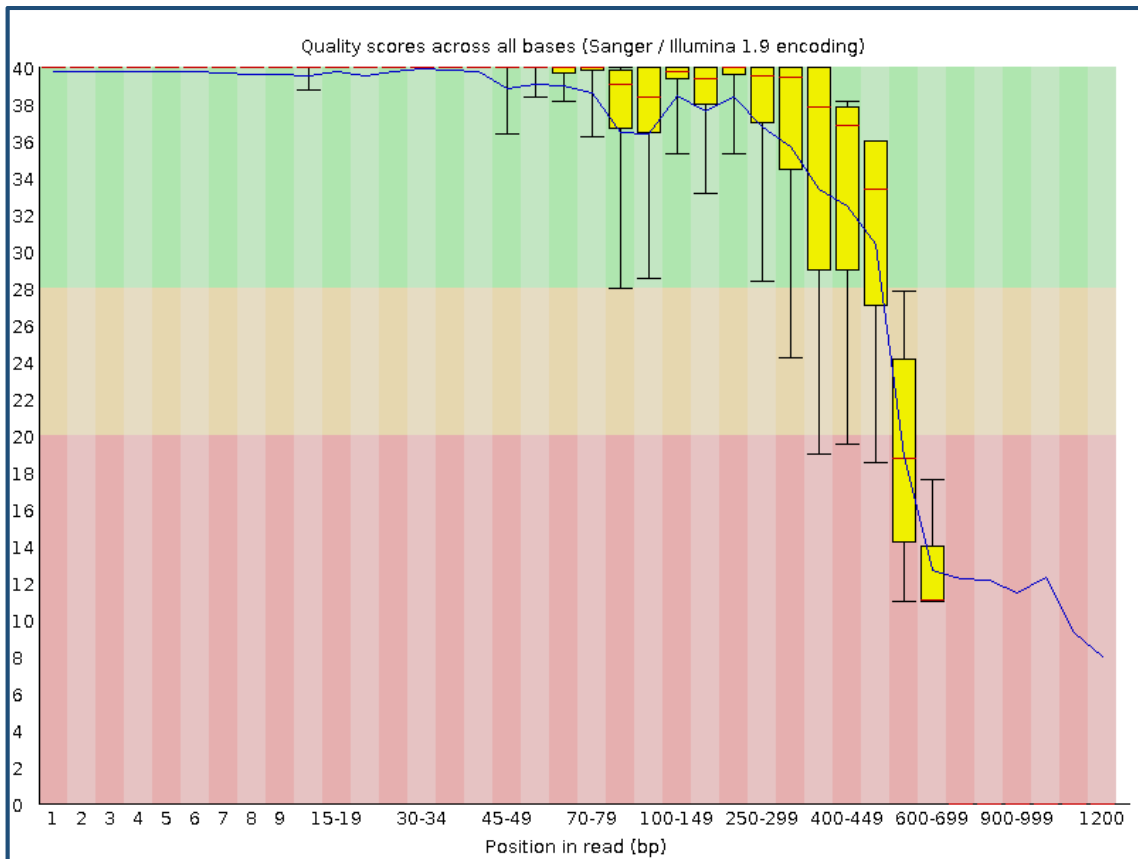


**Figure 3.8:** FastQC quality score of individual position reads of PHS diversity profile sequence data.

### 3.6.2 Phylum Distribution

Diversity profiling revealed bacteria belonging to 21 different phyla from the PHS water sample. Cyanobacteria comprised the largest percentage of detected sequences, with 36.69% of total fragments detected belonging to the phylum. Additionally, Proteobacteria comprised 29.51% of total sequences detected. The remaining 15.62% of sequences belonged to the remaining 21 phyla consisting of 14 cultivated, 6 uncultivated and 1 unclassified groups (Table 3.10; Figure 3.9). The isolates obtained through culture dependent analyses belonged to the phylum Firmicutes and a breakdown of this phyla presented in Table 3.11.

**Table 3.10:** PHS diversity profile sequence distribution organized by phylum. Erroneous sequences removed and relative percentages adjusted.

	Distribution (%)
Taxon (Phylum)	Distribution
Unclassified	0.01%
Acidobacteria	5.41%
Actinobacteria	1.45%
Armatimonadetes	0.01%
BRC1	0.01%
Bacteroidetes	1.15%
Chlorobi	0.17%
Chloroflexi	6.28%
Cyanobacteria	44.84%
Firmicutes	1.36%
Gemmatimonadetes	0.21%
Nitrospirae	0.16%
Planctomycetes	2.16%
Proteobacteria	36.08%
SBR1093	0.03%
Spirochaetes	0.04%
TM6	0.01%
TM7	0.02%
Thermi	0.02%
Verrucomicrobia	0.35%
WPS-2	0.07%
WS3	0.16%
<b>Total</b>	<b>100%</b>

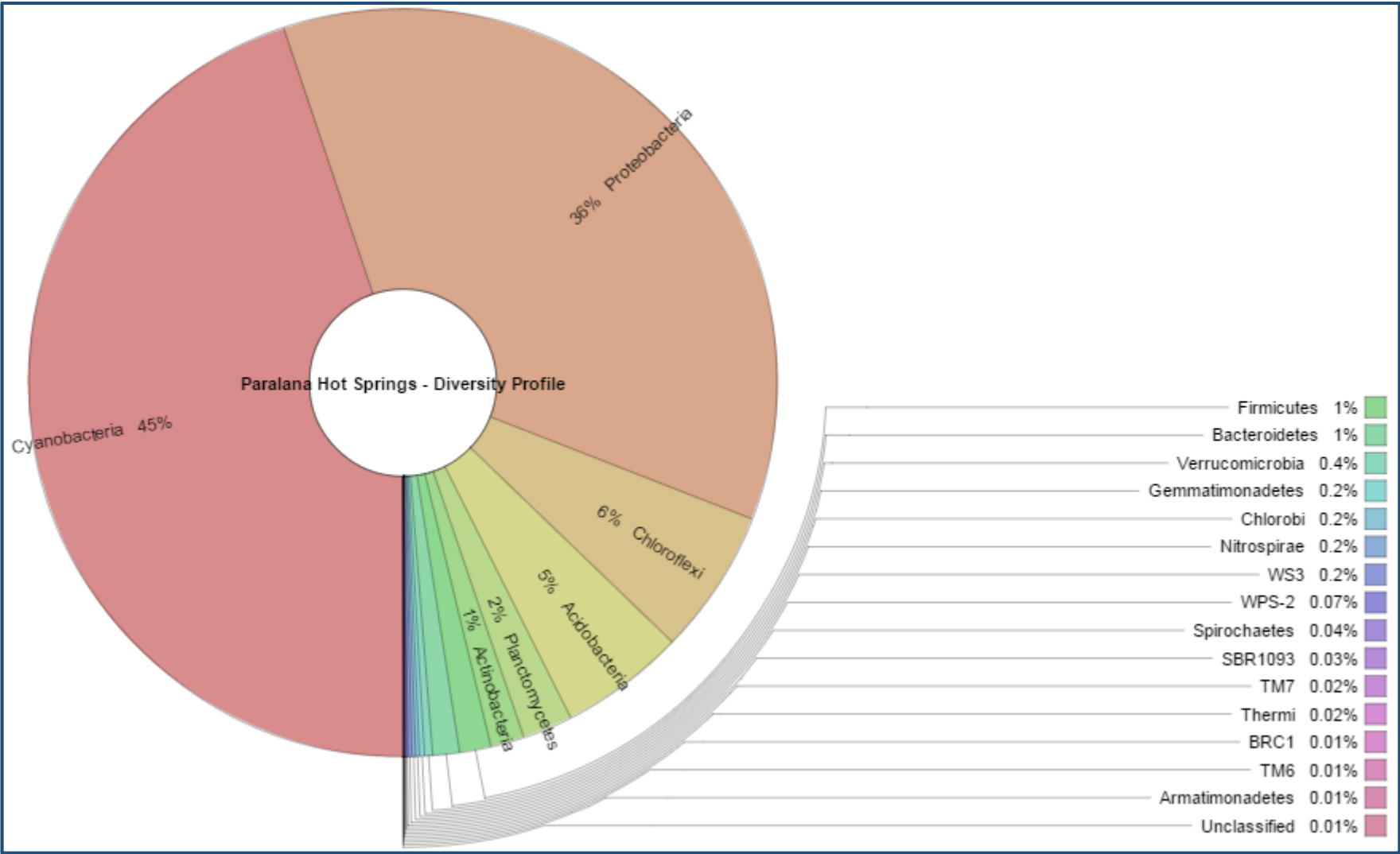


**Figure 3.9:** KRONA diagram depicting relative distributions (phylum) following Metagenomic analysis of PHS diversity profile sequence data.

**Table 3.11:** Detected sequences within the phylum Firmicutes.

Firmicutes				
Class	Order	Family	Genus	Sequences
Unclassified	-	-	-	<b>3</b>
Bacilli	Unclassified	-	-	<b>1</b>
Bacilli	Bacillales	Unclassified	-	<b>5</b>
Bacilli	Bacillales	Bacillaceae	Unclassified	<b>3</b>
Bacilli	Bacillales	Bacillaceae	<i>Bacillus</i>	<b>3</b>
Bacilli	Lactobacillales	Streptococcaceae	<i>Lactococcus</i>	<b>14</b>
Clostridia	Unclassified	-	-	<b>2</b>
Clostridia	Clostridiales	Unclassified	-	<b>2</b>
Clostridia	Clostridiales	Clostridiaceae	Unclassified	<b>11</b>
Clostridia	Clostridiales	Clostridiaceae	<i>Alkaliphilus</i>	<b>35</b>
Clostridia	Clostridiales	Clostridiaceae	<i>Caloramator</i>	<b>50</b>
Clostridia	Clostridiales	Clostridiaceae	<i>Clostridium</i>	<b>1</b>
Clostridia	Coriobacteriales	Coriobacteriaceae	Unclassified	<b>10</b>
<b>Total</b>				<b>154</b>

### 3.6.3 Detection of chlorophylls and bacteriochlorophylls

As the primary group of microbes in PHS were phototrophs, chlorophylls and bacteriochlorophylls in the water were analysed by scanning UV-Vis spectroscopy. Scanning spectroscopy revealed absorbance at 380-500nm and 600-690nm, with major peaks detected at 435nm, 480nm, 615nm and 667nm, confirming the presence of *Chl a*, *Chl b*, *Chl c<sub>1</sub>*, *Chl d* and *Chl f* within the PHS waters (Figure 3.10; Table 3.12). Additionally, scanning spectroscopy resulted in absorbance at 920-980 and 1010-1020nm, with major peaks detected at 883nm, 962nm and 1015nm, revealing the presence of *Bchl a*, *Bchl b*, *Bchl d* and *Bchl e* (Figure 3.11).

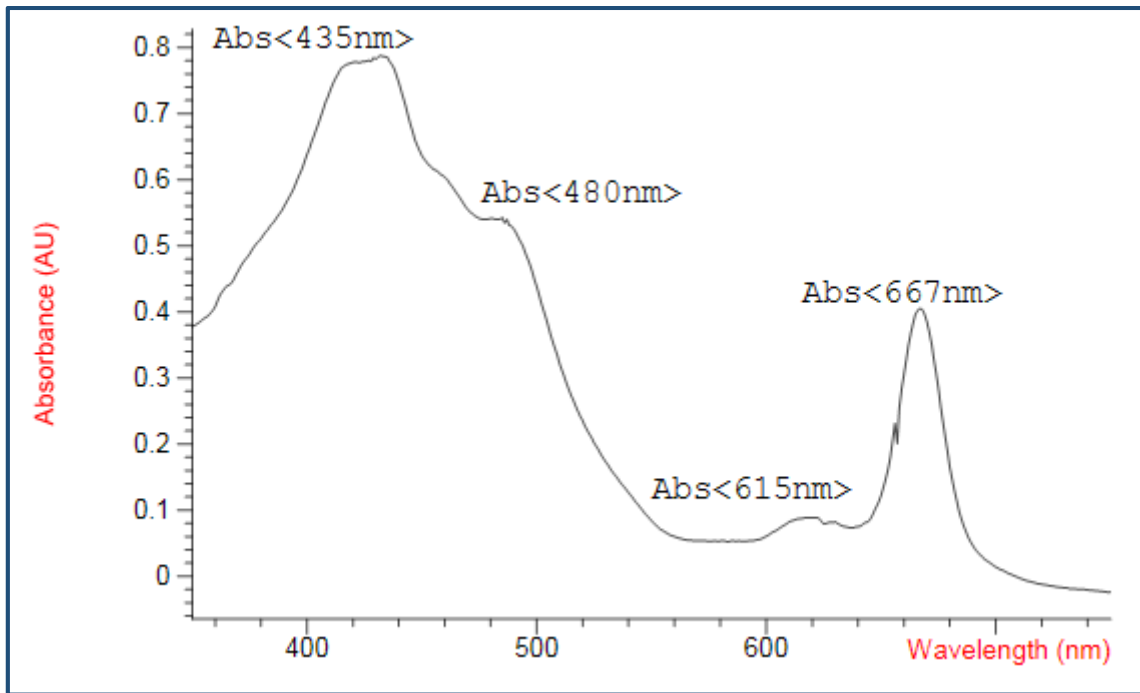


**Figure 3.10:** Chlorophyll detection by scanning UV-Vis spectroscopy (350nm-700nm). Primary absorbance peaks are presented.

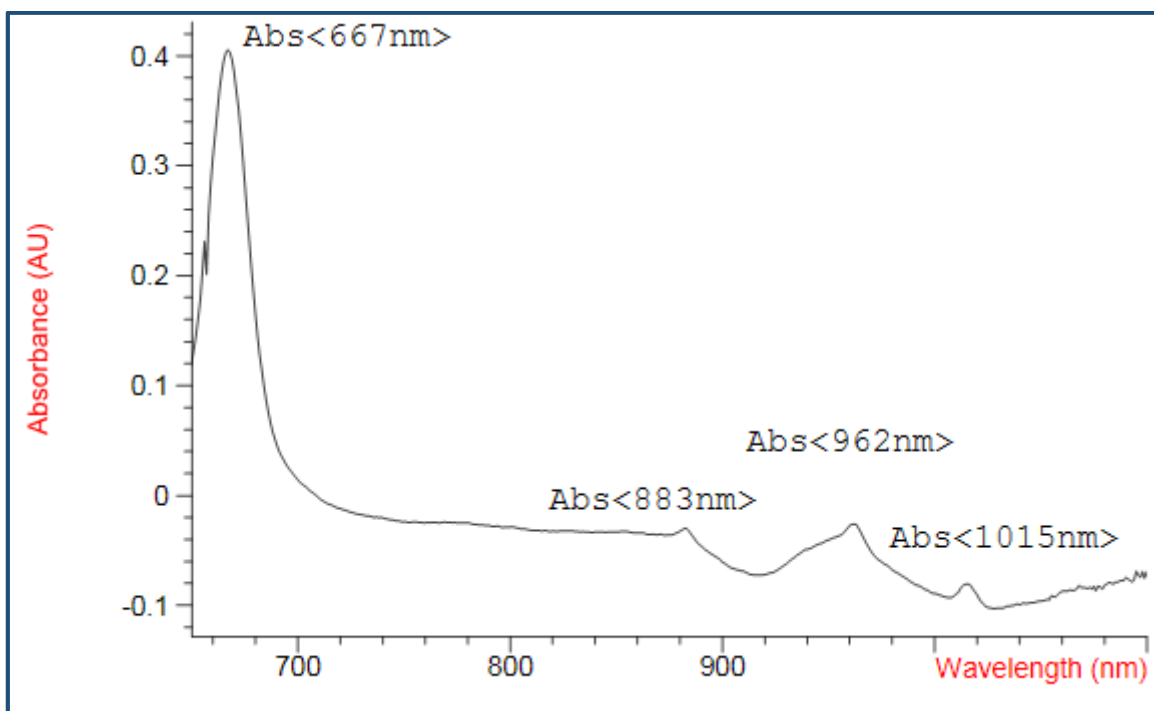


**Figure 3.11:** Bacteriochlorophyll detection by scanning UV-Vis spectroscopy (700nm-1050nm). Primary absorbance peaks are presented.

**Table 3.12:** Major chlorophylls and bacteriochlorophylls and their occurrences in PHS waters.

Chlorophyll	Occurrence	Absorption Peak	Detected in PHS	Reference
<i>Chlorophyll a</i>	Universal	430 nm 665 nm	Yes	Porra <i>et al.</i> , 1989
<i>Chlorophyll b</i>	Predominately plants	450 nm 640 nm	Yes	Porra <i>et al.</i> , 1989
<i>Chlorophyll c<sub>1</sub></i>	Algae	454 nm 630 nm	Yes	Fawley, 1989
<i>Chlorophyll d</i>	Cyanobacteria	446 nm 697 nm	Yes	Miyashita <i>et al.</i> , 1997 Li <i>et al.</i> , 2012
<i>Chlorophyll f</i>	Cyanobacteria	406 nm 706 nm	Yes	Chen <i>et al.</i> , 2010 Li <i>et al.</i> , 2013
<i>Bacteriochlorophyll a</i>	Universal (exc. Cyanobacteria)	800 nm 830-890 nm	Yes	Olsen <i>et al.</i> , 1973 Ponsano <i>et al.</i> , 2008
<i>Bacteriochlorophyll b</i>	Purple bacteria	1020 nm	Yes	Steiner <i>et al.</i> , 1983
<i>Bacteriochlorophyll d</i>	Green sulphur bacteria	429 nm 656 nm	Yes	Borrego <i>et al.</i> , 1998
<i>Bacteriochlorophyll e</i>	Green sulphur bacteria	660 nm	Yes	Borrego <i>et al.</i> , 1999
<i>Bacteriochlorophyll c</i>	Green sulphur bacteria Chloroflexi	740 nm	No	Wang <i>et al.</i> , 2004
<i>Bacteriochlorophyll g</i>	Heliobacteria	770 nm	No	Brockmann Jr & Lipinski, 1983

### 3.7 Discussion

The examination and understanding of the bacteriological makeup within aqueous environments offers insight into the ecological significance that these organisms play in affecting the surrounding physical and chemical conditions. The chapter sought out to identify the most abundant bacteria present both from a culture dependent and independent approach; looking at both aerobic and anaerobic thermophiles. Bacteria belonging to the genera *Anoxybacillus* dominated non-specific aerobic enrichments, identified across all pool samples and over a variety of electron donors. Anaerobic studies revealed primarily low percentage relatives to *Thermobrachium celere*. Additional aerobic enrichments with Mn(II) revealed a number of bacteria capable of manganese oxidation. Finally, culture independent analysis of the spring revealed a diverse range of bacteria belonging numerous phyla, as well as high levels of Cyanobacteria. Paralana hot springs is unique, relatively isolated water source that has an assorted range of metal-transforming, thermophilic and thermotolerant bacteria.

ICP-OES trace analysis of PHS waters detected a variety of metals, including arsenic, chromium, cobalt, iron, magnesium, manganese and vanadium. Of the useable metals in anaerobic respiration, iron was detected in the highest quantities (37ppb and <5ppb in solution, 340 ppb and 2200 ppb in soil). This is indicative of iron cycling within PHS with insoluble iron precipitating out of solution and becoming embedded within the surrounding soils. To a lesser extent this was also evident with manganese, with 0.3 ppb and < 0.1 ppb evident in water samples and 1.9 ppb and 140 ppb detected in soil samples. This predisposition was not observed across any other metals tested. Selenium was included in the ICP-OES analysis and though all returned readings were all <1ppb, positive growth was detected on a single selenium-containing enrichment (Strain MNA-008; 98% similarity to *Anoxybacillus pushchinoensis*). However, there is no visual change in the reduction of selenium in anaerobic respiration; therefore growth under these conditions may have been a result of fermentation as opposed to selenium being used as an electron acceptor.

PHS primary pool samples exhibited growth in both higher levels and on a more diverse range of electron donors/acceptors than the secondary pool samples. When tested under aerobic conditions, both primary pool samples displayed growth on a larger variety of electron donors. While this is only a representative dataset, based on the conditions tested under, it is indicative that microbial activity is highest nearest the heat source. The aerobic MPN studies revealed higher levels of growth in the sediment compared to the liquid samples. It is deduced that as these microorganisms primarily obtain energy as a result of nutrient cycling, so their proximity from the PHS heat source is not vital in supporting aerobic cellular growth. Additionally, hot spring fluids are more likely to be anaerobic. This nutrient cycling also accounts for the increased range of nutrients used by the aqueous communities.

Metal reducing anaerobes were prevalent in PHS primary pool samples and were barely detected in the secondary pool across all tested electron acceptors. P1S, P1W and P2S were found to contain reducers of a variety of metals, including iron, manganese, molybdenum, uranium and vanadium. Conversely, P2W was found only containing a vanadium reducer. Samples obtained from the secondary pool had a significantly higher level of exposure to oxygen and therefore attributes to the lower cell levels through the toxication of obligate anaerobes present in the spring. However, while located in the secondary pool, sedimentary sample P2S was exposed to much less oxygen, which therefore accounts for higher detection of metal reducing bacteria. Furthermore, less microbial activity could have led to a lower supply of recycled nutrients otherwise used to promote bacterial growth.

The 34 aerobic isolates were found most closely related to two distinct genera; *Anoxybacillus* and *Geobacillus* (belonging to the phylum Firmicutes). Interestingly, Firmicutes comprised only 1.11% of detected sequences in the culture-independent analysis of PHS waters. The lack of isolates from more prevalent phyla is most likely due to enrichment conditions favouring the growth of Firmicutes. Specialised media and enrichment conditions (particularly light) would need to be designed to isolate bacteria from Cyanobacteria (highest % detected sequences). Bacteria in the *Bacillaceae* family are extremely versatile and are easy to grow compared to other organisms. They can grow in a range of temperatures, pH and on numerous electron donors and are both aerobic and facultatively anaerobic (Goh *et al.*, 2013). Additionally, they are easily isolated and do not required a specialised growth medium (Inan *et al.*, 2012). It is likely that the robust characteristics of these organisms position them to outgrow bacteria from other genera, and is the reason for their prevalence in the aerobic enrichments.

Culture independent analysis was used to obtain a representative view of the bacterial community in PHS waters. 21 distinct phyla were detected; 14 cultivated, 6 uncultivated and 1 unidentified. Cyanobacteria were the most prevalent, comprising 36.69% of all detected sequences. The PHS water sample was a green-pigment containing sample and it was predicted that photosynthetic bacteria would be the common highly detected. Additionally, phototrophic mats were seen during sample collection (Figure 2.3, Figure 3.1) and made up part of the PHS water composition. 11 of these detected genera have been associated with manganese transforming bacteria; *Bacteroidetes*, *Chlorobi*, *Chloroflexi*, *Nitrospirae*, *Acidobacteria*, *Actinobacteria*, *Cyanobacteria*, *Firmicutes*, *Spirochaetes*, *Proteobacteria* and *TM7* (Tebo et al., 2005). However, further research into these organisms suggests most is limited to three genera; *Firmicutes*, *Actinobacteria* and *Proteobacteria*. Due to the ubiquitous nature of manganese transformers it was predicted that these bacteria would be present in the PHS community study, though based on the low detection percentage of *Firmicutes* the existence of multiple Mn(II) oxidisers was surprising as they are likely to be present in low numbers.

The detection of *Anoxybacillus* spp. in aerobic enrichments was unique as these organisms are facultative anaerobes and it was presumed that strict aerobes would be detected. Specifically, *Anoxybacillus* spp. are moderately thermophilic, rod-shaped bacteria that can be obligately anaerobic or facultatively anaerobic with a growth temperature of 50°C – 65°C (Pikuta et al., 2000; Goh et al., 2013). The anoxic nature of the water at PHS primary heat source combined with the temperature of ~57°C favours the growth of *Anoxybacillus* spp., so it is not unexpected that these bacteria would be detected. The Narayan group found that *Anoxybacillus* spp. was the dominant genus in the Fijian Savusavu hot spring (Narayan et al., 2008). Furthermore, they are commonly found in GAB samples (Ogg, 2011).

Several metal reducing bacteria were isolated through anaerobic enrichments with iron, selenium, uranium, cobalt, molybdenum, arsenic and vanadium used as terminal electron acceptors. Of the sequenced isolates, bacteria primarily belonging to the genus *Thermobrachium* were identified, with the four isolates having a 90% -91% similarity to *Thermobrachium celere*. Further analysis of these four isolates revealed a >99.5% sequence similarity to each other, and it is deduced that this or these are potentially novel multi-metal reducing thermophiles. Similar to the aerobes, *Thermobrachium* are members of the Firmicutes (family *Clostridiaceae*). Again, it is likely that culture conditions selected for these bacteria. *Clostridiaceae* are known for having both metal reducing and fermentative members (Mermelstein *et al.*, 1992; Dobbin *et al.*, 1999; Ogg & Patel, 2009).

Three bacteria in the *Bacillaceae* family were detected as manganese transformers; *Bacillus* sp. PMO, *Bacillus* sp. DLH-1207 and *Paenibacillus* sp. AEM-1106. Similarly, the most studied manganese oxidiser is a *Bacillus* sp, strain SG-1 (Tebo *et al.*, 1998). *Bacillus* sp. SG-1 was first isolated from shallow marine sediment (San Diego, California) and determined to play a role in aquatic manganese cycling (Nealson & Ford, 1980; van Waasbergen *et al.*, 1993). *Anoxybacillus* spp. and *Paenibacillus* spp. share high levels of genetic similarity and the detection of these organisms were expected in an environment containing high levels of heavy metals. This is the first known instance of an isolated manganese oxidiser belonging to the genus *Paenibacillus*.

Two iron reducing bacterial strains, MNA-006 and MNA-008, were isolated and determined to be most similar to *Caloramator australicus*, 96% and 95% respectively. Again, these isolates are from the *Clostridiaceae* family. Due to the relatively low similarity of these strains, it is deduced that further investigation may also result in the discovery of new organisms within the genus. *Caloramator australicus* is an iron reducer first detected in the Great Artesian Basin, a neighbouring subsurface aquifer (Ogg & Patel, 2009). It is theorised that before its geographic isolation, PHS was connected to GAB and that the waters which comprise PHS originated from the basin (Brugger *et al.*, 2004; Figure 3.12). The detection of metal reducers of close 16S evolutionary similarity *Caloramator australicus*, which is to date unique to GAB, reinforces the theory that the two once shared waters.

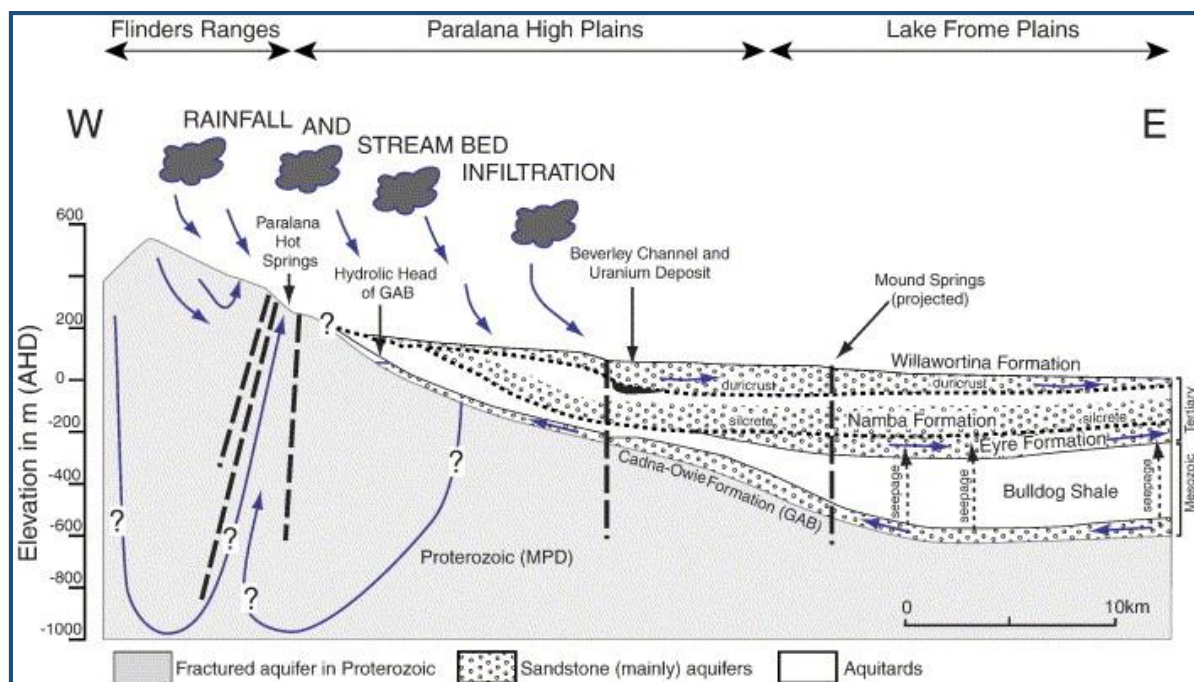


**Figure 3.12:** Cross-section of Paralana hot springs and its surrounding aquifers. The close proximity of the GAB and the springs suggests that the basin may have attributed to the waters of PHS. (Brugger *et al.*, 2005)

Following on from the observation that phototrophic organisms were most abundant in PHS water, the types of chlorophylls (Chl) and bacteriochlorophylls (Bchl) present were investigated. Scanning UV-Vis spectroscopy detected peaks correlating to several chlorophylls and bacteriochlorophylls present in PHS waters. *Chl a* was detected in the highest levels within the waters and as it is the most widespread of all the chlorophylls in nature, this was not unexpected. *Chl a* is found in cyanobacteria, algae and plants. Conversely, *Chl b* (predominately a plant chlorophyll) was also detected, though at much lower levels than *Chl a*. The PHS water sample contained green-algae but little to no plant material, and while *Chl b* is not unique to plants, it is rare in other organism types and as a result detected at significantly lower levels than *Chl a* (Porra *et al.*, 1989). *Chl c<sub>1</sub>* (algal) *Chl d* and *Chl f* (Cyanobacteria) were detected but were also detected at lower levels than *Chl a*.

Several high range peaks were detected associated with various bacteriochlorophylls, which are typically found in anoxygenic phototrophic organisms such as purple and green bacteria. *Bchl a* (Universal phototrophic bacteriochlorophyll excluding Cyanobacteria) was detected at 883nm (Olsen *et al.*, 1973). Additionally, *Bchl b* (Purple bacteria), *Bchl d* and *Bchl f* (Green sulphur bacteria) were also detected, correlating with the metagenomic profile of PHS waters (Steiner *et al.*, 1983; Borrego *et al.*, 1998). Green sulphur bacteria belong to the phylum Chlorobi, which comprised 0.14% of the diversity profile. Comparatively, the peak for *Chl a* was magnitudes higher than those for the bacteriochlorophylls. It is therefore deduced that the primary source of green particulate matter within PHS waters is a result of Cyanobacteria/Algal blooms and non-Cyanobacteria phototrophs are present but comprise a relatively low percentage of the microbial community within the spring.

All of the isolates obtained from culture dependent studies belonged to the phylum Firmicutes, which accounted for only 1.36% (154) amplicons obtained in the metagenomic analyses of the PHS waters. Firmicutes comprise a relatively low percentage in the diversity profile of the spring however were exclusively isolated in the culture dependent assessment of PHS waters. This occurred as the enrichment media and conditions were designed to select for metal transforming organisms. Organisms belonging to the genus *Caloramator*, *Clostridium* and *Bacillus* were detected both in the independent and dependent analyses. While some organisms obtained through isolations were not detected explicitly in the diversity profile (*Anoxybacillus*, *Geobacillus* and *Paenibacillus*), sequences associated with the Family *Bacillaceae* were detected, of which all remaining isolates belonged to.

The only previous microbial study of PHS was a culture independent analysis some ten years ago which used an *E. coli* expression system (Anitori *et al.*, 2002). No culturing or isolation was done in this study. Unlike the current work which focuses waters proximal to the primary water source, Anitori and colleagues compared the bacterial communities at several different locations within the spring. However, the limitations in culture independent analyses at the time resulted in a limited library, with 7-60 unique ribotypes observed under any condition. Furthermore, the pGem-T Easy vector system used was limited in that not all DNA is able to be expressed through this system and can therefore favour the presence of particular organisms over others. Comparatively, advances in culture independent analyses and next generation sequencing resulted in 13,949 sequences belonging to 21 unique phyla in the current study. Similarly however, the previous culture independent analyses of both the Anitori group and the one described in this report both identify *Cyanobacteria* and *Proteobacteria* as the most common bacteria detected.

# Chapter 4

Manganese Transformation

Characteristics of

Paralana Isolates and

*Shewanella* species

## 4.1 Introduction

### 4.1.1 *Shewanella*

Organisms within the genus *Shewanella* are facultatively anaerobic, gram-negative bacteria found predominately in marine environments. The genus contains over 40 species and these bacteria have been discovered in both mesophilic and psychrophilic habitats (Kato & Nogi, 2001). *Shewanella* sp. have been found capable of reducing numerous heavy metals, including Fe(III), V(V), Cr(VI), Mn(IV) and U(VI) as alternatives to oxygen in metabolic respiration (Guha *et al.*, 1987; Myers *et al.*, 2004; Truex *et al.*, 2000). Within this genus, *Shewanella oneidensis* MR-1 has been a focal point of research due to its extensive respiratory abilities. *Shewanella oneidensis* MR-1 is capable of reduction of a variety of metals, many associated with environmental pollution and industrial waste. Genomic sequencing of the bacteria revealed a novel iron hydrogenase and highlights the importance of understanding the reduction mechanisms of this and other *Shewanella* sp. for potential use in bioremediation (Heidelberg *et al.*, 2002).

*Shewanella* spp. represent some of the best known Mn(IV) reducers and are useful representations for comparing with other manganese transforming bacteria (such as those from the PHS). Compared to other genera, *Shewanella* are “the most diverse respiratory organisms described so far” (Hau & Gralnick, 2007). Manganese oxidation by *Shewanella* spp. has not been the focal point of research to date, however due to the transformation characteristics of the genus on manganese and other metals, manganese oxidation may be present in many bacteria within this genus. In fact, *Shewanella* spp. have been found in association with Mn oxidising communities (Anderson *et al.*, 2011; Bräuer *et al.*, 2011). This chapter investigates the manganese transforming characteristics of several *Shewanella* strains alongside isolates from Paralana hot springs.

## 4.2 Visual Inference of Bacterial MnO<sub>2</sub> Production

Bacterial oxidation of manganese was inferred through the production of a dark brown precipitate in the culture medium (Figure 4.1A). Oxide formation appeared approximately 7 days after growth (Figure 4.1B) which was evident in varying degrees of turbidity in the culture medium (relative to growth levels). Chemical oxidation was not normally observed in the control under the conditions used in current work (Figure 4.1C), therefore all MnO<sub>2</sub> was produced biologically. Manganese oxidation can be confirmed using Mn oxide assays with leucoberberlin blue assay (<1mM concentrations; Wang *et al.*, 2011), however all studies performed in this chapter involved concentrations <1mM and therefore the LCV assay was used (Spratt Jr. *et al.*, 1994; Section 2.8.1)

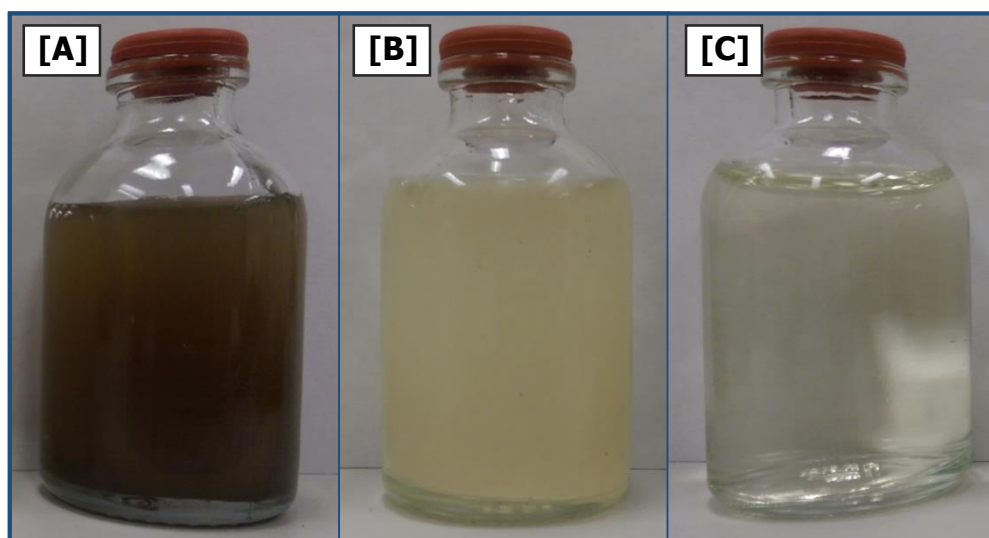


**Figure 4.1:** Bacterial manganese oxidation [A], growth without oxidation [B] and the control [C].

## 4.3 Optimisation Studies

### 4.3.1 Temperature optimum

Isolates were grown under increasing temperatures to establish optimal growth conditions (Figure 4.2). *Shewanella putrefaciens* 200, *Shewanella putrefaciens* CN-32, *Shewanella loihica* PV-4 and *Shewanella denitrificans* OS517 best grew at 40°C and all grew between 20°C and 50°C. Additionally, *Bacillus* sp. PMO also grew optimally at 40°C, however was limited to a temperature range of 30°C – 40°C. *Shewanella oneidensis* MR-1, *Bacillus* sp. DLH-1207 and *Paenibacillus* sp. AEM-1106 had a growth optima of 30°C with a range of 20°C – 40°C.

### 4.3.2 pH optimum

Isolates were grown under various pH increments to establish optimal pH growth conditions (Figure 4.3). All isolates were able to grow in enrichments with pH 6.5 – 8, with >8.5 inhibitory to cellular growth. *Shewanella putrefaciens* CN-32 grew on the largest pH range; exhibiting growth from pH 5 – 8.5. Conversely, *Shewanella denitrificans* OS517 grew on the lowest pH range from 6.5 – 8. Of the eight isolates tested, none grew below pH 5.

### 4.3.3 Salinity optimum

Isolates were grown under increasing salt levels to establish salinity resistance (Figure 4.4). *Shewanella* strains were found to grow best at 1% salinity (excluding *Shewanella loihica* PV-4 which exhibited optimal growth in the absence of salt). Conversely, Paralana isolates were found to grow best at 2.5% salt. All bacteria were inhibited in enrichments containing  $\geq 5\%$  salinity.

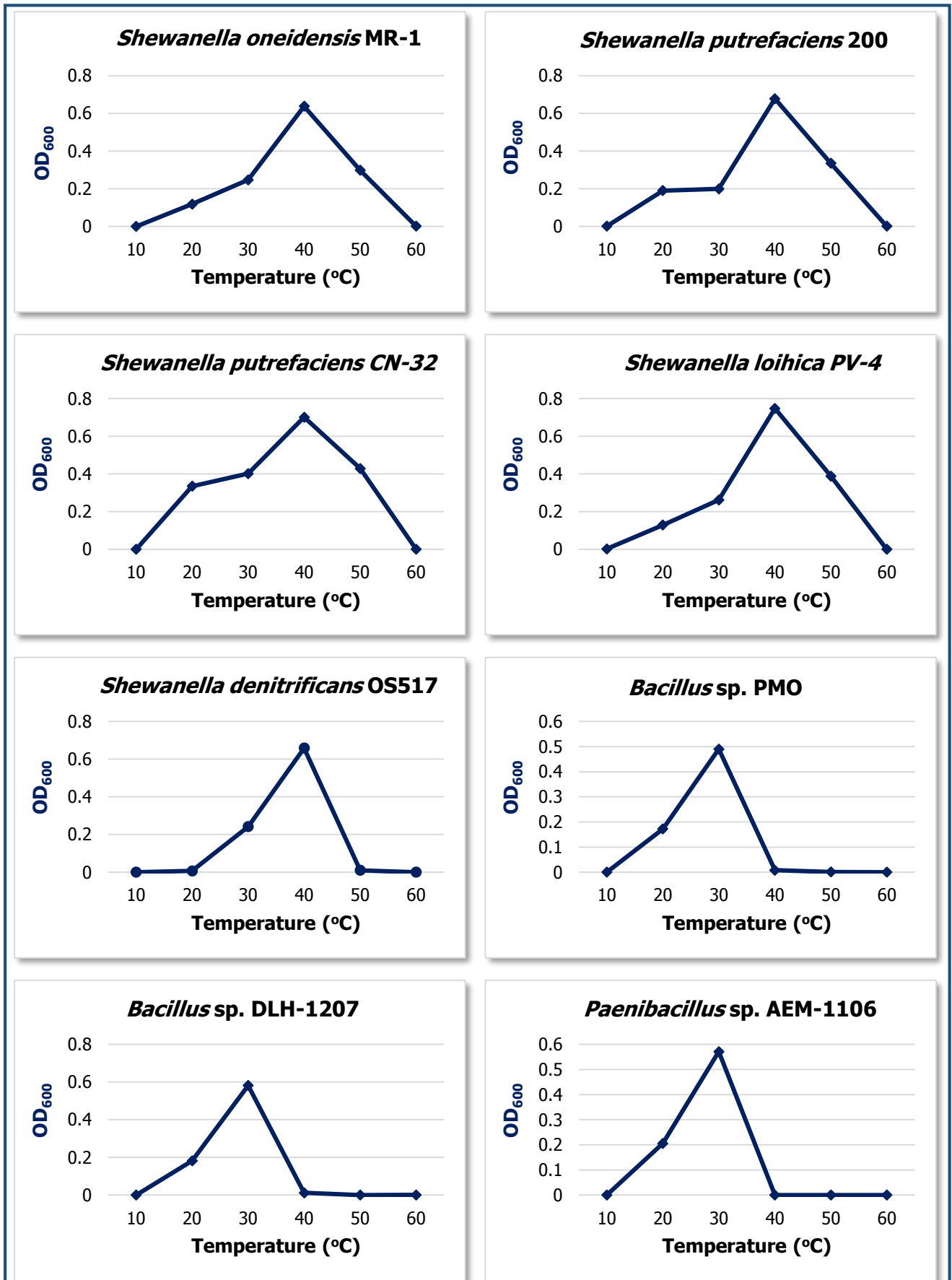


**Figure 4.2:** Growth curves of *Shewanella* sp. and Paralana isolates. Grown aerobically on PYE media, 0.2% yeast extract, pH 7.

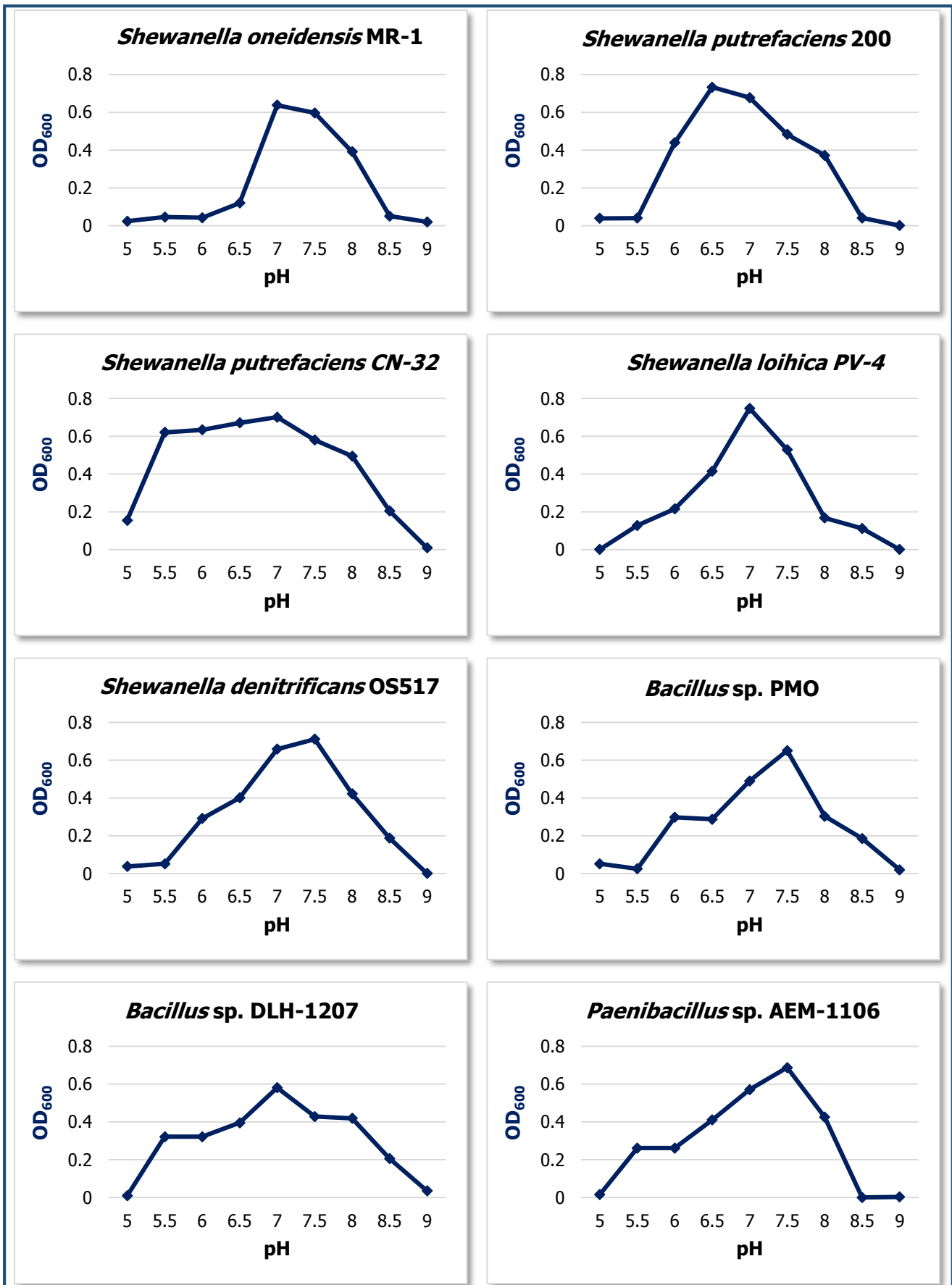


**Figure 4.3:** pH curves of *Shewanella* sp. and Paralana isolates. Grown aerobically on PYE media, 0.2% yeast extract, under optimal temperature.

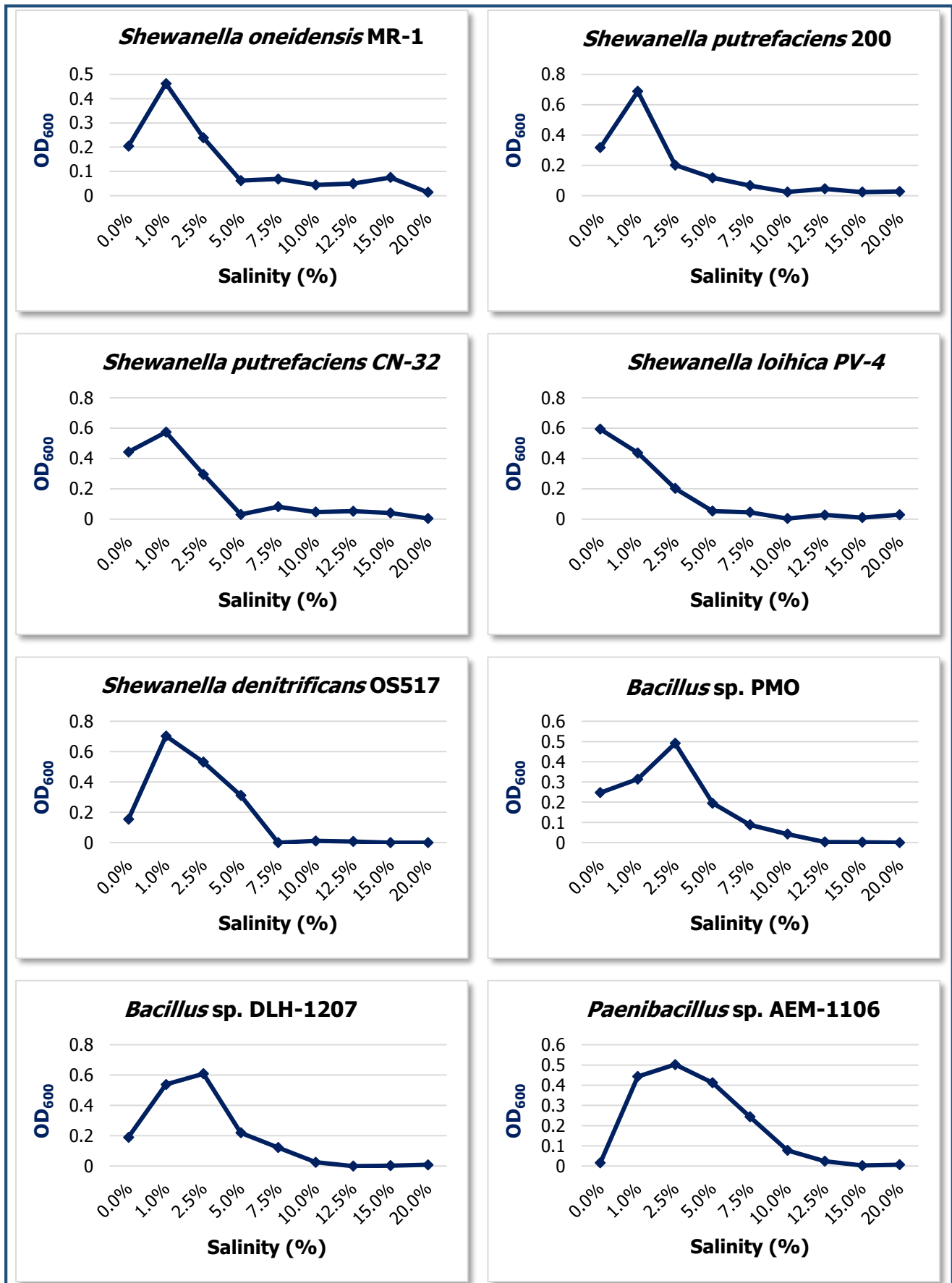


Figure 4.4: Salinity curves of *Shewanella* sp. and *Paralana* isolates. Grown aerobically on PYE media, 0.2% yeast extract, under optimal temperature and pH.

#### 4.3.4 Antibiotic susceptibility

The isolates were tested for antibiotic susceptibility against a range of antibiotics (Tetracycline; Gentamycin; Cephazolin; Ciprofloxacin; Ampicillin; and Chloramphenicol). Very little antibiotic resistance was observed from any isolate against any of the tested antibiotics. *Shewanella denitrificans* OS517 showed resistance to Cephazolin and Ampicillin and *Bacillus* sp. DLH-1207 also grew in the presence of Cephazolin (Table 4.1).

**Table 4.1:** Antibiotic susceptibility across the *Shewanella* spp. (CN-32, PV-4, 200, OS517 and MR-1) and PHS isolates (PMO, DLH-1207 and AEM-1106). Samples were tested on PYE media agar plates and grown under optimal conditions.

+ indicates the isolate was resistant against a tested antibiotic.

Antibiotic		Antibiotic Resistance							
Antibiotic	Conc.	CN-32	PV-4	PMO	200	OS517	MR-1	DLH-1207	AEM-1106
Tetracycline	30µg	–	–	–	–	–	–	–	–
Gentamycin	10µg	–	–	–	–	–	–	–	–
Cephazolin	30µg	–	–	–	–	+	–	+	–
Ciprofloxacin	5µg	–	–	–	–	–	–	–	–
Ampicillin	10µg	–	–	–	–	+	–	–	–
Chloramphenicol	10µg	–	–	–	–	–	–	–	–

### 4.3.5 Electron donor utilisation

Various electron donors were tested for utilisation in aerobic respiration (Table 4.2). All isolates were able to use the organic extracts (yeast extract and casamino acids) and a high range of growth was exhibited on glucose. Fructose was also a widely used donor, with positive growth in 6 of 8 of the strains that were tested. *Shewanella oneidensis* MR-1 grew on the largest range of donors; with growth evident in all enrichments except lactose. Aside from MR-1, the remaining *Shewanella* isolates were unable to utilise most of the tested donors; the least being *Shewanella denitrificans* OS517 which was only able to use organic extracts.

**Table 4.2:** Electron donor utilisation across the *Shewanella* spp. (CN-32, PV-4, 200, OS517 and MR-1) and PHS isolates (PMO, DLH-1207 and AEM-1106). Samples were tested aerobically on PYE media and grown under optimal conditions.

Electron Donor		Utilisation							
Donor	Conc.	CN-32	PV-4	PMO	200	OS517	MR-1	DLH-1207	AEM-1106
Yeast extract	0.2%	+	+	+	+	+	+	+	+
Casamino acids	0.2%	+	+	+	+	+	+	+	+
Glucose	10mM	–	–	+	–	–	+	+	+
Lactose	10mM	–	–	–	–	–	–	–	–
Xylose	10mM	–	–	–	–	–	+	–	–
Arabinose	10mM	–	–	–	–	–	+	–	–
Glycine	10mM	–	–	–	–	–	+	+	–
Fructose	10mM	–	+	+	+	+	+	+	–
Mannitol	10mM	–	–	+	+	–	–	–	–
Raffinose	10mM	–	–	–	–	–	+	+	+

### 4.3.6 Electron acceptor utilisation

The PHS isolates and *Shewanella* spp. were tested for anaerobic growth. All were capable of linking growth to the reduction of electron acceptors. Various electron acceptors were tested for utilisation in anaerobic respiration (Table 4.3). All isolates were able to couple nitrate and manganese with cellular respiration, and 7 out of 8 iron enrichments also resulted in positive growth (all isolates except *Shewanella denitrificans* OS517). *Shewanella loihica* PV-4 and *Shewanella oneidensis* MR-1 were able to reduce the widest variety of acceptors, with evidence of growth and reduction across all conditions. Comparatively, *Shewanella* isolates were able to reduce a much wider range of acceptors than the Paralana isolates, the lowest being *Bacillus* sp. DLH-1207 which was only able to utilise nitrate and manganese. *Shewanella oneidensis* MR-1, *Shewanella putrefaciens* CN-32 and *Shewanella loihica* PV-4 were able to reduce uranium.

**Table 4.3:** Electron acceptor utilisation across the *Shewanella* spp. (CN-32, PV-4, 200, OS517 and MR-1) and PHS isolates (PMO, DLH-1207 and AEM-1106). Samples were tested on PYE media and grown under optimal conditions, 0.2% yeast extract.

Electron Acceptors		Reduction							
Acceptor	Conc.	CN-32	PV-4	PMO	200	OS517	MR-1	DLH-1207	AEM-1106
Iron	0.2%	+	+	+	+	+	+	+	+
Oxygen	N/A	+	+	+	+	+	+	+	+
Manganese	1mM	+	+	+	+	+	+	+	+
Vanadium	2mM	–	+	+	+	–	+	+	–
Uranium	4mM	+	+	–	–	–	+	–	–
Cobalt	0.1%	–	+	–	–	+	+	+	–
Nitrate	1mM	+	+	+	+	+	+	+	+
None	-	–	–	+	–	–	–	+	–

## 4.4 Manganese Transformation Characteristics

### 4.4.1 Manganese reduction

Increasing concentrations of manganese dioxide were tested for reduction by the eight isolates (Figure 4.5). All of the tested isolates were able to reduce manganese (Section 4.3.6). *Bacillus* sp. PMO and *Shewanella putrefaciens* CN-32 were able to reduce the highest concentration of MnO<sub>2</sub>; with reduction at widest concentrations of  $\leq 12\text{mM}$  (28.00% and 5.62% reduction respectively). Conversely, *Paenibacillus* sp. AEM-1106 was able to reduce the lowest concentration of manganese, with inhibition evident at concentrations  $\leq 7\text{mM}$  (3.94% reduction).

Manganese dioxide reduction (3mM) was tested as a function against time to determine the rate of conversion by the isolates (Figure 4.6). Reduction was first observed after 12 hours in all the isolates except *Shewanella oneidensis* MR-1 and *Shewanella putrefaciens* CN-32, with reduction first evident after 18 hours. Complete reduction occurred between 24-42 hours and was most quickly reduced by *Bacillus* sp. PMO, *Shewanella loihica* PV-4 and *Shewanella putrefaciens* 200. Negative controls did not detect any chemical oxidation across any conditions.

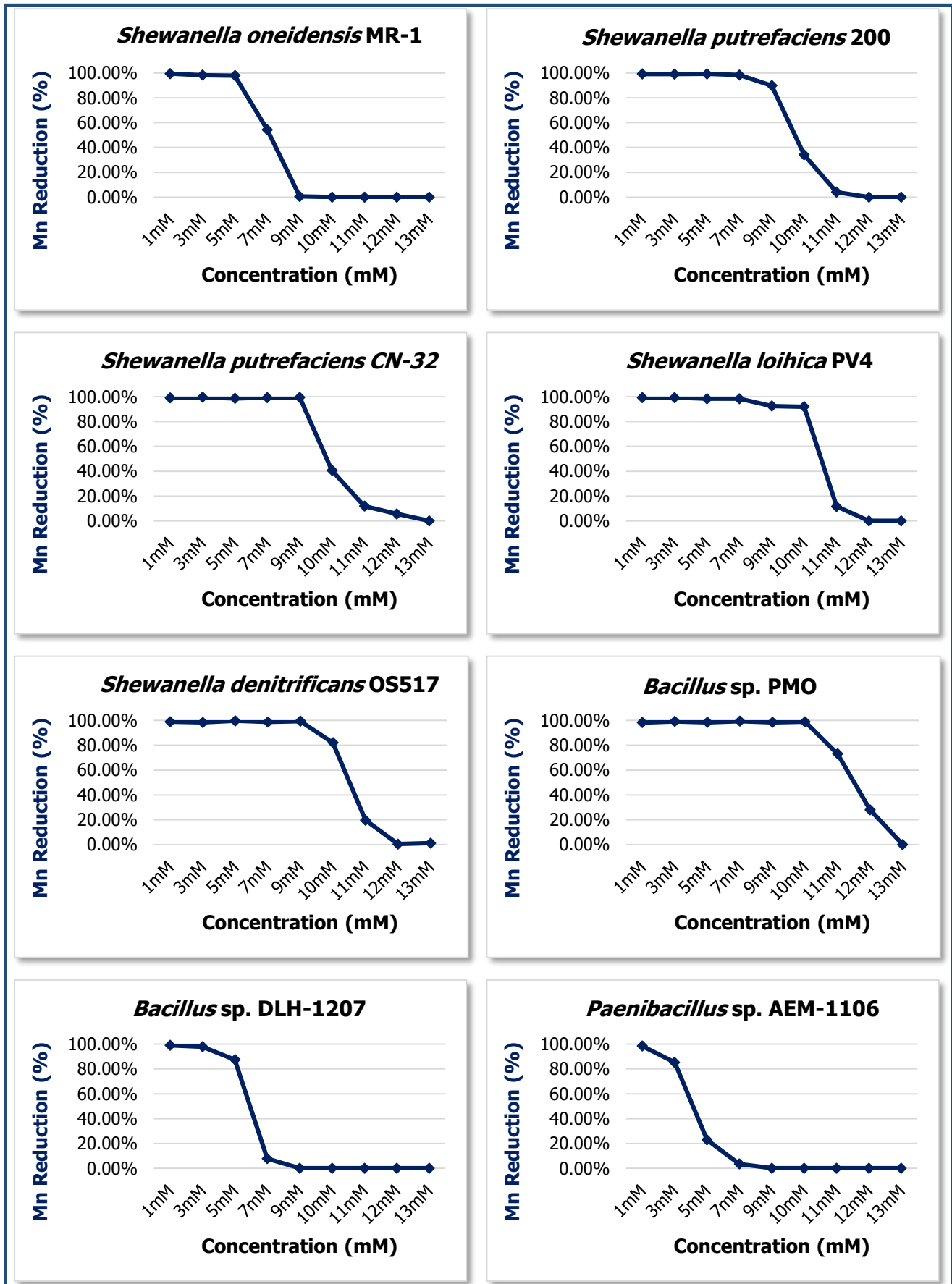


Figure 4.5: Manganese reduction curves of *Shewanella* sp. and PHS isolates. Grown aerobically on PYE media, 0.2% yeast extract, under optimal temperature and pH.

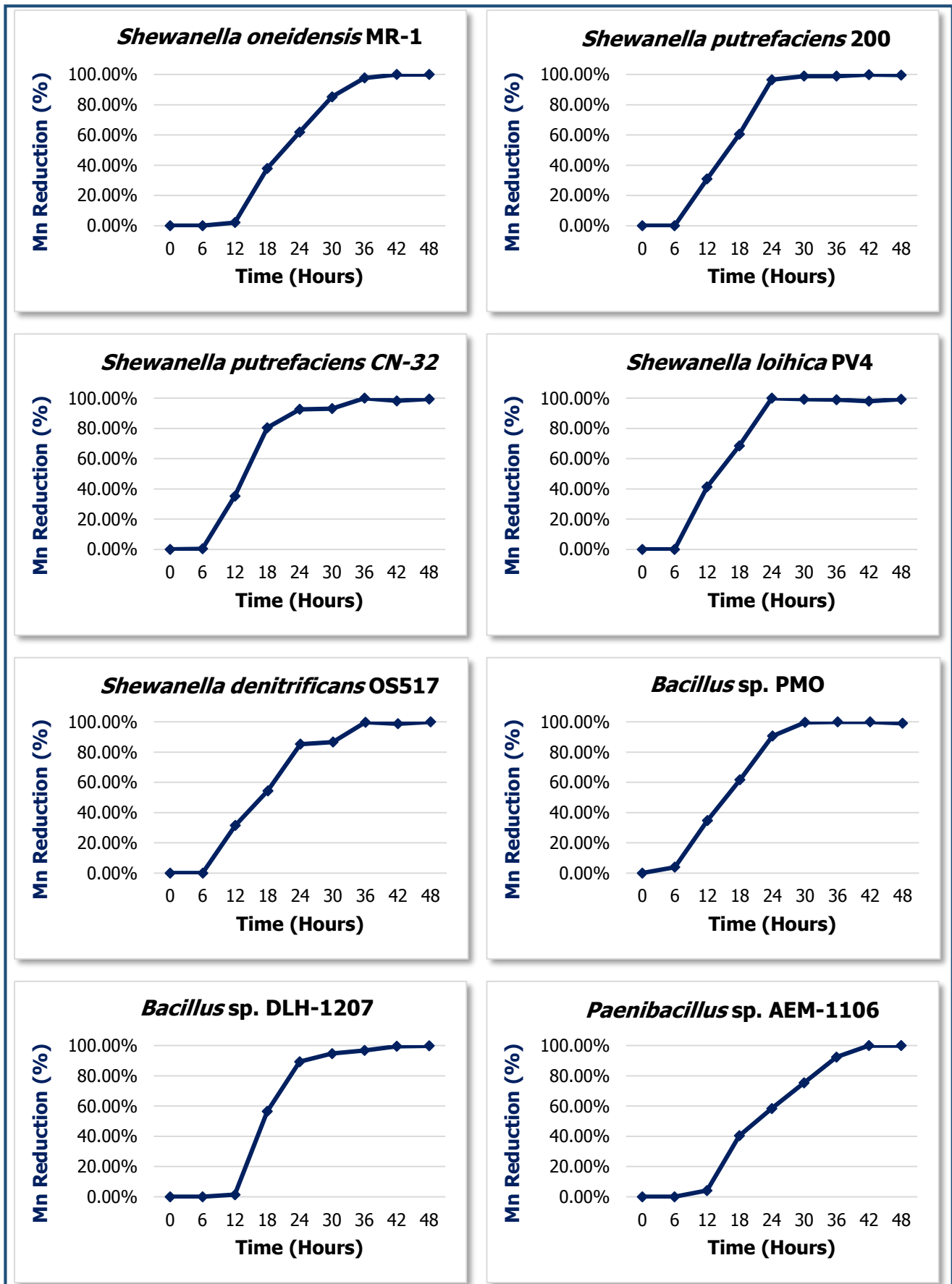


Figure 4.6: Manganese reduction time curves of *Shewanella* sp. and PHS isolates. Grown aerobically on PYE media, 0.2% yeast extract, 3mM manganese dioxide under optimal temperature and pH.

#### 4.4.2 Manganese oxidation

While the PHS strains were isolated as Mn oxidisers, the ability of *Shewanella* to oxidise Mn is largely unknown. Increasing concentrations of Mn(II) were tested for oxidation by the eight isolates (Figure 4.7). All of the tested isolates were able to oxidise manganese. *Shewanella putrefaciens* 200 and *Shewanella loihica* PV-4 were able to oxidise the highest concentration of Mn(II), up to 8mM. Conversely, *Shewanella oneidensis* MR-1 was able to oxidise the lowest concentration of manganese, with inhibition occurring at concentrations 3mM or above.

Manganese transformation of the isolates was tested as a function against time and cellular growth (Figure 4.8). Isolates were grown aerobically with 3mM Mn(II) for 21 days. In all cases oxidation occurred, so the cultures were then transferred to serum bottles, deoxygenated with N<sub>2</sub> gas and an additional 0.2% yeast extract added to determine if the biogenic oxide was reduced. Initial oxidation occurred 2-3 days after initial growth began and maximum oxidation was observed 10-15 days after. Under anaerobic conditions, reduction occurred with all isolates after a further 1-2 days. All isolates were able to reduce and oxidise manganese under the different conditions. Negative controls did not detect any chemical oxidation across any conditions.

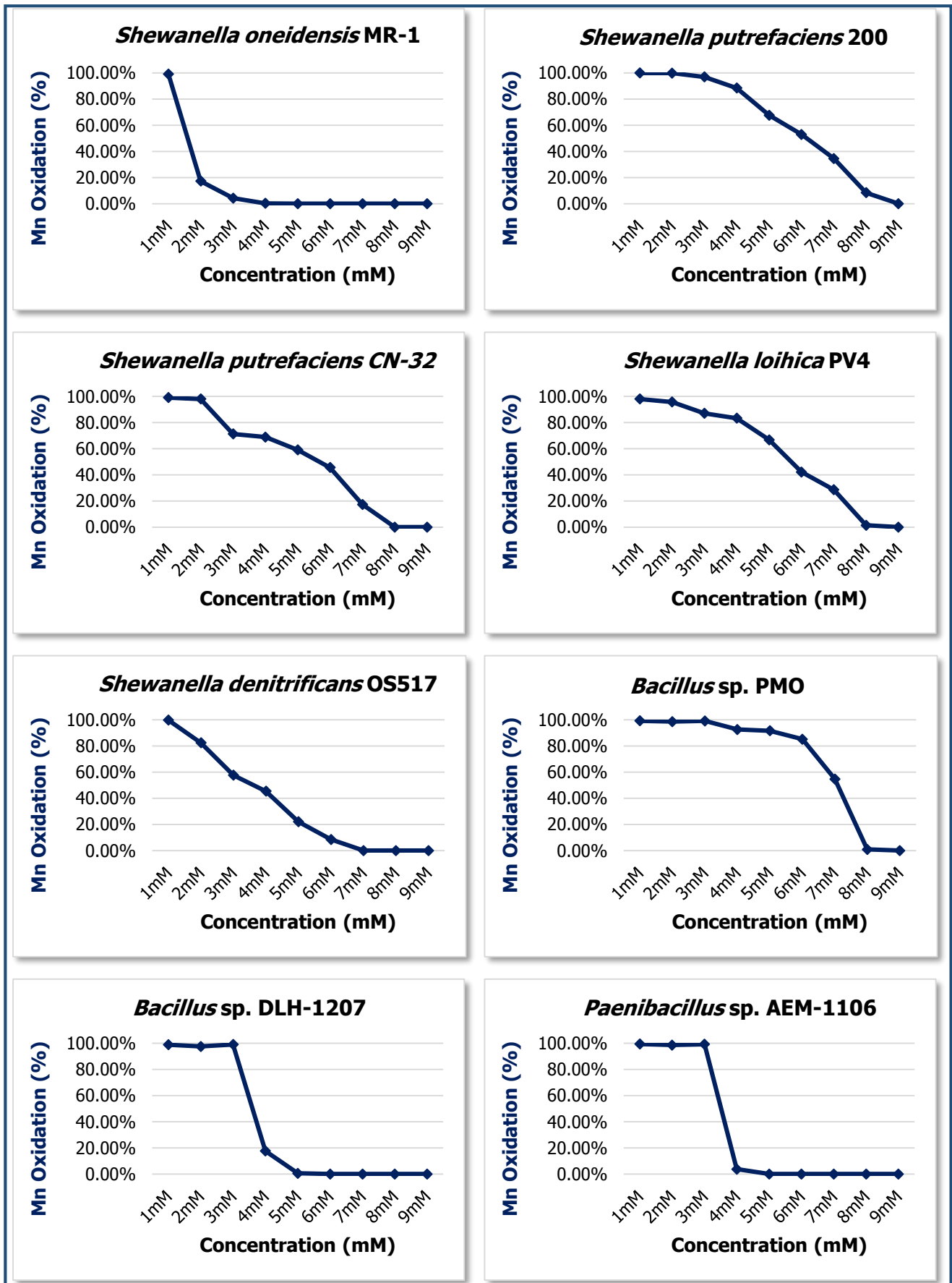
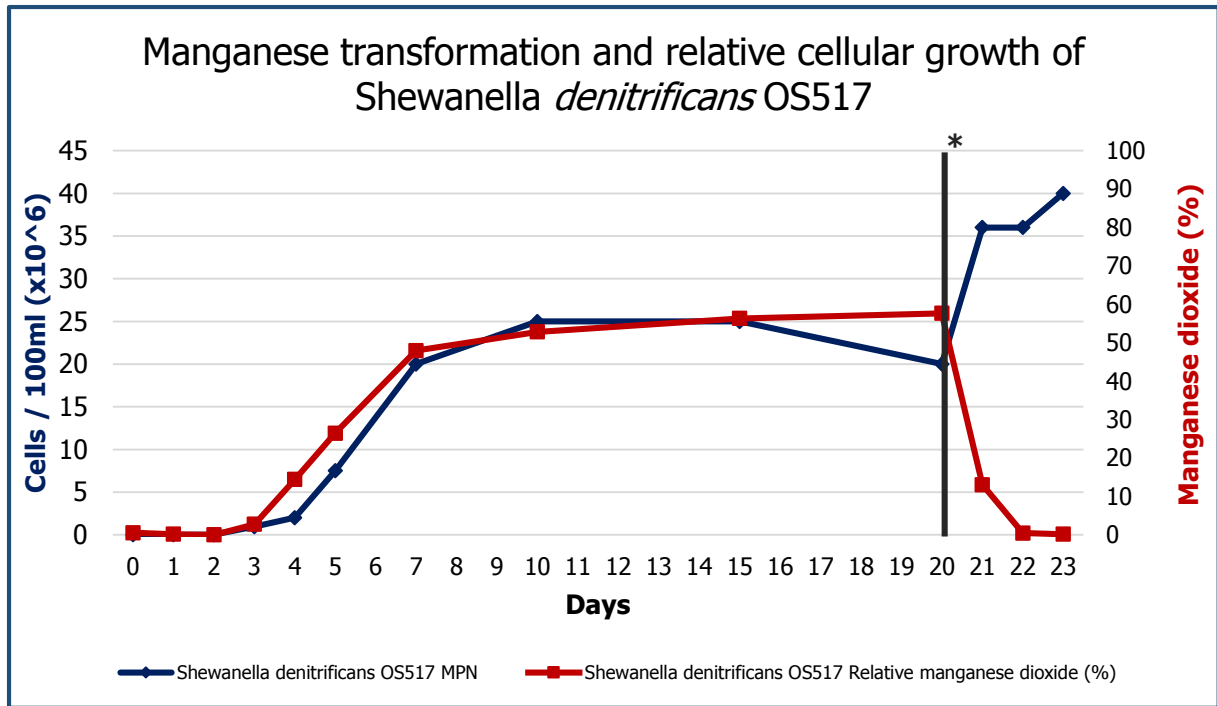


Figure 4.7: Manganese oxidation curves of *Shewanella* sp. and PHS isolates. Grown aerobically on PYE media, 0.2% yeast extract, under optimal temperature and pH.



**Figure 4.8a:** Manganese transformation and relative cellular growth of *Shewanella denitrificans* OS517.

Grown aerobically on PYE media, 0.02% yeast extract, 3mM Mn(IV), under optimal temperature and pH.

*\*Isolates were deoxygenated with N<sub>2</sub> gas and re-enriched with 0.2% yeast extract.*

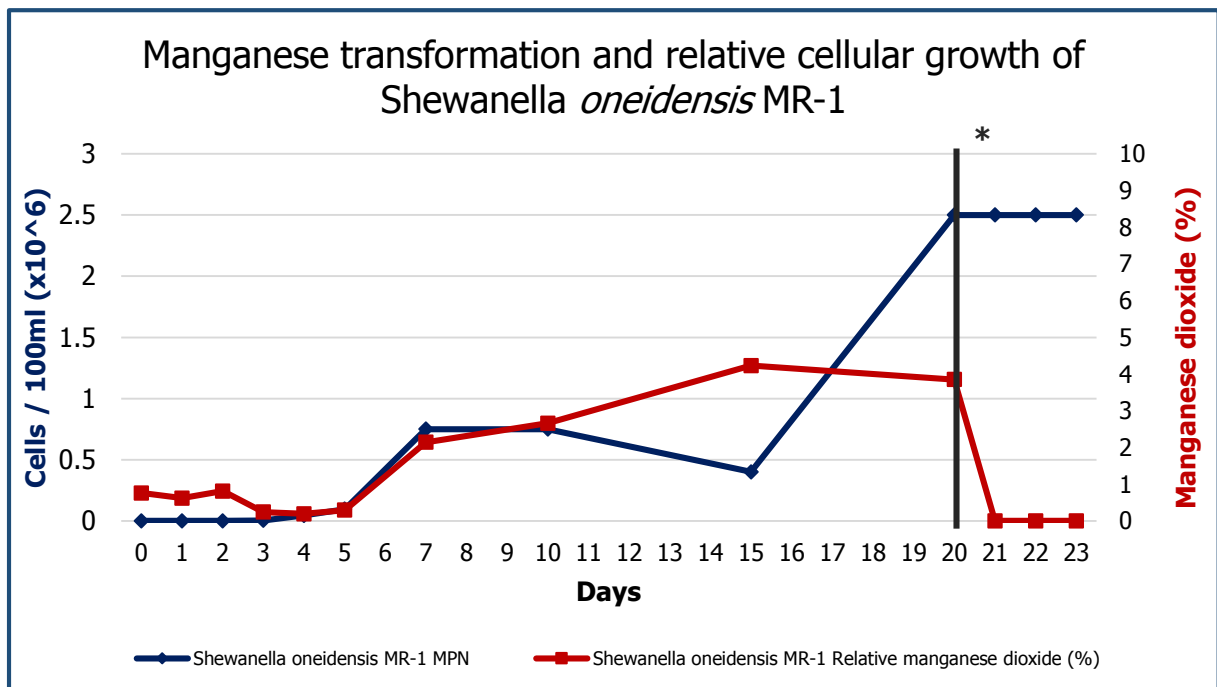


**Figure 4.8b:** Manganese transformation and relative cellular growth of *Shewanella oneidensis* MR-1.

Grown aerobically on PYE media, 0.02% yeast extract, 3mM Mn(IV), under optimal temperature and pH.

*\*Isolates were deoxygenated with N<sub>2</sub> gas and re-enriched with 0.2% yeast extract.*

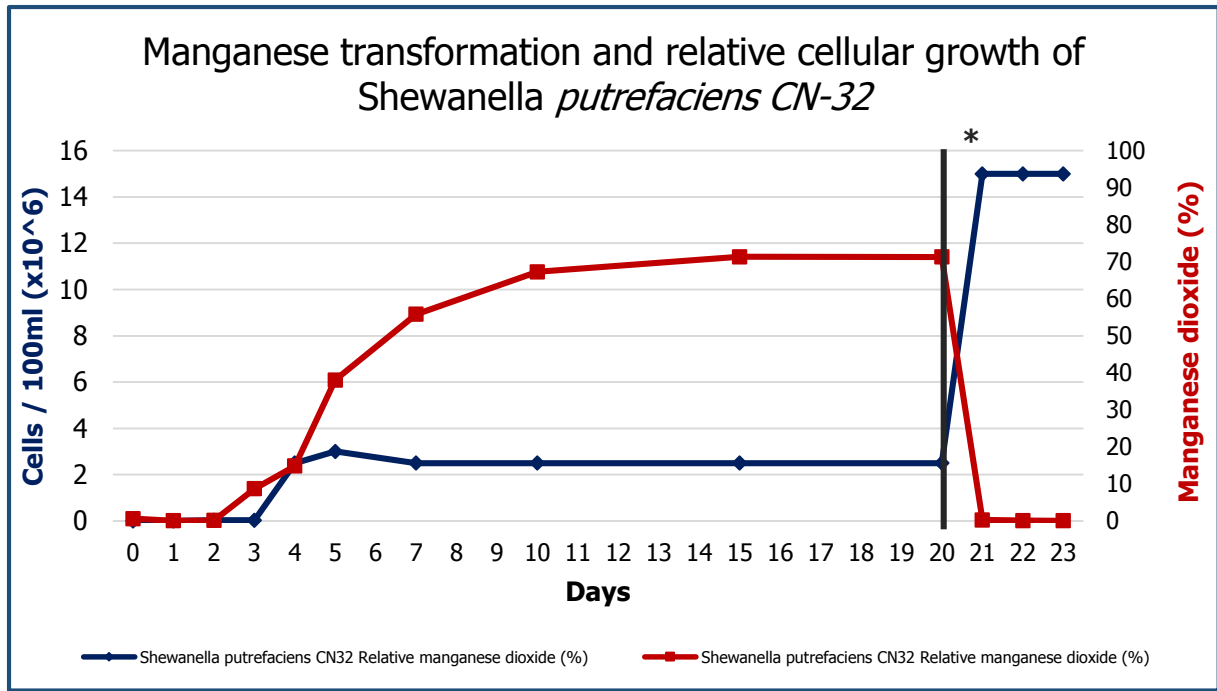


**Figure 4.8c:** Manganese transformation and relative cellular growth of *Shewanella putrefaciens* CN-32.

Grown aerobically on PYE media, 0.02% yeast extract, 3mM Mn(IV), under optimal temperature and pH.

\*Isolates were deoxygenated with N<sub>2</sub> gas and re-enriched with 0.2% yeast extract.

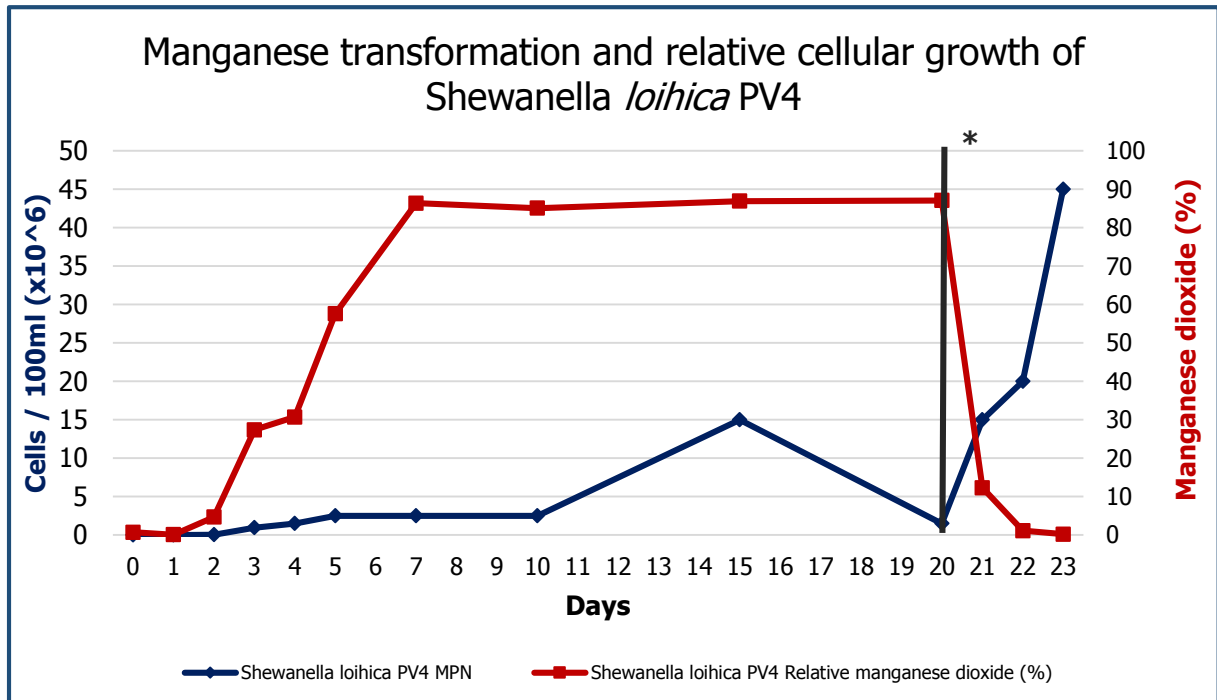


**Figure 4.8d:** Manganese transformation and relative cellular growth of *Shewanella loihica* PV4. Grown

aerobically on PYE media, 0.02% yeast extract, 3mM Mn(IV), under optimal temperature and pH.

\*Isolates were deoxygenated with N<sub>2</sub> gas and re-enriched with 0.2% yeast extract.

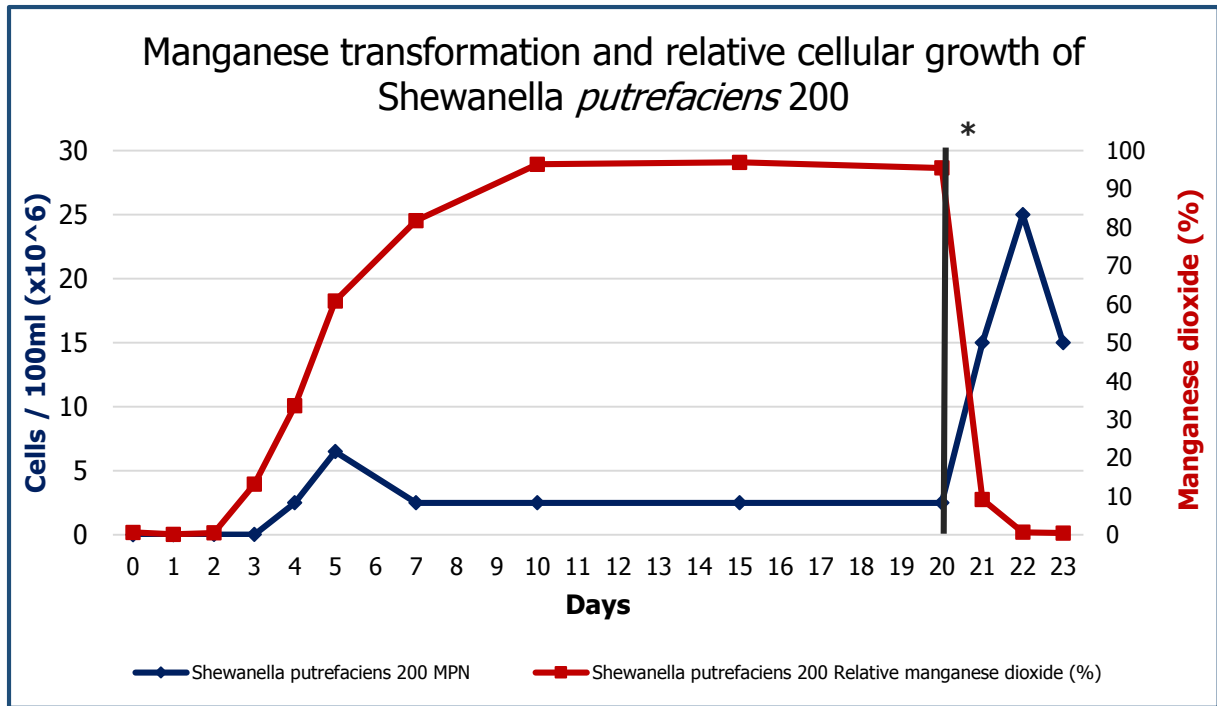


**Figure 4.8e:** Manganese transformation and relative cellular growth of *Shewanella putrefaciens* 200.

Grown aerobically on PYE media, 0.02% yeast extract, 3mM Mn(IV), under optimal temperature and pH.

*\*Isolates were deoxygenated with N<sub>2</sub> gas and re-enriched with 0.2% yeast extract.*

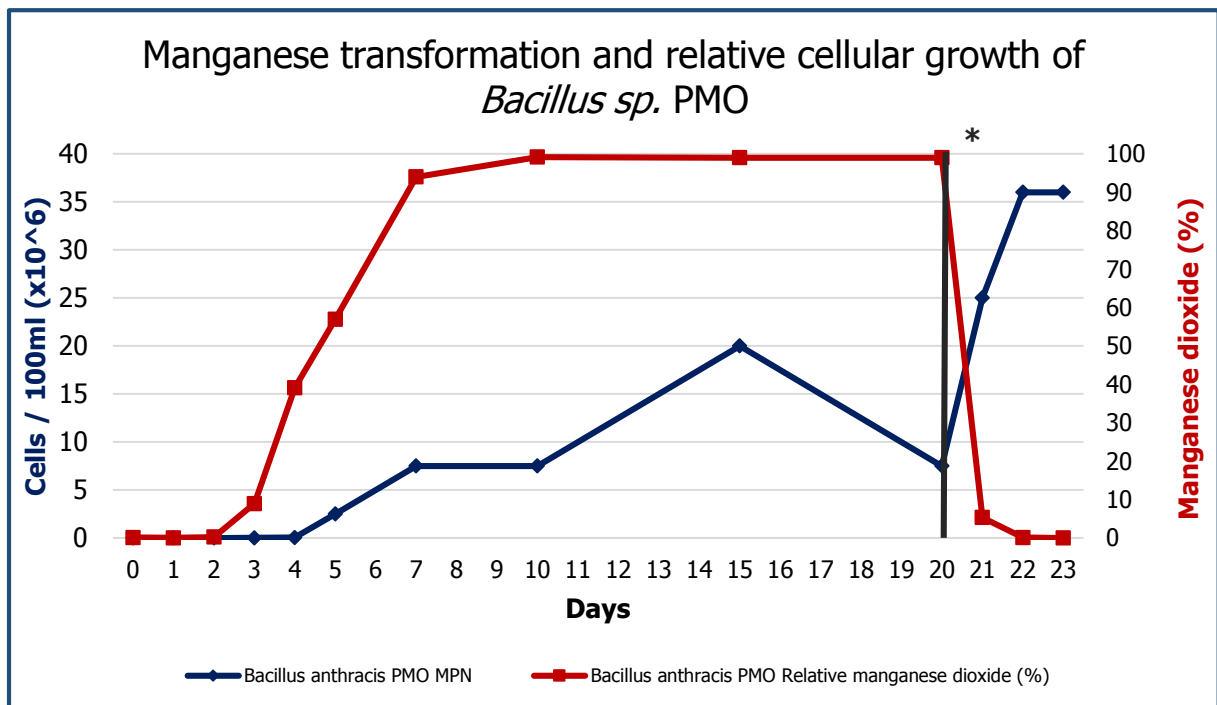


**Figure 4.8f:** Manganese transformation and relative cellular growth of *Bacillus sp.* PMO. Grown aerobically on PYE media, 0.02% yeast extract, 3mM Mn(IV), under optimal temperature and pH.

*\*Isolates were deoxygenated with N<sub>2</sub> gas and re-enriched with 0.2% yeast extract.*

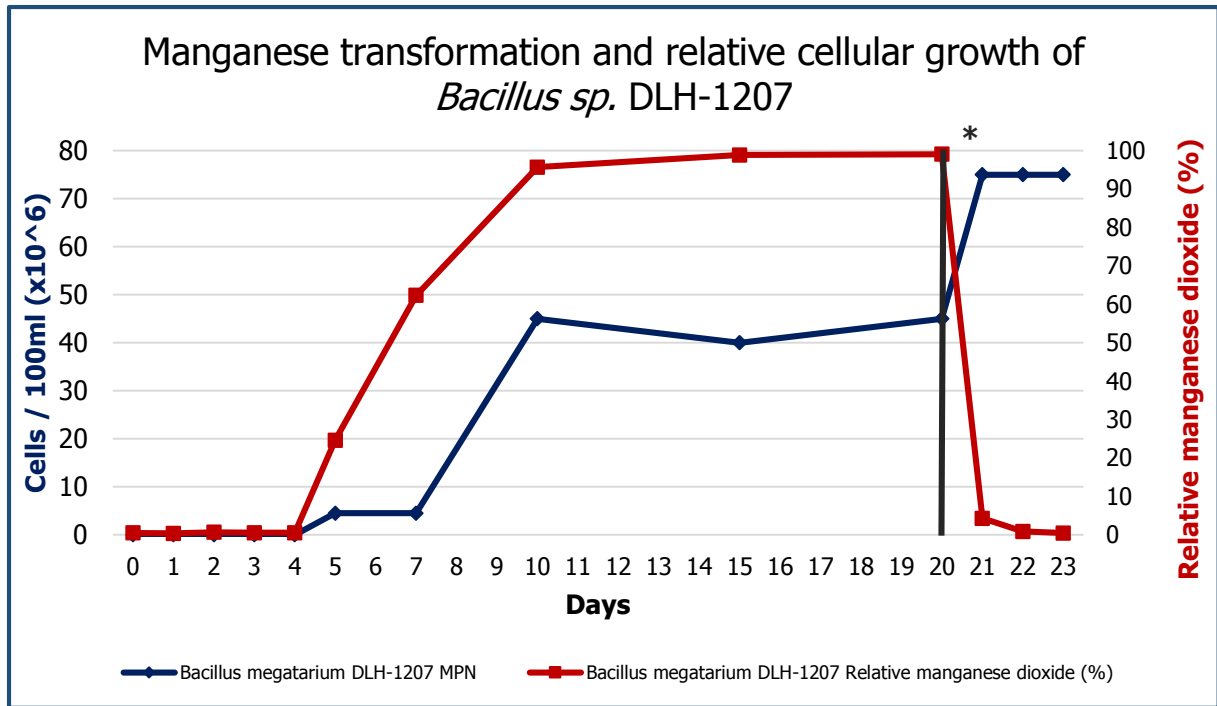


**Figure 4.8g:** Manganese transformation and relative cellular growth of *Bacillus sp.* DLH-1207. Grown aerobically on PYE media, 0.02% yeast extract, 3mM Mn(IV), under optimal temperature and pH..

*\*Isolates were deoxygenated with N<sub>2</sub> gas and re-enriched with 0.2% yeast extract.*

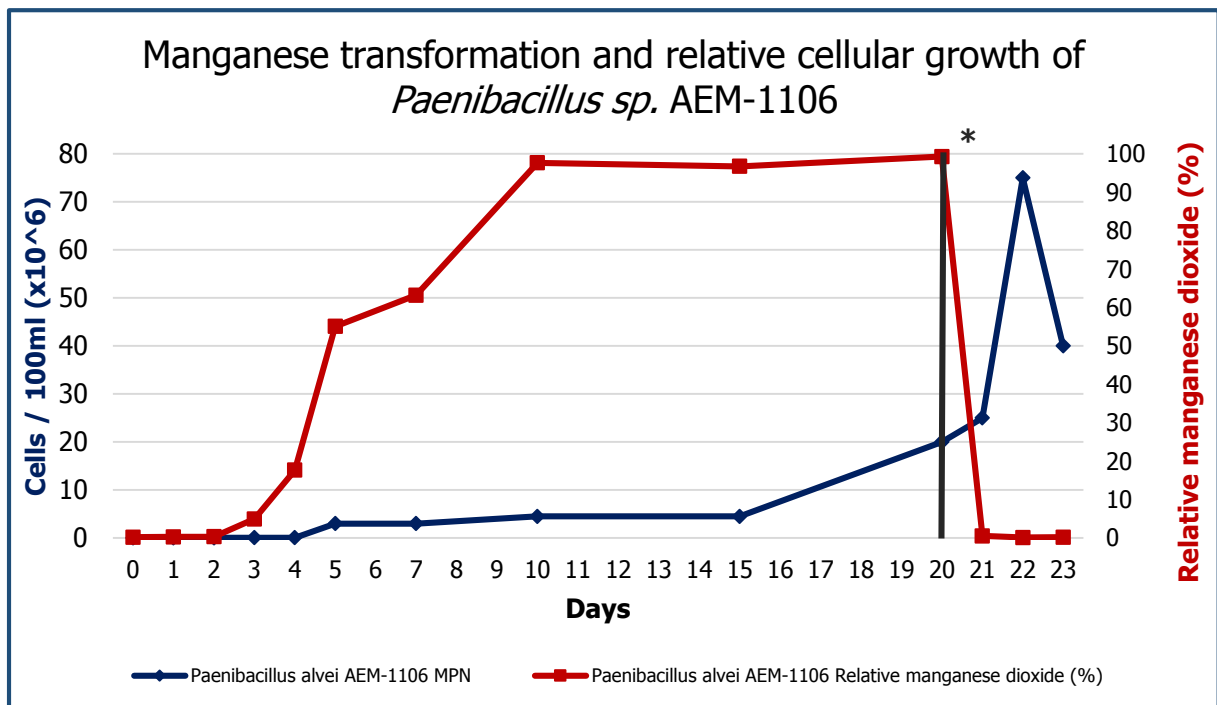


**Figure 4.8h:** Manganese transformation and relative cellular growth of *Paenibacillus sp.* AEM-1106.

Grown aerobically on PYE media, 0.02% yeast extract, 3mM Mn(IV), under optimal temperature and pH.

*\*Isolates were deoxygenated with N<sub>2</sub> gas and re-enriched with 0.2% yeast extract.*

## 4.5 Manganese Oxide Characterisation

### 4.5.1 Average oxidation states of oxides

The manganese oxide produced by several of the strains was characterised in terms of physical properties and chemical composition. The average oxidation states of the bacterially formed, analytical grade and chemically synthesised oxides were performed to determine the relative concentrations of MnO<sub>2</sub> within each sample (Table 4.4). It was observed that the analytical grade MnO<sub>2</sub> had an average oxidation state of 1.99, indicative of an extremely high level of purity. The manganese oxide content of the analytical grade manganese was 100%. Similarly, the chemically synthesised MnO<sub>2</sub> had an average oxidation state of 1.98 with a manganese oxide content of 99.6%. The average oxidation states of oxides produced by *Shewanella putrefaciens* CN-32, *Shewanella loihica* PV-4 and *Bacillus* sp. PMO were 1.93, 1.93 and 1.92 respectively. The manganese oxide content of these samples were 92%, 91.6% and 90.8%.

**Table 4.4:** Relative oxidation states and manganese oxide content of chemically synthesised, analytical grade MnO<sub>2</sub> and the produced oxides by *Shewanella putrefaciens* CN-32, *Shewanella loihica* PV-4 and *Bacillus* sp. PMO

Oxide Sample	Average Oxidation State	Manganese oxide content (%)
Analytical Grade MnO <sub>2</sub>	1.99	100%
Chemically synthesised MnO <sub>2</sub>	1.98	99.6%
<i>Shewanella putrefaciens</i> CN-32 produced MnO <sub>2</sub>	1.93	92.0%
<i>Shewanella loihica</i> PV-4 produced MnO <sub>2</sub>	1.93	91.6%
<i>Bacillus</i> sp. PMO produced MnO <sub>2</sub>	1.92	90.8%

#### 4.5.2 Scanning electron microscopy (SEM) of oxides

SEM images of the biogenic manganese oxides were compared against analytical grade (Figure 4.9) and chemically produced  $\text{MnO}_2$  (Figure 4.10). The oxide production of *Shewanella putrefaciens* CN-32 (Figure 4.11), *Shewanella loihica* PV-4 (Figure 4.12) and *Bacillus* sp. PMO (Figure 4.13) all produced powder-like  $\text{MnO}_2$ , structurally similar to the chemically produced oxide. In addition, bacteria can be clearly seen in the 5,000x magnification of the EM images. The analytical grade oxide was dissimilar to the other samples with significantly larger granules evident when viewed on the SEM.

#### 4.5.3 FTIR analysis of oxides

FTIR-Spectroscopy was used to compare the infrared spectrums of produced oxides with both analytical grade and chemically produced  $\text{MnO}_2$ . Spectra analysis of the analytical grade  $\text{MnO}_2$  revealed a distinct peak at  $487.23\text{cm}^{-1}$ , with lesser peaks observed at  $1238.24\text{cm}^{-1}$  –  $967.72\text{cm}^{-1}$ . Comparatively, the chemically produced oxide provided a distinct peak at  $495.29\text{cm}^{-1}$  and a secondary peak at  $1633.87\text{cm}^{-1}$  (Figure 4.14). *Shewanella putrefaciens* CN-32, *Shewanella loihica* PV-4 and *Bacillus* sp. PMO had nearly identical peaks at higher magnifications  $\sim 525\text{cm}^{-1}$ , however distinct secondary peaks were evident at  $\sim 1000\text{cm}^{-1}$  (Figure 4.15) that were not evident in the manganese controls.

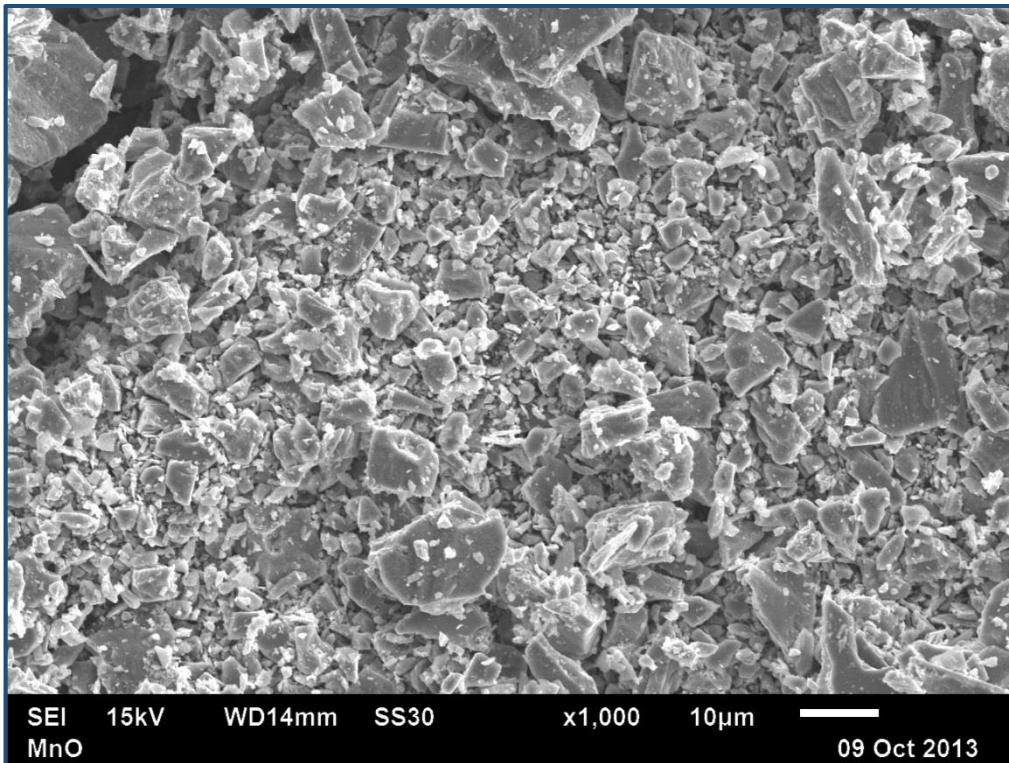


**Figure 4.9a:** Scanning electron microscopy of analytical grade manganese dioxide.

*Bar = 10µm (1,000x magnification).*

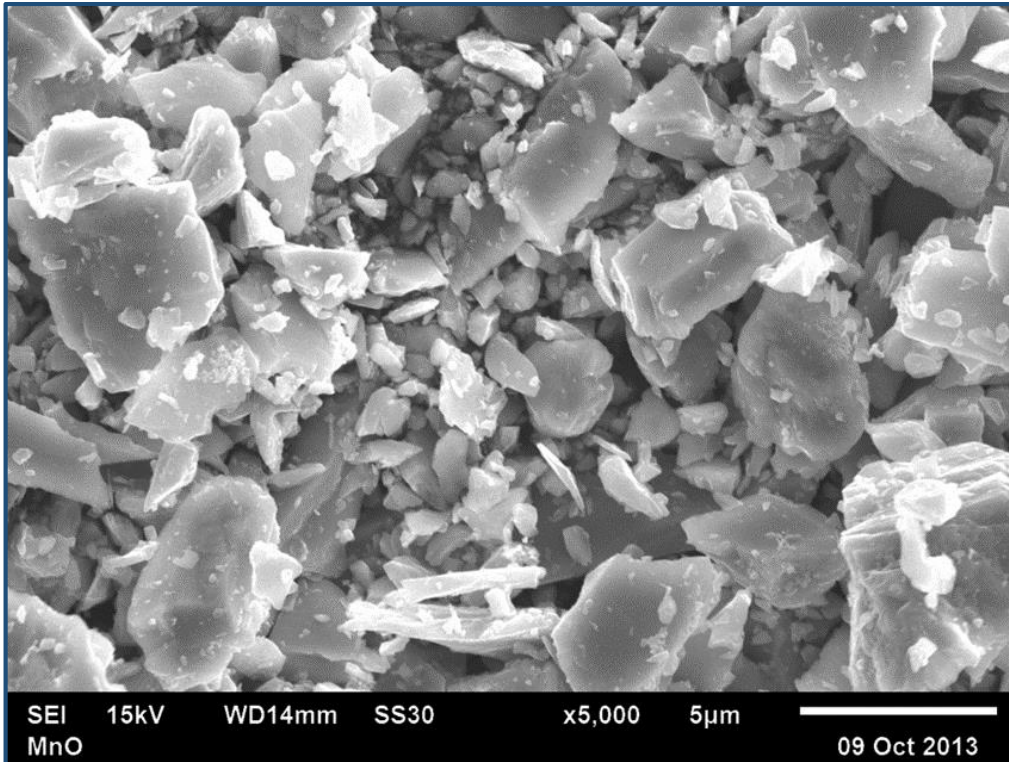


**Figure 4.9b:** Scanning electron microscopy of analytical grade manganese dioxide.

*Bar = 5µm (5,000x magnification).*

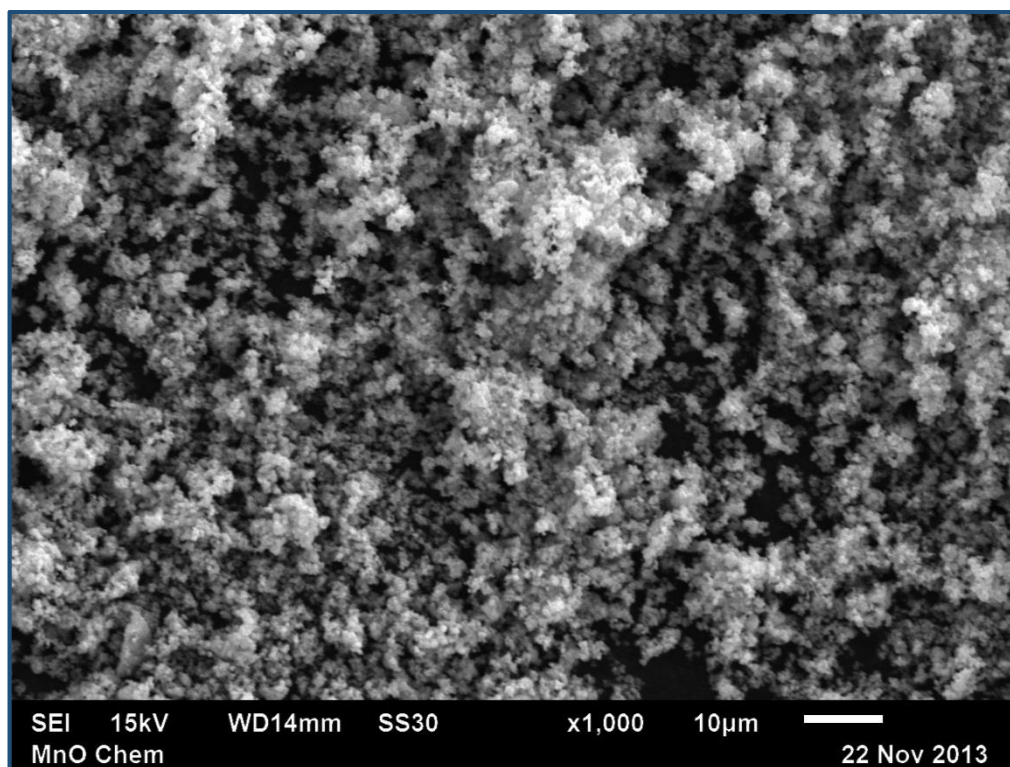


**Figure 4.10a:** Scanning electron microscopy of chemically synthesised manganese dioxide.

*Bar = 10µm (1,000x magnification).*

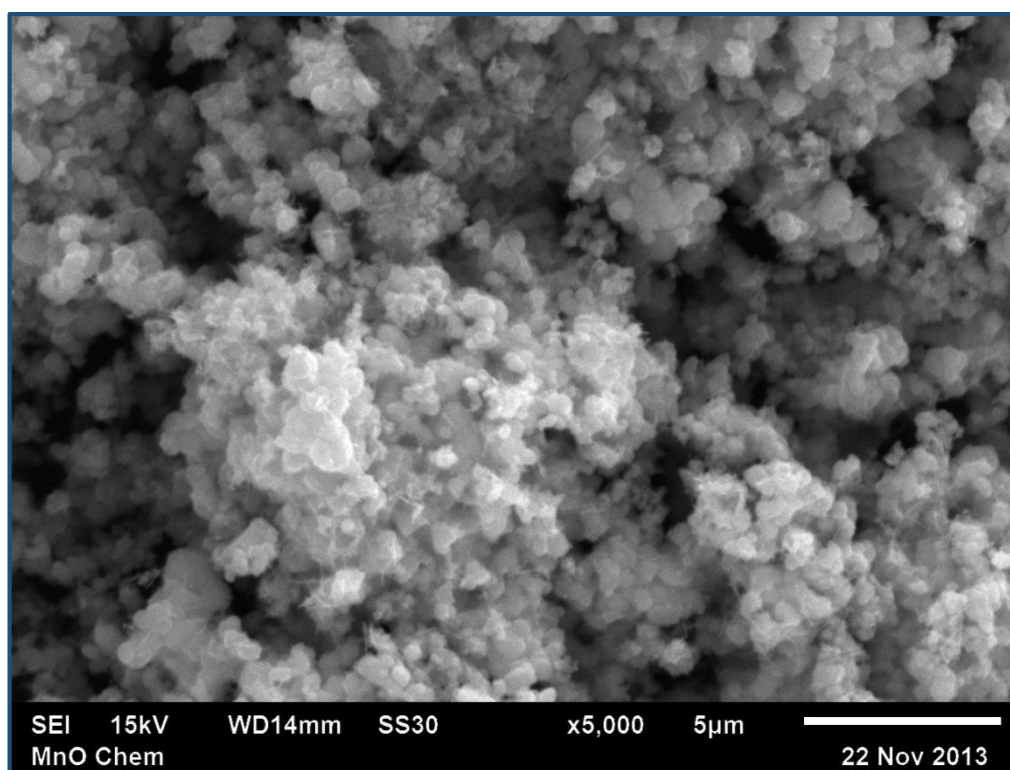


**Figure 4.10b:** Scanning electron microscopy of chemically synthesised manganese dioxide.

*Bar = 5µm (5,000x magnification).*

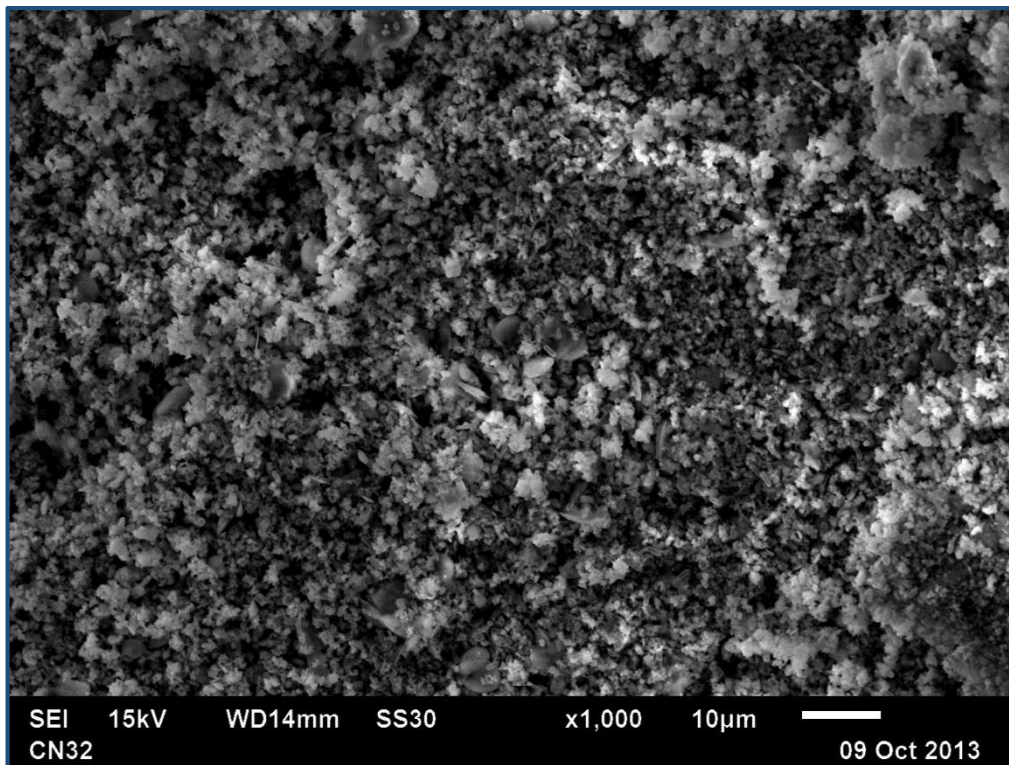


**Figure 4.11a:** Scanning electron microscopy of manganese dioxide transformed by *Shewanella putrefaciens* CN-32. Bar = 10µm (1,000x magnification).

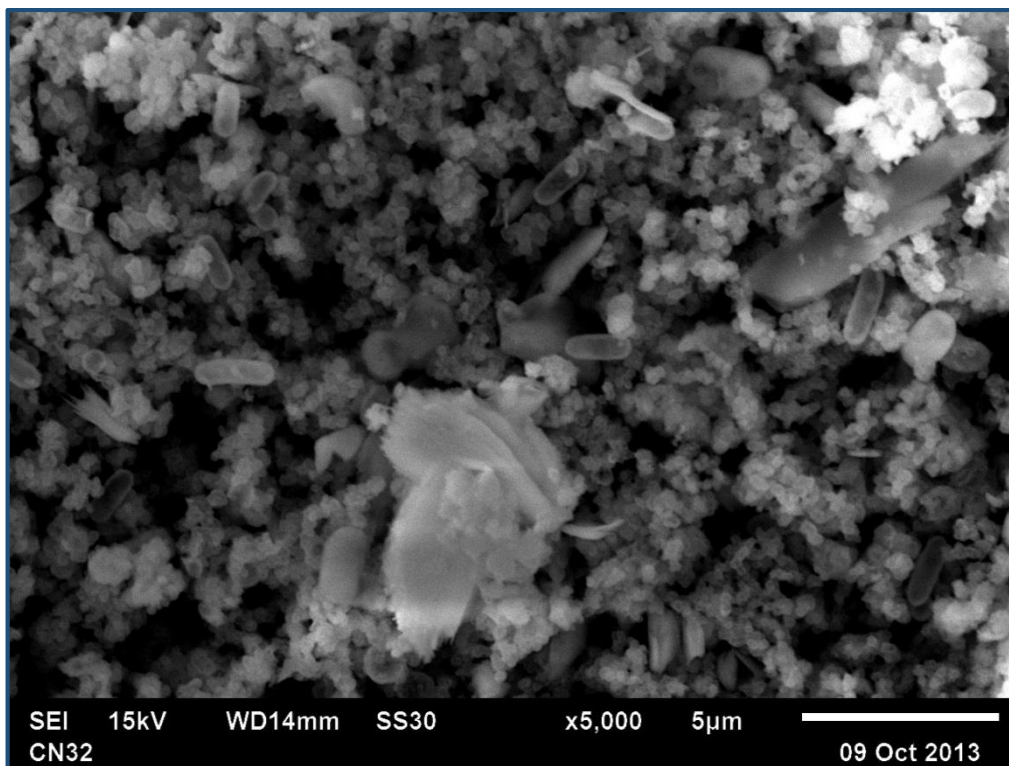


**Figure 4.11b:** Scanning electron microscopy of *Shewanella putrefaciens* CN-32 and the produced manganese dioxide. Bar = 5µm (5,000x magnification).

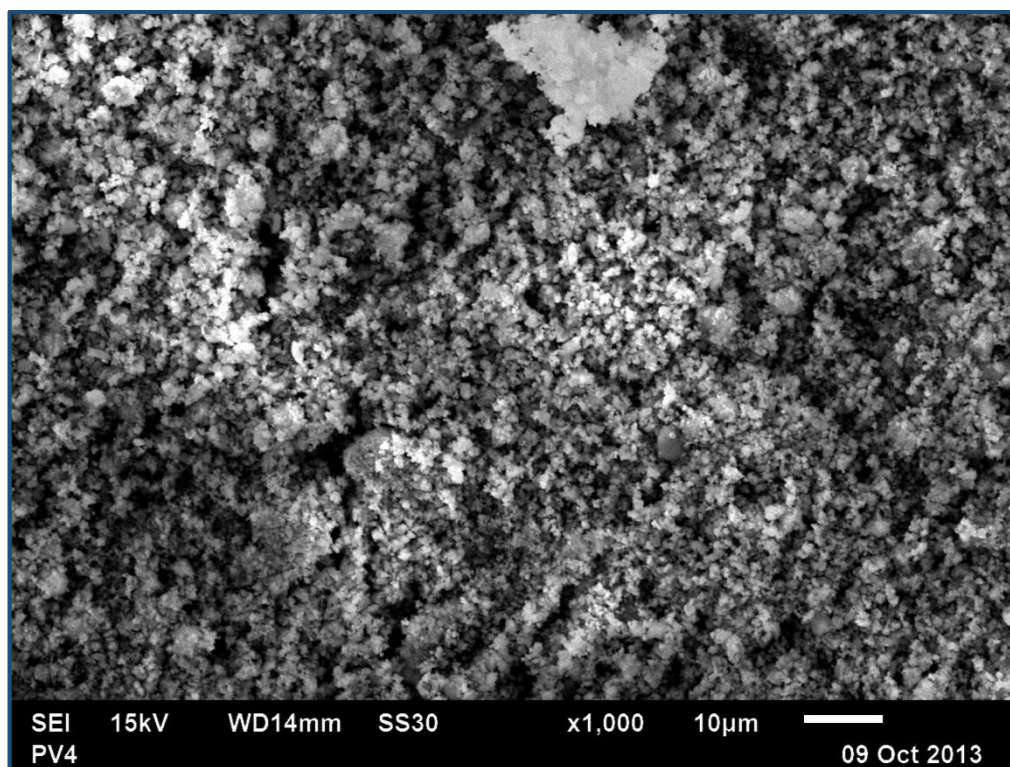


**Figure 4.12a:** Scanning electron microscopy of manganese dioxide transformed by *Shewanella loihica* PV-4. Bar = 10µm (1,000x magnification).

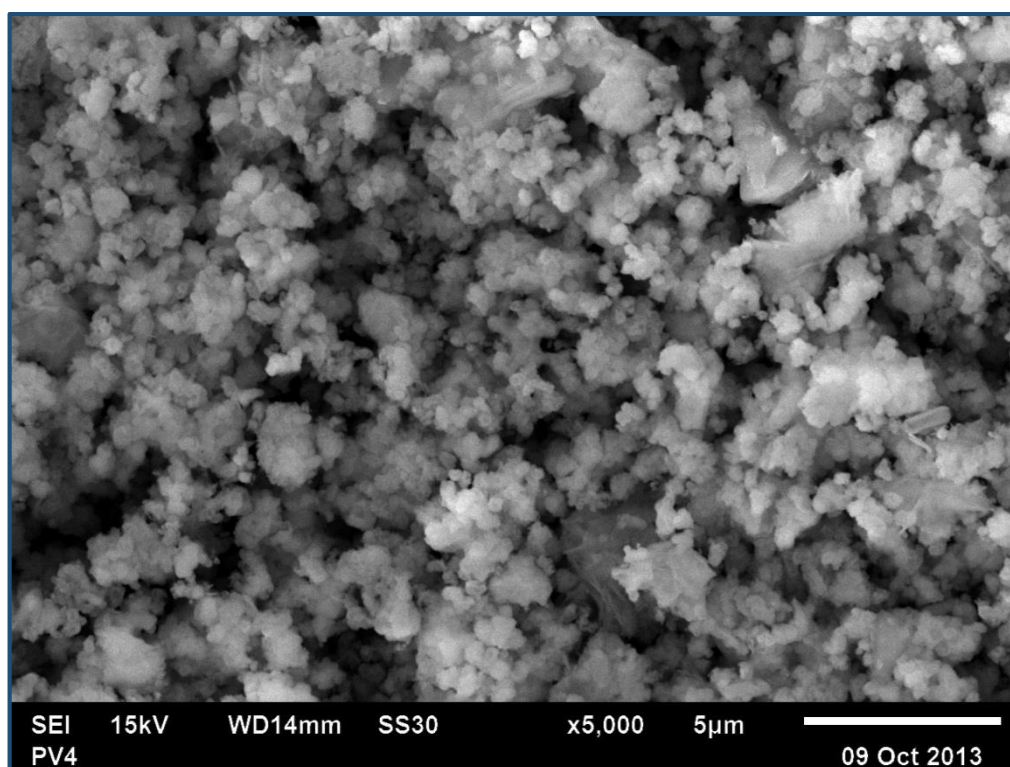


**Figure 4.12b:** Scanning electron microscopy of *Shewanella loihica* PV-4 and the produced manganese dioxide. Bar = 5µm (5,000x magnification).

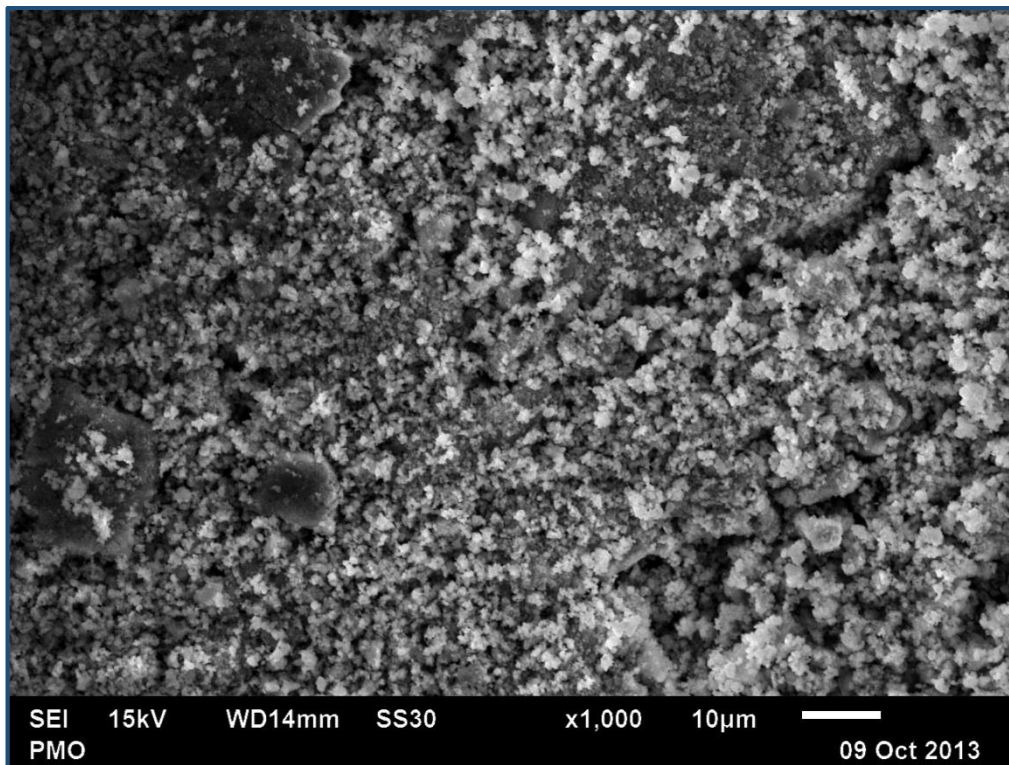


**Figure 4.13a:** Scanning electron microscopy of manganese dioxide transformed by *Bacillus* sp. PMO. Bar = 10µm (1,000x magnification).

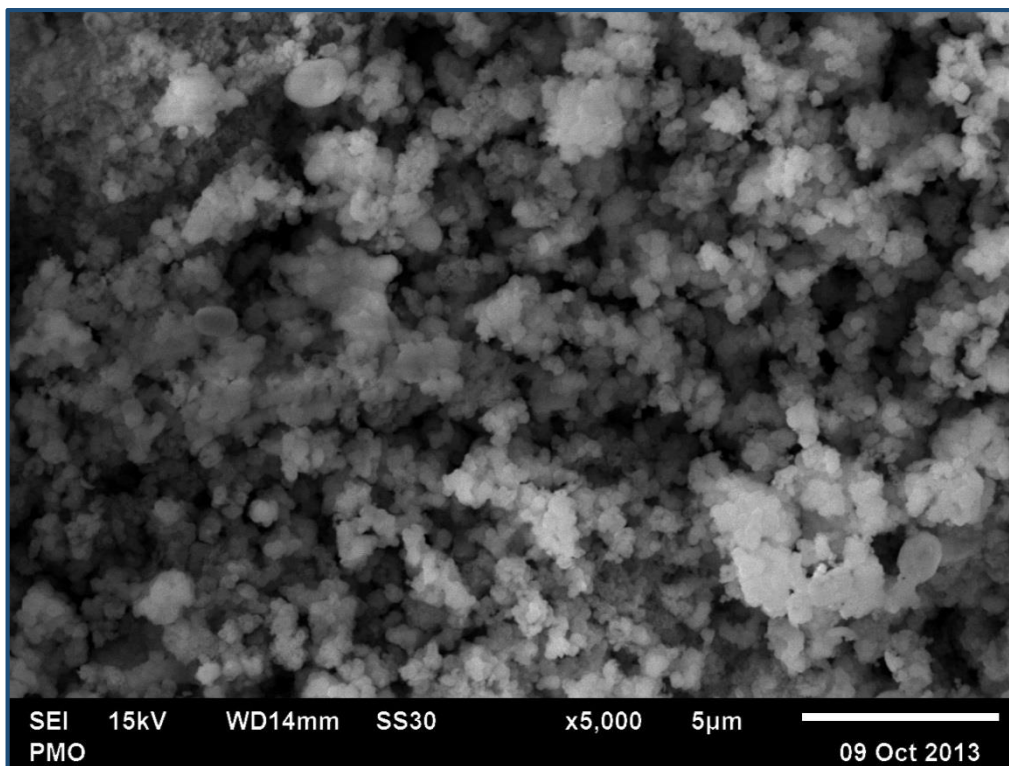


**Figure 4.13b:** Scanning electron microscopy of *Bacillus* sp. PMO and the produced manganese dioxide. Bar = 5µm (5,000x magnification).

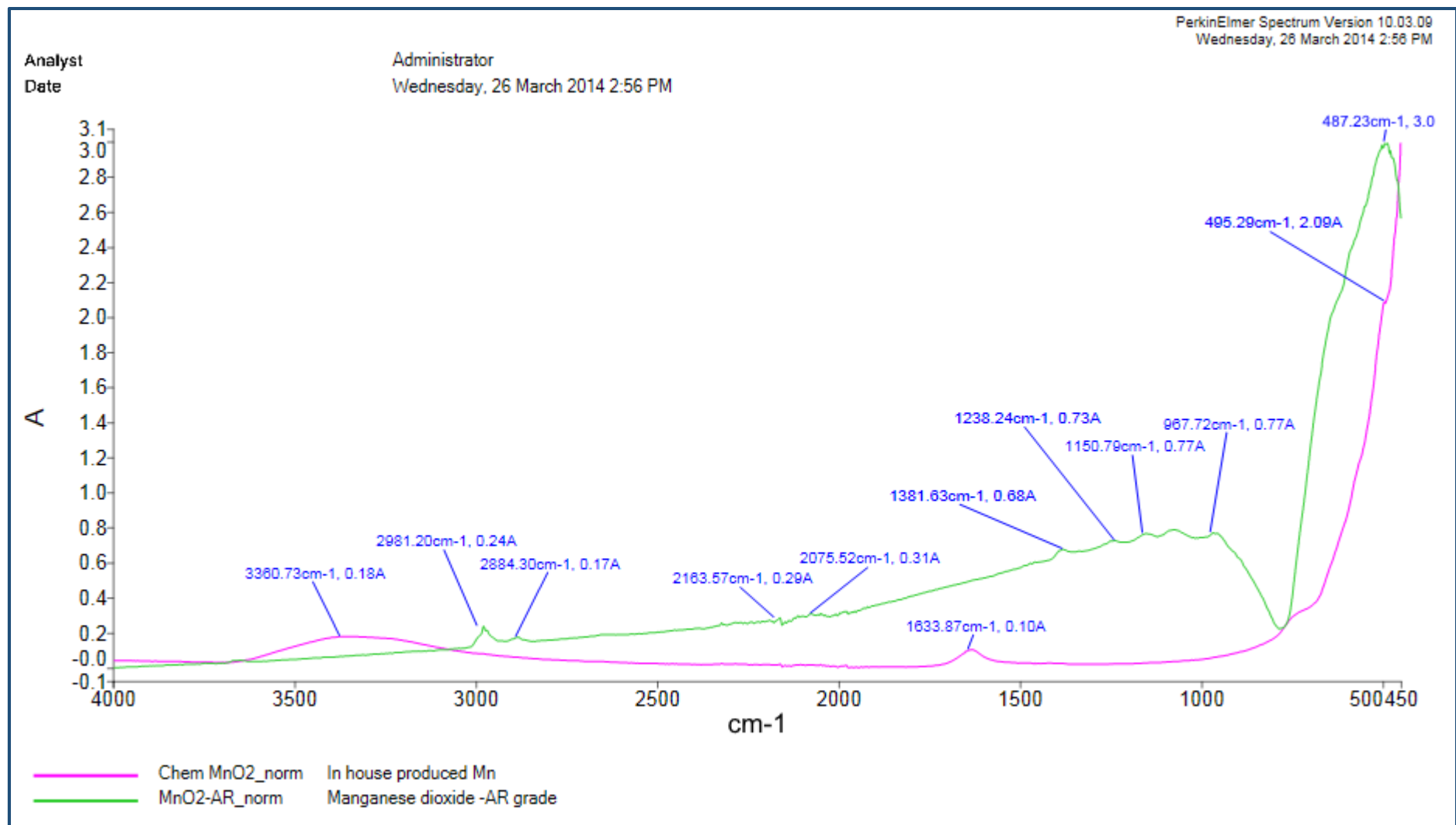


**Figure 4.14:** FTIR-Spectroscopy of organically produced manganese samples of analytical grade and chemically produced MnO<sub>2</sub>. Major absorbance peaks are displayed.

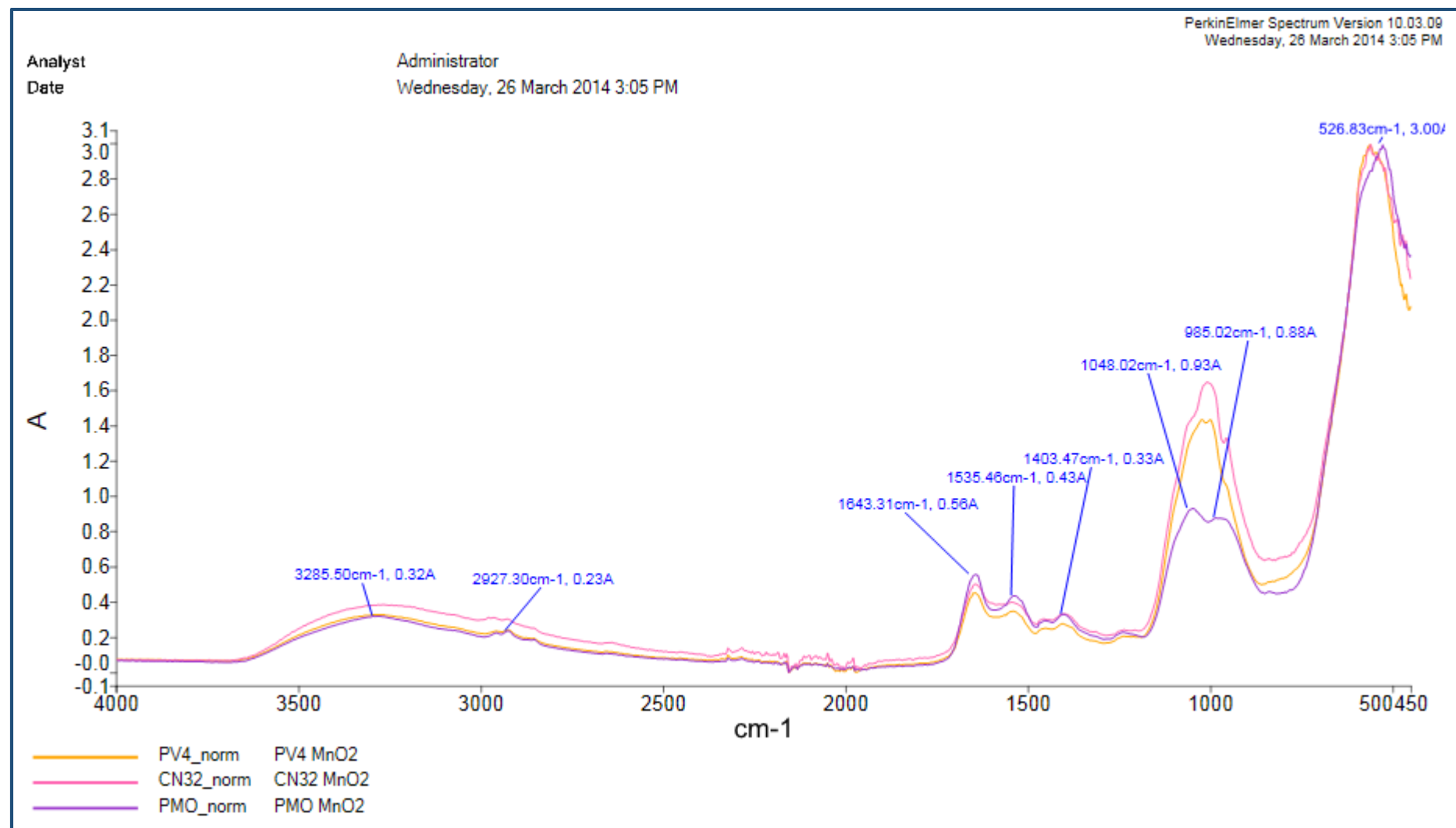


**Figure 4.15:** FTIR-Spectroscopy of organically produced manganese samples of *Shewanella putrefaciens* CN-32, *Shewanella loihica* PV-4 and *Bacillus* sp. PMO. Major absorbance peaks of *Bacillus* sp. PMO are displayed.

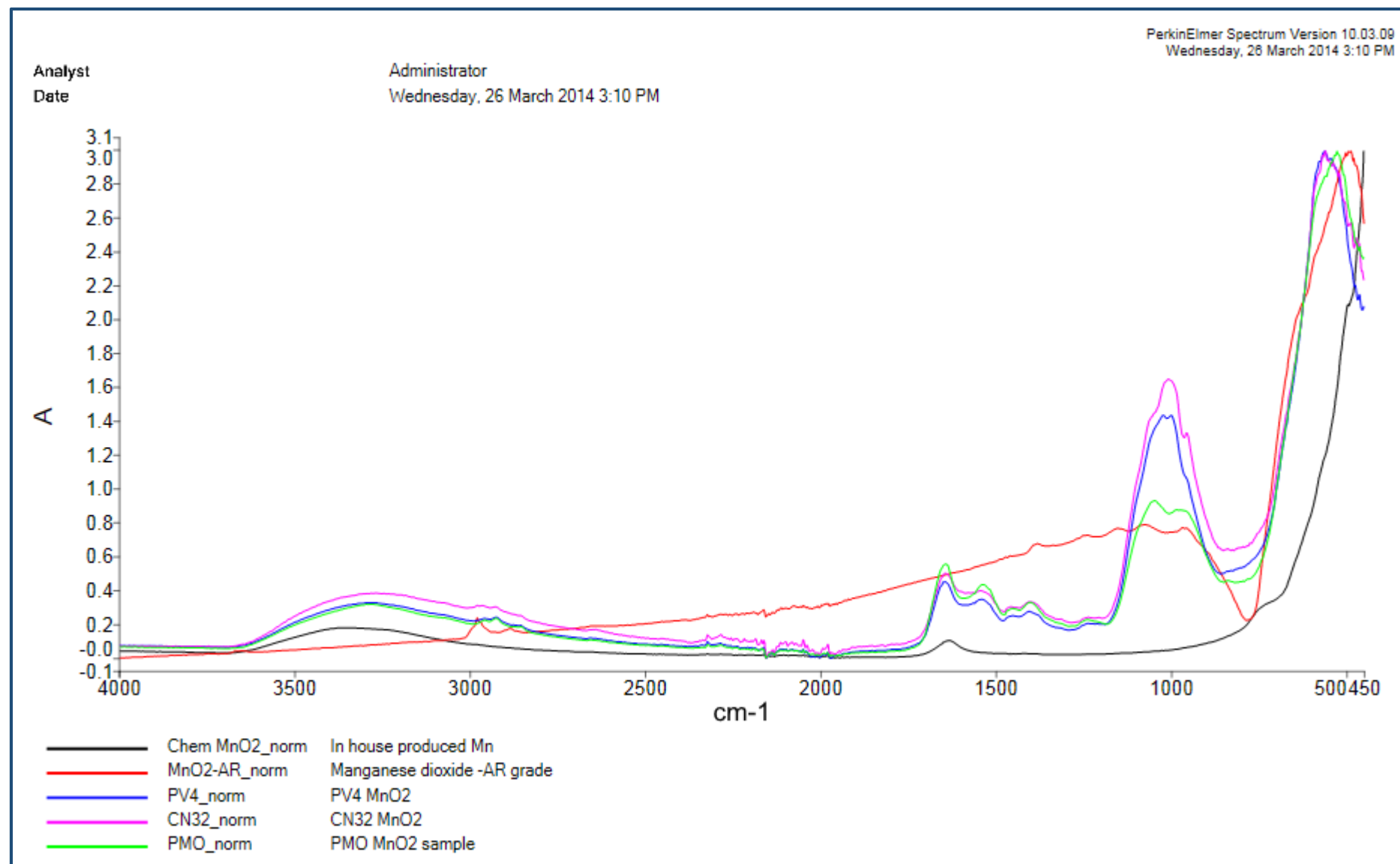


**Figure 4.16:** FTIR-Spectroscopy overlay of the bacterially produced, analytical grade and chemically produced manganese samples.

## 4.6 Discussion

Bacterial manganese cycling is an important biological process in the environment for both the energy demands of microorganisms, and the balancing of Mn(II) → Mn(IV) in the environment. This chapter sought to investigate the oxidation and reduction of manganese transformers isolated from PHS and to increase the knowledge base of the characteristics of organisms within the genera *Shewanella*. *Shewanella* spp. are the most studied manganese reducers to date, but little is known about their ability to oxidise manganese. The chapter focused both on obtained isolates from culture collections (*Shewanella*), as well as bacteria that were isolated from an environment rich in metals (PHS). Characterisation studies were performed to assess the conditions under which to conduct the manganese redox studies. All of the isolates were able to both oxidise and reduce manganese at a range of concentrations. Microbial reduction was rapid and generally commenced within 24 hours whereas oxidation which took 2-3 days, with maximum oxidation occurring between 10-15 days. After 20 days incubation a relatively pure Mn(IV) oxide was created by the isolates.

It was determined that all of the isolates were facultative, mesophilic and able to metabolise a variety of different electron acceptors besides Mn(IV). *Shewanella* isolates grew best at around 40°C, while isolates obtained from PHS grew at an optimal temperature of 30°C. Despite the PHS water having an average temperature of 57°C, the localised heat source actually gave the pool a temperature gradient away from the source, thus providing suitable growth conditions for mesophiles in addition to thermophiles. The isolation of mesophiles from an environment with an average temperature of 57°C is attributed to the temperature gradient of the water within the spring; with generally lower temperatures near the edges and sediments. Samples were taken from various locations in the spring and those from which the strains were isolated were away from the source.

The isolates were able to use various electron donors in cellular metabolism. Organic extracts were found to be the most widely used electron donors of those tested and positive growth evident in all isolates. Simple sugars (glucose, fructose) were also used by a range of isolates (4/8 and 6/8 respectively). However, *Shewanella oneidensis* MR-1 was the most biologically active of all the isolates with growth present in 8/10 electron donors tested, consistent with previous studies which emphasises its nutritional versatility (Gao *et al.*, 2006; Pinchuck *et al.*, 2011; Yoon *et al.*, 2013). PHS isolates were able to utilise raffinose, a trisaccharide composed of glucose, galactose and fructose (found in various plants). PHS isolates obtain energy through nutrient recycling and presence of plant and algal material would account for the presence of Raffinose-degrading enzymes within these organisms. Furthermore, the abundance of microbial life in PHS would account for the use of all extracts such as yeast extract. This is observed in bacteria isolated from the GAB which also use raffinose in cellular metabolism (Ogg & Patel, 2009).

Several electron acceptors were able to be used in cellular respiration as an alternative to oxygen. The isolates were tested for growth in conjunction with a variety of metals found in trace concentrations in environmental waters and of these, Fe(III) and Mn(IV) were found to be the most widely used; with growth in 7/8 and 8/8 conditions respectively. Reduction of vanadium and cobalt was evident in several isolates, with the largest variety of reduction by *Shewanella loihica* PV-4 and the PHS isolate *Bacillus* sp. DLH-1207. Uranium reduction was only evident by *Shewanella oneidensis* MR-1 and *Shewanella putrefaciens* CN-32. Uranium reduction in *Shewanella* spp. has been well recognised, with extensive studies on the mechanisms and bioremediation potential of both *Shewanella oneidensis* MR-1 and *Shewanella putrefaciens* CN-32 as reducers of the toxic affluent (Gao *et al.*, 2006; Fredrickson *et al.*, 2002; Sheng *et al.*, 2011; Sheng and Fein, 2014). From a bioremediation perspective, microorganisms capable of multi-metal reduction are advantageous as pollutants are rarely pure and often contain several toxic metals. Though under anoxic conditions, these metals may be coupled with cellular respiration and subsequently detoxified.

As stated, both the *Shewanella* and PHS isolates were able to reduce and oxidise manganese. Reduction studies revealed the isolates capable of reducing MnO<sub>2</sub> at concentrations  $\leq 12$  mM, with complete reduction occurring at 24-36 hours after incubation. Microbial oxidation was only evident in concentrations  $\leq 7$  mM, occurring 2-3 days after initial growth was observed and complete oxidation after 10-15 days. Comparatively, reduction occurred at both at a faster rate and at higher concentrations than oxidation. The isolates were also able to reduce biogenic MnO<sub>2</sub> for cellular respiration under anaerobic conditions.

The ability of bacteria to both oxidise and reduce manganese has been rarely investigated as many oxidisers are strict aerobes and many reducers are strict anaerobes. However it is possible that facultative transformers may be capable of both processes and be very important in manganese cycling. An early study by Bromfield and David (1976) observed that *Arthrobacter* spp. were capable of manganese oxidation in shallow aerated vessels and reduction as well when transferred to deep static cultures. The present study supports the findings these authors and suggests that bacteria capable of both oxidation and reduction may be more widespread in natural environments.

Unexpectedly, growth inhibition was detected in cultures containing high levels of Mn(IV). Manganese dioxide is a solid that settles at the bottom of the stagnant culture media and it was assumed that Mn(IV) concentration would be independent of cellular growth, however this was not the case. The most likely cause of inhibition is the build-up of Mn(II) when it is reduced by the manganese transformers. As Mn(II) is reduced, it is also solubilised and is distributed throughout the medium. As the intracellular concentration increases, it is probable that this becomes toxic to the cells and subsequently inhibits cellular growth. This is further highlighted through the detection of growth inhibition in cultures containing Mn(II).

It was observed that manganese oxidation did not occur as a direct response to cellular growth, but rather appeared to be an independent process. In the transformation studies, oxidation was only observed after growth had begun. Total oxidation increased with growth; however these processes do not appear to be linked. Based on these observations, it is theorised that manganese oxidation is most likely an energy storing mechanism performed by cells (under aerobic conditions) and that the reduction of Mn(IV)  $\rightarrow$  Mn(II) provides an alternate electron acceptor to oxygen (under anoxic conditions). While Mn(II) oxidation to Mn(III)/Mn(IV) is

thermodynamically favourable, there has been no previous research supporting that this is an energy storing mechanism by bacteria (Tebo *et al.*, 2005).

The average oxidation states of samples were assessed between the control and the bacterially formed oxides. Note that the obtained values do not definitively distinguish between two oxidation states; but rather offers an average oxidation state. The analytical grade manganese gave an average oxidation state of 1.99 and manganese oxide content of 100%. The value 1.99 refers to  $\text{MnO}_{1.99}$  and is as close as experimentally possible to  $\text{MnO}_2$ , which is virtually complete Mn(IV). Analytical grade  $\text{MnO}_2$  is pyrolusite, a highly pure form of  $\text{MnO}_2$ . The analytical  $\text{MnO}_2$  has a minimal purity of 99.9% (Sigma-Aldrich, 2014) and the obtained values are very close to the theoretical values. Conversely, the chemically produced oxide gave an average oxidation state of 1.98 and manganese oxide content of 99.6%. The differences in purity are attributed to the chemical processing and purification of the oxide in chemical synthesis verses the purification processing of the analytical grade  $\text{MnO}_2$ . The average oxidation states of oxides produced by *Shewanella putrefaciens* CN-32, *Shewanella loihica* PV-4 and *Bacillus* sp. PMO were 1.93, 1.93 and 1.92 respectively. The result is  $\text{MnO}_{1.92/1.93}$  which is consistent with microbially formed manganese oxides, likely due to a lower crystalline content and some partially oxidised Mn(III) (Greene & Madgwick, 1991). The manganese oxide content of these samples were 92%, 91.6% and 90.8%. The lower manganese oxide content values of these samples are a result of contamination of residual organic materials (cellular components, metabolic products, adsorbed ions, etc.).

Scanning Electron Microscopy compared the relative sizes and structures between biogenic, chemically produced and analytical grade manganese dioxides. SEM revealed the analytical grade was significantly different to both the biologically and chemically synthesised equivalents. Imaging of the analytical grade  $\text{MnO}_2$  revealed large crystal-like structures, ranging from 0.3-5 $\mu\text{m}$  in size. Conversely, the chemically synthesised and biogenic  $\text{MnO}_2$  consisted of smaller, powder like compounds; with no visual difference between these two. Oxidation of manganese by bacteria occurs at a microscopic level, accounting for small particle production of  $\text{MnO}_2$ . Conversely, analytical grade  $\text{MnO}_2$  is mined pyrolusite and accounts for the difference in particle size between the particle size of the analytical from chemical and biogenic oxides.

Bacteria were visualised in the *Shewanella* spp. SEM images but were absent in the *Bacillus* sp. PMO photographs. Instead, SEM imagery of *Bacillus* sp. PMO revealed the presence of spores. Manganese oxidation by *Bacillus* sp. SG-1 can be achieved by bacterial spores, and it is deduced that the presence of these spores are responsible for the surrounding Mn(II) oxidation (Tebo *et al.*, 1998). It is assumed that bacterial cells are present, however are encrusted with oxide and difficult to visualise under electron microscopy.  $\text{MnO}_2$  production by bacterial spores supports the theory that oxidation is a response to energy generation, as dormant spores under anoxic conditions may oxidise this manganese to produce a terminal electron donor for use in anaerobic respiration.

FTIR spectroscopy was employed to compare the purity and differences of analytical grade manganese dioxide against both the chemical and biogenic oxides. The analytical grade  $\text{MnO}_2$  produced a distinct peak at  $487.23\text{cm}^{-1}$  which falls within the peak spectra for Mn(IV) products (Moy, 1998). Likewise, the chemically produced  $\text{MnO}_2$  was close to the analytical grade  $\text{MnO}_2$  at  $495.29\text{cm}^{-1}$  and lower wavenumbers. The differences in absorbance readings between the two samples are a result of impurities generated during the synthesis process of chemically produced manganese dioxide. During the chemical synthesis of  $\text{MnO}_2$ , residual manganese (from  $\text{KmnO}_4$  /  $\text{MnCl}$ ) can remain post purification as well as other the formation of other manganese compounds ( $\gamma\text{-MnO}_2$ ;  $\text{Mn}_3\text{O}_4$ ;  $\gamma\text{-MnOOH}$ ); however this occurs at significantly lower levels than  $\text{MnO}_2$  (Spiro *et al.*, 2010). The variations in the major peaks in the FTIR are likely reflective of the structural differences in the manganese oxides.

The biogenic oxides showed quite dissimilar, large peaks at  $526.83\text{cm}^{-1}$  when visualised on the FTIR spectrometer. The peaks at  $\sim 526\text{cm}^{-1}$  indicate a less crystalline  $\text{MnO}_2$  which is typical of biogenic oxides (Greene & Madgwick, 1991). However, secondary peaks were also detected at varying points between  $1238.24\text{cm}^{-1}$  –  $967.72\text{cm}^{-1}$ . These peaks are most likely residual biological matter from the oxidising bacteria. Though the oxide cultures were lysed and acid washed, it is possible that organic matter was not removed or got trapped within the residual oxide. François *et al.* (2012) performed FTIR on mercury tolerant bacteria and an almost identical peak at  $\sim 1000\text{cm}^{-1}$  was present within their FTIR analysis. This is confirmed in the manganese oxide % analysis of these samples, revealed 8% - 9.2% of unknown material present in the samples. It is therefore deduced that these peaks are residual matter left over from the enrichment cultures.

# Chapter 5

Immobilisation of Toxic  
Metals by Biogenic MnO<sub>2</sub>

## 5.1 Introduction

### 5.1.1 Metal immobilization by biogenic MnO<sub>2</sub>

Manganese(IV) oxides are able to immobilise numerous toxic metals present in the environment. The negative charged, layered structures and high specific surface areas of manganese oxides result in high levels of adsorption of toxic metals (Miyata *et al.*, 2007). Adsorption of toxic metals effectively immobilises them from their soluble form; playing a pivotal role in the geochemical cycling of these pollutants, removing them from the environment. MnO<sub>2</sub> adsorption has been detected in arsenic, cadmium, calcium, cobalt, copper, iron, lead, mercury, nickel, plutonium, polonium, radium, selenium, tin, thorium, uranium and zinc (Tebo *et al.*, 2004). This occurs at significant levels and has potential applications in bioremediation and biogenic MnO<sub>2</sub> have significantly greater absorption capacities than abiotically produced oxides (Stuetz *et al.*, 1996; Francis & Tebo, 2001; Tebo *et al.*, 2004).

There have been extensive studies on the mechanisms behind manganese-driven heavy metal immobilisation. Biogenic manganese oxides form sheet-structures in nature (attributing to Mn nodules found in nature) and these sheets can immobilise metal ions through edge-sharing, double edge sharing (DES) or triple corner sharing (TCS) (Figure 5.1). These edges form complexes with free metal ions, binding them and effectively immobilising them. Figure 5.2 highlights the mechanisms behind DES and TCS bonding of Pb(II).

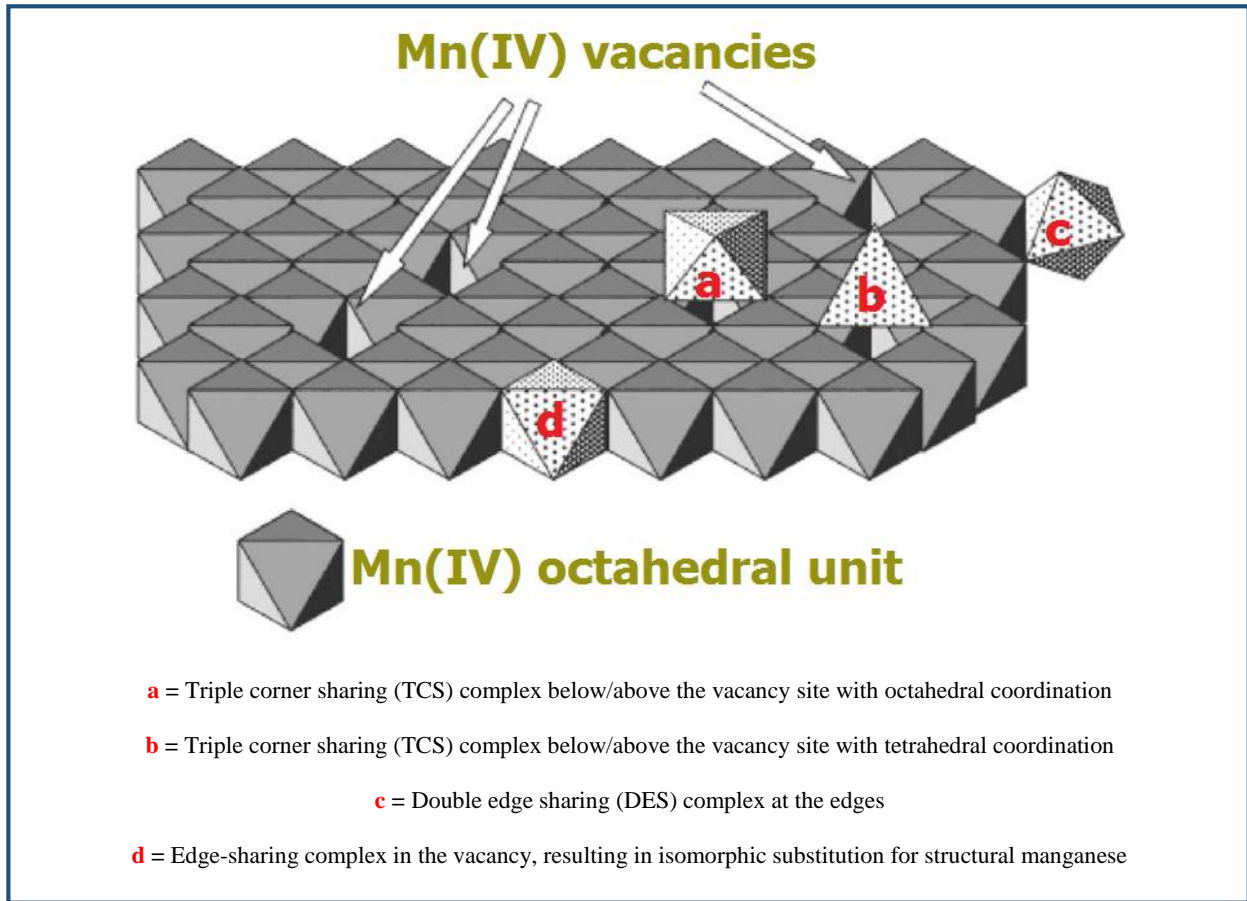


**Figure 5.1:** Structural model of biogenic manganese oxides and subsequent adsorption of metals (as ions) on hexagonal birnessite. Mn(IV) vacancies are compensated by charge-balancing cations (excluded from diagram). Adapted from Miyata *et al.*, 2007.

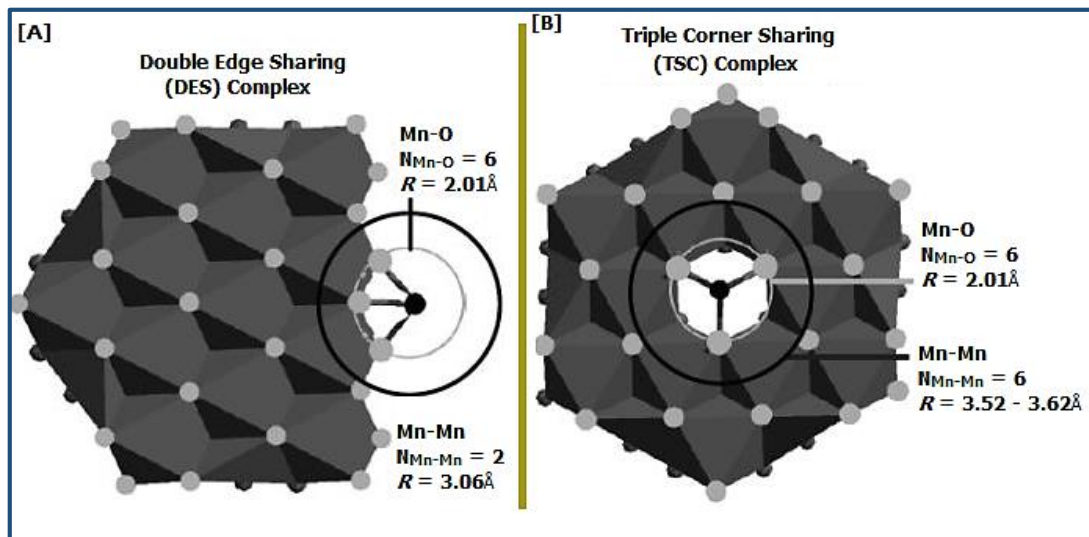


**Figure 5.2:** Adsorbed Pb(II) on hexagonal birnessite, depicting [A] double edged sharing and [B] triple corner sharing to lead. Adapted from Spiro *et al.*, 2010.

### 5.1.2 Bioremediation

Bioremediation is a waste management technique that uses microorganisms to breakdown toxic materials into less harmful or nontoxic by-products. Contamination through poor industrial practices or chemical spillages can result in toxic wastes that can pollute environments with hazardous materials. These materials can include heavy metals, hydrocarbons and various other organic and inorganic compounds. Physical neutralisation (removal by manual extraction) and chemical neutralisation (treatment of contaminants with other chemicals) are often cost ineffective or impractical (Yang *et al.*, 1999). Microbial decontamination offers an alternative to traditional environmental remediation; enzymatically converting or breaking down waste products into more manageable compounds.

The process of bioremediation can be sub-categorised into three stages: bioattenuation; biostimulation; and bioaugmentation). Bioattenuation is a preliminary step which involves the monitoring of the contamination site as natural bioremediation may occur, avoiding the need for additional intervention. If natural site restoration fails, biostimulation of the contaminated site is attempted. This process involves environmental modifications to promote the growth of already present bacteria for use in bioremediation. This occurs through the alteration of pH/temperature, the inclusion of organics (Methanol, acetate, etc.), inorganic compounds (Nitrogen, Phosphorus), and/or electron. If this fails, bioaugmentation (the induction of microbes capable of environmental restoration) are applied to the contamination site. Microbial bioremediation has risks however; primarily the introduction of foreign microbes in high numbers can potentially upset the microbial flora, disrupting the ecosystem of the waste site. However the microbial cell numbers typically reduce significantly after bioremediation has been achieved (Iwamoto & Nasu, 2001).

## 5.2 Single Metal Immobilisation by Manganese Oxides

The adsorption potential of manganese oxides produced by *Bacillus* sp. PMO, *Shewanella putrefaciens* CN-32 and *Shewanella loihica* PV-4 was tested against 6µg/mL concentrations of copper, chromium, lithium, lead, cobalt, arsenic and nickel (Figure 5.3, Figure 5.4, Figure 5.5). Additionally, adsorption was tested concurrently with bacterial growth/Mn oxidation and also with the addition of oxidised cultures to waters containing individual metals. Of the 42 conditions tested, varying degrees of adsorption was observed in every instance. There were only minor differences between adsorption by the different strains, however there were significant differences between the metal addition and metal pre-treatment conditions. Additionally, there were significant differences between the total adsorption levels of each metal. With the exception of nickel, all metals showed higher adsorption rates when growth/oxidation occurred simultaneously compared to direct addition. Immobilisation of lead occurred at the greatest levels, with 44.3% to 84.5% (post-growth) and 92.98% to 96.86% (during growth) removed (Table 5.1). Conversely, nickel did not follow the observed trend; with no significant differences observed.

**Table 5.1:** Metal immobilisation of individual metals by bacterially produced manganese oxides.

Immobilisations at percentages  $\geq 90\%$  are highlighted in bold.

Strain	Condition	Metal Immobilisation (%)						
		Cu	Cr	Li	Pb	Co	As	Ni
CN-32	Concurrent	62.51%	50.00%	73.01%	<b>92.98%</b>	47.78%	78.25%	22.46%
	Post oxidation	33.4%	32.4%	44.05%	79.06%	15.41%	20.90%	35.98%
PV-4	Concurrent	82.26%	74.33%	73.01%	<b>96.86%</b>	68.56%	81.96%	34.95%
	Post oxidation	2.86%	26.25%	42.33%	44.30%	12.96%	16.38%	33.61%
PMO	Concurrent	80.25%	75.00%	74.08%	<b>95.28%</b>	71.23%	57.43%	27.30%
	Post oxidation	44.50%	25.30%	42.61%	84.51%	26.55%	38.30%	43.11%

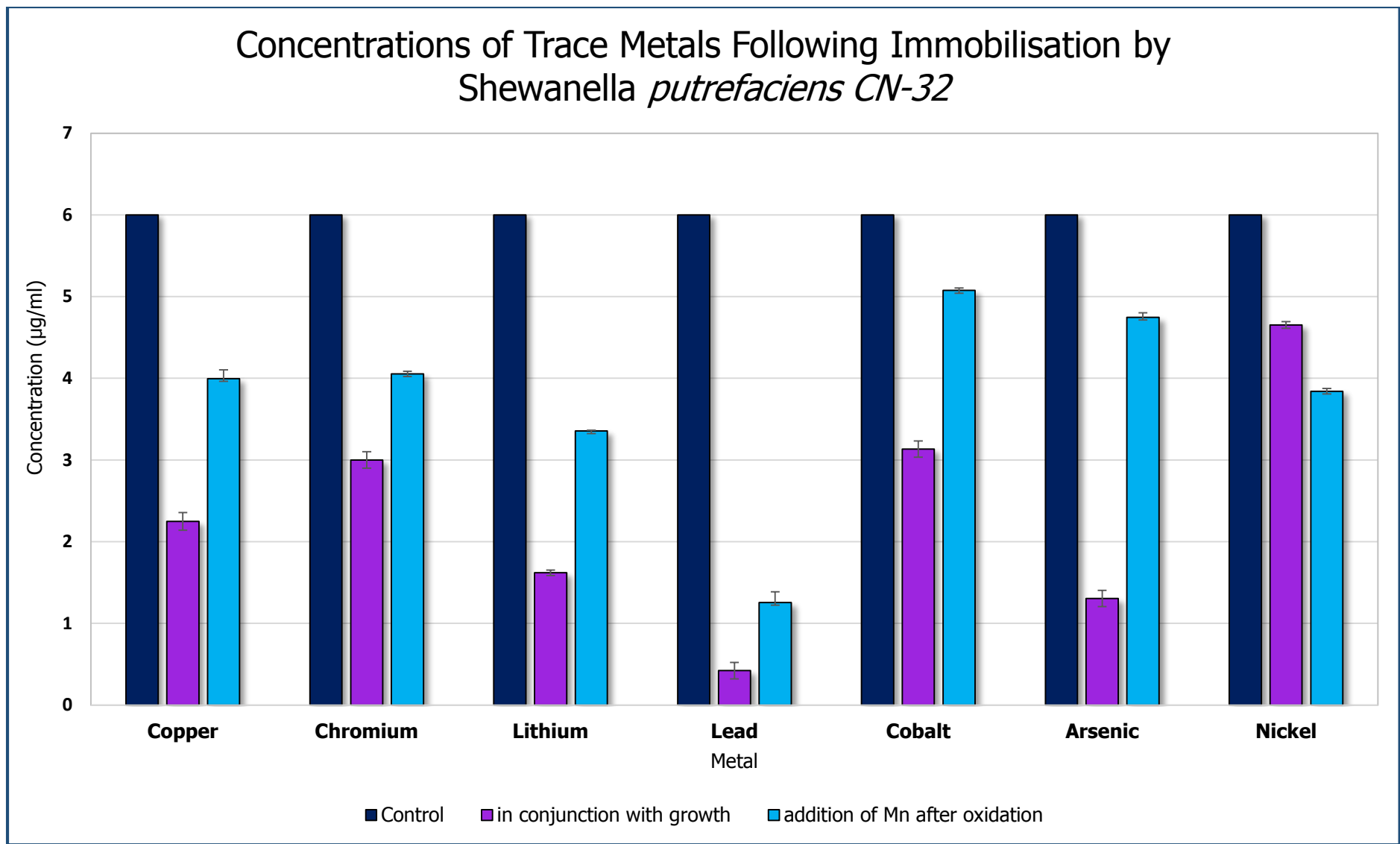


**Figure 5.3:** Adsorption of various metals by biogenic manganese oxides (oxidised by *Shewanella putrefaciens* CN-32) in conjunction with bacterial growth and after growth/oxidation.

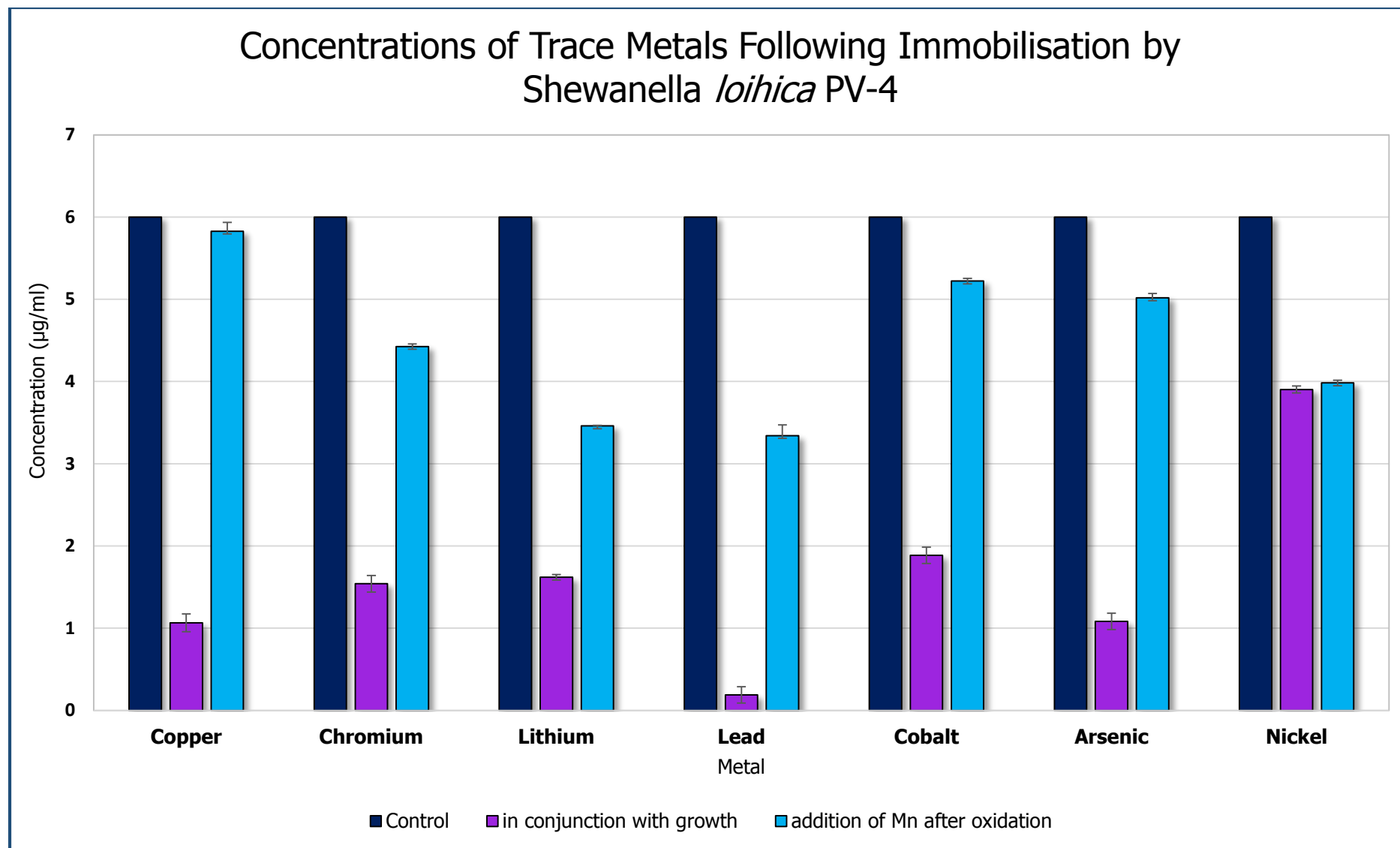


**Figure 5.4:** Adsorption of various metals by biogenic manganese oxides (oxidised by *Shewanella loihica* PV-4) in conjunction with bacterial growth and after growth/oxidation.

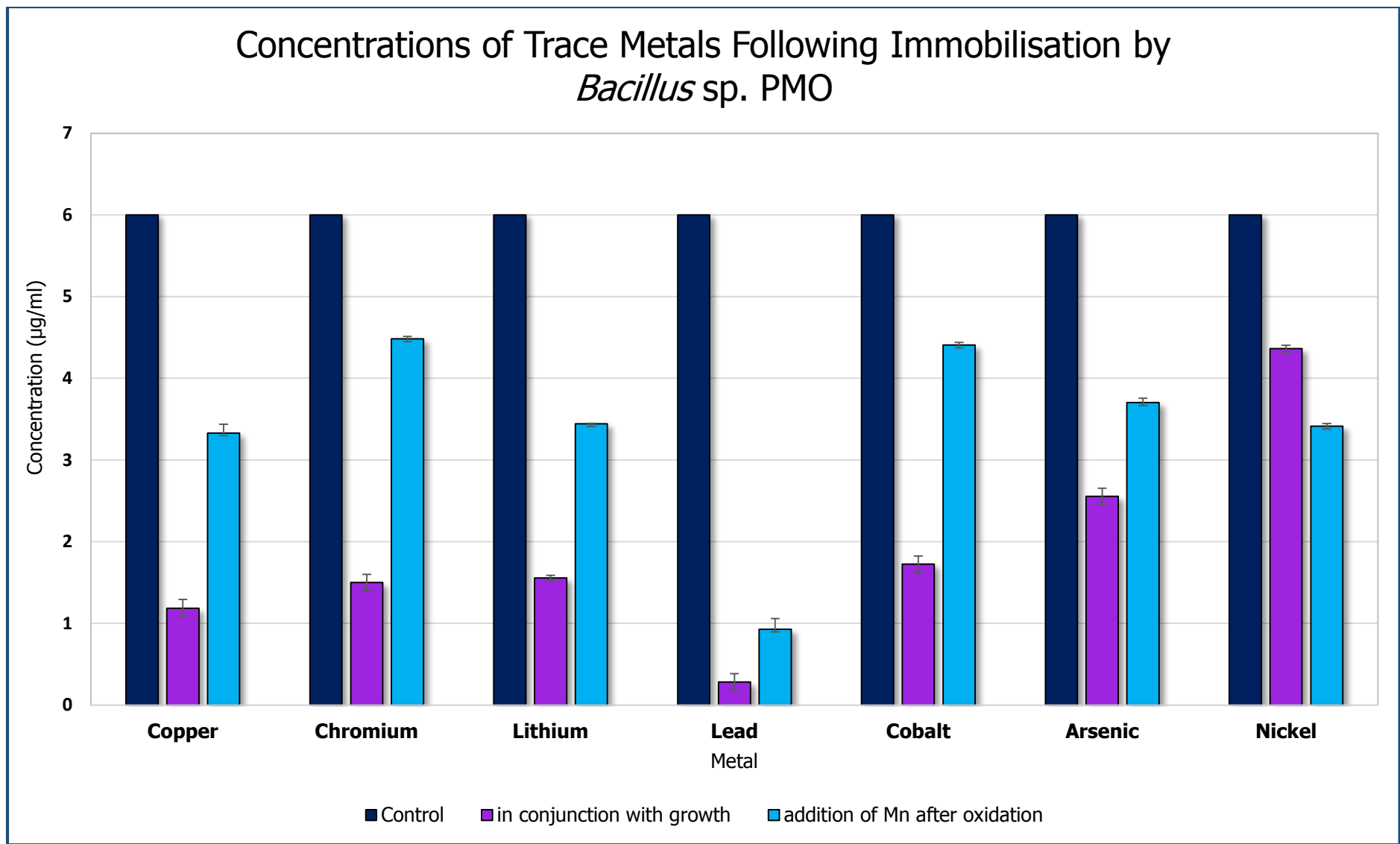


**Figure 5.5:** Adsorption of various metals by biogenic manganese oxides (oxidised by *Bacillus* sp. PMO) in conjunction with bacterial growth and after growth/oxidation.

### 5.3 Bioremediation of Waste Waters by Biogenic Oxides

Manganese oxide-containing cultures of *Bacillus sp.* PMO, *Shewanella putrefaciens* CN-32 and *Shewanella loihica* PV-4 were directly applied to simulated waste waters to assess the bioremediation potential of metal immobilisation (Figure 5.6, Figure 5.7, Figure 5.8). Neat (identical concentrations to those in the waste waters), 1:10 and 1:100 dilutions were analysed by ICP-OES before and after application of MnO<sub>2</sub>. Immobilisation was detected across all metals and in all conditions, with complete removal revealed under all conditions in the 1:100 dilutions. Zinc was the most readily immobilised metal, with >75% immobilisation detected in the neat metal composite sample and >99% removal observed in the 1:10 and 1:100 dilutions. Conversely, chromium was removed in low percentages in the neat and 1:10 dilutions, however was completely removed in the 1:100 dilution sample. There were no significant differences between any of the three organisms tested (Table 5.2).

**Table 5.2:** Metal immobilisation of simulated waste waters by bacterially produced manganese oxides. Immobilisations at percentages  $\geq 90\%$  are highlighted in bold.

Strain	Conc.	Metal Immobilisation (%)				
		Zn	Cu	Ni	Cd	Cr
CN-32	Undiluted	79.07%	81.22%	26.95%	32.83%	8.54%
	1:10 dilution	<b>100%</b>	35.03%	33.95%	<b>93.57%</b>	5.67%
	1:100 dilution	<b>100%</b>	<b>100%</b>	<b>100%</b>	<b>100%</b>	<b>100%</b>
PV-4	Neat	77.24%	19.72%	22.53%	46.23%	7.36%
	1:10 dilution	<b>99.27%</b>	39.40%	21.99%	87.9%	9.08%
	1:100 dilution	<b>100%</b>	<b>100%</b>	<b>100%</b>	<b>100%</b>	<b>100%</b>
PMO	Neat	77.17%	77.10%	27.81%	41.11%	11.31%
	1:10 dilution	<b>100%</b>	60.29%	35.24%	<b>94.80%</b>	3.86%
	1:100 dilution	<b>100%</b>	<b>100%</b>	<b>100%</b>	<b>100%</b>	<b>100%</b>

Concentrations of Trace Metals in Simulated Waste Water Following Immobilisation by

*Shewanella putrefaciens* CN-32

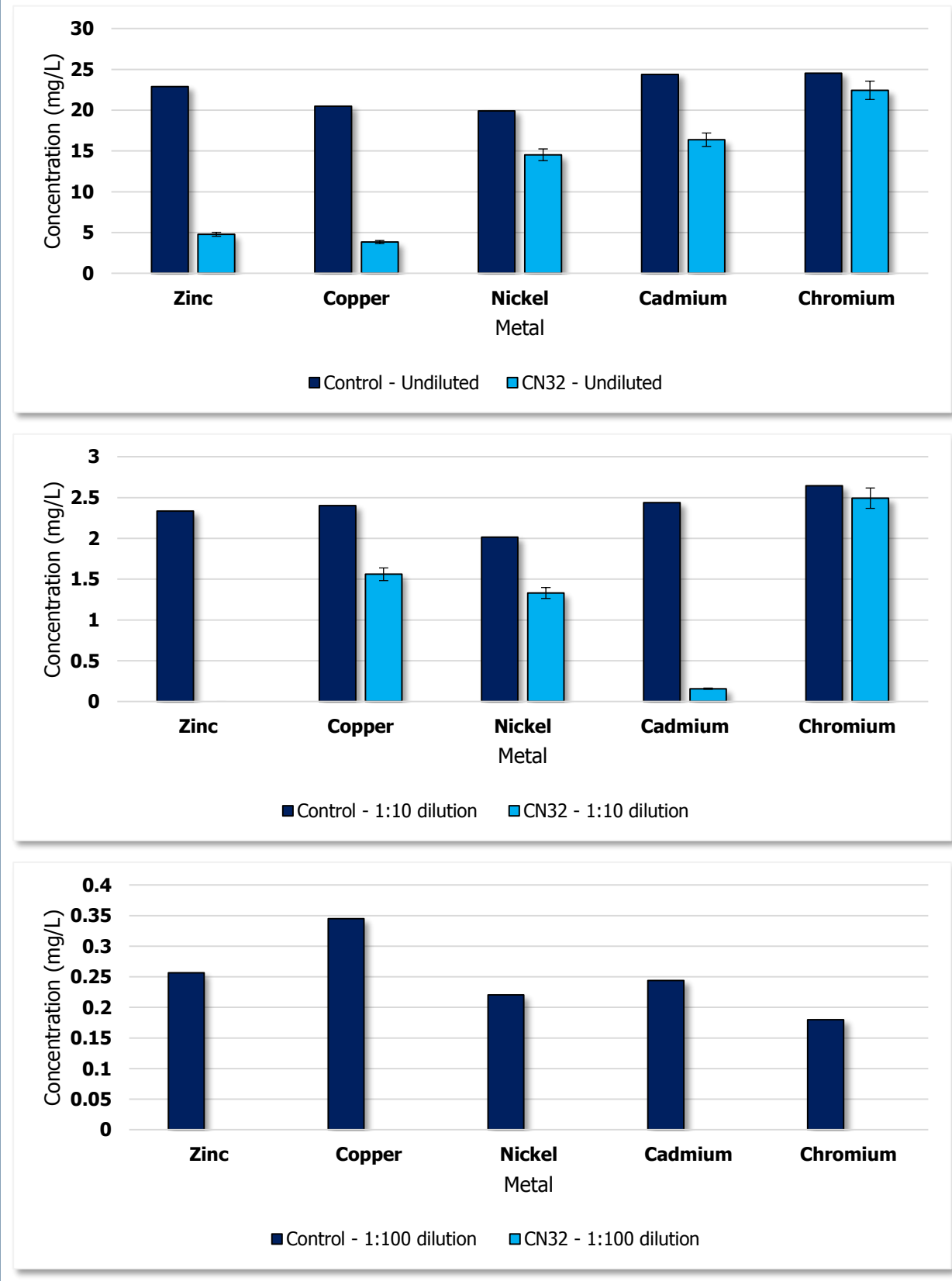


Figure 5.6: Metal immobilisation of simulated waste waters by manganese oxides produced by *Shewanella putrefaciens* CN-32.

Concentrations of Trace Metals in Simulated Waste Water Following Immobilisation by

*Shewanella loihica* PV-4

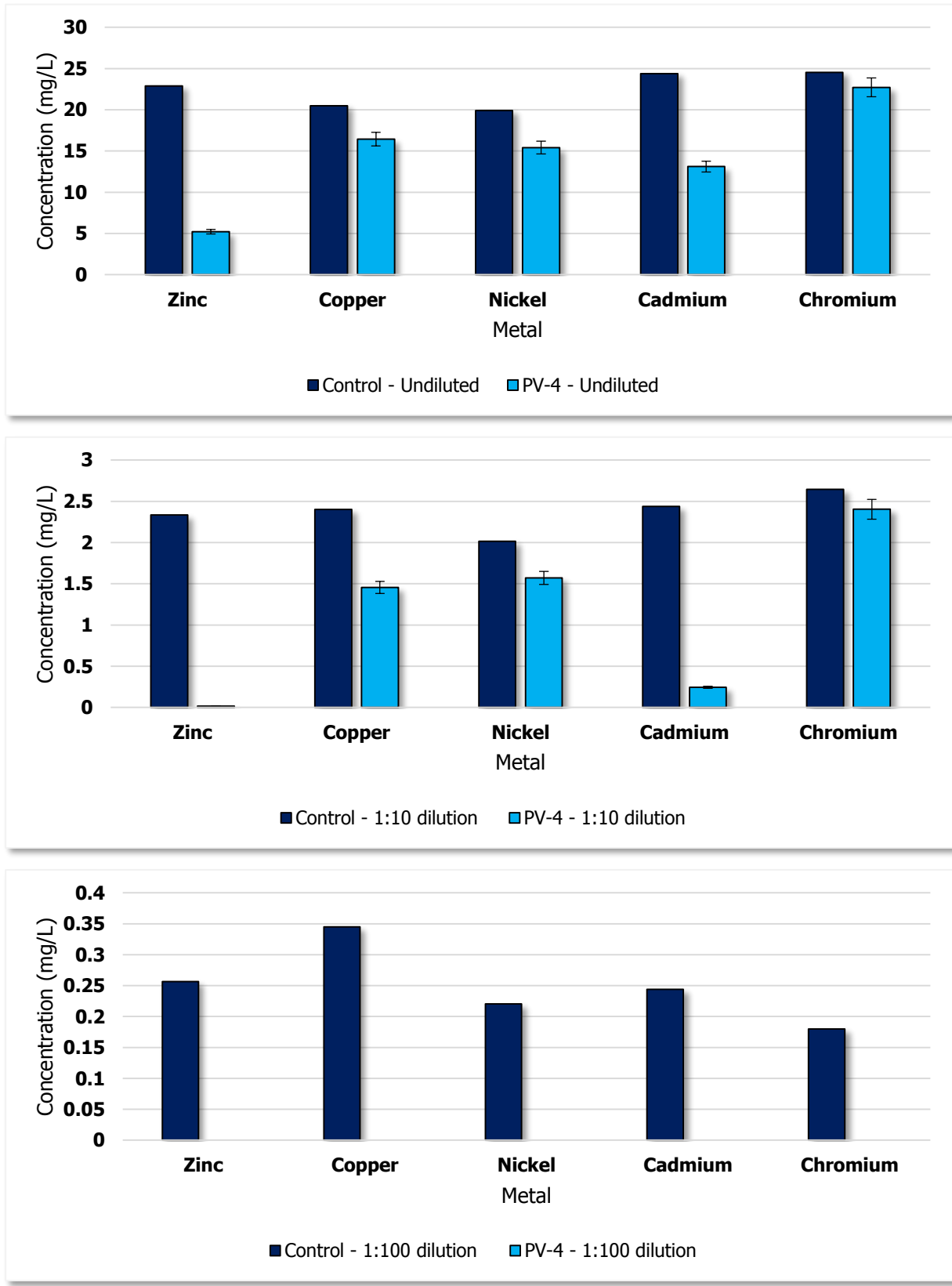


Figure 5.7: Metal immobilisation of simulated waste waters by manganese oxides produced by *Shewanella loihica* PV-4.

Concentrations of Trace Metals in Simulated Waste Water Following Immobilisation by

*Bacillus sp. PMO*

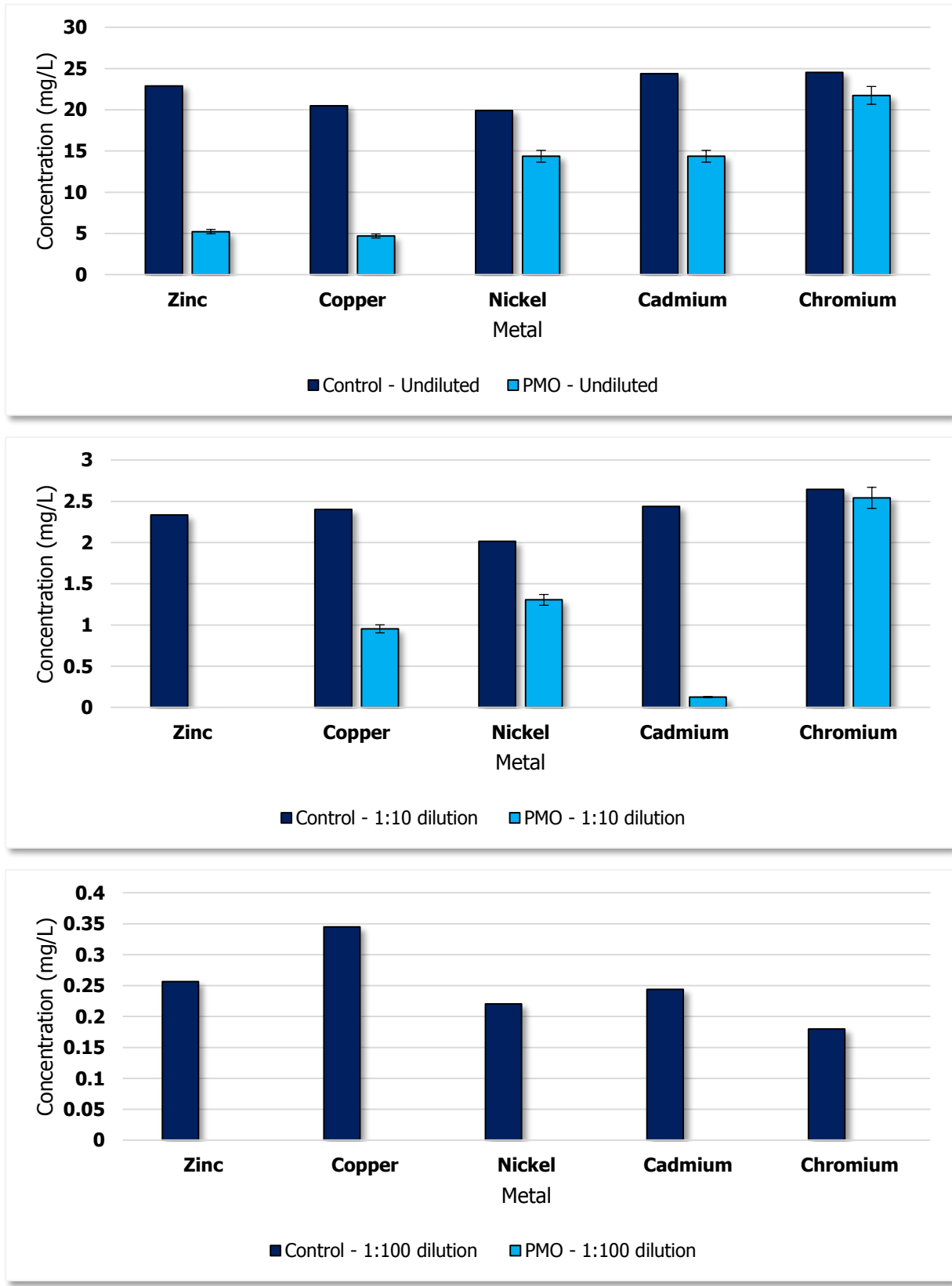


Figure 5.8: Metal immobilisation of simulated waste waters by manganese oxides produced by *Bacillus sp. PMO*.

## 5.4 Discussion

Immobilisation of metals using biogenic MnO<sub>2</sub> has the potential to remove environmental and industrial toxic effluents. This chapter sought to investigate the immobilisation characteristics of manganese oxides produced by *Shewanella putrefaciens* CN-32, *Shewanella loihica* PV-4 and *Bacillus* sp. PMO. This chapter focused on both the immobilisation of individual metals and the removal of metals from simulated waste waters. Two conditions were tested in the removal of individual metals. Firstly, manganese oxides were produced initially by bacteria then used to immobilise metals in solution. Secondly, metals were added to media prior to the production of MnO<sub>2</sub> by bacteria. Immobilisation was evident across a variety of metals under both these conditions. Greater levels of metals were immobilised when metals were incorporated to the media prior to oxide formation.

In single metal studies, immobilisation was detected in varying degrees against all metals tested (copper, chromium, lithium, lead, cobalt, arsenic and nickel). With the exception of nickel, all metal immobilisation occurred at greater levels when oxidation occurred concurrently. The lack of significant difference in the removal of nickel (irrespective of when oxidised manganese was added) is likely a result of maximum immobilisation occurring in both conditions. While simultaneous growth offers greater levels of immobilisation, the presence of these metals in higher concentrations may be toxic and inhibit cellular growth and oxide production. Conversely, the addition of biogenic MnO<sub>2</sub> alleviates growth inhibition but lowers the effectiveness of immobilisation.

The remediation potential of biogenic MnO<sub>2</sub> against simulated industrial waste waters resulted in substantial removal of metals tested under all conditions (Undiluted, 1:10 and 1:100 dilutions of simulated wastewaters). Metal removal through manganese oxide immobilisation was found to be non-specific. Zinc was most readily immobilised within the waste waters, with 77.17% - 79.07% adsorption observed in the neat and 100% adsorption in the 1:10 and 1:100 conditions. Chromium was the least adsorbed of all the metals, with 7.36% - 11.31% detected in the neat waters, 3.86% - 9.08% in the 1:10 dilution and 100% removal in the 1:100 dilution. This correlates with data described by the Tebo and colleagues (2004), who previously reported that adsorption has been detected in zinc, copper, cadmium and nickel. Chromium was not reported as a metal that can be immobilised by manganese oxide.

The relatively low levels of adsorption of chromium may have been due to adherence to glass flasks or cell binding, though it is likely a result of auto-oxidation. Chromium concentrates were significantly removed in single metal manganese oxide studies but were not reduced in simulated waste water studies, and is due to the interacting nature of MnO<sub>2</sub> and Cr(III). MnO<sub>2</sub> in solution oxidises Cr(III) rather than immobilising it, producing Cr(VI) which is much more soluble than Cr(III) and can then be adsorbed by MnO<sub>2</sub> (Guha *et al.*, 2001). It is theorised that in the simulated waste water studies, the manganese oxide was inundated with other toxic metals in the neat and 1:10 dilutions, leaving Cr(III) which was unable to be adsorbed from solution. Conversely, with the 1:100 dilution there was lower levels of metals to bind with MnO<sub>2</sub>, therefore there was still adequate oxide to convert Cr(III) → Cr(VI) and adsorb all the other trace metals present within the solution. This theory also applies to chromium in the single metal analyses, however in these studies there was sufficient MnO<sub>2</sub> available for adsorption to occur.

Various studies on the immobilisation of lead by biogenic manganese have been performed previously, including using simulated bioreactors (Ervin *et al.*, 2005; Villalobos *et al.*, 2005; Hua *et al.*, 2012). Compared to other heavy metals, lead has been the focal point of most research relating to the immobilisation of heavy metals by oxides. This research however focused on typical waste waters produced by industrial processing, as well as comparing the immobilisation potential of cultures growing alongside heavy metals and also the direct application of oxides. Similar to the current study, MnO<sub>2</sub> produced by the isolates could immobilise significant levels of lead.

# Chapter 6

Genomic Analysis of

*Bacillus* sp. PMO

## 6.1 Introduction

### 6.1.1 Whole genome sequencing

Whole genome sequencing (WGS) provides an entire DNA sequence analysis of an organism. WGS is different to traditional methods of sequencing as it ‘shotgun’ sequences the DNA of a particular organism, rather than focusing on a particular gene of interest (for example, 16S rRNA sequencing for bacterial identification). This is particularly useful in clinical analysis as it can identify an individual’s genetic predisposition to a particular disease. (Gonzaga-Jauregui *et al.*, 2012). In prokaryotic analysis, WGS is used to identify genes of interest that a particular organism possesses, including metabolic pathways, antibiotic resistances and secretory systems. Moreover, genes responsible for the transformation of metals can be identified in a microorganism, even if microbial conversion is undetectable in laboratory conditions. WGS is becoming increasingly more viable as a means of identifying and understanding the molecular properties of organisms due to the moderate costs and manageable/straightforward sequencing data produced from this method (Pabinger *et al.*, 2012).

### 6.1.2 Genes associated with manganese oxide reduction

Biological reduction of manganese is achieved through the coupling of Mn(IV) with an appropriate electron donor in cellular respiration. Unlike most metals utilised by DMRB, manganese oxides are environmentally insoluble and thus impermeable for uptake into the cellular matrix. Two major subsystems have been identified responsible for reduction of manganese located in the genera *Shewanella* and *Geobacter*. *Shewanella* spp. employ a type II secretion system, where enzymatic translocation from the outer membrane to the bacterial cell surfaces forms a protein:metal complex with the manganese oxide, which is then reduced from Mn(IV)  $\rightarrow$  Mn(II). *Geobacter* spp. form protein:metal complexes, however electron transfer is achieved through type IV pili that relay electrons to the solid Mn(IV) (Shi *et al.*, 2007). These are illustrative systems used (Figure 6.1); however microbial respiration of manganese is a very diverse trait observed in a multitude of bacteria. Table 6.1 shows a representative list of known genes involved in Mn(IV) oxide reduction.

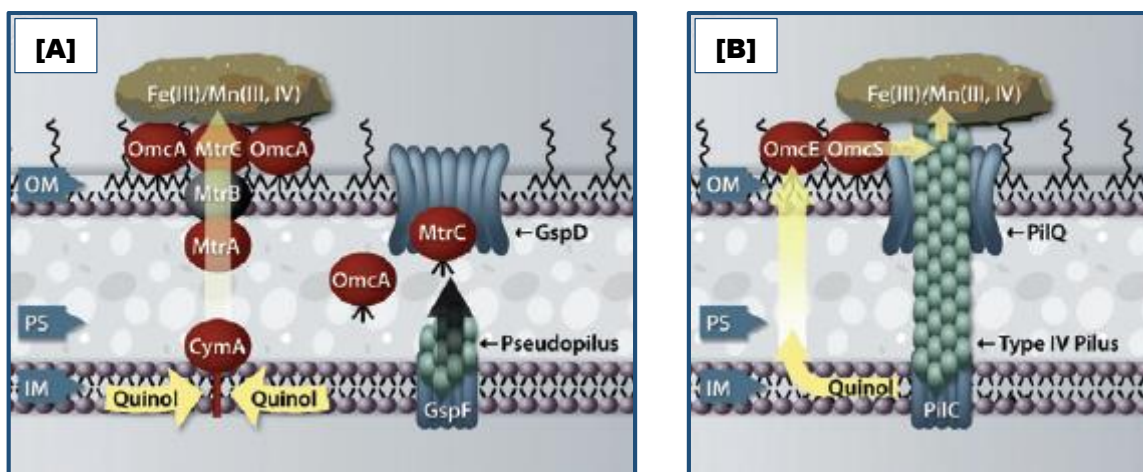


**Figure 6.1:** Electron transfer pathways for *Shewanella* spp. [A] and *Geobacter* spp. [B] during reduction of solid metal oxides. In system [A], proteins form complexes with the metal oxide and subsequent reduction transpires, while in system [B] electron transfer is conferred through type IV pili.

Important proteins are visualised (red) and their encoding genes are detailed in Table 6.1. Figure

adapted from Shi *et al.*, 2007.

**Table 6.1:** Representative genes associated with Mn(IV) oxide reduction.

Gene	Description of gene	Strain	References
<i>CymA</i>	Periplasmic c-type cytochrome	<i>Shewanella putrefaciens</i> CN-32	Murphy & Saltikov, 2007
<i>MtrA</i>	Periplasmic c-type cytochrome	<i>Shewanella putrefaciens</i> MR-1	Beliaev <i>et al.</i> , 2001
<i>MtrB</i>	Outer membrane c-type cytochrome	<i>Shewanella putrefaciens</i> MR-1	Beliaev & Saffarini, 1998
<i>MtrC</i>	Outer membrane c-type cytochrome	<i>Shewanella putrefaciens</i> MR-1	Beliaev <i>et al.</i> , 2001
<i>OmaB</i>	Outer membrane c-type cytochrome	<i>Geobacter sulfurreducens</i>	Ding <i>et al.</i> , 2006
<i>OmaC</i>	Outer membrane c-type cytochrome	<i>Geobacter sulfurreducens</i>	Ding <i>et al.</i> , 2006
<i>OmcB</i>	Outer membrane c-type cytochrome	<i>Geobacter sulfurreducens</i>	Kim <i>et al.</i> , 2006
<i>OmcC</i>	Outer membrane c-type cytochrome	<i>Geobacter sulfurreducens</i>	Mehta <i>et al.</i> , 2005
<i>OmcE</i>	Outer membrane c-type cytochrome	<i>Geobacter sulfurreducens</i>	Mehta <i>et al.</i> , 2005
<i>OmcS</i>	Outer membrane c-type cytochrome	<i>Geobacter sulfurreducens</i>	Leang <i>et al.</i> , 2010
<i>OmcT</i>	Outer membrane c-type cytochrome	<i>Geobacter sulfurreducens</i>	Mehta <i>et al.</i> , 2005
<i>OmcZ</i>	Outer membrane c-type cytochrome	<i>Geobacter sulfurreducens</i>	Nevin <i>et al.</i> , 2009
<i>OmpC</i>	Multi copper oxidase	<i>Geobacter sulfurreducens</i>	Holmes <i>et al.</i> , 2008
<i>PccR</i>	Periplasmic c-type cytochrome	<i>Geobacter sulfurreducens</i>	Aklujkar <i>et al.</i> , 2013
<i>PgcA</i>	Periplasmic c-type cytochrome	<i>Geobacter sulfurreducens</i>	Aklujkar <i>et al.</i> , 2013
<i>PpcA</i>	Periplasmic c-type cytochrome	<i>Geobacter sulfurreducens</i>	Lloyd <i>et al.</i> , 2003
<i>PpcA</i>	Periplasmic c-type cytochrome	<i>Geobacter sulfurreducens</i>	Aklujkar <i>et al.</i> , 2013
<i>PpcD</i>	Periplasmic c-type cytochrome	<i>Geobacter sulfurreducens</i>	Aklujkar <i>et al.</i> , 2013

### 6.1.3 Genes associated with manganese oxidation

Bacteria utilise numerous pathways in manganese oxidation. The most prevalent means of oxidation is the enzymatic conversion by multi-copper oxidases (MCOs), however it has been discovered that many other genes have a direct relationship with Mn(II) oxidation (Spiro *et al.*, 2010). While the genes involved vary from organism to organism, the detection of Mn(III) intermediates during oxide formation suggest a two-step electron transfer process that either involves multiple systems or a complex enzyme complex capable of the microbial conversion of Mn(II) → Mn(III) → Mn(IV). Research into the MCO enzyme *MnxG* has suggested that it is capable of performing both steps, however other enzymes determined to be used in manganese oxidation cannot complete both steps individually (Tebo *et al.*, 2005). Table 6.2 shows a representative list of known genes involved in Mn(II) oxidation and illustrates the variability in genes involved in manganese oxidation in different organisms.

**Table 6.2:** Representative genes associated with Mn(II) oxidation.

Gene	Description of gene	Strain	References
<i>aceA</i>	Lipoate acetyltransferase (subunit of pyruvate dh complex)	<i>Pseudomonas putida</i> MnB1	Caspi <i>et al.</i> , 1998
<i>ccmA</i>	c-type cytochrome (biogenesis)	<i>Pseudomonas putida</i> MnB1	Caspi <i>et al.</i> , 1998
<i>ccmE</i>	c-type cytochrome (biogenesis)	<i>Pseudomonas putida</i> MnB1	Caspi <i>et al.</i> , 1998
<i>ccmF</i>	c-type cytochrome (biogenesis)	<i>Pseudomonas putida</i> MnB1	Caspi <i>et al.</i> , 1998
<i>cumA</i>	Multi copper oxidase	<i>Pseudomonas putida</i> GB-1	Brouwers <i>et al.</i> , 1999
<i>icd</i>	Isocitrate dh	<i>Pseudomonas putida</i> MnB1	Caspi <i>et al.</i> , 1998
<i>mnxA</i>	No homology	<i>Bacillus</i> sp. SG-1	van Waasbergen <i>et al.</i> , 1996
<i>mnxB</i>	No homology	<i>Bacillus</i> sp. SG-1	van Waasbergen <i>et al.</i> , 1996
<i>mnxC</i>	Required for cytochrome c oxidase activity	<i>Bacillus</i> sp. SG-1	van Waasbergen <i>et al.</i> , 1996
<i>mnxD</i>	No homology	<i>Bacillus</i> sp. SG-1	van Waasbergen <i>et al.</i> , 1996
<i>mnxE</i>	No homology	<i>Bacillus</i> sp. SG-1	van Waasbergen <i>et al.</i> , 1996
<i>mnxF</i>	No homology	<i>Bacillus</i> sp. SG-1	van Waasbergen <i>et al.</i> , 1996
<i>mnxG</i>	Multi copper oxidase	<i>Bacillus</i> sp. SG-1	van Waasbergen <i>et al.</i> , 1996
<i>mofA</i>	Multi copper oxidase	<i>Leptothrix discophora</i> SS-1	Corstjens and De Vrind, 1997
<i>mofB</i>	Peptidyl-prolyl-cis-trans isomerase (involved in protein folding) and macrophage infectivity potentiator	<i>Leptothrix discophora</i> SS-1	Brouwers <i>et al.</i> , 2000
<i>mofC</i>	Cytochrome C family protein	<i>Leptothrix discophora</i> SS-1	Brouwers <i>et al.</i> , 2000
<i>moxA</i>	Multi copper oxidase	<i>Pedomicrobium</i> sp. ACM 3067	Ridge <i>et al.</i> , 2007
<i>sdhABCD</i>	Succinate dehydrogenase complex	<i>Pseudomonas putida</i> MnB1	Caspi <i>et al.</i> , 1998
<i>trpE</i>	Subunit of anthranilate synthetase	<i>Pseudomonas putida</i> MnB1	Caspi <i>et al.</i> , 1998
<i>xcpA</i>	General secretory pathway	<i>Pseudomonas putida</i> GB-1	De Vrind <i>et al.</i> , 2003
<i>xcpT</i>	General secretory pathway	<i>Pseudomonas putida</i> GB-1	De Vrind <i>et al.</i> , 2003

## 6.2 Genomic Analysis of *Bacillus* sp. PMO

Genomic analysis of *Bacillus* sp. PMO was performed as it was the PHS isolate able to oxidise the highest levels of manganese (compared to AEM-1106 and DLH-1207). 5,446 putative genes were detected within the genome of *Bacillus* sp. PMO which was 3,090,173bp in length. While 16S rRNA sequencing determined that this organism was 99% similar to *Bacillus anthracis*, metabolically it was most similar to *Labrenzia alexandrii* DFL-11 (against organisms that have had whole genome analysis performed). Genes associated with subsystems and their relative distributions are visualised in Figure 6.2.

Based on genomic analysis, it is determined that *Bacillus* sp. PMO is metabolically diverse, with a number of genes associated with the utilisation of electron donors and acceptors present. Systems linked to nutrient metabolism included carbohydrate metabolism of sugars, aminosugars, organic acids, monosaccharides, polysaccharides and aromatic degradation are present. Reduction pathways of nitrate and sulphate were detected as well as a system for fermentation, consistent with the anaerobic growth of the bacteria. Additionally, the detection of an iron siderophore system were revealed. Genes associated with the transport of manganese, manganese oxidation and reduction were also present.

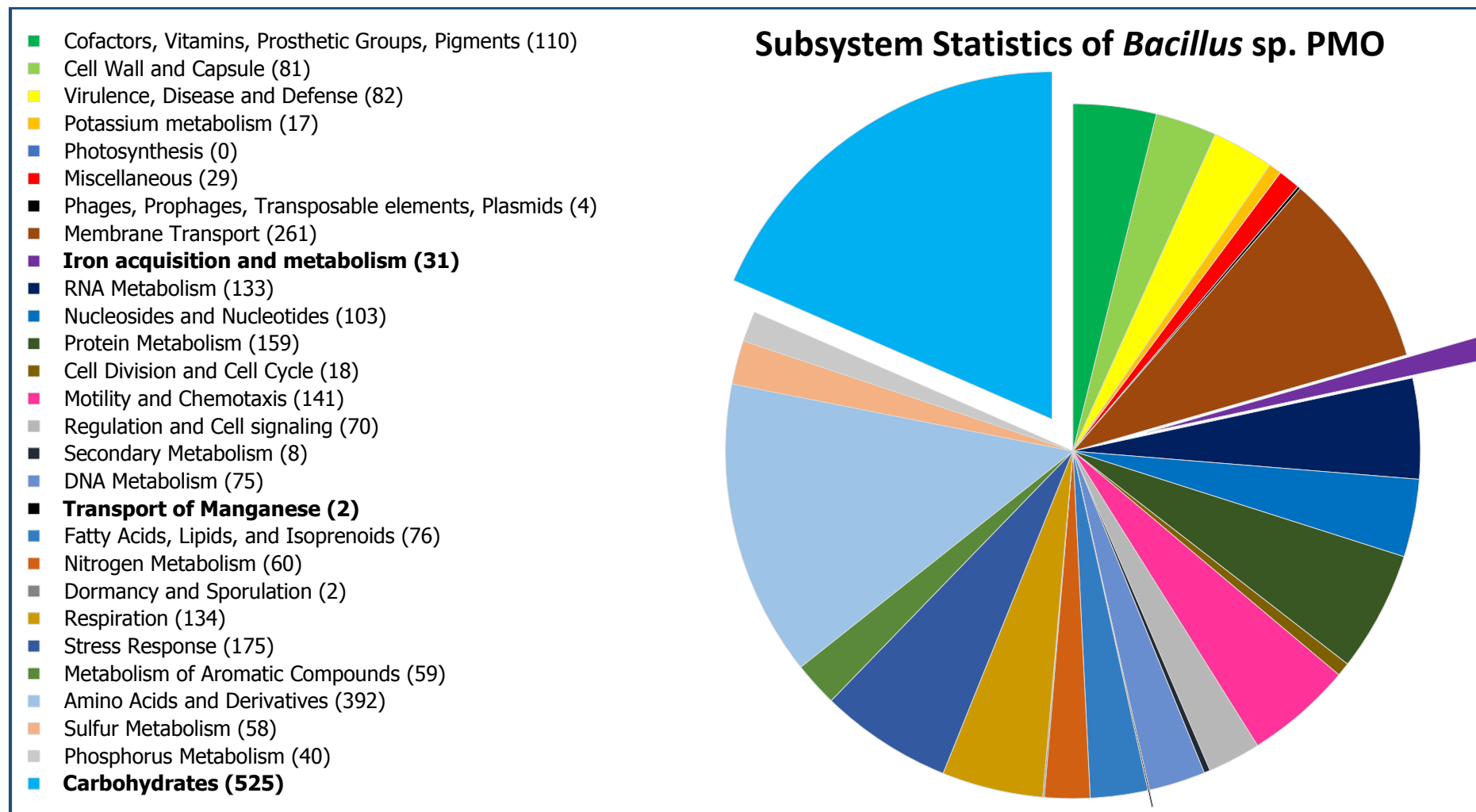


**Figure 6.2:** Genes associated with subsystems and their distributions in different subsystems as identified by RAST. Subsystems in bold are discussed in more detail in this chapter.

## 6.3 Genes Associated with Carbohydrate Metabolism

### 6.3.1 Overview

Figure 6.3 shows 525 putative genes and subsystems that were identified that were involved in carbohydrate metabolism. The genes detected were primarily within the subsystem *central carbohydrate metabolism*, and included those associated with Glycolysis and Gluconeogenesis, Pyruvate metabolism II: acetyl-CoA, acetogenesis from pyruvate and the TCA cycle. Monosaccharide metabolism genes were detected (Mannose, D-Ribose, Xylose, D-Gluconate, D-Galacturonate and D-Glucuronate) in addition to genes associated with the utilisation of the polysaccharide  $\alpha$ -amylase. Numerous genes linked to fermentation and were also revealed.

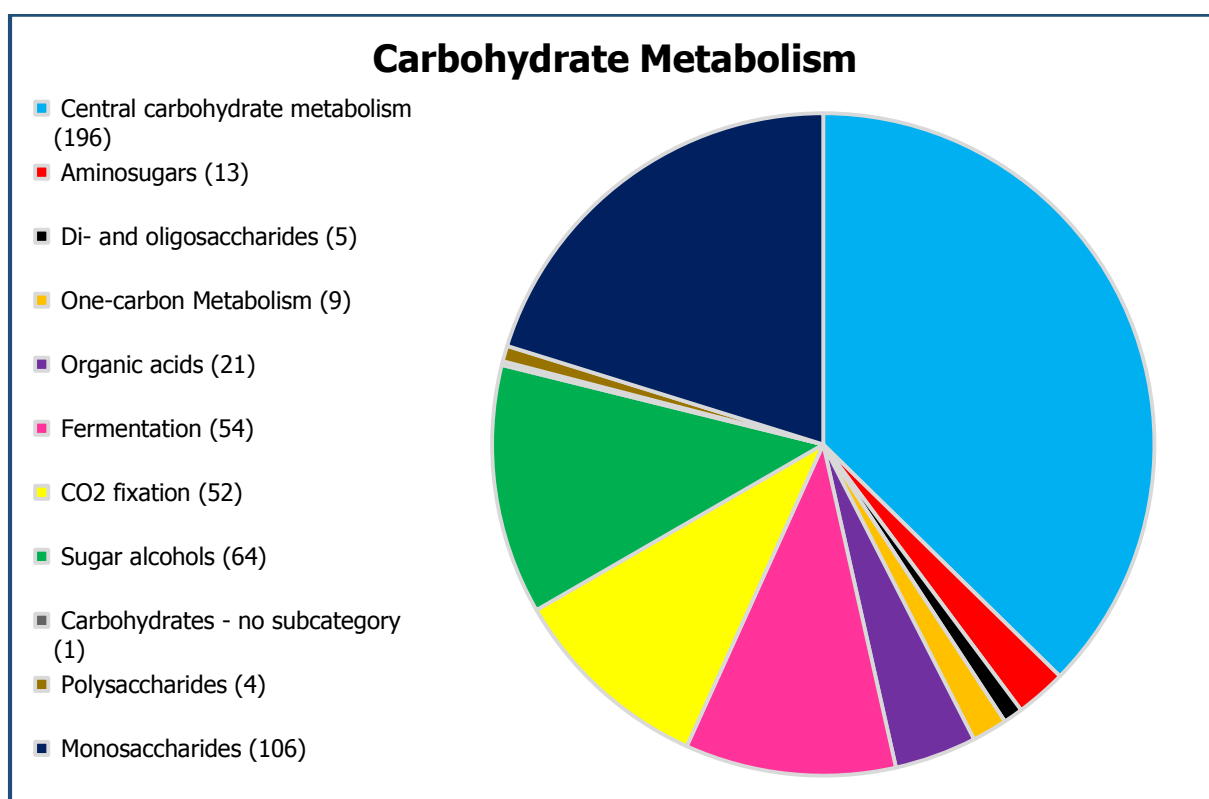


**Figure 6.3:** Genes associated with carbohydrate metabolism, further classified into subcategories.

## 6.4 Genes Associated with Iron Acquisition and Electron Transfer

### 6.4.1 Overview

31 putative genes were identified that are involved in metabolism of iron. The genes detected were primarily responsible for iron uptake, however several components of a siderophore system were detected. These include those coding for the iron siderophore sensor and receptor system and the ABC transporter responsible for iron acquisition. Figure 6.4 depicts subcategories of genes detected in the *iron acquisition and metabolism* subsystem and are comprehensively listed in Table 6.3.

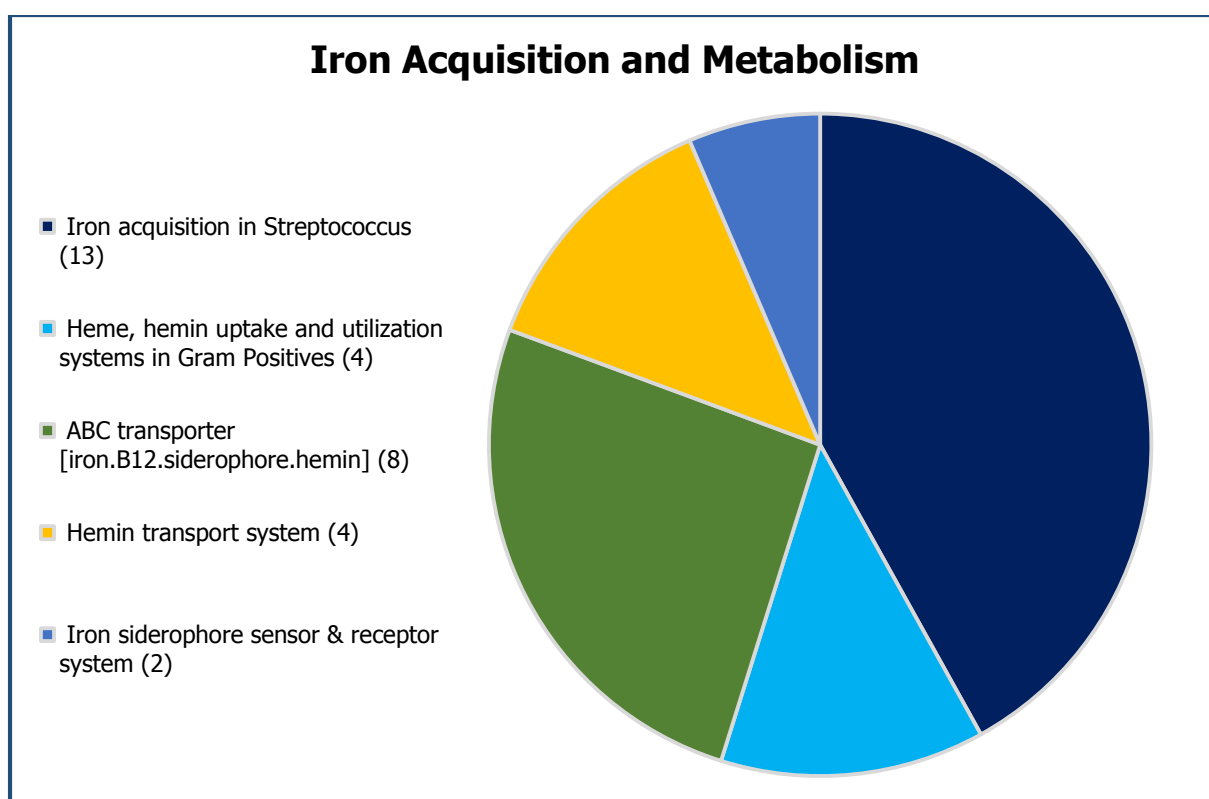


**Figure 6.4:** Genes associated with iron acquisition and metabolism, further classified into subcategories; iron acquisition in *Streptococcus* (13 genes; 42%), heme, hemin uptake and utilization systems in Gram Positives (4 genes; 13%), ABC transporter [iron.B12.siderophore.hemin] (8 genes; 26%), hemin transport system (4 genes; 13%) and iron siderophore sensor and receptor system (2 genes; 6%).

**Table 6.3:** Genes, roles and features associated with iron acquisition and metabolism.

Subcategory	Subsystem	Role	Features Detected
Siderophores	Iron siderophore sensor & receptor system	FIG006045: Sigma factor, ECF subfamily	fig 6666666.75011.peg.3255
Siderophores	Iron siderophore sensor & receptor system	Iron siderophore receptor protein	fig 6666666.75011.peg.2100
Iron acquisition and metabolism - no subcategory	Iron acquisition in <i>Streptococcus</i>	Ferric iron ABC transporter, ATP-binding protein	fig 6666666.75011.peg.2912 fig 6666666.75011.peg.2921
Iron acquisition and metabolism - no subcategory	Iron acquisition in <i>Streptococcus</i>	Ferric iron ABC transporter, iron-binding protein	fig 6666666.75011.peg.686 fig 6666666.75011.peg.687 fig 6666666.75011.peg.3293 fig 6666666.75011.peg.4972
Iron acquisition and metabolism - no subcategory	Iron acquisition in <i>Streptococcus</i>	Ferric iron ABC transporter, permease protein	fig 6666666.75011.peg.1063 fig 6666666.75011.peg.1064 fig 6666666.75011.peg.1065 fig 6666666.75011.peg.2730 fig 6666666.75011.peg.2731 fig 6666666.75011.peg.3487 fig 6666666.75011.peg.4918
Iron acquisition and metabolism - no subcategory	ABC transporter [iron.B12.siderophore.hemin]	ABC transporter (iron.B12.siderophore.hemin), permease component	fig 6666666.75011.peg.3803 fig 6666666.75011.peg.4879
Iron acquisition and metabolism - no subcategory	ABC transporter [iron.B12.siderophore.hemin]	ABC transporter (iron.B12.siderophore.hemin), ATP-binding component	fig 6666666.75011.peg.1435 fig 6666666.75011.peg.2878
Iron acquisition and metabolism - no subcategory	ABC transporter [iron.B12.siderophore.hemin]	ABC transporter (iron.B12.siderophore.hemin), periplasmic substrate-binding component	fig 6666666.75011.peg.285 fig 6666666.75011.peg.1432 fig 6666666.75011.peg.1433 fig 6666666.75011.peg.1434

### 6.4.2 Siderophore genes

Two siderophore genes were detected through genomic analysis of *Bacillus* sp. PMO, hemophore/receptor (*HasA/HasR*) and an associated sigma factor (*ECF subfamily*). The system functions as followed; the *HasA* protein is secreted into the extracellular medium (via a Type I ABC secretion pathway) where the ultra-high affinity for iron causes binding to the *HasA* protein which then returns to the *HasR* receptor (Figure 6.5). Both the loading and unloading of the *HasA* protein is energy independent. Iron acquisition through this system is non-specific, and both Fe(II) and Fe(III) can be obtained in this way. Additionally, this process is not solely for the procurement of iron for anaerobic respiration, but is also used for the acquisition of nutritional iron (Cescau *et al.*, 2007). Due to the detection of iron reduction by *Bacillus* sp. PMO, it is predicted that this is one of the systems responsible.

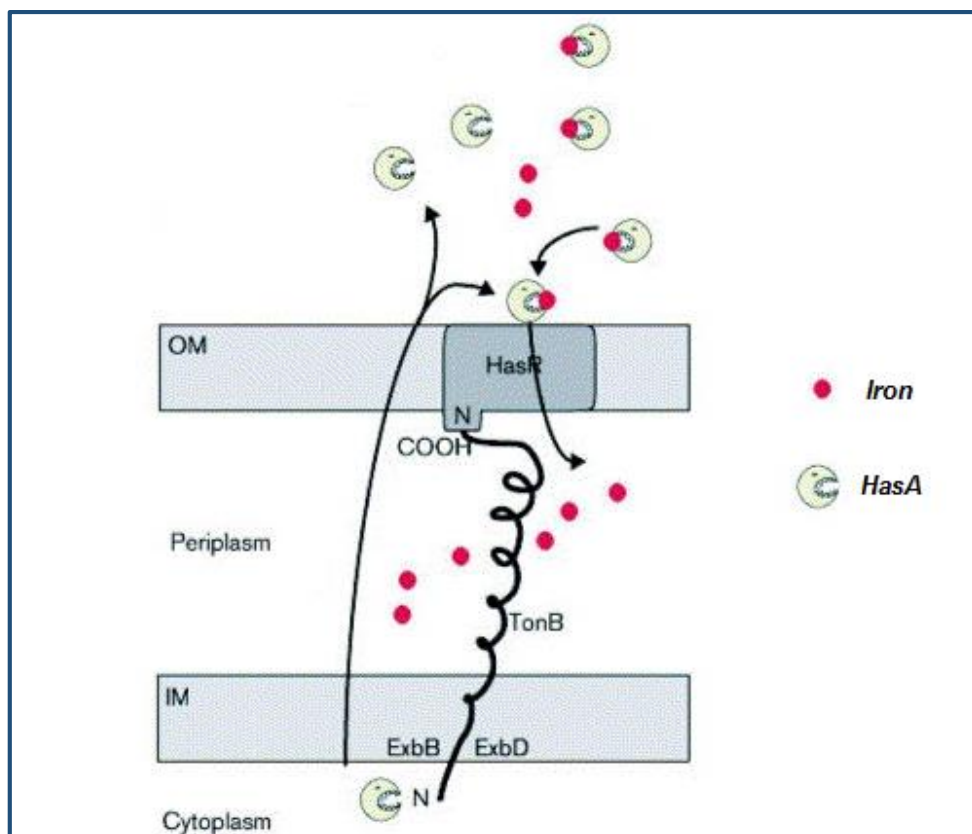


**Figure 6.5:** *HasA* hemophore binding to extracellular iron. The hemophore delivers the bound iron to the *HasR* receptor and transported into the cell by the *TonB* system. Diagram adapted from Wandersman and Stojiljkovic, 2000.

## 6.5 Genes Associated with the Transport of Manganese

### 6.5.1 Overview

Two putative genes encoding for a manganese ABC transporter system were detected within the genome of *Bacillus* sp. PMO. Specifically, the detected genes encoded for the protein *SitB* (252bp) and the protein *SitC* (336bp). Probing for the gene encoding the protein *SitA* proved unsuccessful.

### 6.5.2 *SitABC* manganese transporter system

The *SitABC* transporter system is an ABC-type manganese permease complex that transports  $\text{Fe}^{2+}$  and  $\text{Mn}^{2+}$  (Sabri *et al.*, 2006). The system is capable of both iron and manganese uptake, however catalyses  $\text{Mn}^{2+}$  uptake better than  $\text{Fe}^{2+}$  (Nies & Silver, 2007). The *SitB* and *SitC* are not associated with the reduction or oxidation of manganese, rather with the transport of  $\text{Mn}^{2+}$ . The detected *SitB* gene encodes for an ATP-binding protein while the *SitC* gene encodes for an inner membrane permease protein within the manganese ABC-transporter system.

## 6.6 Genes Associated With Manganese Oxidation

### 6.6.1 Identification of associated manganese oxidation genes

Genomic analysis of *Bacillus* sp. PMO resulted in the detection of two putative genes of significance to manganese oxidation; a c-type cytochrome involved in biogenesis (*ccmA*) associated with Mn(II) oxidation in *Pseudomonas putida*, and a multicopper oxidase gene (*MCO*) with no previous association with manganese oxidation in other organisms. Probing of *Bacillus* sp. PMO for major Mn(II) oxidation genes found in *Bacillus* sp. SG-1 (*mnxA-G*) proved unsuccessful, and it is theorised that *Bacillus* sp. PMO uses a unique, sole MCO in biological manganese oxidation. While *ccmA* has been characterised as a cytochrome associated with manganese in *Pseudomonas putida*, it is possible that it may also aid in oxidation.

### 6.6.2 Multicopper oxidase gene analysis

Genomic analysis revealed a 948bp putative gene encoding for a multicopper oxidase. BLAST analysis of the predicted *MCO* protein revealed a 99.04% similarity to another *MCO* (GenBank: WP\_009880000.1) belonging to *Bacillus anthracis* CDC 684, another subspecies of *B. anthracis* that has had complete genomic sequence analyses (Okinaka *et al.*, 2011; GenBank: CP001216.1). Further BLAST analysis determined that the identified MCO is highly conserved amongst select *Firmicutes*, and is not limited to the *Bacillus* genus. Figure 6.6 provides an *MCO* amino acid sequence CLUSTAL alignment of the MCO detected in *Bacillus* sp. PMO against other *MCOs* of high similarity.

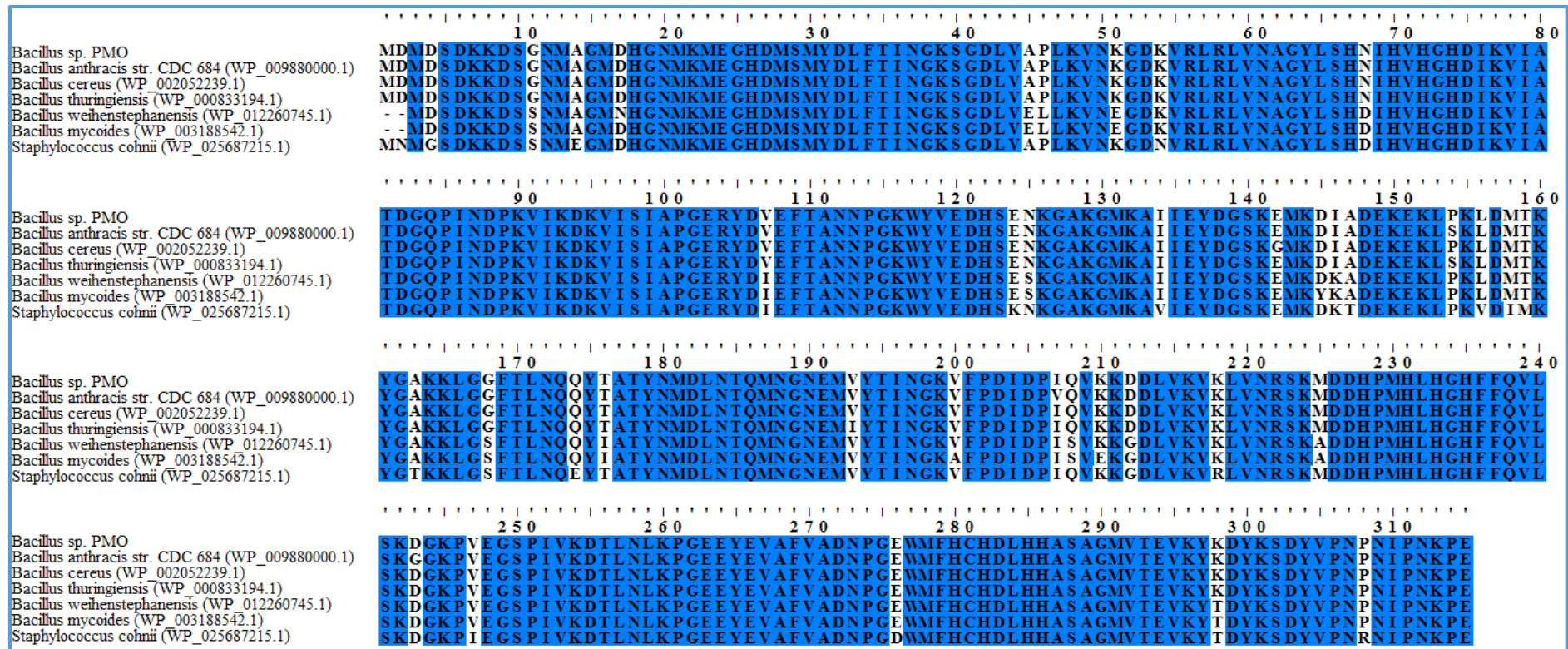


**Figure 6.6:** Multiple alignment of *MCO* amino acid sequence (*Bacillus* sp. PMO) against other *MCO* proteins of significant similarity by use of CLUSTAL. Shaded amino acids represent identical residues between all *MCO* proteins. GenBank accession numbers: *Bacillus anthracis* CDC 684 (WP\_009880000.1), *Bacillus cereus* (WP\_002052239.1), *Bacillus thuringiensis* (WP\_000833194.1), *Staphylococcus cohnii* (WP\_025687215.1), *Bacillus weihenstephanensis* (WP\_012260745.1), *Bacillus mycooides* (WP\_003188542.1).

### 6.6.3 Predicted role of MCO in Mn(II) oxidation

Based on the absence of other multicopper oxidases or genes associated with manganese oxidation, it is predicted that the enzyme encoded by the MCO gene detected in *Bacillus* sp. PMO oxidises both Mn(II) into its Mn(III) intermediate and then catalyses the conversion of the Mn(III) intermediate into Mn(IV)-oxide. The absence of other manganese oxidising genes suggests that the *MCO* may be the sole protein responsible for the oxidation of Mn(II) → Mn(IV), unlike the *Bacillus* sp. SG-1 system that employs multiple enzymes. Therefore, the likely pathway for Mn(II) oxidation in *Bacillus* sp. PMO is as followed (Figure 6.7):

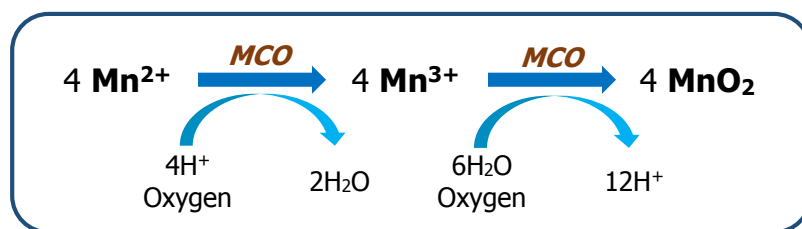


**Figure 6.7:** The predicted role of *MCO* in the two-step oxidation of Mn(II) to Mn(IV).

### 6.6.4 Significance of the MCO enzyme

Manganese is found at significant levels in water and oxidation of naturally present Mn(II) → Mn(IV) has been observed in bacteria across multiple genera. Several Mn(II) oxidising enzymes have been detected, including those specific to one step and also enzymes capable of oxidising both intermediates. Although enzymatic oxidation is independent of cellular metabolism, MnO<sub>2</sub> can be used in oxidative phosphorylation and thus this process may be an energy saving mechanism. Under anoxic conditions, anaerobes (including the facultative *Bacillus* sp. PMO) can use Mn(IV) as a terminal electron acceptor in cellular respiration. Therefore, *MCO* plays a pivotal role in the geochemical cycling of manganese in the environment.

## 6.7 Discussion

The MCO gene was detected in strain PMO and several other closely associated bacteria but it is not inclusive to the *Bacillus* genus. Figure 6.6 compares the MCO amino acid sequence of strain PMO and other organisms, highlighting extensive the conserved regions shared between them. The mechanisms of microbial manganese oxidation have been studied extensively in several bacteria; however the diversity of bacteria capable of manganese oxidation is relatively unknown. Chapter 4 describes a new genus (*Shewanella*) capable of biogenic Mn(II) oxidation, however based on this observations it is likely that many more species and genera exist with this trait but have not been tested. In fact, it may be a common trait of facultative manganese reducing bacteria such as *Shewanella*.

The MCO amino acid sequence was compared against most researched Mn(II) oxidising organism, *Bacillus* sp. SG-1. Protein BLAST analysis revealed a 29%-43% similarities (multiple alignments against conserved regions) to a multicopper oxidase 1217 amino acids in length (WP\_006837219.1). Conserved regions were detected in 4 distinct regions; positions 51-94, 253-316, 690-724 and 1093-1139 (Figure 6.8). Comparatively, the multicopper oxidase gene present in *Bacillus* sp. SG-1 is much larger than the one present in *Bacillus* sp. PMO, 1217 amino acids to 315. There is presently no research into the biochemical role of this MCO in Mn(II) oxidation, and through this data it inconclusive if the MCO enzyme produced by *Bacillus* sp. SG-1 would oxidise Mn(II), and would depend on the active site(s) responsible for manganese oxidation. The degree of homology indicates a level of evolutionary similarity, however it is deduced that multicopper oxidases of these two *Bacilli* are quite dissimilar. Additional research into the enzymatic activity between this MCO and Mn(II) may result in the identification of another manganese oxidising enzyme within *Bacillus* sp. SG-1 and it is possible that the conserved regions are active sites for manganese oxidation.

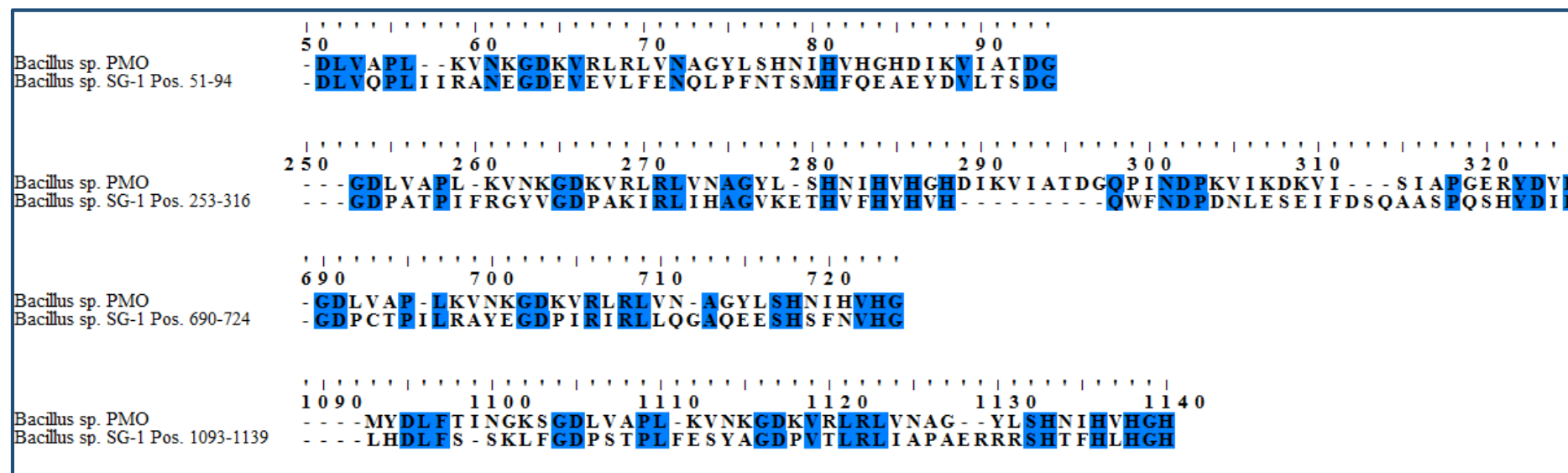


**Figure 6.8:** Multiple alignment of *MCO* amino acid sequence (*Bacillus* sp. PMO) against the *MCO* enzyme of *Bacillus* sp. SG-1 (WP\_006837219.1) by use of CLUSTAL. Sequence alignment revealed similarity at four sites on the *Bacillus* sp. SG-1 *MCO* protein; positions **51-94** (14/44 matches, 32% similarity), **253-316** (21/73 matches, 29% similarity), **690-724** (15/35 matches, 43% similarity) and **1093-1139** (19/48 matches; 40% similarity).

# Chapter 7

Thesis Summary and

Future Directions

## 7.1 Thesis Summary

The thesis focused on manganese transformation (reduction and/or oxidation) by bacteria. PHS was used as a model environment for investigating microbial diversity and for the isolation of manganese transformers. This particular hot spring was chosen because of the high metal content and gradient of temperature from thermophilic to mesophilic. In Chapter 3, PHS was investigated from both a culture dependent and independent perspective; studying the mechanisms and types of bacteria present. The chapter focused on the presence and diversity of manganese transforming bacteria (through both isolations and metagenomic analysis). Initially, microbial levels and physiochemical characteristics of the spring were quantified to understand the geochemistry of the mineral rich, radioactive hot spring and as a base for enrichment studies. The culture dependent assessment of PHS waters provided a summary of typical bacteria present and the transformation diversities of these organisms. From these enrichments, three manganese transformers were identified (and assessed further in Chapter 4); *Bacillus* sp. PMO, *Paenibacillus* sp. AEM-1106 and *Bacillus* sp. DLH-1207. Culture independent studies were undertaken in the exploration of the spring's biodiversity through 16S rRNA metagenomic analysis. This not only provided a representative model of bacteria present in these types of waters but revealed several genera associated with microbial manganese transformation. However, the PHS water sample was rich in green microbial matter and predominately bacteria from *Cyanobacteria* were detected, which were consequently screened for presence of chlorophylls and bacteriochlorophylls. It was concluded that PHS is an environment rich in microbial diversity and contains organisms capable of microbial transformation of several metals, including manganese, however was dominated by phototrophic organisms. This is understandable as the high mineral content of the water, water temperatures and constant exposure to sunlight is conducive to phototrophs.

In Chapter 4, the physiology and manganese transformation potential of PHS isolates were investigated (isolated in Chapter 3). As a comparative measure, several species of *Shewanella* were tested alongside alongside the PHS isolates. *Shewanella* were chosen as they are the most studied manganese reducing bacteria. The chapter focused the manganese transformation properties of the isolates, characterising the rates of oxidation and reduction along with optimisation studies to gain better insight into these organisms. Manganese transformation studies revealed that all the isolates were able to both reduce and oxidise manganese (a combined trait rarely examined in bacteria), and in the case of *Shewanella*, this is the first reported manganese oxidation study of bacteria within the genus. Additionally, it was discovered that the isolates were able to oxidise manganese aerobically and then when deoxygenated, were able to use the produced oxide which could then be used as a terminal electron acceptor in anaerobic respiration; converting Mn(IV) back into Mn(II) (coupled with an appropriate electron donor). This highlights the manganese cycling nature of both the *Shewanella* isolates from marine environments and PHS strains from a heated spring rich in metals. Finally, the chapter focused on the characteristics of the biogenically produced oxides. Various analyses were performed on the oxides generated by select isolates (*Bacillus* sp. PMO, *Shewanella putrefaciens* CN-32 and *Shewanella loihica* PV-4) from both a physical and chemical standpoint. Analyses included Scanning Electron Microscopy, ICP-OES O/Mn ratio determination and FTIR analysis. Through these it was determined that high purity MnO<sub>2</sub> was produced through microbial oxidation. It was concluded that these organisms produced an oxide that offered potential for bioremediation studies (through metal immobilisation by MnO<sub>2</sub>) to be investigated further.

In Chapter 5, the immobilisation potential of biogenic oxides against heavy metals was tested and assessed. The biogenic manganese oxides induced the immobilisation of a range of metals when added individually at set concentrations and when added as part of a simulated wastewater study. Studies of  $\text{MnO}_2$  immobilisation by single metals revealed significant levels of adsorption against all tested metals, whether the metals were added after  $\text{MnO}_2$  formation or with coprecipitation of the oxides. However, it was discovered that when the oxidation transpired in the presence of trace metals the overall immobilisation was greater than when separately added. Similarly, studies of simulated waste waters also resulted in high levels of immobilisation across difference concentrations (undiluted, 1:10 and 1:100 dilutions), with complete removal occurring in the 1:100 dilution. It was determined that biogenic  $\text{MnO}_2$  offers the possibility of the removal of toxic metals from waste waters through adsorption and subsequent removal of the oxide. However, if this was applied in the clean up of actual wastewater, care would have to be taken so the conditions did not turn anaerobic and induce microbial reduction of  $\text{MnO}_2$ .

In Chapter 6, genomic analysis was performed on one of the isolates, *Bacillus* sp. PMO, to determine the genes associated with manganese oxidation and reduction within the bacteria. This chapter focused on the subsystems pertaining to carbohydrate and iron metabolism, as well as the the analysis of a multicopper oxidase responsible for manganese oxidation. It was discovered that *Bacillus* sp. PMO was a nutritionally diverse bacterium with a number metabolic and transportation systems for both iron and manganese. In addition to iron and manganese transport systems which have roles in reduction, a putative MCO gene was detected and determined to be a multi-step manganese oxidiser. When compared genetically to the most widely researched manganese oxidiser, *Bacillus* sp. PMO, four homologous sites were found to be shared between the two genes. BLAST analysis revealed the MCO gene in a variety of other organisms (not limited to *Bacillus* spp.) and indicates that manganese oxidation may be much more widespread within the *Firmicute* phylum.

## 7.2 Future Directions

From the culture dependent and independent studies (Chapter 3), a number of novel strains were isolated from PHS, however were not characterised as they were not identified as manganese transforming bacteria (Table 3.8). Despite this, the low similarity to their nearest phylogenetic neighbours suggests that these are likely to be novel organisms. Future studies may include full characterisation of these organisms, investigating the characteristics and assessing the metal transforming capabilities of the isolates. Additionally, PHS is heated by radioactive decay and it is possible that the long term exposure may have resulted in cellular mutations or radioactive resistances in the bacteria present. Genetic investigation into metal, radionuclide and ultraviolet light resistance by *Bacillus* sp. PMO and other bacteria present in the spring could be performed, which may result in the identification of novel enzymatic radiation resistances. Thermophilic manganese reducers were detected in enrichment cultures from the spring, but were not isolated or sequenced. Based on the fact that no thermophilic oxidisers were detected in enrichments, these organisms are likely to be strictly anaerobic manganese reducers, however may be of interest in understanding the mechanisms of manganese reduction in a radioactive environment. This would be of interest from an astrobiology perspective. Finally, culture independent analyses of PHS revealed the presence of 11 phyla known to contain manganese oxidisers. Further studies could involve the targeting of these organisms for isolation and probing for multicopper oxidase and other manganese oxidising genes in the waters.

In manganese transformation studies (Chapter 4), the reduction characteristics of the isolates were tested with a number of other metals known to be coupled in anaerobic respiration. Isolates *Bacillus* sp. DLH-1207 and *Paenibacillus* sp. AEM-1106 were the subject of initial growth characterisation and metal transforming analyses; however due to time constraints genome sequencing was not performed. Genomic analysis may reveal further interesting characteristics. Finally, average oxidation state analysis revealed that the biogenic oxides produced did not contain pure MnO<sub>2</sub>; however these findings did not reveal what other manganese variants were present in the sample. Future exploration into both the structure of the produced impurities and the cause of their presence could help in understanding the mechanisms of microbial oxidation on a molecular level.

In the metal immobilisation studies (Chapter 5), more extensive studies involving a wider range of metals could be tested. The immobilisation of metals in simulated waste waters was performed as an individual study; with the only condition tested being immobilisation after the addition of a preformed oxide. Preliminary results proved promising; however for bioremediation it would be optimal that oxide production occurred *in situ*. Therefore, toxicity studies of various metal compositions should be established for future research into the bioremediation potential of these organisms. Additionally, a bioreactor-style study with close control of conditions could see the effective removal of toxic effluents by biologically produced MnO<sub>2</sub>.

In Chapter 6, the genomic and metabolic profile of *Bacillus* sp. PMO was assessed in detail. While a number of genes involved in both iron and manganese transport and metabolism were detected, the localisation of manganese oxidation was not determined through genomic analysis. Localisation studies of the oxidising activity would increase knowledge of the mechanisms utilised by *Bacillus* sp. PMO in biogenic oxidation of Mn(II). Oxidation by *Bacillus* sp. SG-1 was detected in spores, however due to the pathogenic nature of *Bacillus anthracis* (the closest phylogenetic relative) and health and safety restrictions, detailed sporulation studies were not performed. Additionally, subsystems pertaining to metabolic processes were assessed in detail, however deeper probing into the various other subsystems detected within *Bacillus* sp. PMO could reveal other novel proteins/pathways previously undiscovered within the *Bacillus* genus.

# References

## 8.1 Reference List

**Aklujkar, M., Coppi, M.V., Leang, C., Kim, B.C., Chavan, M.A., Perpetua, L.A., Giloteaux, L., Lui, A. & Holmes, D.E.** (2013). Proteins involved in electron transfer to Fe(III) and Mn(IV) oxides by *Geobacter sulfurreducens* and *Geobacter uraniireducens*. *Microbiology*. **159**, pp. 515-535.

**Altshul, S.F., Gish, W., Miller, W., Myers, E.W. & Lipman, D.J.** (2001). Basic local alignment search tool. *J. Mol. Biol.* **215**. pp. 403-410.

**Anderson, C.R., Davis, R.E., Bandolin, N.S., Baptista, A.M., Tebo, B.M.** (2011). Analysis of in situ manganese(II) oxidation in the Columbia River and offshore plume: linking *Aurantimonas* and the associated microbial community to an active biogeochemical cycle. *Environ. Microbiol.* **13**(6), pp. 1561-1576.

**Anitori, R.P., Trott, C., Saul, D.J., Bergquist, P.L. & Walter, M.R.** (2002). A Culture-Independent Survey of the Bacterial Community in a Radon Hot Spring. *Astrobiology* 2, pp. 255-270.

**Anisimova, M. & Gascuel O.** (2006). Approximate likelihood ratio test for branches: A fast, accurate and powerful alternative. *Syst Biol.* **55**(4), pp.539-552.

**Avoscan, L., Untereiner, G., Degrouard, J., Carriere, M. & Gouget, B.** (2007). Uranium and selenium resistance in *Cupriavidus metallidurans* CH34. *Toxicology Letters* **172**(1), pp. 157

**Aziz, R.K., Bartels, D., Best, A.A., DeJongh, M., Disz, T., Edwards, R.A., Formsmas, K., Gerdes, S., Glass, E.M., Kubal, M., Meyer, F., Olsen, G.J., Olson, R., Osterman, A.L., Overbeek, R.A., McNeil, L.K., Paarmann, D., Paczian, T., Parrello, B., Pusch, G.D., Reich, C., Stevens, R., Vassieva, O., Vonstein, V., Wilke, A. & Zagnitko, O.** (2008). The RAST Server: rapid annotations using subsystems technology. *BMC Genomics*. **8**(9), pp. 75.

**Barbeau, K., Rue, E.L., Bruland, K.W. & Butler, A.** (2001). Photochemical cycling of iron in the surface ocean mediated by microbial iron(III)-binding ligands. *Nature*. **413**, pp. 409-413.

**Baron, V., Gutzmer, J., Rundlof, H. & Tellgren, R.** (1998). The influence of iron substitution on the magnetic properties of hausmannite,  $Mn(Fe,Mn)_2O_4$ , Sample at  $T = 295$  K. *Natura. American Mineralogist*. **83**, pp.786-793.

**Bekesi, G., Tyler, M., Niejalke, D. & Waterhouse, J.** (2013). Improved regulation of Water Supply for the Olympic Dam Mine, South Australia. *International Mine Water Association*.

**Beliaev, A.S. & Saffarini, D.A.** (2001). MtrB, *Shewanella putrefaciens* MtrB encodes an outer membrane protein required for Fe(III) and Mn(IV) reduction. *J. Bacteriol.* **180**, pp. 6292-6297.

**Beliaev, A.S., Saffarini, D.A., McLaughlin, J.L. & Hunnicutt, D.** (2001). MtrC, an outer membrane decahaem c cytochrome required for metal reduction in *Shewanella putrefaciens* MR-1. *Molecular Microbiology*. **39**(3), pp. 722-730.

**Berg, J.M., Tymoczko, J.L. & Stryer L.** (2002). Biochemistry. 5th edition. *W H Freeman (New York, United States of America)*.

**Bhattacharyya-Pakrasi, M.B., Pakrasi, H.B., Ogawa, T. & Aurora, R.** (2002). Manganese transport and its regulation in bacteria. *Biochemical Society Transactions*. pp. 768-770.

- Bontidean, I., Lloyd, J.R., Hobman, J.L., Brown, N.L., Wilson, J.R. Csoregi, E., Mattiasson, B. & Brown, N.L.** (2000). Bacterial metal resistance proteins and their use in biosensors for detection of bioavailable heavy metals. *J. Inorg. Biochem.* **79**, pp. 225-229.
- Borrego, C.M., Garcia-Gil, J., Christina, X.P., Vila, X. & Abella, C.A.** (1998). Occurrence of new bacteriochlorophyll d forms in natural populations of green photosynthetic sulfur bacteria. *FEMS Microbiology Ecology.* **26**(4), pp. 257-267.
- Bräuer, S.L., Adams, C., Kranzler, K. Murphy, D., Xu, M., Zuber, P., Simon, H.M., Baptista, A.M. & Tebo, B.M.** (2011). Culturable *Rhodobacter* and *Shewanella* species are abundant in estuarine turbidity maxima of the Columbia River. *Environ. Microbiol.* **13**(3), pp. 589-603.
- Brockmann Jr, H. & Lipinski, A.** (1983). Bacteriochlorophyll g. A new bacteriochlorophyll from *Heliobacterium chlorum*. *Archives of Microbiology.* **136**(1), pp. 17-19.
- Bromfield, S.M.** (1974). Bacterial oxidation of manganous ions as affected by organic substrate concentration and composition. *Soil Biology and Biochemistry.* **6**(6), pp. 383-392.
- Bromfield, S.M. & David, D.J.** (1976). Sorption And Oxidation Of Manganous Ions And Reduction Of Manganese Oxide By Cell Suspensions Of A Manganese Oxidizing Bacterium. *Soil. Biol. Biochem.* **8**, pp. 37-43.
- Brosius, J., Dull, T.J., Sleeter, D.D. & Noller, H.F.** (1981). Gene organization and primary structure of a ribosomal RNA operon from *Escherichia coli*. *J. Mol. Bio.* **148**(2), pp. 107-127.
- Brouwers, G.J., Vijgenboom, E., Corstjens, P.L.A.M., de Vrind, J.P.M. & de Vrind-de Jong, E.W.** (2000). Bacterial Mn<sup>2+</sup> Oxidizing Systems and Multicopper Oxidases: An Overview of Mechanisms and Functions. *Geomicrobiol.* **17**(1), pp. 1-24.

- Brouwers, G.J., de Vrind, J.P., Corstjens, P.L., Cornelis, P., Baysse, C. & de Vrind-de Jong, E.W.** (1999) *cumA*, a gene encoding a multicopper oxidase, is involved in Mn<sup>2+</sup> oxidation in *Pseudomonas putida* GB-1. *Appl. Environ. Microbiol.* **65**, pp. 1762–1768.
- Brugger, J., Ngaire, L., McPhail, D.C. & Plimer, I.** (2005). An active amagmatic hydrothermal system: The Paralana hot springs, Northern Flinders Ranges, South Australia. *Clinical Geology* **222**, pp. 35-64.
- Burg, B.V.D.** (2003). Extremophiles as a source for novel enzymes. *Current Opinion in Microbiology* **6**(3), pp. 213-218
- Caporaso, J.G., Kuczynski, J., Stombaugh, J., Bittinger, K., Bushman, F.D., Costello, E.K., Fierer, N., Penttilde, A.G., Goodrich, J.K., Gordon, J.I., Huttley, G.A., Kelley, S.T., Knights, D., Koenig, J.E., Ley, R.E., Lozupone, C.A., McDonald, D., Muegge, B.D., Pirrung, M., Redder, J., Sevinsky, J.R., Turnbaugh, P.J., Walters, W.A., Widmann, J., Yasunenko, T., Zaneveld, J. & Knight, R.** (2010). QIIME allows analysis of high-throughput community sequencing data. *Nature Methods*. **7**, pp. 335-336.
- Cardenas, E., Wu, W.M., Leigh, M.B., Carley, J., Carroll, S., Gentry, T. & Luo, J.** (2008). Microbial Communities in Contaminated Sediments, Associated with Bioremediation of Uranium to Submicromolar Levels. *American Society for Microbiology*. **74**(12), pp. 3718-3729.
- Carpentier, W., Sandra, K., De Smet, I., Brige A., De Smet, L. & Van Beeumen, J.** (2003). Microbial reduction and precipitation of vanadium by *Shewanella oneidensis*. *Int. J. Syst. Evol. Microbiol.* **69**, pp. 3636-3639.
- Caspi, R., Tebo, B.M. & Haygood, M.G.** (1998). c-type cytochromes and manganese oxidation in *Pseudomonas putida* MnB1. *Appl. Environ. Microbiol.* **64**(10), pp. 3549-3555.

**Castresana J.** (2000). Selection of conserved blocks from multiple alignments for their use in phylogenetic analysis. *Mol Biol Evol.* **17**(4), pp. 540-552.

**Cerrato, J.M., Falkinham, J.O., Dietrich, A.M., Knocke, W.R., McKinney, C.W. & Pruden, A.** (2010). Manganese-oxidizing and -reducing microorganisms isolated from biofilms in chlorinated drinking water systems. *Water Research.* **44**, pp. 3935-3945.

**Cescau, S., Cwerman, H., Létoffé, S., Delepelaire, P., Wandersman, C. & Biville F.** (2007). Heme acquisition by hemophores. *Biometals.* **20**(3-4), pp. 603-613.

**Chen, M., Schliep, M., Willows, R.D., Cai, Z.L., Neilan, B.A. & Scheer, H.** (2010). A red-shifted chlorophyll. *Science.* **329**(5997), pp. 1318-1319.

**Chevenet, F., Brun, C., Banuls, AL., Jacq, B. & Chisten R.** (2006). TreeDyn: towards dynamic graphics and annotations for analyses of trees. *BMC Bioinformatics.* **7**, pp. 439.

**Chukhrov, F.V., Gorshkov, A.I., Rudnitskaya, E.S., Beresovskaya, V.V. & Sivtsov, A.V.S.** (1980). Manganese minerals in clays: A review. *Clays and Clay Minerals* **28**(5), pp. 346-354.

**Cole, J.R., Wang, Q., Fish, J.A., Chai, B., McGarrell, D.M., Sun, Y., Brown, C.T., Porrás-Alfaro, A., Kuske, C.R. & Tiedje, J.M.** (2014). Ribosomal Database Project: data and tools for high throughput rRNA analysis. *Nucl. Acids Res.* **41**.

**Corstjens, P.L.A.M. & De Vrind, J.P.M.** (1997). Identification and molecular analysis of the *Leptothrix discophora* SS-1mofA gene, a gene putatively encoding a manganese-oxidizing protein with copper domains. *Geomicrobiol. J.* **14**, pp. 91-108.

**Dastur, Y.N. & Leslie, W.C.** (1981). Mechanism of work hardening in Hadfield manganese steel. *Metallurgical Transactions A.* **12**(5), pp. 749-759.

- Deppenmeier, U., Müller V. & Gottschalk G.** (1996). Pathways of energy conservation in methanogenic bacteria. *Arch.microbiol.* **165**, pp. 149-163.
- Dereeper, A., Audic, S., Claverie, J.M. & Blanc G.** (2010) BLAST-EXPLORER helps you building datasets for phylogenetic analysis. *BMC Evol Biol.* **12**(10), pp. 8.
- Dereeper A., Guignon V., Blanc G., Audic S., Buffet S., Chevenet F., Dufayard J.F., Guindon S., Lefort V., Lescot M., Claverie J.M., & Gascuel O.** (2008). Phylogeny.fr: robust phylogenetic analysis for the non-specialist. *Nucleic Acids Research.* **1**(36), pp. 465-469.
- de Vrind, J.P., Brouwers, G.J., Corstjens, P.L., den Dulk, J. & de Vrind-de Jong, E.W.** (1998) The cytochrome c maturation operon is involved in manganese oxidation in *Pseudomonas putida* GB-1. *Appl. Environ. Microbiol.* **64**, pp. 3556–3562.
- de Vrind, J.P., De Groot, A., Brouwers, G.J., Tommassen, J. & de Vrind-de Jong, E.W.** (2003) Identification of a novel Gsp-related pathway required for secretion of the manganese-oxidizing factor of *Pseudomonas putida* GB-1. *Mol. Microbiol.* **47**(4), pp. 993-1006.
- D'Amico, S., Collins, T., Marx, J.C., Feller, G. & Gerday, C.** (2006). Psychrophilic microorganisms: challenges for life. *EMBO Rep.* **7**(4), pp. 385-389.
- Ding, Y.H.R., Hixson, K.K., Giometti, C.S., Stanley, A., Esteve-Nunez, A., Khare, T., Tollaksen, S.L., Zhu, W.H., Adkins, J.N., Lipton, M.S., Smith, R.D., Mester, T. & Lovley, D.R.** (2006). The proteome of dissimilatory metal-reducing microorganism *Geobacter sulfurreducens* under various growth conditions. *Biochim Biophys Acta.* **1764**, pp. 1198-1206.
- Duxbury, T. & Bicknell, B.** (1983), Metal-tolerant bacterial populations from natural and metal-polluted soils. *Soil Biology and Biochemistry.* **15**(3), pp. 243-250.

- Edgar, R.C.** (2004). MUSCLE: multiple sequence alignment with high accuracy and high throughput. *Nucleic Acids Res.* **32**(5), pp. 1792-1797.
- Emerson, D. & Floyd, M.M.** (2005). Enrichment and isolation of iron-oxidizing bacteria at neutral pH. *Methods Enzymol.* **397**, pp. 112-123.
- Ervin, J.S.** (2005). Toxic Trace Metal Removal Using Biogenic Manganese Oxide In A Packed-Bed Bioreactor. *California Polytechnic State University, California, USA.*
- Fawley, M.W.** (1989). A New Form of Chlorophyll c Involved in Light-Harvesting. *Plant Physiol.* **91**, pp. 727-732.
- Francis, C.A. & Tebo, B.M.** (2002). Enzymatic Manganese(II) Oxidation by Metabolically Dormant Spores of Diverse *Bacillus* Species. *Appl. Environ. Microbiol.* **68**(2), pp. 874-880.
- François, F., Lombard, C., Guigner, J-M., Soreau, P., Brian-Jaisson, F., Martino, G., Vandercennet, M., Garcia, D., Molinier, A-L., Pignol, D., Peduzzi, J., Zirah, S. & Rebuffat, S.** (2012). Isolation and Characterization of Environmental Bacteria Capable of Extracellular Biosorption of Mercury. *Appl. Environ. Microbiol.* **78**(4), pp. 1097-1106.
- Frank, A.J., Reich, C.I., Sharma, S., Weisbaum, J.S., Wilson, B.A. & Olsen, G.J.** (2008). Critical Evaluation of Two Primers Commonly Used for Amplification of Bacterial 16S rRNA Genes. *Appl. & Environ. Micro.* **74**(8), pp. 2461-2470.
- Fredrickson, J.K., Zachara, J.M., Kennedy, D., Lui, C. & Martine, D.** (2002). Influence of Mn oxides on the uranium(VI) by the metal-reducing bacterium *Shewanella putrefaciens*. *Geochimica et Cosmochimica Acta.* **66**(18), pp. 3247-3262.

- Friedl, G., Wehrli, B. & Manceau, A.** (1997). Solid phases in the cycling of manganese in eutrophic lakes: New insights from EXAFS spectroscopy. *Geochirica et Cosmochirica Acta*. **61**(2), pp. 275-290.
- Gao, W. & Francis, A.J.** (2008). Reduction of Uranium(VI) to Uranium(IV) by Clostridia. *American Society for Microbiology*.
- Gao, H.A., Obraztova, A., Stewart, N., Popa, R., Fredrickson, J.K., Tiedje, J.M., Nealson, K.H. & Zhou J.** (2006). *Shewanella loihica* sp. nov., isolated from iron-rich microbial mats in the Pacific Ocean. *Int. J. Syst. Evol. Microbiol.* **56**, pp. 1911-1916.
- Gardner, W.H. & Klute, A.** (1986). Methods of soil analysis: Part 1. Physical and mineralogical methods. pp. 493-544.
- Gheriany, I.A., Bocioaga, D., Hay, A.G., Ghoirse, W.C., Shuler, M.L. & Lion, L.W.** (2011). An uncertain role for Cu(II) in stimulating Mn(II) oxidation by *Leptothrix discophora* SS-1. *Arch. Microbiol.* **193**, pp. 89-93.
- Goh, M.K., Kahar, U.M., Chai, Y.Y., Chong, C.S., Chai, K.P., Ranjani, V., Illias, R.M. & Chan, K.** (2013). Recent discoveries and applications of *Anoxybacillus*. *Appl. Microbiol. Biotechnol.* **97**, pp. 1475-1488.
- Gonzaga-Jauregui, C., Lupski, J.R. & Gibbs, R.A.** (2012). Human genome sequencing in health and disease. *Annu. Rev. Med.* **63**, pp. 35-61.
- Guha, H., Jayachandran, K. & Maurrasse, F.** (2001). Kinetics of chromium (VI) reduction by a type strain *Shewanella* alga under different growth conditions. *Europe Pub Med Central*.

- Guha, H., Saiers, J.E., Brooks, S., Jardine, P. & Jayachandran, K.** (2001). Chromium transport, oxidation, and adsorption in manganese-coated sand. *Journal of Contaminant Hydrology*. **49**, pp. 311-334.
- Graf, D.L.** (1961). Crystallographic tables for the rhombohedral carbonates. *American Mineralogist*. **46**, pp. 1283-1316.
- Greenberg, A.E., Clesceri, L.S. & Eaton, A.D.** (1992). Estimation of bacterial density. *Standard Methods for the Examination of Water and Waste Water, Washington, DC: American Society for Microbiology*. pp. 49–50.
- Greene, A.C. & Madgwick, J.C.** (1991). Microbial formation of manganese oxides. *Appl. Environ. Microbiol.* **57**(4), pp. 1114-1120.
- Guindon, S. & Gascuel, O.** (2003). A simple, fast, and accurate algorithm to estimate large phylogenies by maximum likelihood. *Syst Biol.* **52**(5), pp. 696-704.
- Hall, T.A.** (1999). BioEdit: a user-friendly biological sequence alignment editor and analysis program for Windows 95/98/NT. *Nucl. Acids Symp. Ser.* **41**, pp. 95-98.
- Halvorsen, H.O. & Ziegler, N.H.** (1933). Application of statistics to problems in bacteriology; a means of determining populations by the dilution method, *J. Bacteriology*. **25**, pp. 101-121.
- Hassen, A., Saidi, N., Cherif, M. & Boudabous, A.** (1998). Resistance of environmental bacteria to heavy metals. *Bioresource Technology*. **64**(1), pp. 7-15.
- Hau, H.H. & Gralnick, J.A.** (2007). Ecology and Biotechnology of the Genus *Shewanella*. *Annu. Rev. Microbiol.* **61**, pp. 237-258.

**Hedrich, S., Schlömann, M. & Johnson, D.B.** (2011). The iron-oxidizing Proteobacteria. *Microbiology*. **157**(6), pp. 1551-1564.

**Heidelberg, J.F.I., Paulsen, I.T., Nelson, K.E., Gaidos, E.J., Nelson, W.C., Read, T.D., Eisen, J.A., Seshadri, R., Ward, N., Methe, B., Clayton, R.A., Meyer, T., Tsapin, A., Scott, J., Beanan, M., Brinkac, L., Daugherty, S., DeBoy, R.T., Dodson, R.J., Durkin, A.S., Haft, D.H., Kolonay, J.F., Madupu, R., Peterson, J.D., Umayam, L.A., White, O., Wolf, A.M., Vamathevan, J., Weidman, J., Impraim, M., Lee, K., Berry, K., Lee, C., Mueller, J., Khouri, H., Gill, J., Utterback, T.R., McDonald, L.A., Feldblyum, T.V., Smith, H.O., Venter, J.C., Nealon, K.H. & Fraser, C.M.** (2002). Genome sequence of the dissimilatory metal ion-reducing bacterium *Shewanella oneidensis*. *Nat. Biotechnol.* **20**(11), pp. 1118-1123.

**Higgins, C.F., Hiles, I.D., Salmond, G.P.C., Gill, D.R., Downie, J.A., Evans, I.J., Holland, I.B., Gray, L., Buckel, S.D., Bell, A.W. & Hermodson, M.A.** (1986). A family of related ATP-binding subunits coupled to many distinct biological processes in bacteria. *Nature*. pp. 448-450.

**Holmes, D.E., Mester, T., O'Neil, R.A., Perpetua, L.A., Larrahondo, M.J., Glaven, R., Sharma, M.L., Ward, J.E., Nevin, K.P. & Lovley, D.R.** (2008). Genes for two multicopper proteins required for Fe(III) oxide reduction in *Geobacter sulfurreducens* have different expression patterns both in the subsurface and on energy-harvesting electrodes. *Microbiology*. **154**, pp. 1422-1435.

**Holmes, R.A.** (1994). Manganese Minerals. *Industrial Minerals and Rocks*. pp. 657.

- Hua, M., Zhang, S., Pan, B., Zhang, W., Lu, L. & Zhang, Q.** (2012). Heavy metal removal from water/wastewater by nanosized metal oxides: A review. *Journal of Hazardous Materials*. **211-212**, pp. 317-331.
- Hucker, G.J. & Conn, H.J.** (1923). Methods of Gram staining. *Tech. Bull. New York*. **93**, pp. 37.
- Hullo, M.F., Moszer, I., Danchin, A. & Martin-Verstraete I.** (2001). CotA of *Bacillus subtilis* is a copper-dependent laccase. *J. Bacteriol.* **183**, pp. 5426-30.
- Hungate, R.E.** (1950). The anaerobic mesophilic cellulolytic bacteria. *Bacteriol. Rev.* **14**(1), pp. 1-49.
- Inan, K. & Canakci, S.** (2012). *Anoxybacillus kaynarcensis* sp. nov., a moderately thermophilic, xylanase producing bacterium. *J. Basic Microbiol.*
- Iwamoto, T. & Nasu, M.** (2001). Current bioremediation practice and perspective. *J. Biosci. Bioeng.* **92**(1), pp. 1-8.
- Jones, T.S.** (2000). Manganese. *U.S. Geological Survey Minerals Yearbook*. **50**, pp. 1-18.
- Jurtshuk Jr., P.** (1996). Medical Microbiology. 4<sup>th</sup> edition. *University of Texas Medical Branch at Galveston (Texas, United States of America)*.
- Kanso, S., Greene, A.C. & Patel, B.K.C.** (2002). *Bacillus subterraneus* sp. nov., an iron- and manganese-reducing bacterium from a deep subsurface Australian thermal aquifer. *IJSEM*. **52**, pp. 869-874.

- Kemp, G.J., Roussel, M., Bendahan, D., Le Fur, Y. & Cozzone, P.J.** (2001). Interrelations of ATP synthesis and proton handling in ischaemically exercising human forearm muscle studied by  $^{31}\text{P}$  magnetic resonance spectroscopy. *Journal of Physiology*. **535**(3), pp. 901-928.
- Leang, C., Qian, X., Mester, T. & Lovley, D.R.** (2010). Alignment of the c-Type Cytochrome *OmcS* along Pili of *Geobacter sulfurreducens*. *Appl. Environ. Microbiol.* **76**(12), pp. 4080-4084.
- Learman, D.R. & Voelker, B.M.** (2011). Formation of manganese oxides by bacterially generated superoxide. *Nature Geoscience*. **4**, pp. 95-98.
- Li, Y., Cai, Z.L. & Chen, M.** (2013). Spectroscopic properties of *Chlorophyll f*. *J. Phys. Chem. B*. **117**, pp. 11309-11317.
- Li, W.F. & Lu, Z.P.** (2005). Structural features of thermozymes. *Biotechnology Advances*. **25**, pp. 271-281.
- Li, Y., Scales, N., Blankenship, R.E., Willows, R.D. & Chen, M.** (2012). Extinction coefficient for red-shifted chlorophylls: Chlorophyll d and *chlorophyll f*. *Biochimica et Biophysica Acta (BBA) – Bioenergetics*. **1817**(8), pp. 1292-1298.
- Liang, S., Squier, T.C., Zachara, J.M. & Fredrickson, J.K.** (2007). Respiration of metal (hydr)oxides by *Shewanella* and *Geobacter*: a key role for multiheme c-type cytochromes. *Molecular Microbiology*. **65**(1), pp. 12-20.
- Lloyd, J.R., Leang, C., Hodges-Myerson, A.L., Coppi, M.V., Ciuffo, S., Methe, B., Sandler, S.J. & Lovley, D.R.** (2003). Biochemical and genetic characterization of *PpcA*, a periplasmic c-type cytochrome in *Geobacter sulfurreducens*. *Biochem J*. **369**, pp. 153-161.

- Lokhande, R.S., Singare, P.U. & Pimple, D.S.** (2011). Quantification Study of Toxic Heavy Metal Pollutants in Sediment Samples Collected From Kasardi River Flowing Along the Taloja Industrial Area of Mumbai, India. *New York Science Journal*. **4**(9), pp. 66-71.
- Lovley D.R.** (1991). Dissimilatory Fe(III) and Mn(IV) Reduction. *Microbiological Reviews*. **55**(2), pp. 259-287.
- Lovley, D.R.** (2001). Anaerobes to the Rescue, *Science* **293**, pp. 1444-1446.
- Lovley, D.R. & Blunt-Harris, E.L.** (1999). Role of Humic-Bound Iron as an Electron Transfer Agent in Dissimilatory Fe(III) Reduction. *Appl. Environ. Microbiol.* **65**(9), pp. 4252-4254.
- Lovley, D.R. & Philips, E.J.P.** (1986). Availability of Ferric Iron for Microbial Reduction in Bottom Sediments of the Freshwater Tidal Potomac River. *Appl. Environ. Microbiol.* **52**(4), pp. 751-757.
- Lovley D.R., Phillips E.J.P, Gorby Y.A. and Landa E.R.** (1991). Microbial reduction of Uranium. *Nature* **350**, pp. 413-416.
- Lucchesi, S., Russo, U. & Della Giusta, A.** (1997). Crystal chemistry and cation distribution in some, Mn-rich natural and synthetic spinels, Sample: JBS1. *European Journal of Mineralogy*. **9**, pp. 31-42.
- Lyle S.J. & Tamizi, M.** (1978). A study of the direct spectrophotometric determination of uranium(VI) in trialkylamine extracts with 2-(5-bromo-2-pyridylazo)-5-diethylaminophenol. *University of Kent*.
- Kato, C. & Nogi, K.** (2001). Correlation between phylogenetic structure and function: examples from deep-sea *Shewanella*. *FEMS Microbiology Ecology*. **35**(3), pp. 223-230

**Kim, B.C., Qian, X.L., Leang, C., Coppi, M.V. & Lovley, D.R.** (2006). Two putative c-type multiheme cytochromes required for the expression of *OmcB*, an outer membrane protein essential for optimal Fe(III) reduction in *Geobacter sulfurreducens*. *J Bacteriol.* **188**, pp. 3138-3142.

**Kohler, T., Armbruster, T. & Libowitzky, E.** (1997). Hydrogen bonding and Jahn-Teller distortion in groutite, alpha-MnOOH, and manganite, gamma-MnOOH, and their relations to the manganese, dioxides ramsdellite and pyrolusite. *Journal of Solid State Chemistry.* **133**, pp. 486-500.

**Kouzuma A., Hashimoto K. & Watanabe K.** (2012). Roles of siderophore in manganese-oxide reduction by *Shewanella oneidensis* MR-1. *FEMS Microbiol. Lett.* **326**(1), pp. 91-98.

**Mao, Y., Zhang, L., Li, D., Shi, H., Lui, Y. & Cai, L.** (2010). Power generation from a biocathode microbial fuel cell biocatalyzed by ferro/manganese-oxidizing bacteria. *Electrochimica Acta.* **55**, pp. 7804-7808.

**Marmur, M.** (1961). A procedure for the isolation of Deoxyribonucleic acid from microorganism. *J. Mol. Biol.* **3**, pp. 208-218.

**Marshall, K.C.** (1979). Chapter 5: Biogeochemistry of Manganese Metals. *Studies in Environmental Science.* **3**, pp. 253-292.

**McCammion, C.A.** (1991). Static compression of alpha-MnS at 298 K to 21 GPa, Sample: P = 0 GPa. *Physics and Chemistry of Minerals.* **17**, pp. 636-641.

- Mehta, T., Coppi, M.V., Childers, S.E. & Lovley, D.R.** (2005). Outer membrane c-type cytochromes required for Fe(III) and Mn(IV) oxide reduction in *Geobacter sulfurreducens*. *Appl. Environ. Microbiol.* **71**, pp. 8634-8641.
- Mermelstein, L.D., Welker, N.E., Bennett, G.N. & Papoutsakis, E.T.** (1992). Expression of Cloned Homologous Fermentative Genes in *Clostridium Acetobutylicum* ATCC 824. *Nature Biotechnology.* **10**, pp. 190-195.
- Miyashita, H., Adachi, K., Kurano, N., Ikemot, H., Chihara, M. & Miyach, S.** (1997). Pigment Composition of a Novel Oxygenic Photosynthetic Prokaryote Containing Chlorophyll d as the Major Chlorophyll. *Plant and Cell Physiology.* **38**(3), pp. 274-281.
- Miyata, N., Sugiyama, D., Tani, Y., Tsuno, H., Seyama, H., Sakata, M. & Iwahori, K.** (2007). Production of Biogenic Manganese Oxides by Repeated-Batch Cultures of Laboratory Microcosms. *J. Bioscience. Bioengineering.* **103**(5), pp. 443-439.
- Miyata, N., Tani, Y., Sakata, M. & Iwahori, K.** (2007). Microbial Manganese Oxide Formation and Interaction with Toxic Metal Ions. *J. Bioscience. Bioengineering.* **104**(1), pp. 1-8.
- Murphy, J.L. & Saltikov, C.W.** (2007). The *cymA* Gene, Encoding a Tetraheme c-Type Cytochrome, Is Required for Arsenate Respiration in *Shewanella* Species. *J. Bacteriol.* **189**(6), pp. 2283-2290.
- Murray, J.W., Balistrieri, L.S. & Paul, B.** (1984). The oxidation state of manganese in marine sediments and ferromanganese nodules. *Geochimica et Cosmochimica Acta.* **48**(6), pp. 1237-1247.

- Myers, J.M., Antholine, W.E. & Myers, C.R.** (2004). Vanadium(V) Reduction by *Shewanella oneidensis* MR-1 Requires Menaquinone and Cytochromes from the Cytoplasmic and Outer Membranes. *Appl. Environ. Microbiol.* **70**(3), pp. 1405-1412.
- Narayan, V.V., Hatha, M.A., Morgan, H.W. & Rao, D.** (2008). Isolation and characterization of aerobic thermophilic bacteria from the Savusavu hot springs in Fiji. *Microbes Environ.* **23**, pp. 350-352.
- Nealson, K.H.** (1983). The microbial manganese cycle. *Microbial Geochemistry – Blackwell Scientific Publications*. Oxford. pp. 191-221.
- Nealson, K.H.** (2006). The Manganese-Oxidizing Bacteria. *Prokaryotes*. **5**, pp. 222-231.
- Nealson, K.H. & Ford, J.** (1980). Surface Enhancement of Bacterial Manganese Oxidation: Implications for Aquatic Environments. *Geomicrobiology Journal*. **2**(1), pp. 21-37.
- Nealson, K.H., Tebo, B.M. & Rosson, R.A.** (1988). Occurrence and mechanisms of microbial oxidation of manganese. *Adv. Appl. Microbiol.* **33**, pp. 279-318.
- Nevin, K.P., Kim, B.C., Glaven, R.H., Johnson, J.P., Woodard, T.L., Methe, B.A., Didonato, R.J., Covalla, S.F., Franks, A.E., Lui, A. & Lovley, D.R.** (2009). Anode biofilm transcriptomics reveals outer surface components essential for high density current production in *Geobacter sulfurreducens* fuel cells. *PLoS ONE*. **4**(5), pp. e5628.
- Nevin, K.P., Finneran, K.T. & Lovley, D.R.** (2003). Microorganisms Associated with Uranium Bioremediation in a High-Salinity Subsurface Sediment. *Appl. Environ. Microbiol.* **69**(6), pp. 3672-3675.

**Nies, D.H. & Silver, S.** (2007). *Molecular Microbiology of Heavy Metals. Springer Science & Business Media.*

**Ogg, C.D.** (2011). *Thermophiles from Deep Subsurface Waters – Thesis (PhD Doctorate). Griffith University, Brisbane.*

**Ogg, C.D. & Patel, B.K.C.** (2009). *Caloramator australicus* sp. nov., a thermophilic, anaerobic bacterium from the Great Artesian Basin of Australia. *International Journal of Systematic and Evolutionary Microbiology.* **59**, pp. 95-101.

**Okinaka, R.T., Price, E.P., Wolken, S.R., Gruendike, J.M., Chung, W.K., Pearson, T., Xie, G., Munk, C., Hill, K.K., Challacombe, J., Ivins, B.E., Schupp, J.M., Beckstrom-Sternberg, S.M., Friedlander, A. & Keim, P.** (2011). An attenuated strain of *Bacillus anthracis* (CDC 684) has a large chromosomal inversion and altered growth kinetics. *BCM Genomics.* **12**(477), pp. 1-13.

**Olsen, J.M., Philipson, K.D. & Sauer, K.** (1973). Circular Dichroism And Absorption Spectra Of Bacterio-Chlorophyll-Protein And Reaction Center Complexes From *Chlorobium Thiosulfatophilum*. *Biochimica et Biophysica Acta.* **292**, pp. 206-217.

**Ondov, B.D., Bergman, N.H. & Phillippy, A.M.** (2011). Interactive metagenomic visualization in a Web browser. *BMC Bioinformatics.* **12**(1), pp. 385.

**Orchid Bioinformatics.** (2013). Phylogenetic Tree of Life. *Orchid Bioinformatics.* Viewed May 14<sup>th</sup>, 2014. <[http://www.exploreorchid.com/wp-content/uploads/2013/09/phylogenetic\\_tree.png](http://www.exploreorchid.com/wp-content/uploads/2013/09/phylogenetic_tree.png)>

**Overbeek, R., Begley, T., Butler, R.M., Choudhuri, J.V., Chuang, H-Y., Cohoon, M., Crécy-Lagard, V.D., Diaz, N., Disz, T., Edwards, R., Fonstein, M., Frank, E.D., Gerdes,**

S., Glass, E.M., Goesmann, A., Hanson, A., Iwata-Reuyl, D., Jensen, R., Jamshidi, N., Krause, L., Kubal, M., Larsen, N., Linke, B., McHardy, A.C., Meyer, F., Neuweger, H., Olsen, G., Olson, R., Osterman, A., Portnoy, V., Pusch, G.D., Rodionov, D.A., Rückert, C., Steiner, J., Stevens, R., Thiele, I., Vassieva, O., Ye, Y., Zagnitko, O. & Vonstein, V. (2005). The Subsystems Approach to Genome Annotation and its Use in the Project to Annotate 1000 Genomes. *Nucleic Acids Res.* **33**(17), pp. 5691-5702.

Pabinger, S., Dander, A., Fischer, M., Snajder, R., Sperk, M., Efremova, M., Krabichler, B., Speicher, M.R., Zschocke, J. & Trajanoski, Z. (2012). A survey of tools for variant analysis of next-generation genome sequencing data. *Briefings in Bioinformatics.* pp. 1-23.

Pacalo, R.E.G. & Graham E.K. (1991). Pressure and temperature dependence of the elastic, properties of synthetic MnO, Sample: 1. *Physics and Chemistry of Minerals.* **18**, pp. 69-80.

Paustian, T. (2000). Metabolism – Fermentation. *University of Madison-Wisconsin.*

Pikuta, E., Lysenko, A., Chuvilskaya, N., Mendrock, U., Hippe, H., Suzina, N., Nikitin, D., Osipov, G. & Laurinavichius K. (2000). *Anoxybacillus pushchinensis* gen. nov., sp. nov., a novel anaerobic, alkaliphilic, moderately thermophilic bacterium from manure, and description of *Anoxybacillus flavitherms* comb. nov. *Int. J. Syst. Evol. Microbiol.* **50**(6), pp. 2109-2107.

Pinchuk, G.E., Geydebrekht1, O.V., Hill, E.A., Reed, J.L., Konopka1, A.E., Beliaev, A.E. & Fredrickson, J.K. (2011). Pyruvate and Lactate Metabolism by *Shewanella oneidensis* MR-1 under Fermentation, Oxygen Limitation, and Fumarate Respiration Conditions. *Appl. Environ. Microbiol.* **77**(23), pp. 8234-8240.

- Ponsano, E.H.G, Paulino, C.Z. & Pinto, M.F.** (2008). Phototrophic growth of *Rubrivivax gelatinosus* in poultry slaughterhouse wastewater. *Bioresource Technology*. **99**(9), pp. 3836-3842.
- Porra, R.J., Thompson, W.A. & Kriedemann, P.E.** (1989). Determination of accurate extinction coefficients and simultaneous equations for assaying *chlorophylls a* and *chlorophylls b* extracted with four different solvents: verification of the concentration of chlorophyll standards ' by atomic absorption spectroscopy *Biochimica et Biophysica Acta*. **975**, pp. 384-394.
- Post, J.E.** (1999). Manganese oxide minerals: Crystal structures and economic and environmental significance. *Proc. Natl. Acad. Sci.* **96**(7), pp. 3447-3454.
- Post, J.E. & Heaney, P.J.** (2004). Neutron and synchrotron X-ray diffraction study of the structures and dehydration behaviors of ramsdellite and "groutellite". *American Mineralogist*. **89**, pp. 969-975.
- Post, J.E. & Veblen, D.R.** (1990). Crystal structure determinations of synthetic sodium, magnesium and potassium, birnessite using TEM and the Rietveld method. *American Mineralogist*. **75**, pp. 477-489.
- Post, J.E., Von Dreele, R.B. & Buseck, P.R.** (1982). Symmetry and cation displacements in hollandites:., structure refinements of hollandite, cryptomelane and priderite. *Acta Crystallographica*. **38**, pp.1056-1065.
- Reguera, G., McCarthy, K.D., Mehta, T., Nicoll, J.S., Tuominen, M.T. & Lovley, D.R.** (2005). Extracellular electron transfer via microbial nanowires. *Nature*. **435**(7045), pp. 1098-1101.

- Rehder, D.** (1991). The bioorganic chemistry of vanadium. *Angew. Chemistry*. **30**, pp. 148-167.
- Rehder, D.** (1992). Structure and function of vanadium compounds in living organisms. *Biometals*. **5**, pp. 3-12.
- Richardson, L.L., Aguilar, C. & Nealson, K.H.** (1988). Manganese oxidation in pH and O<sub>2</sub> microenvironments produced by phytoplankton. *Limnol. Oceanogr.* **33**, pp. 352–63.
- Ridge, J.P., Marianna, L., Eloise, I.L., Fegan, M., McEwan, A.G. & Sly, L.I.** (2007). A multicopper oxidase is essential for manganese oxidation and laccase-like activity in *Pedomicrobium* sp. ACM 3067. *Environmental Microbiology*. **9**(4), pp. 944-953.
- Romano, A.H. & Conway, T.** (1996). Evolution of carbohydrate metabolic pathways. *Res. Microbiol.* **147**(6-7), pp. 448-455.
- Rothschild, L.J. & Mancinelli, R.L.** (2001). Life in extreme environments. *Nature*. **409**, pp. 1092-1101.
- Sabri, M., Léveillé, S. & Dozois, C.M.** (2005). A SitABCD homologue from an avian pathogenic *Escherichia coli* strain mediates transport of iron and manganese and resistance to hydrogen peroxide. *Microbiology*. **152**(3), pp. 745-758.
- Santelli, C.M., Pfister, D.H., Lazarus, D., Sun, L., Burgos W.D. & Hansel, C.M.** (2010). Promotion of Mn(II) oxidation and remediation of coal mine drainage in passive treatment systems by diverse fungal and bacterial communities. *Appl. Environ. Microbiol.* **76**(14), pp. 4871-4875.

- Schiebe, T.D., Fang, R.M., Garg, S., Long, P.E. & Lovley, D.R.** (2009), Coupling a genome-scale metabolic model with a reactive transport model to describe *in situ* uranium bioremediation., *Microbial Biotechnology* **2**, pp. 274-286.
- Sheng, L.I.** (2011). Uranium speciation on the rate of U(VI) reduction by *Shewanella oneidensis* MR-1. *Geochimica et Cosmochimica Acta.* **75**(12), pp. 3558-3567.
- Sheng, L.I. & Fein, J.B.** (2014). Uranium Reduction by *Shewanella oneidensis* MR-1 as a Function of NaHCO<sub>3</sub> Concentration: Surface Complexation Control of Reduction Kinetics. *Environ. Sci. Technol.* ePub ahead of print.
- Shi, L, Squier, T.C., Zachara, J.M. & Fredrickson, J.K.** (2007). Respiration of metal (hydr)oxides by *Shewanella* and *Geobacter*: a key role for multiheme *c*-type cytochromes. *Molecular Microbiology.* **65**(1), pp. 12-20.
- Shivaji, S., Pratibha, M.S., Sailaja, B., Hara Kishore, K., Singh, A.K., Begrum, Z., Anarasi, U., Prabakaran, S.R., Reddy, G.S.N & Srinivas, T.N.R.** (2011). Bacterial diversity of soil in the vicinity of Pindari glacier, Himalayan mountain ranges, India, using culturable bacteria and soil 16S rRNA gene clones. *Extremophiles.* **15**(1), pp. 1-22.
- Smith, T.F. & Waterman, M.S.** (1981). Identification of common molecular subsequences. *J. Mol. Biol.* **147**, pp. 195-197.
- Spiro, T.G., Bargar, J.R., Sposito, G. & Tebo, B.M.** (2010). Bacteriogenic Manganese Oxides. *Accounts of Chemical Research.* **43**(1), pp. 2-9.
- Sørensen, J.** (1981). Reduction of Ferric Iron in Anaerobic, Marine Sediment and Interaction with Reduction of Nitrate and Sulfate. *Appl. & Environ. Micro.* **43**(2), pp. 319-324.

- Spratt Jr, H.G., Siekmann, E.C. & Hodson, R.E.** (1994). Microbial Manganese Oxidation in Saltmarsh Surface Sediments Using a Leuco Crystal Violet Manganese Oxide Detection Technique. *Estuarine, Coastal and Shelf Science*. **38**(1), pp. 91-112.
- Steiner, R., Cmiel, E. & Scheer, H.** (1983). Chemistry of Bacteriochlorophyll b: Identification of Some (Photo)Oxidation Products. *Z. Naturforsch.* **38c**, pp. 748-752.
- Stetter, K.O.** (1999) . Extremophiles and their adaptation to hot environments. *FEBS Letters*. **452**(1-2), pp. 22-25.
- Straub, K.L., Benz, M. & Schink, B.** (2001). Iron metabolism in anoxic environments at near neutral pH. *Microbiol. Ecol.* **34**(3), pp. 181-186.
- Stuetz, R.M., Greene, A.C. & Madgwick, J.C.** (1996). The Potential Use Of Manganese Oxidation In Treating Metal Effluents. *Minerals Engineering*. **9**(12), pp. 1253-1261.
- Stuetz, R.M., Greene, A.C. & Madgwick, J.C.** (1996). Microalgal-facilitated bacterial oxidation of manganese. *Journal of Industrial Microbiology*. **16**(5), pp. 267-273.
- Tebo, B.M., Bargar, J.R., Clement, B., Dick, G., Murray K.J., Parker, D., Verity, R. & Webb, S.** (2004). Biogenic manganese oxides: Properties and mechanisms of formation. *Annual Reviews of Earth and Planetary Sciences*. **32**, pp. 287–328.
- Tebo, B.M., Johnson, H.A., McCarthy, J.K. & Templeton, A.S.** (2005). Geomicrobiology of manganese(II) oxidation. *Trends in Microbiology*. **13**(9), pp. 421-428.
- Tebo, B.M., van Waasbergen, L.G., Francis, C.A., He, L.M., Edwards, D.B. & Casciotti, K.** (1998). Manganese Oxidation by Spores of the Marine *Bacillus* sp. Strain SG-1. *New Developments in Marine Biotechnology*. pp. 177-180.

- Thauer, R.K., Jungermann, K. & Decker, K.** (1977). Energy conservation in chemotrophic anaerobic bacteria. *Bacteriol. Rev.* **41**(1), pp. 100-180.
- Thompson, I.A., Huber, D.M., Guest, C.A. & Schulze, D.G.** (2005). Fungal manganese oxidation in a reduced soil. *Environ. Microbiol.* **7**(9), pp. 1480-1487.
- Trivedi, U.H., Cézard, T., Bridgett, S., Montazam, A., Nichols, J., Blaxter, M. & Gharbi, K.** (2014). Quality control of next-generation sequencing data without a reference. *Front Genet.*
- Trudinger, P.A & Swaine, D.J.** (1979). Biogeochemical Cycling of Mineral-Forming Elements. *Elsevier Science.*
- Truex, M.J., Peyton, B.M., Valentine, N.B. & Gorby, Y.A.** (2000). Kinetics of U(VI) reduction by a dissimilatory Fe(III)-reducing bacterium under non-growth conditions. *Biotechnology and Bioengineering.*
- Turner, S. & Post, J.E.** (1988). Refinement of the substructure and superstructure of romanechite. *American Mineralogist.* **73**, pp. 1155-1161.
- Valdés, J., Pedroso, I., Quatrini, R., Dodson, R.J., Tettelin, H., Blake, R., Eisen, J.A. & Holmes, D.S.** (2008). Acidithiobacillus ferrooxidans metabolism: from genome sequence to industrial applications. *BMC Genomics.* **11**(9), pp. 597.
- Valley, J.W.** (2005). A Cool Early Earth? *Scientific American.* pp. 59-65.
- van Waasbergen, L.G., Hildebrand, M. & Tebo, B.M.** (1996). Identification and characterization of a gene cluster involved in manganese oxidation by spores of the marine *Bacillus sp.* strain SG-1. *J. Bacteriol.* **178**, pp. 3517–3530.

- van Waasbergen, L.G., Hoch, J.A. & Tebo, B.M.** (1993). Genetic analysis of the marine manganese-oxidizing *Bacillus* sp. strain SG-1: protoplast transformation, Tn917 mutagenesis, and identification of chromosomal loci involved in manganese oxidation. *J. Bacteriol.* **175**(23), pp. 7594-7603.
- Villalobos, M., Toner, B., Bargar, J. & Sposito, G.** (2003). Characterization of the manganese oxide produced by *Pseudomonas putida* strain MnB1. *Geochimica et Cosmochimica Acta.* **67**(14), pp. 2649-2662.
- Wandersman, C. & Stojiljkovic, I.** (2000). Bacterial heme sources: the role of heme, hemoprotein receptors and hemophores. *Current Opinion in Microbiology.* **3**, pp. 215-220.
- Wang, Z.Y., Kadota, T., Kobayashi, M., Kasuya, A. & Nozawa, T.** (2004). NMR Relaxation Study of the Bacteriochlorophyll c in Solutions. *J. Phys. Chem. B.* **108**, pp. 15422-15428.
- Wang X., Schröder H.C., Wiens M., Schlossmacher U. & Müller W.E.G.** (2009). Manganese/polymetallic nodules: micro-structural characterization of exolithobiontic- and endolithobiontic microbial biofilms by scanning electron microscopy. *Micron.* **40**(3), pp. 350-358.
- Wang, X., Wiens, M., Divekar, M., Grebenjuk, V.A., Schröder H.C, Batel, R. & Müller W.E.G.** (2011). Isolation and Characterization of a Mn(II)-Oxidizing Bacillus Strain from the Demosponge *Suberites domuncula*. *Mar. Drugs.* **9**, pp. 1-28.
- Webb, S.M., Dick, G.J., Bargar, J.R. & Tebo, B.M.** (2005). Evidence for the presence of Mn(III) intermediates in the bacterial oxidation of Mn(II). *The National Academy of Sciences.* **102**(15), pp. 5558-5563.

**Weber K. A., Achenbach L. A., Coates J. D.** (2006). Microorganisms pumping iron: anaerobic microbial iron oxidation and reduction. *Nat. Rev. Microbiol.* **4**, pp. 752-764.

**Weidemeier, T.H.** (1999). Natural Attenuation of Fuels and Chlorinated Solvents in the Subsurface. John Wiley & Sons, Inc. New York, ISBN: 0-471-19749-1.

**Wolin, E.A., Wolin, M.J. & Wolfe, R.S.** (1963). Formation of methane by bacterial extracts. *J. Biol. Chem.* **238**, pp. 2882-2886.

**Wright, M.H.** (2010). Thermophilic metal reducing bacteria from Paralana hot springs. *Griffith University - Australia*.

**Wyckoff, R.W.G.** (1963). Note: beta phase of MnO<sub>2</sub>, rutile structure. *Crystal Structures - Second edition. Interscience Publishers, New York.* **1**, pp. 239-444.

**Yang, L., Chang, Y. & Chou, M.S.** (1999), Feasibility of bioremediation of trichloroethylene contaminated sites by nitrifying bacteria through co-metabolism with ammonia. *J. Hazardous Metals* **69**(1), pp. 111-126.

**Yoon, S., Sanford, R.A. & Löffler, F.E.** (2013). *Shewanella* spp. Use Acetate as an Electron Donor for Denitrification but Not Ferric Iron or Fumarate Reduction. *Appl. Environ. Microbiol.* **79**(8), pp. 2818-2822.

**Zhang, W. & Cheng, C.Y.** (2007). Manganese metallurgy review. Part I: Leaching of ores/secondary materials and recovery of electrolytic/chemical manganese dioxide. *Hydrometallurgy.* **89**(3-4), pp. 137-159.

**Zeikus, J.G., Hegge, P.W. & Anderson, M.A.** (1979). *Thermoanaerobium brockii* gen. nov. and sp. nov., a new chemoorganotrophic, caldoactive, anaerobic bacterium. *Arch. Microbiol.* **122**, pp. 41-48

# Appendices

**Appendix 1**

**Most Probable Number (MPN) Table**

X Dilution	Y Dilution	Z Dilution	MPN of micro-organisms per mL of x dilution
0	0	0	0
0	0	1	0.1
0	1	0	0.3
0	1	1	0.6
0	2	0	0.6
1	0	0	0.6
1	0	1	0.9
1	0	2	1.1
1	1	0	0.9
1	1	1	1.1
1	2	0	1.1
1	2	1	1.5
1	3	0	1.0
2	0	0	0.8
2	0	1	1.0
2	0	2	2.0
2	1	0	1.5
2	1	1	2.0
2	1	2	3.0
2	2	0	2.0
2	2	1	3.0
2	2	2	3.5
2	2	3	4.0
2	3	0	3.0
2	3	1	3.5
2	3	2	4.0
3	0	0	2.5
3	0	1	4.0
3	0	2	6.5
3	1	0	4.5
3	1	1	7.5
3	1	2	11.5
3	2	3	10
3	2	0	9.5
3	3	1	15.0

Consider the case where the following pattern is seen 24 days after incubation:

- 1 dilution: all three bottles show turbidity
- 2 dilution: all two bottles show turbidity
- 3 dilution: all one bottles show turbidity
- 4 dilution: no bottles show turbidity

This result would be as followed:

	1a +	2a +	3a -	4a -
	1b +	2b -	3b -	4b -
	1c +	2c +	3c +	4c -
<b>Total:</b>	3	2	1	0

From the MPN table this result can be read:

a)	X dilution	Y Dilution	Z Dilution	MPN
	3	2	1	15
Or... b)	X dilution	Y Dilution	Z Dilution	MPN
	2	1	0	1.5

In a), the MPN table value is 15.0. The x dilution is 1:10, thus the bacteria per ml. is 150 (15 \* 10)

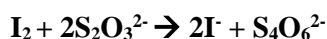
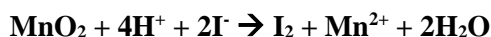
In b), the MPN table value is 1.5. The x dilution is 1:100, thus the bacteria per ml. is 150 (1.5 \* 100)

Thus both interpretations yield the same result

## Appendix 2

### Calculation of Average Oxidation States (O/Mn ratio)

The method to determine the average oxidation states theoretically is given in the following chemical equations:



The O/Mn ratio (as  $\text{MnO}_x$ ) is calculable from the following formula:

$$x = 1 + \frac{A}{B} \quad (\text{Murray } et \text{ al.}, 1984)$$

Where:

**A** = The total oxidised equivalents (i.e. number of moles of  $\text{S}_2\text{O}_3^{2-}$  used)  
5mM solution was used (i.e. 5nmol/L)

Total number of moles =  $5.a \times 10^{-6}$

Where a = the volume (mL) of  $\text{S}_2\text{O}_3^{2-}$  used in the titration.

**B** = The moles of Mn(II)

The concentration of Mn(II) was determined using ICP-OES with a total volume of 100ml

Mn(II) molarity = b mg/L

$$= b/55\text{mmoles/L}$$

$$= b/0.0055$$

**Therefore, using the above values the overall equation is...**

$$x = 1 + \frac{275.a}{100.b}$$